Streptococcus pneumoniae carriage

The impact of intranasal vaccination and mucosal immunity

Kirsten Kuipers

Streptococcus pneumoniae carriage

The impact of intranasal vaccination and mucosal immunity

Kirsten Kuipers

***Streptococcus pneumoniae* carriage**
The impact of intranasal vaccination and mucosal immunity
PhD thesis, Radboud University, The Netherlands

Author
Kirsten Kuipers

ISBN
978-94-028-0624-3

Design/lay-out
Promotie In Zicht, Arnhem

Print
Ipskamp Printing, Enschede

About the cover
The cover image represents the storm that arises during the growth of a tree in a human individual. The initial planting of *Streptococcus pneumoniae*, represented by the tree, is harmless to the host at first. However, danger lurks ahead as the roots begin to take hold, allowing the pneumococcus to grow in the unknowing host. This metaphor depicts the critical step of successful colonization of *S. pneumoniae* in the progression towards disease (the storm).

Printing of this thesis was kindly financially supported by
the Radboud University, the Netherlands Society for Microbiology (NVMM) / the Royal Netherlands Society for Microbiology (KNVM), Pfizer bv, and Fysiozorg Rijssen.

Streptococcus pneumoniae carriage

The impact of intranasal vaccination and mucosal immunity

Proefschrift

ter verkrijging van de graad van doctor
aan de Radboud Universiteit Nijmegen
op gezag van de rector magnificus Prof. dr. J.H.J.M. van Krieken,
volgens besluit van het college van decanen
in het openbaar te verdedigen op maandag 29 mei 2017
om 12.30 precies

door

Kirsten Kuipers
geboren op 11 november 1988
te Almelo

Promotor
Prof. dr. R de Groot

Copromotor
Dr. M.I. de Jonge

Manuscriptcommissie
Prof. dr. A.J.A.M. van der Ven
Prof. dr. H.F.L. Wertheim
Prof. dr. J.N. Weiser (New York University, Verenigde Staten)

Voor Pap en Mam

omdat jullie altijd voor mij klaar staan
en niets jullie te veel is

CONTENTS

1

General introduction

GENERAL INTRODUCTION

The burden of *Streptococcus pneumoniae*

Respiratory infections caused by bacteria and viruses remain a major burden of disease contributing to significant morbidity and mortality within the human population. Globally, lower respiratory tract infections are ranked 4th in the top 10 causes of death[1]. Pneumonia alone is responsible for 15% of child deaths below the age of five years[2]. The most common cause of pneumonia in children and the elderly is *Streptococcus pneumoniae*, a human specific bacterium that stands out among respiratory pathogens as a global health problem[2-6]. *S. pneumoniae*, or pneumococcus, is a gram-positive bacterium and a commensal colonizer that is part of the nasopharyngeal microbiome[4,7]. Carriage of the pneumococcus is primarily asymptomatic. However, infrequently *S. pneumoniae* invades otherwise sterile compartments leading to disease (Figure 1). Pneumococcal disease primarily presents as mild infections, such as sinusitis and otitis

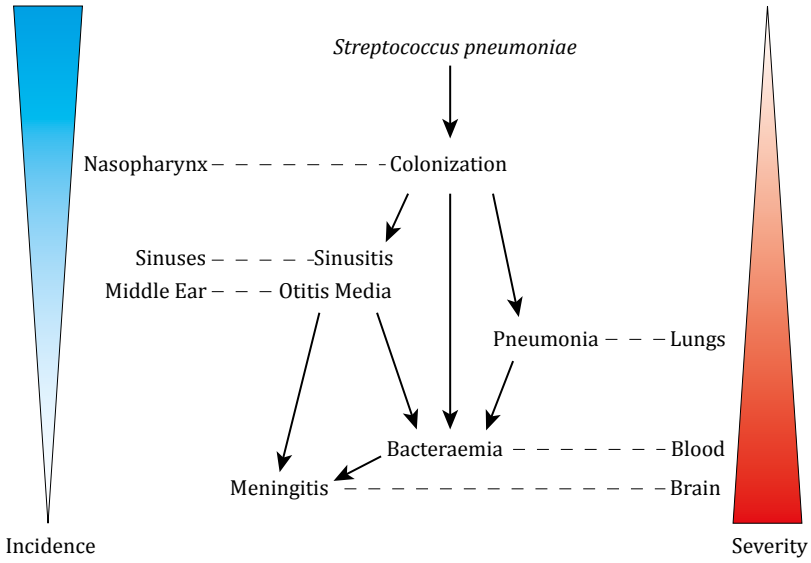

Figure 1 Overview of the range of diseases caused by *Streptococcus pneumoniae*.

Figure is adjusted from Jambo *et al.* 2010[12]. Acquisition of *S. pneumoniae* starts with colonization of the nasopharynx. In some occasions, *S. pneumoniae* transits into other niches, including the sinuses, the middle ear and the lungs, causing sinusitis, otitis media, and pneumonia respectively. The pneumococcus is able to enter otherwise sterile compartments of the human body, such as the blood (bacteraemia) and the brain where it could lead to septicemia and meningitis. Notably, the incidence of different pneumococcal stages of disease is inversely correlated with disease severity.

media (OM)[4,6]. These clinical entities form an important cause for child physician visits and annual antibiotic prescriptions[4,6]. Serious invasive illnesses caused by *S. pneumoniae* include pneumonia, bacteraemia, sepsis, and meningitis[3-6]. Pneumococcal disease primarily affects young children, the elderly, and immune compromised individuals[3-6,8]. Globally, pneumococcal disease accounts for over 800,000 deaths among young children each year with a major impact on mortality particularly in developing countries[3]. Among elderly between the ages of 65 to 85 years, 15% succumbs to pneumococcal pneumonia. Mortality rates further increase to 30-45% for individuals 85 years or older, which explains why the pneumococcus is called *"the old man's friend"* as first posed by Sir William Osler in 1909[4,6,9]. Pneumococcal infection is treatable with antibiotics. However, the continuing emergence and spread of antibiotic resistant strains increasingly restrict the options for adequate antimicrobial therapy[10]. Vaccination against colonization and disease is a commonly accepted approach for eradication of (resistant) pneumococcal serotypes included in the vaccine[4,8,11].

Pneumococcal vaccination strategies

In 1911, the first pneumococcal killed whole cell vaccine was tested in a clinical trial[4,13,14]. Decades later in 1945 this was followed by studies with a capsular polysaccharide vaccine. The capsular polysaccharide surrounding the pneumococcal cell wall is considered a major virulence factor and used for classification of *S. pneumoniae* into distinct serotypes, of which more than 95 have been described[4,7]. In 1977 and 1983, vaccines containing 14 and 23 purified capsular polysaccharides (PPSV23), respectively, were approved for vaccination. PPSV23, also known as Pneumovax 23, reduced pneumococcal disease incidence in the elderly[4,15,16]. PPSV23 was introduced in the US for adults over 65 years of age, but vaccine effectiveness against invasive pneumococcal disease remains controversial[4,15-18]. The polysaccharide vaccines were not protective in children below the age of 2 years nor did they induce a memory response[19,20].

In 1929 it was discovered that the conjugation of the capsular polysaccharides to a carrier protein increased vaccine immunogenicity leading to improved memory and enhanced immune responses also in young children[4,21,22]. Nowadays, pneumococcal conjugate vaccines (PCVs) are introduced in many industrialized countries for childhood vaccination included in the national vaccination programs[4]. Prevnar 7 (US) or Prevenar 7 (Europe) is a 7-valent PCV that includes polysaccharides from serotypes 4, 6B, 9V, 14, 18C, 19F and 23F. Selection of these serotypes was based on their prevalence and strong association with invasive pneumococcal disease in the Western world. However, the disease burden is highest in developing countries where different serotypes are circulating and causing disease. The next generation of PCVs are PCV10 and PCV13[4]. These

vaccines both include the same serotypes as in PCV7 to which 3, 6A, 19A are added. PCV13 additionally contains serotypes 1, 5, and 7F. Introduction of PCVs in industrialized countries has greatly reduced pneumococcal disease and carriage by serotypes included in the vaccine (i.e. vaccine (sero)types; VTs)[4,6,23,24]. The elderly may benefit from introduction of PCV13. The Dutch CAPiTA study illustrated that the use of PCV13 resulted in a cost-effective reduction in serotype specific disease in adults over 65 years of age[25]. Following PCV introduction, non-vaccine (sero)types (NVTs) are increasingly isolated from patients with invasive disease[26-30]. The decrease in VT carriage caused by PCV immunization has also led to an increased carriage of NVTs, also referred to as serotype replacement, which is thought to be a result of changes in the nasopharyngeal microbiome[26,27,31]. Theoretically, infections resulting from serotype replacement can be solved by including more serotypes in the PCVs. However, the number of capsular polysaccharides that can be coupled to a carrier protein is limited due to the complexity of the manufacturing process. The addition of polysaccharides also leads to a sharp increase in the vaccine production costs. Furthermore, immunological restrictions such as too much carrier antigen may impair antibody responses by polysaccharide antigen competition or carrier-mediated epitope suppression[22,32].

Despite the availability of vaccines and antibiotics, *S. pneumoniae* still causes approximately 1.3 million deaths yearly[5]. Alternative vaccine strategies addressing the limitations of the currently applied strategies are therefore required to reduce the global burden of pneumococcal disease. Experimental vaccine development focuses on the use of, preferably highly conserved, pneumococcal proteins that are present in all serotypes[4,14,22,33,34]. These may potentially be incorporated in a universal vaccine, protecting against all circulating strains. Important candidates for a protein-based vaccine include virulence proteins, such as pneumococcal surface protein A (PspA), C (PspC), and pneumolysin[4,14,22,33,34]. Although some protein-based vaccines have been tested in clinical trials they are still far away from marked approval.

Streptococcus pneumoniae colonization: a prerequisite for disease

Colonization of the nasopharynx by pneumococci is a highly dynamic process and an essential step preceding pneumococcal disease (Figure 1)[4,35]. Although persons from all ages acquire and become colonized by *S. pneumoniae*, the highest colonization rates are found in children. The average time of a first pneumococcal colonization event for a child is around the age of 6 months in industrialized countries. The duration of colonization with a specific serotype is highly variable and can range between 1-30 weeks depending on the type and the individual's age[4,35-37]. Other factors that impact pneumococcal

acquisition and duration of colonization include breast-feeding, antibiotic use, and co-infection with other respiratory pathogens[4,38-40]. Prolonged carriage is characteristic for young children. Colonization duration decreases with increasing age, e.g. carriage peaks during the first 2 years of life and decreases to 10% in infants over 5 years of age[4,8,41,42]. In industrialized countries, the incidence of pneumococcal carriage varies between 20 and 50% in children below the age of 3 years, whereas in developing countries, typically all 3-month-old children are carrying *S. pneumoniae*[4,8,43]. It is therefore not surprising that young children are considered the natural reservoir for *S. pneumoniae* and thus are primarily responsible for pneumococcal transmission.

PCVs were initially designed to protect against invasive disease via induction of systemic anti-capsular antibodies and complement activity that mediate pneumococcal opsonization and killing by phagocytic cells[4,44,45]. However, there is increasing evidence that PCVs also reduce the circulation of VTs, suggesting that PCVs directly affect VT carriage[26,27,31]. Indeed, a recent clinical trial demonstrated that in participants who received PCV *S. pneumoniae* colonization was reduced after intranasal challenge[46]. It has been postulated that the strong reduction of VT-induced pneumococcal disease by PCVs may primarily be caused by the PCV's reduction of VT carriage.

A reduction in pneumococcal colonization can be caused by distinct mucosal immune mechanisms (Figure 2). The mechanisms underlying PCV-mediated reduction in *S. pneumoniae* carriage are not yet completely understood, but these likely involve agglutination, in which capsular-specific antibodies agglutinate bacterial cells and prevent pneumococcal adherence to the nasospharyngeal epithelium[47]. These pneumococcal-specific antibodies contribute to a reduction in colonization by blocking acquisition in mice, although it was repetitively shown that antibodies are not essential for protection against pneumococcal colonization[48-50]. Alternatively, a memory Th17 response was responsible for protection against pneumococcal colonization in mice as shown with a whole cell vaccine (WCV), e.g. heat-inactivated *S. pneumoniae* vaccine adjuvanted with cholera toxin (CT)[49,51]. This memory Th17 response is accomplished by memory $CD4^+$ T cells that produce IL17A upon recognition of pneumococcal antigen leading to an influx of neutrophils, thereby clearing *S. pneumoniae* at the nasopharyngeal niche. Notably, a Th17 response against *S. pneumoniae* in the nasopharynx has not yet been described in humans, but pneumococcal specific $CD4^+Th17^+$ T cells have been detected in the mucosal tissue of the human respiratory tract[52]. However, for clearance of colonizing pneumococci during a first *S. pneumoniae* colonization event when pneumococcal specific memory responses are not yet established, not a neutrophil influx, but the recruitment of macrophages is essential[53].

The presence of a relationship between pneumococcal carriage and disease has been demonstrated by studies in both mice and men in which increased pneumococcal densities in the nasopharynx are associated with disease progression[38,54-56]. This relation is further supported by the observed parallel decrease in carriage and invasive pneumococcal disease by VTs following introduction of PCVs[8,33]. Importantly, during the carriage stage pneumococcal DNA derived from lysed cells is taken up by neighbouring pneumococci and integrated in their genome[57]. This horizontal gene transfer is the most important determinant for the emergence of new variants and selection of antibiotic resistance. Therefore, a vaccine that reduces or restricts pneumococcal carriage may be an attractive option to prevent disease progression, but also to reduce pneumococcal transmission. Such a vaccine may simultaneously decrease the risk of horizontal transfer and the occurrence of new variants and antibiotic-

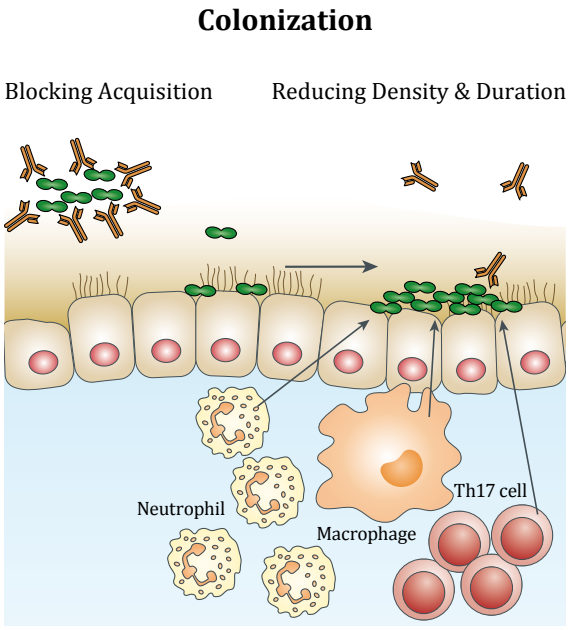

Figure 2 Distinct mucosal immune mechanisms reduce colonization of *S. pneumoniae*.

An overview of the different types of mucosal cellular and humoral responses that influence pneumococcal colonization. *S. pneumoniae* carriage starts by acquisition of the bacterium, which can be prevented via agglutination by pneumococcal specific antibodies. Once *S. pneumoniae* colonization is established, mucosal neutrophils, macrophages, and Th17 cells directly affect colonizing pneumococci, by reducing colonization density and/or decreasing colonization duration.

resistant strains. Although there is not yet a licensed vaccine available that targets bacterial carriage, the observed reduction in bacterial colonization in clinical trials is widely accepted as an endpoint and used as a correlate of protection to determine vaccine efficacy[8,58-60].

A mucosal vaccination approach to target pneumococcal carriage

Vaccination has been one of the most successful strategies to reduce morbidity and mortality caused by respiratory infections. Mucosal vaccination is particularly appealing as protection can be offered at the site of pathogen entry and provides strong mucosal as well as systemic immunity with long lasting memory[12,61]. There are different routes for mucosal vaccination, but the oral and intranasal applications are the most accessible and acceptable. Intranasal vaccination offers additional advantages compared to the parenterally applied PCV. It is easy to administer, needle-free and therefore administration does not require medical staff. It also mimics the natural route of infection potentially inducing the most effective immune response. It has been shown that pneumococcal infection of the nasopharyngeal mucosa protects against both colonization and disease in mice[62]. Additionally, different experimental vaccines strongly reduce pneumococcal colonization after intranasal immunization[49,63,64]. We therefore hypothesize that an intranasal vaccine targeting pneumococcal carriage will further reduce pneumococcal morbidity and mortality worldwide in both industrialized and developing countries. Currently, there is only one licensed intranasal vaccine, Flumist, which consists of live attenuated influenza and has shown to be protective against influenza in children[65,66].

An important challenge in the development of mucosal vaccines is the lack of suitable adjuvants that are strong enough to break immunological tolerance[12,61]. In experimental research, cholera toxin (CT) and non-toxic derivatives of subunit A (CTA) and B (CTB) are strong and widely used mucosal adjuvants, but not yet approved for human application. Alternatively, bacterial outer membrane vesicles (OMVs) represent an interesting novel strategy to deliver vaccine antigens and are considered natural adjuvants, because of their intrinsic stimulatory properties to activate the immune system and their particulate nature[67,68]. Recently, OMVs were engineered for recombinant expression of (pneumococcal) antigens, combining antigen delivery and natural adjuvanticity in a single particle (Figure 3)[63,69-71]. Importantly, OMVs are strong mucosal adjuvants, as it was recently shown that intranasally delivered *Escherichia coli* OMVs had comparable adjuvant activity as CT[72]. Compared to the currently used pneumococcal conjugate vaccines, OMVs are much simpler to produce at a lower cost, which allows for easier implementation in developing countries. Currently, there is a licensed parenterally administered OMV-based vaccine against

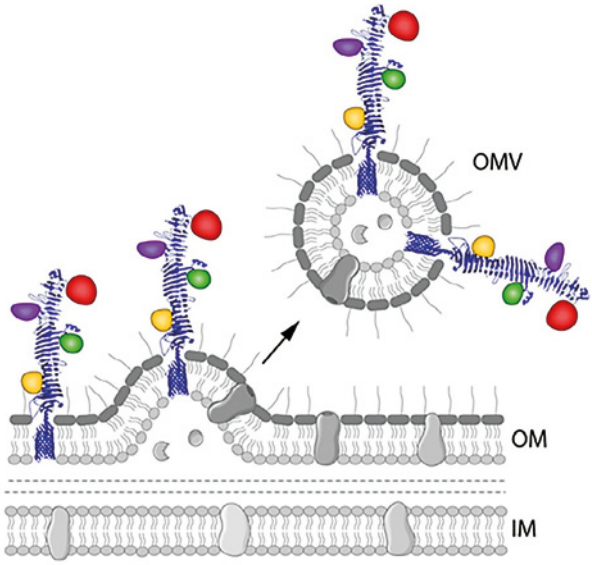

Figure 3 Salmonella OMVs surface displaying heterologous antigens.

Salmonella was engineered to express an *E. coli* autotransporter protein (Hbp) fused to multiple antigens or antigen fragments from *S. pneumoniae* at the membrane surface. OMVs are formed during growth through bulging and pinching off the outer membrane[63,69,70].

Neisseria meningitidis, Bexsero, that is proven to be safe and effective in humans[73,74].

The **aim of this thesis** is to study the impact of intranasal vaccination on pneumococcal colonization and to explore the mucosal immune responses that affect *S. pneumoniae* densities in the nasopharynx. In **Chapter 2** of this thesis we investigated the applicability of an OMV-based vaccine containing pneumococcal model antigens (PspA and pneumolysin) to protect against pneumococcal colonization. Conserved pneumococcal proteins are incorporated in vaccines to induce broader protection. **Chapter 3** therefore describes the role of highly conserved protein SP1298, renamed as PapP. This study set out to explain the reduction in virulence of *S. pneumoniae* deficient for SP1298, as previously observed in animal models of pneumococcal disease[75]. So far it is unclear whether a vaccine inducing Th17-mediated immunity that utilizes variable proteins can offer broad protection against pneumococcal colonization. In **Chapter 4** we explored the feasibility of using a variable pneumococcal protein, namely PspA, at the basis of broadly protective vaccine against *S. pneumoniae*

colonization. We selected the part that induced the strongest protection, i.e. the N-terminal α1α2 domain. The α1α2 sequences derived from clinical isolates were aligned and Th17 memory cross-reactivity of the vaccine with sequenced clinical isolates were assessed in *ex vivo* and *in vivo* studies. Certain adjuvants that are part of the vaccine formulation may induce 'non-specific' protection against respiratory infections independently of the co-administered antigens. In **Chapter 5**, we assessed the effect of mucosal adjuvant CTB on pneumococcal densities in the murine nasopharynx. We studied the role of CTB in pneumococcal clearance by using different knockout mouse strains deficient for caspase 1/11, T cells, and macrophages. Also we explored the associated mucosal immune mechanisms and focused on T helper cytokines and immune cells with a known role in pneumococcal clearance. Efficacy of vaccine-induced responses is primarily defined by the vaccine formulation, e.g. antigen and adjuvant used, but are also influenced by the host. In **Chapter 6** we studied the effect of mouse genetic backgrounds on vaccine-induced reduction in pneumococcal colonization. We studied pneumococcal clearance in C57BL/6, BALB/c, and CB6F1 mice following vaccination. Furthermore we explored the mucosal immune responses, e.g. by measuring T helper cytokines in nasal tissue, for an association with reduction in pneumococcal colonization. **Chapter 7** discusses the age-related susceptibility to pneumococcal infection in infants and elderly and offers insight into why infections occur at the age extremes of life. Susceptibility to infection is illustrated as prolonged colonization of *S. pneumoniae* in the nasopharynx. This is attributed to altered monocyte biology driven by high baseline inflammation in both age groups. Lastly, **Chapter 8** provides a discussion of the major findings in light of the current literature and future perspectives within the field of pneumococcal vaccination, carriage and disease.

REFERENCES

1 Organization, W. H. *Top 10 causes of death*, <http://www.who.int/mediacentre/factsheets/fs310/en/> (2015).
2 Organization, W. H. *Pneumonia*, <http://www.who.int/mediacentre/factsheets/fs331/en/> (2015).
3 O'Brien, K. L. *et al.* Burden of disease caused by *Streptococcus pneumoniae* in children younger than 5 years: global estimates. *Lancet* **374**, 893-902, doi:10.1016/s0140-6736(09)61204-6 (2009).
4 Brown, J., Hammerschmidt, S. & Orihuela, C. *Streptococcus pneumoniae molecular mechanisms of host-pathogen interactions*. (Elsevier, 2015).
5 Walker, C. L. *et al.* Global burden of childhood pneumonia and diarrhoea. *Lancet* **381**, 1405-1416, doi:10.1016/s0140-6736(13)60222-6 (2013).
6 Drijkoningen, J. J. & Rohde, G. G. Pneumococcal infection in adults: burden of disease. *Clin Microbiol Infect* **20 Suppl 5**, 45-51, doi:10.1111/1469-0691.12461 (2014).
7 Kadioglu, A., Weiser, J. N., Paton, J. C. & Andrew, P. W. The role of *Streptococcus pneumoniae* virulence factors in host respiratory colonization and disease. *Nat Rev Microbiol* **6**, 288-301, doi:10.1038/nrmicro1871 (2008).
8 Simell, B. *et al.* The fundamental link between pneumococcal carriage and disease. *Expert Rev Vaccines* **11**, 841-855, doi:10.1586/erv.12.53 (2012).
9 Osler, W. *The Principles and Practice of Medicine*. 7th edition edn, (Appleton, D. , 1909).
10 Organization, W. H. *Antimicrobial resistance*, <http://www.who.int/mediacentre/factsheets/fs194/en/> (2015).
11 Organization, W. H. *Children Reducing mortality*, <http://www.who.int/mediacentre/factsheets/fs178/en/> (2016).
12 Jambo, K. C., Sepako, E., Heyderman, R. S. & Gordon, S. B. Potential role for mucosally active vaccines against pneumococcal pneumonia. *Trends Microbiol* **18**, 81-89, doi:10.1016/j.tim.2009.12.001 (2010).
13 Macleod, C. M., Hodges, R. G., Heidelberger, M. & Bernhard, W. G. PREVENTION OF PNEUMOCOCCAL PNEUMONIA BY IMMUNIZATION WITH SPECIFIC CAPSULAR POLYSACCHARIDES. *J Exp Med* **82**, 445-465 (1945).
14 Malley, R. & Anderson, P. W. Serotype-independent pneumococcal experimental vaccines that induce cellular as well as humoral immunity. *Proc Natl Acad Sci U S A* **109**, 3623-3627, doi:10.1073/pnas.1121383109 (2012).
15 Jackson, L. A. *et al.* Effectiveness of pneumococcal polysaccharide vaccine in older adults. *N Engl J Med* **348**, 1747-1755, doi:10.1056/NEJMoa022678 (2003).
16 Mangtani, P., Cutts, F. & Hall, A. J. Efficacy of polysaccharide pneumococcal vaccine in adults in more developed countries: the state of the evidence. *Lancet Infect Dis* **3**, 71-78 (2003).
17 23-valent pneumococcal polysaccharide vaccine. WHO position paper. *Releve epidemiologique hebdomadaire / Section d'hygiene du Secretariat de la Societe des Nations = Weekly epidemiological record / Health Section of the Secretariat of the League of Nations* **83**, 373-384 (2008).
18 Bridges, C. B., Woods, L. & Coyne-Beasley, T. Advisory Committee on Immunization Practices (ACIP) recommended immunization schedule for adults aged 19 years and older--United States, 2013. *MMWR supplements* **62**, 9-19 (2013).
19 Douglas, R. M., Paton, J. C., Duncan, S. J. & Hansman, D. J. Antibody response to pneumococcal vaccination in children younger than five years of age. *J Infect Dis* **148**, 131-137 (1983).
20 Leinonen, M. *et al.* Antibody response to 14-valent pneumococcal capsular polysaccharide vaccine in pre-school age children. *Pediatr Infect Dis* **5**, 39-44 (1986).
21 Poland, G. A. The burden of pneumococcal disease: the role of conjugate vaccines. *Vaccine* **17**, 1674-1679 (1999).
22 Bogaert, D., Hermans, P. W., Adrian, P. V., Rumke, H. C. & de Groot, R. Pneumococcal vaccines: an update on current strategies. *Vaccine* **22**, 2209-2220, doi:10.1016/j.vaccine.2003.11.038 (2004).

23 Keller, L. E., Robinson, D. A. & McDaniel, L. S. Nonencapsulated *Streptococcus pneumoniae*: Emergence and Pathogenesis. *MBio* **7**, doi:10.1128/mBio.01792-15 (2016).

24 Feldman, C. & Anderson, R. Review: current and new generation pneumococcal vaccines. *J Infect* **69**, 309-325, doi:10.1016/j.jinf.2014.06.006 (2014).

25 van Werkhoven, C. H. & Bonten, M. J. The Community-Acquired Pneumonia immunization Trial in Adults (CAPiTA): what is the future of pneumococcal conjugate vaccination in elderly? *Future Microbiol* **10**, 1405-1413, doi:10.2217/fmb.15.80 (2015).

26 Hanage, W. P. *et al.* Evidence that pneumococcal serotype replacement in Massachusetts following conjugate vaccination is now complete. *Epidemics* **2**, 80-84, doi:10.1016/j.epidem.2010.03.005 (2010).

27 Weinberger, D. M., Malley, R. & Lipsitch, M. Serotype replacement in disease after pneumococcal vaccination. *Lancet* **378**, 1962-1973, doi:10.1016/s0140-6736(10)62225-8 (2011).

28 Hicks, L. A. *et al.* Incidence of pneumococcal disease due to non-pneumococcal conjugate vaccine (PCV7) serotypes in the United States during the era of widespread PCV7 vaccination, 1998-2004. *J Infect Dis* **196**, 1346-1354, doi:10.1086/521626 (2007).

29 Lexau, C. A. *et al.* Changing epidemiology of invasive pneumococcal disease among older adults in the era of pediatric pneumococcal conjugate vaccine. *Jama* **294**, 2043-2051, doi:10.1001/jama.294.16.2043 (2005).

30 Miller, E., Andrews, N. J., Waight, P. A., Slack, M. P. & George, R. C. Herd immunity and serotype replacement 4 years after seven-valent pneumococcal conjugate vaccination in England and Wales: an observational cohort study. *Lancet Infect Dis* **11**, 760-768, doi:10.1016/s1473-3099(11)70090-1 (2011).

31 Nzenze, S. A. *et al.* Temporal association of infant immunisation with pneumococcal conjugate vaccine on the ecology of *Streptococcus pneumoniae*, Haemophilus influenzae and Staphylococcus aureus nasopharyngeal colonisation in a rural South African community. *Vaccine* **32**, 5520-5530, doi:10.1016/j.vaccine.2014.06.091 (2014).

32 Di John, D. *et al.* Effect of priming with carrier on response to conjugate vaccine. *Lancet* **2**, 1415-1418 (1989).

33 Jefferies, J. M., Clarke, S. C., Webb, J. S. & Kraaijeveld, A. R. Risk of red queen dynamics in pneumococcal vaccine strategy. *Trends Microbiol* **19**, 377-381, doi:10.1016/j.tim.2011.06.001 (2011).

34 Miyaji, E. N., Oliveira, M. L., Carvalho, E. & Ho, P. L. Serotype-independent pneumococcal vaccines. *Cell Mol Life Sci* **70**, 3303-3326, doi:10.1007/s00018-012-1234-8 (2013).

35 Bogaert, D., De Groot, R. & Hermans, P. W. *Streptococcus pneumoniae* colonisation: the key to pneumococcal disease. *Lancet Infect Dis* **4**, 144-154, doi:10.1016/s1473-3099(04)00938-7 (2004).

36 Gray, B. M., Converse, G. M., 3rd & Dillon, H. C., Jr. Epidemiologic studies of *Streptococcus pneumoniae* in infants: acquisition, carriage, and infection during the first 24 months of life. *J Infect Dis* **142**, 923-933 (1980).

37 Sleeman, K. L. *et al.* Capsular serotype-specific attack rates and duration of carriage of *Streptococcus pneumoniae* in a population of children. *J Infect Dis* **194**, 682-688, doi:10.1086/505710 (2006).

38 Short, K. R., Reading, P. C., Wang, N., Diavatopoulos, D. A. & Wijburg, O. L. Increased nasopharyngeal bacterial titers and local inflammation facilitate transmission of *Streptococcus pneumoniae*. *MBio* **3**, doi:10.1128/mBio.00255-12 (2012).

39 Siegel, S. J. & Weiser, J. N. Mechanisms of Bacterial Colonization of the Respiratory Tract. *Annu Rev Microbiol* **69**, 425-444, doi:10.1146/annurev-micro-091014-104209 (2015).

40 Lysenko, E. S., Ratner, A. J., Nelson, A. L. & Weiser, J. N. The role of innate immune responses in the outcome of interspecies competition for colonization of mucosal surfaces. *PLoS Pathog* **1**, e1, doi:10.1371/journal.ppat.0010001 (2005).

41 Lipsitch, M. *et al.* Estimating rates of carriage acquisition and clearance and competitive ability for pneumococcal serotypes in Kenya with a Markov transition model. *Epidemiology* **23**, 510-519, doi:10.1097/EDE.0b013e31824f2f32 (2012).

42 Hogberg, L. *et al.* Age- and serogroup-related differences in observed durations of nasopharyngeal carriage of penicillin-resistant pneumococci. *J Clin Microbiol* **45**, 948-952, doi:10.1128/jcm.01913-06 (2007).

43 Montgomery, J. M. *et al.* Bacterial colonization of the upper respiratory tract and its association with acute lower respiratory tract infections in Highland children of Papua New Guinea. *Rev Infect Dis* **12 Suppl 8**, S1006-1016 (1990).

44 AlonsoDeVelasco, E., Verheul, A. F., Verhoef, J. & Snippe, H. *Streptococcus pneumoniae*: virulence factors, pathogenesis, and vaccines. *Microbiol Rev* **59**, 591-603 (1995).

45 Kim, J. O. *et al.* Relationship between cell surface carbohydrates and intrastrain variation on opsonophagocytosis of *Streptococcus pneumoniae*. *Infect Immun* **67**, 2327-2333 (1999).

46 Collins, A. M. *et al.* First human challenge testing of a pneumococcal vaccine. Double-blind randomized controlled trial. *Am J Respir Crit Care Med* **192**, 853-858, doi:10.1164/rccm.201503-0542OC (2015).

47 Roche, A. M., Richard, A. L., Rahkola, J. T., Janoff, E. N. & Weiser, J. N. Antibody blocks acquisition of bacterial colonization through agglutination. *Mucosal Immunol* **8**, 176-185, doi:10.1038/mi.2014.55 (2015).

48 Basset, A. *et al.* Antibody-independent, CD4+ T-cell-dependent protection against pneumococcal colonization elicited by intranasal immunization with purified pneumococcal proteins. *Infect Immun* **75**, 5460-5464, doi:10.1128/iai.00773-07 (2007).

49 Malley, R. *et al.* CD4+ T cells mediate antibody-independent acquired immunity to pneumococcal colonization. *Proc Natl Acad Sci U S A* **102**, 4848-4853, doi:10.1073/pnas.0501254102 (2005).

50 McCool, T. L. & Weiser, J. N. Limited role of antibody in clearance of *Streptococcus pneumoniae* in a murine model of colonization. *Infect Immun* **72**, 5807-5813, doi:10.1128/iai.72.10.5807-5813.2004 (2004).

51 Lu, Y. J. *et al.* Interleukin-17A mediates acquired immunity to pneumococcal colonization. *PLoS Pathog* **4**, e1000159, doi:10.1371/journal.ppat.1000159 (2008).

52 Pido-Lopez, J., Kwok, W. W., Mitchell, T. J., Heyderman, R. S. & Williams, N. A. Acquisition of pneumococci specific effector and regulatory Cd4+ T cells localising within human upper respiratory-tract mucosal lymphoid tissue. *PLoS Pathog* **7**, e1002396, doi:10.1371/journal.ppat.1002396 (2011).

53 Zhang, Z., Clarke, T. B. & Weiser, J. N. Cellular effectors mediating Th17-dependent clearance of pneumococcal colonization in mice. *J Clin Invest* **119**, 1899-1909, doi:10.1172/jci36731 (2009).

54 Diavatopoulos, D. A. *et al.* Influenza A virus facilitates *Streptococcus pneumoniae* transmission and disease. *FASEB J* **24**, 1789-1798, doi:10.1096/fj.09-146779 (2010).

55 Mina, M. J., Klugman, K. P. & McCullers, J. A. Live attenuated influenza vaccine, but not pneumococcal conjugate vaccine, protects against increased density and duration of pneumococcal carriage after influenza infection in pneumococcal colonized mice. *J Infect Dis* **208**, 1281-1285, doi:10.1093/infdis/jit317 (2013).

56 Vu, H. T. *et al.* Association between nasopharyngeal load of *Streptococcus pneumoniae*, viral coinfection, and radiologically confirmed pneumonia in Vietnamese children. *Pediatr Infect Dis J* **30**, 11-18, doi:10.1097/INF.0b013e3181f111a2 (2011).

57 Marks, L. R., Reddinger, R. M. & Hakansson, A. P. High levels of genetic recombination during nasopharyngeal carriage and biofilm formation in *Streptococcus pneumoniae*. *MBio* **3**, doi:10.1128/mBio.00200-12 (2012).

58 Auranen, K. *et al.* Design questions for *Streptococcus pneumoniae* vaccine trials with a colonisation endpoint. *Vaccine* **32**, 159-164, doi:10.1016/j.vaccine.2013.06.105 (2013).

59 Auranen, K. *et al.* Colonisation endpoints in *Streptococcus pneumoniae* vaccine trials. *Vaccine* **32**, 153-158, doi:10.1016/j.vaccine.2013.08.061 (2013).

60 Goldblatt, D., Ramakrishnan, M. & O'Brien, K. Using the impact of pneumococcal vaccines on nasopharyngeal carriage to aid licensing and vaccine implementation; a PneumoCarr meeting report March 27-28, 2012, Geneva. *Vaccine* **32**, 146-152, doi:10.1016/j.vaccine.2013.06.040 (2013).

61 Lycke, N. Recent progress in mucosal vaccine development: potential and limitations. *Nat Rev Immunol* **12**, 592-605, doi:10.1038/nri3251 (2012).
62 Malley, R. *et al.* Intranasal immunization with killed unencapsulated whole cells prevents colonization and invasive disease by capsulated pneumococci. *Infect Immun* **69**, 4870-4873, doi:10.1128/iai.69.8.4870-4873.2001 (2001).
63 Kuipers, K. *et al.* Salmonella outer membrane vesicles displaying high densities of pneumococcal antigen at the surface offer protection against colonization. *Vaccine* **33**, 2022-2029, doi:10.1016/j.vaccine.2015.03.010 (2015).
64 Kuipers, K. v. S., S.; van Opzeeland, F., Langereis, J.D., Verhagen, L. M.; Diavatopoulos, D. A.; de Jonge, M. I. *The influence of genetic diversity on vaccine-induced reduction of pneumococcal colonization* (2016).
65 Belshe, R. B. *et al.* Live attenuated versus inactivated influenza vaccine in infants and young children. *N Engl J Med* **356**, 685-696, doi:10.1056/NEJMoa065368 (2007).
66 Carter, N. J. & Curran, M. P. Live attenuated influenza vaccine (FluMist(R); Fluenz): a review of its use in the prevention of seasonal influenza in children and adults. *Drugs* **71**, 1591-1622, doi:10.2165/11206860-000000000-00000 (2011).
67 Bergman, M. A. *et al.* CD4+ T cells and toll-like receptors recognize Salmonella antigens expressed in bacterial surface organelles. *Infect Immun* **73**, 1350-1356, doi:10.1128/iai.73.3.1350-1356.2005 (2005).
68 Ellis, T. N. & Kuehn, M. J. Virulence and immunomodulatory roles of bacterial outer membrane vesicles. *Microbiol Mol Biol Rev* **74**, 81-94, doi:10.1128/mmbr.00031-09 (2010).
69 Daleke-Schermerhorn, M. H. *et al.* Decoration of outer membrane vesicles with multiple antigens by using an autotransporter approach. *Appl Environ Microbiol* **80**, 5854-5865, doi:10.1128/aem.01941-14 (2014).
70 Jong, W. S. *et al.* An autotransporter display platform for the development of multivalent recombinant bacterial vector vaccines. *Microb Cell Fact* **13**, 162, doi:10.1186/s12934-014-0162-8 (2014).
71 Underhill, D. M. & Goodridge, H. S. Information processing during phagocytosis. *Nat Rev Immunol* **12**, 492-502, doi:10.1038/nri3244 (2012).
72 Pritsch, M. *et al.* Comparison of Intranasal Outer Membrane Vesicles with Cholera Toxin and Injected MF59C.1 as Adjuvants for Malaria Transmission Blocking Antigens AnAPN1 and Pfs48/45. *Journal of immunology research* **2016**, 3576028, doi:10.1155/2016/3576028 (2016).
73 Holst, J. *et al.* Properties and clinical performance of vaccines containing outer membrane vesicles from Neisseria meningitidis. *Vaccine* **27 Suppl 2**, B3-12, doi:10.1016/j.vaccine.2009.04.071 (2009).
74 Holst, J. *et al.* Vaccines against meningococcal serogroup B disease containing outer membrane vesicles (OMV): lessons from past programs and implications for the future. *Hum Vaccin Immunother* **9**, 1241-1253, doi:10.4161/hv.24129 (2013).
75 Cron, L. E. *et al.* Two DHH subfamily 1 proteins contribute to pneumococcal virulence and confer protection against pneumococcal disease. *Infect Immun* **79**, 3697-3710, doi:10.1128/iai.01383-10 (2011).

2

Salmonella outer membrane vesicles displaying high densities of pneumococcal antigen at the surface offer protection against colonization

Kirsten Kuipers*, Maria H. Daleke-Schermerhorn*, Wouter S.P. Jong, Corinne M. ten Hagen-Jongman, Fred van Opzeeland, Elles Simonetti, Joen Luirink, Marien I. de Jonge

*Equal contribution

Vaccine. 2015 Apr 21;33(17):2022-9. doi: 10.1016/j.vaccine.2015.03.010.

ABSTRACT

Bacterial outer membrane vesicles (OMVs) are attractive vaccine formulations because they have intrinsic immunostimulatory properties. In principle, heterologous antigens incorporated into OMVs will elicit specific immune responses, especially if presented at the vesicle surface and thus optimally exposed to the immune system. In this study, we explored the feasibility of our recently developed autotransporter Hbp platform, designed to efficiently and simultaneously display multiple antigens at the surface of bacterial OMVs, for vaccine development. Using two *Streptococcus pneumoniae* proteins as model antigens, we showed that intranasally administered *Salmonella* OMVs displaying high levels of antigens at the surface induced strong protection in a murine model of pneumococcal colonization, without the need for a mucosal adjuvant. Importantly, reduction in bacterial recovery from the nasal cavity was correlated with local production of antigen-specific IL-17A. Furthermore, the protective efficacy and the production of antigen-specific IL-17A, and local and systemic IgGs, were all improved at increased concentrations of the displayed antigen. This discovery highlights the importance of an adequate antigen expression system for development of recombinant OMV vaccines. In conclusion, our findings demonstrate the suitability of the Hbp platform for development of a new generation of OMV vaccines, and illustrate the potential of using this approach to develop a broadly protective mucosal pneumococcal vaccine.

INTRODUCTION

Outer membrane vesicles (OMVs), ubiquitously released from the outer membrane (OM) of Gram-negative bacteria, are promising as vaccines because they combine antigen and adjuvant in a single formulation. The intrinsic adjuvant activity provided by the presence of various pathogen recognition receptor ligands, such as lipopolysaccharide and immunogenic surface proteins, forms an attractive combination with the non-living, particulate nature of the OMVs[1-3]. OMVs have protected animals against various pathogens[4,5], and a licensed OMV vaccine against *Neisseria meningitidis* has been proven safe and protective in humans[6]. The interest in OMVs expanded as heterologous proteins were successfully incorporated into vesicles[7-11], and engineered OMVs were shown to elicit antigen-specific immune responses[9-11] and protection in mice[9].

Accumulating evidence indicates that both the magnitude and the breadth of the immune response can be improved by secreting or displaying antigens at the surface of bacterial and viral vaccine vectors[12-17]. Instigated by these observations, we recently engineered the *Escherichia coli* autotransporter (AT) Hemoglobin protease (Hbp) into a platform for efficient display of heterologous polypeptides at the surface of live bacteria[18,19], bacterial ghosts[20] and OMVs[21]. The AT pathway is the most widespread system for transport of proteins across the Gram-negative cell envelope, employing a relatively simple two-step mechanism. The AT is first transported across the inner membrane by the Sec machinery, after which its C-terminal domain inserts into the OM and forms a β-barrel that together with a central linker domain mediates transport of the functional N-terminal passenger domain to the cell surface or medium[22]. Based on the available crystal structure of the Hbp passenger[23], a side-domain replacement strategy was developed that allows fusion of multiple heterologous sequences to a single, stable Hbp scaffold[18]. Using various mycobacterial, chlamydial and influenza antigens, the Hbp platform was demonstrated to be a versatile tool for the simultaneous display of multiple sizeable antigens at the surface of live bacteria[19] and OMVs[21].

Here, we set out to test the applicability of the Hbp platform for development of recombinant OMV vaccines, using as model antigens the well-known protective proteins pneumococcal surface protein A (PspA) and pneumolysin (Ply) of the nasopharyngeal colonizer *Streptococcus pneumoniae*[24-26]. Current pneumococcal conjugate vaccines (PCVs), consisting of capsular polysaccharides, have strongly reduced the incidence of severe disease caused by vaccine-specific *S. pneumoniae* serotypes[27]. However, the efficacy of PCVs is reduced by serotype replacement[28-30] and capsular switching events[31], and their accessibility in developing countries is restricted by complex, costly manufacturing and the requirement for

needle-based administration. These limitations can potentially be overcome by development of a novel vaccine based on conserved, non-capsular, proteinaceous antigens that is suitable for intranasal administration. We describe here the first *in vivo* challenge study designed to test a vaccine formulation consisting of OMVs that display heterologous proteins at the surface. We investigated whether intranasal immunization with *Salmonella enterica* serovar Typhimurium OMVs efficiently displaying sizeable fragments of PspA and Ply at the surface could protect mice against pneumococcal colonization. By assessing immune responses and bacterial load following intranasal *S. pneumoniae* challenge in mice immunized with various vaccine formulations and regimes, we demonstrate the potential of the Hbp platform for recombinant OMV vaccine development and we identified parameters that are critical for obtaining protective efficacy.

MATERIALS AND METHODS

Bacterial strains and growth conditions

S. Typhimurium SL3261 Δ*tolRA*[21], and *E. coli* TOP10F' and BL21(DE3) were grown at 37°C in LB medium containing 0.2% glucose. When appropriate, kanamycin was used at a concentration of 25 μg/ml and chloramphenicol at 30 μg/ml. *S. pneumoniae* TIGR4[32] was grown and vaccination stocks containing 10^6 colony forming units (CFU)/10 μL in phosphate buffered saline (PBS) were prepared as described[33].

Plasmid construction

Construction of pEH3-based[34] plasmids for expression of Hbp fused to pneumococcal antigen fragments and pET16b(+) vectors (Novagen) for expression of PspA and the PdT derivative of Ply[35] is described in the Supplementary Materials and Methods.

Hbp expression, OMV isolation and protein analysis

S. Typhimurium SL3261 Δ*tolRA* harboring pEH3 vectors was grown until an OD_{660} of ~0.6, at which expression of Hbp derivatives was induced from the *lacUV5* promoter in the presence of 1 or 100 μM IPTG for 1 hour.

To isolate OMVs, culture supernatants obtained by low-speed centrifugation were passed through 0.45-μm-pore-size filters (Millipore) and centrifuged at 208'000×*g* for 60 min, separating OMVs from soluble proteins. Pelleted OMVs were washed by resuspension in PBS containing 500 mM NaCl (1 OD unit of OMVs per μl) and centrifugation at 440'000×*g* for 2 h, after which they were taken up in PBS containing 15% glycerol (1 OD unit of OMVs per μl). An amount of 1 OD unit of OMVs is derived from 1 OD_{660} unit of cells.

Proteinase K accessibility of OMV proteins was analysed as described[21], and proteins were analysed by SDS-PAGE and Coomassie G-250 (BioRad) staining or immunoblotting using antisera recognizing the β-domain of Hbp (SN477)[36], PspA or pneumolysoid, the detoxified derivative of Ply (own lab collection). Densitometric analysis on Coomassie-stained gels was carried out using a Molecular Imager GS-800 Calibrated Densitometer (Biorad) and Quantity One software (Biorad).

Mouse immunizations and challenge

Seven week-old female C57BL/6 mice (Charles River Laboratories) were intranasally (i.n.) immunized three, two or one time(s) with 8 OD units of OMVs (corresponding to ~4 μg total protein) in a volume of 10 μL, at two-week intervals, under anaesthetics (2.5% v/v isoflurane, AU Veterinary Services). Three weeks after the final immunization mice were challenged i.n. with 10^6 CFU of *S. pneumoniae* TIGR4 [33]. Three days after infection, mice were euthanized, and blood and mucosal nasal tissue were harvested. Nasal tissue was homogenized using an IKA T10 basic blender, and serially diluted samples were plated on Gentamicin Blood Agar (Mediaproducts BV) to determine bacterial recovery (log CFU/organ). All animal work was performed with approval of the Radboud University Medical Center Committee for Animal Ethics. Consequently, three mice were euthanized and excluded from further experimental analysis after reaching a humane endpoint, i.e. over 20% weight loss, potentially caused by a reaction to lipopolysaccharide present in the OMVs.

Detection of antibody responses by enzyme-linked immunosorbent assay analysis

Antigen and OMV-specific IgG in nasal samples and sera were detected as described in the Supplementary Materials and Methods.

Measurement of local IFNγ and IL-17A

Cytokine production in mouse nasal samples were determined with Cytometric Bead Array (Becton Dickinson) according to manufacturer's instructions, using the Mouse Enhanced Sensitivity buffer kit in combination with the Enhanced Sensitivity Flex set for IFNγ and IL-17A (Becton Dickinson). Concentrations were calculated using Soft Flow FCAP Array v1.0 (Becton Dickinson).

Statistical analyses

All statistical analyses were performed using GraphPad Prism version 5.0 (Graphpad Software). For bacterial recovery data, the Grubbs outlier test was used to test for significant outliers. The One-Way Anova Kruskall Wallis with

Bonferroni post-test for multiple groups or Mann-Whitney t test for two groups were used for comparisons of protection and immune responses. To determine the relation between IL-17A and protection, a Spearman Correlation test was applied.

RESULTS

Selection and fusion of PspA and pneumolysin fragments to Hbp

To facilitate efficient expression of the model antigens PspA and Ply via the Hbp display system, these two complex, multi-domain proteins were split into shorter fragments (Figure 1A). To avoid potential destruction of immune epitopes, fragments were designed to partially overlap with adjacent sequences. PspA was divided into four fragments that cover the N-terminal, surface-exposed part of the protein (Figure 1A). Of these, two fragments derived from the N-terminal portion of α-helical coiled coil domain ('α1' and 'α2') were fused to a single Hbp carrier, yielding HbpD-PspA[α1-α2] (Figure 1B). A second construct, HbpD-PspA[LFBD-PRR] (Figure 1B), was created by combining Hbp with two fragments corresponding to the lactoferrin-binding domain ('LFBD') and the conserved Pro-rich region ('PRR') of PspA, respectively. Similarly, pneumolysin was divided into three fragments (Figure 1A), of which an N-terminal ('F1') and a C-terminal fragment ('F3') were fused to a single Hbp carrier to create HbpD-Ply[F1-F3] (Figure 1B). Unfortunately, the central pneumolysin fragment ('F2'; Figure 1A), that includes the membrane-penetrating D3 domain[19], caused lysis upon expression in the context of Hbp and was therefore excluded from further studies.

Efficient display of PspA and pneumolysin fragments at the surface of *Salmonella* OMVs

The three Hbp chimeras were expressed under control of a *lacUV5* promoter in a previously described Δ*tolRA* derivative of the attenuated *Salmonella* Typhimurium strain SL3261 that produces large amounts of OMVs[21]. A display derivative of Hbp lacking domain d1, HbpD (Figure 1B)[18], was produced in the same strain and the resulting vesicles served as a negative control in subsequent studies. OMVs were isolated from cell-free culture supernatants by ultracentrifugation, after which they were washed with PBS containing a high concentration of NaCl to remove peripherally attached soluble contaminants. The absence of live bacteria was verified by plating, and OMVs were confirmed to contain the Hbp-antigen chimera by SDS-PAGE (Figure 2A) and immunoblotting (Figure 2B). Importantly, and similar to the HbpD control, all three chimeras were exposed at the OMV surface as judged by their sensitivity to externally added Proteinase K

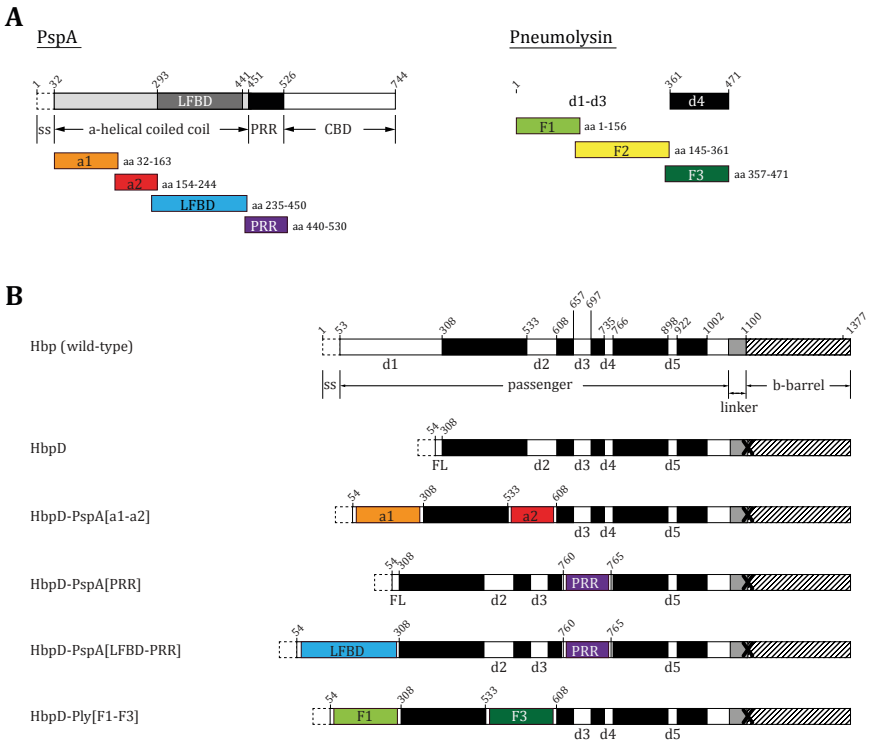

Figure 1 Vaccine design.

(**A**) Schematic representations of PspA and pneumolysin. The slightly overlapping fragments that were selected for fusion to HbpD cover the α-helical coiled coil domain (α1 and α2), the lactoferrin-binding domain (*LFBD*) and the Pro-rich region (*PRR*) but not the cell wall-anchoring choline-binding domain (*CBD*) of PspA, and the entire Ply sequence. Numbers above the diagrams and boundaries next to the fragments correspond to aa positions calculated from the N termini of full-length PspA and Ply. (**B**) Wild-type Hbp (included for reference) comprises an N-terminal cleavable signal sequence (*ss*), a secreted passenger domain, and a linker (grey) and a C-terminal domain that inserts into the OM as a β-barrel, which together facilitate translocation of the passenger. Side domains *d1-d5*, which are dispensable for secretion and can be replaced by heterologous polypeptides, are indicated, while the remainder of the passenger domain is black. Point mutations D1100G and D1101G (denoted ***X***) prevent autocatalytic cleavage after translocation across the OM, creating a surface-exposed (display; D) version of Hbp[48]. Numbers above the diagrams correspond to the aa positions of the wt Hbp precursor, calculated from the N terminus. Insertion of the pneumococcal PspA fragments, defined in *A*, are highlighted. Each insert is flanked by short flexible Gly/Ser linkers (*FL*).

(Figures 2B and C). In contrast, degradation of the protease-sensitive C-terminal periplasmic domain of OmpA occurred only after permeabilization of the OMVs with Triton X-100, confirming the integrity and membrane orientation of the

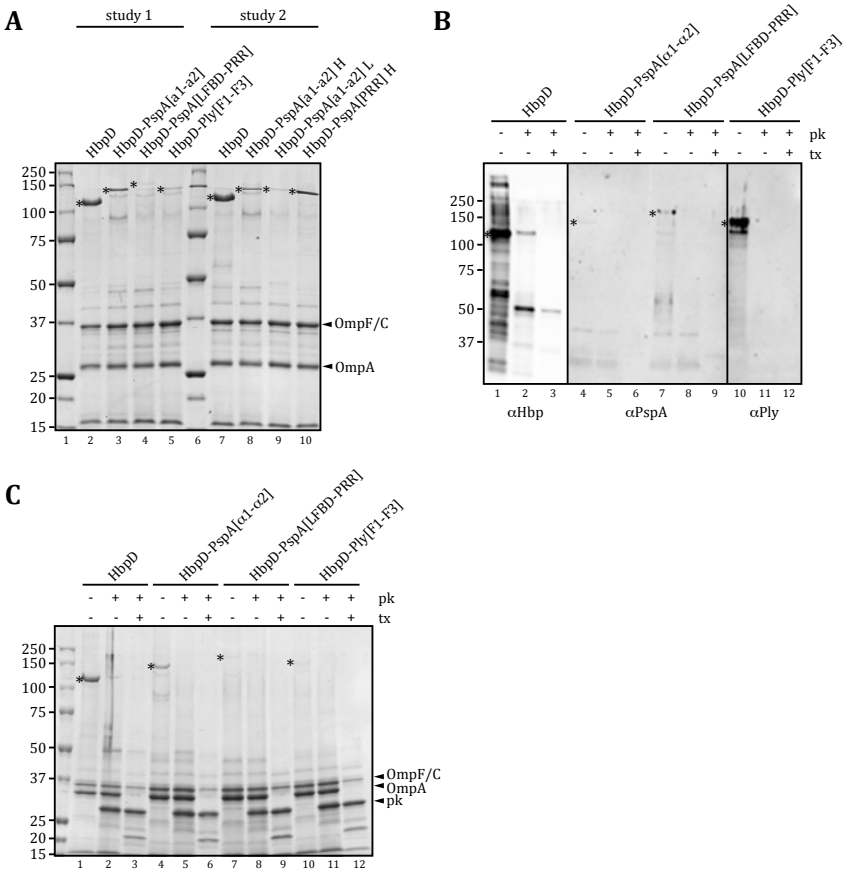

Figure 2 Vaccine production.

(**A**) SDS-PAGE/Coomassie analysis of the vaccine stocks used in the two studies. Equivalent volumes of vaccine stock containing equivalent amounts of OMVs, based on OD units of the original cultures, were isolated from *S.* Typhimurium SL3261 Δ*tolRA* expressing HbpD or the indicated HbpD-antigen chimera were loaded. All constructs were expressed in the presence of 100 µM IPTG (unlabeled or H; high), except for HbpD-PspA[α1-α2] L (low), which was expressed in the presence of 1 µM IPTG. Below the panel, relative amounts of Hbp chimera's and OmpA in OMV samples are displayed as determined by densitometric analysis. Highest measured densities were put at 100%. *B-C*, Equal amounts of intact (- tx) and Triton X-100-permeabilized (+ tx) OMVs described in *A* were incubated with Proteinase K (+ pk) or mock treated (- pk), separated by SDS-PAGE and detected with (**B**) immunoblotting using indicated antibodies, and (**C**) Coomassie staining. An amount of 0.5 OD units of OMV material was loaded in each lane. The Hbp (chimeras) are marked by *asterisks*, and the OMV marker proteins OmpF/C and OmpA, and Proteinase K are indicated with *arrowheads*.

vesicles (Figure 2C). Differences in expression levels of the various HbpD-antigen fusion proteins are likely determined by the difference in complexity of the inserted fragments. Nevertheless, all Hbp-antigen fusions were visible after Coomassie staining indicating that the expression levels are substantial.

Salmonella OMVs displaying PspA fragments protect against pneumococcal colonization

To investigate whether *Salmonella* OMVs displaying PspA and Ply fragments at the surface can confer protection against pneumococcal colonization, we made use of a previously established mouse model[37]. Mice were intranasally immunized three times with two-week intervals, and three weeks after the final immunization, they were intranasally inoculated with the *S. pneumoniae* serotype 4 TIGR4 strain. Recovery of live pneumococci from nasal tissue three days post-infection revealed that mice immunized with OMVs displaying HbpD-PspA[α1-α2] were significantly protected compared to mice that received OMVs displaying HbpD (Figure 3A). Remarkably, over 50% of the mice that received OMVs/HbpD-PspA [α1-α2] completely cleared the pneumococci within three days post-infection. In contrast, mice immunized with OMVs displaying either HbpD-PspA[LFBD-PRR] or HbpD-Ply[F1-F3] showed little, and in the case of HbpD-PspA[LFBD-PRR] rather variable protection, which did not significantly differ from the negative control. To investigate whether the reduced protection may be due to insufficient expression levels of HbpD-PspA[LFBD-PRR] and HbpD-Ply[F1-F3] (Figure 2A), immunization was repeated with OMVs displaying one of the antigen fragments, i.e. PspA[PRR] (Figure 2A, lane 10), at even ~3-fold higher levels than PspA[α1-α2] (Figure 2A, lane 8). However, no reduction in bacterial load was observed (Figure S1), suggesting that protection depends on intrinsic features of the displayed fragments. As an α-helical, potentially coiled coil-forming fragment of the surface-exposed *S. pneumoniae* polyhistidine triad protein D was previously shown to be highly immunogenic and more protective than the full-length protein in a murine sepsis model[38], these properties might be related to the α-helical coiled coil structure of the PspA[α1-α2] fragment[25,39]. Together these data show that the OMV/Hbp platform is suitable for intranasal antigen delivery. Furthermore, the N-terminal half of the α-helical coiled coil domain of PspA is able to induce protection against pneumococcal colonization.

Immunogenicity of *Salmonella* OMVs displaying pneumococcal antigens

Immunity to *S. pneumoniae* infection has been reported to depend on IFNγ and/or IL-17A-mediated recruitment of various effector cells including neutrophils and macrophages that can phagocytose and kill pneumococci[40-42]. To shed light

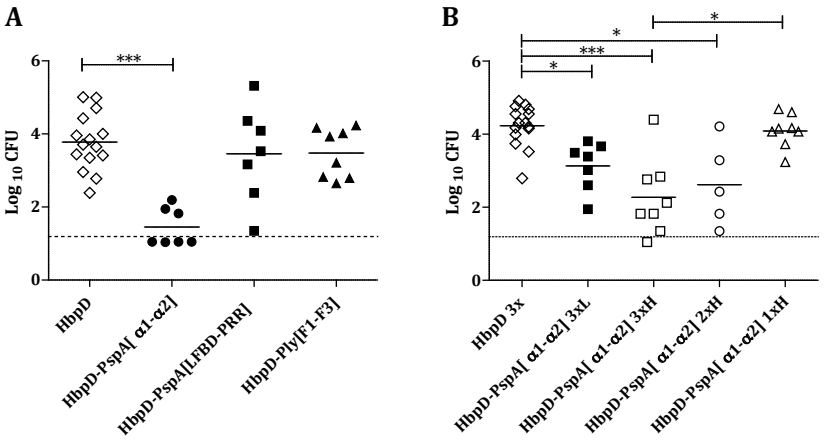

Figure 3 OMV/Hbp platform-induced protection is influenced by choice of antigen fragment, antigen amount, and immunization number.

Bacterial recovery of *S. pneumoniae* from nasal tissue three days post intranasal challenge of C57BL/6 mice that received (**A**) three intranasal immunizations with OMVs displaying HbpD, HbpD-PspA[α1-α2], HbpD-PspA[LFBD-PRR] or HbpD-Ply[F1-F3], or (**B**) three, two or one intranasal immunization(s) (3x; 2x; 1x) with OMVs expressing HbpD or high (H) or 7-fold lower (L) levels of HbpD-PspA[α1-α2]. Symbols indicate individual mice (n = 5-15 per group), bars represent group mean and the dotted line indicates the lower limit of detection. *, $p < 0.05$; **, $p < 0.01$; *** $p < 0.001$.

on the underlying mechanism behind the observed protection, we quantified the levels of IFNγ and IL-17A in nasal tissue of mice immunized with OMVs displaying HbpD-PspA[α1-α2] or the control protein HbpD. Of note, because the vaccinated mice were subjected to subsequent pneumococcal infection, the cytokine levels measured at three days post-challenge reflect recall responses of immunization-induced memory towards the pneumococcal antigen fragments. Interestingly, while both groups produced similar levels of IFNγ (Figure 4A), mice immunized with OMVs/HbpD-PspA[α1-α2] produced significantly higher levels of IL-17A levels compared to control mice (Figure 4B). This strongly suggests that local production of IL-17A, but not IFNγ, is important for protection against pneumococcal colonization.

Because IgGs are important for bacterial opsonization and initiation of robust immune responses, we determined the levels of PspA- and Ply-specific IgGs and IgAs in nasal tissue homogenates and sera of immunized mice (Figures 5A, S2A and S3A). Interestingly, significant yet variable local and systemic antigen-specific IgG production was detected upon immunization with OMVs/HbpD-PspA[α1-α2]. In contrast, with the exception of apparently lower local

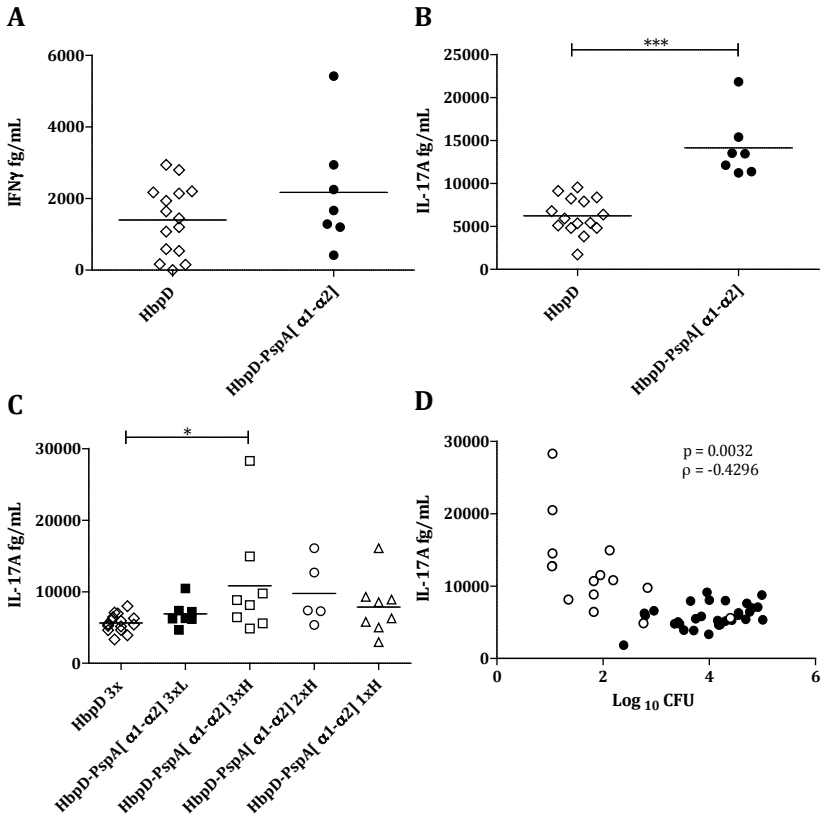

Figure 4 Protective immunity correlates with intranasal IL-17A levels.

Nasopharyngeal (**A**) IFNγ and (**B**) IL-17A three days post-infection in mice immunized three times with OMVs expressing HbpD or HbpD-PspA[α1-α2]. (**C**) Nasopharyngeal IL-17A three days post-infection in mice immunized three, two or one times (3x; 2x; 1x) with OMVs expressing HbpD or high (H) or 7-fold lower (L) levels of HbpD-PspA[α1-α2]. *A-C*, *, $p < 0.05$; **, $p < 0.01$; *** $p < 0.001$. *D*, Pooled data from study 1 and 2 for nasopharyngeal IL-17A and number of CFU three days post-infection of mice. Symbols represent individual mice (n = 5-15 per group) immunized three times with OMV-HbpD (filled symbols) or with OMV-HbpD-PspA[α1-α2] (open symbols), and bars represent group mean. Spearman's correlation coefficient (ρ) and p-value are indicated.

IgGs induced by OMVs/HbpD-Ply[F1-F3], no antibody responses were detected in the other groups. Moreover, there were no differences observed for local IgA production between the treatment groups. Together these results show that the OMV/Hbp platform induces local antigen-specific IL-17A responses. Additionally, the platform can induce local and systemic humoral responses.

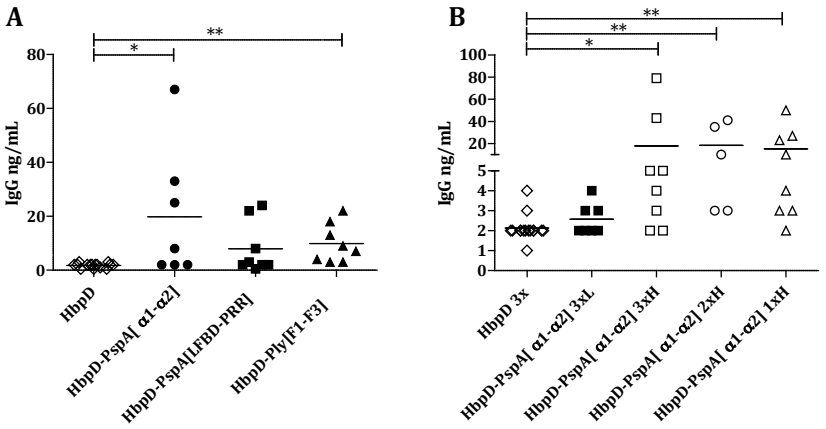

Figure 5 Intranasal antigen-specific IgG is influenced by antigen amount.

Nasal antigen-specific IgG responses directed against the whole protein, i.e. PspA and pneumolysin, in mice immunized (**A**) three times with OMVs displaying the indicated HbpD (chimera), or (**B**) three, two or one times (3x; 2x; 1x) with OMVs displaying HbpD, or HbpD-PspA[α1-α2] with varying antigen amount (H; high or L; 7-fold lower). Symbols represent individual mice, and bars represent mean of groups of 5-15 mice. *, $p < 0.05$; **, $p < 0.01$; *** $p < 0.001$.

Level of protection is influenced by the vaccine-associated antigen load and the number of immunizations

Although intrinsic properties of the α1/α2 fragments of PspA are apparently crucial for protection, the strikingly high expression levels of HbpD-PspA[α1-α2] (Figure 2A) prompted us to investigate whether antigen levels represent an important determinant for immune responses and protection. To this end, mice were immunized with two new batches of OMVs displaying HbpD-PspA[α1-α2] at high levels similar to the first batch or at approximately ~7-fold lower levels (Figure 2A). Similar to the previous experiment, mice immunized with OMVs expressing high levels of HbpD-PspA[α1-α2] produced significantly elevated levels of antigen-specific IL-17A in nasal tissue (Figure 4C), and local and systemic antigen-specific IgG, but not local antigen-specific IgA (Figures 5B, S2B and S3B). In contrast, IL-17A and IgG levels were low or undetectable in samples from mice immunized with OMVs displaying low levels of HbpD-PspA[α1-α2], and did not significantly differ from those of control mice that received three doses of OMVs without pneumococcal protein fragments (Figures 4C, 5B and S2B). Furthermore, although low PspA[α1-α2] induced some protection against pneumococcal colonization, a clear trend suggested that enhanced expression of PspA[α1-α2] improved protection (Figure 3B).

To investigate whether similar levels of protection could be reached with fewer immunizations, two additional groups of mice were included that received one or two immunizations with OMVs expressing high levels of HbpD-PspA[α1-α2]. Antibody analysis revealed significantly elevated local and systemic IgG, but not local IgA levels independently of the number of immunizations (Figures 5B, S2B and S3B). However, although slightly more IL-17A was detected after two vaccinations, three immunizations were required to induce significantly higher IL-17A production compared to control mice (Figure 4C). Moreover, three immunizations offered significantly better protection than two immunizations, while one immunization was not sufficient to induce protection as compared with the control (Figure 3B).

In conclusion, the antigen abundance and the number of immunizations directly influence the levels of nasal IL-17A and protection against *S. pneumoniae* colonization. Importantly, production of nasopharyngeal IL-17A significantly correlated with reduced bacterial recovery from the nasal tissue ($p = 0.0032$) (Figure 4D), suggesting that local IL-17A responses are crucial for protective memory responses induced by our OMV/Hbp antigen display platform.

DISCUSSION

The potential of bacterial OMVs, initially restricted to development of vaccines targeting infection with the parent bacterial species, was further expanded by the possibility of engineering OMVs to contain heterologous antigens[7-11]. We recently developed a platform for efficient, simultaneous transport of multiple heterologous polypeptides to the OMV surface[19,21]. Here we demonstrate for the first time, using pneumococcal proteins as model antigens and a murine *S. pneumoniae* colonization model, that intranasally administered OMVs decorated with heterologous antigens at the surface induce strong protection that correlates with local IL-17A production. The advantage of displaying antigens was highlighted in previous vaccine studies showing that secreted or surface-exposed antigens elicit strong cellular immune responses, because of superior antigen processing, and that physical association of PAMPs might play a role in enhanced responses[12,14-16]. Importantly, modulation of antigen levels revealed that both immune responses and protection are improved as antigen concentrations in the vaccine formulation are increased (Figures 3B, 4C and 5B). This highlights the importance of an adequate antigen expression system, such as the Hbp platform, which mediates expression at strikingly high levels that are easily detectable by Coomassie staining.

Intranasally administered *Salmonella* OMVs loaded with PspA in the lumen previously protected mice against lethal *S. pneumoniae* infection in an intra-

peritoneal challenge model[9], showcasing that OMV vaccines can be used to prevent invasive pneumococcal disease. Although this strategy is used to induce broad protection against invasive disease, we decided here to focus on prevention of *S. pneumoniae* colonization. Undeniably, targeting the nasopharyngeal carriage state with an intranasal vaccine would likely not only protect against disease, but also prevent transmission, thereby providing herd immunity and simultaneously reducing emergence of DNA exchange-mediated antigenic variants[43]. The potential of our approach is underlined by the observed correlation between protection and local IL-17A production, which confirms and extends previous findings regarding the importance of IL-17A in mucosal immunity to *S. pneumoniae*[42]. While others showed systemic *ex vivo* Th17 responses associated with protection measured at six days or longer after pneumococcal challenge[40,42,44,45], we observed that nasopharyngeal IL-17A levels, as early as three days post-challenge, correlated with protection. Although it is currently not clear how the OMVs precisely induce IL-17A production, our findings are consistent with a previous report on *E. coli* OMVs[46]. Possibly, lipoproteins in the OMVs are involved, as lipoproteins have been shown to have a strong Th17 inducing capacity and are directly linked to clearance of colonizing pneumococci[47]. Encouraged by the promising results obtained with the PspA model antigen, we are currently incorporating additional highly conserved antigens with the aim of developing a pneumococcal vaccine that can induce serotype-independent protection.

In conclusion, our results demonstrate the potential of the *Salmonella* OMV surface display platform in vaccine development. The ability to induce strong protection and local IL-17A production without the requirement of an external adjuvant is particularly interesting for development of intranasal vaccines against mucosal pathogens, a strategy that is currently hampered by the lack of suitable mucosal adjuvants. Furthermore, the autotransporter Hbp mediates remarkably high antigen densities at the OMV surface, which we showed is important for induction of protective responses. Considering its compatibility with antigens of diverse origins[19] and the availability of easy manufacturing methods using a hypervesiculating attenuated *S.* Typhimurium strain, the OMV/Hbp platform holds promise for developing safe yet immunogenic, needle-free and affordable recombinant OMV vaccines, applicable to a broad range of diseases. Moreover, by allowing simultaneous fusion of multiple antigens to the same carrier, the platform opens up the possibility of creating multivalent vaccines containing several antigens from the same pathogen or antigens from several different pathogens.

Acknowledgements
This research was supported by Agentschap NL [PneumoVac, nr. OM111009] (K.K. and M.d.J.) and by Vinnova [Eureka grant 7200 PneumoVac] (C.M.t.H.J. and J.L.).

REFERENCES

1 Bergman, M. A. *et al.* CD4+ T cells and toll-like receptors recognize Salmonella antigens expressed in bacterial surface organelles. *Infect Immun* **73**, 1350-1356 (2005).
2 Ellis, T. N. & Kuehn, M. J. Virulence and immunomodulatory roles of bacterial outer membrane vesicles. *Microbiology and molecular biology reviews : MMBR* **74**, 81-94 (2010).
3 Underhill, D. M. & Goodridge, H. S. Information processing during phagocytosis. *Nat Rev Immunol* **12**, 492-502 (2012).
4 Roberts, R. *et al.* Outer membrane vesicles as acellular vaccine against pertussis. *Vaccine* **26**, 4639-4646 (2008).
5 Roier, S. *et al.* Intranasal immunization with nontypeable Haemophilus influenzae outer membrane vesicles induces cross-protective immunity in mice. *PLoS One* **7**, e42664 (2012).
6 Holst, J. *et al.* Properties and clinical performance of vaccines containing outer membrane vesicles from Neisseria meningitidis. *Vaccine* **27 Suppl 2**, B3-12 (2009).
7 Kesty, N. C. & Kuehn, M. J. Incorporation of heterologous outer membrane and periplasmic proteins into Escherichia coli outer membrane vesicles. *The Journal of biological chemistry* **279**, 2069-2076, doi:10.1074/jbc.M307628200 (2004).
8 Kim, J. Y. *et al.* Engineered bacterial outer membrane vesicles with enhanced functionality. *J Mol Biol* **380**, 51-66 (2008).
9 Muralinath, M., Kuehn, M. J., Roland, K. L. & Curtiss, R., 3rd. Immunization with Salmonella enterica serovar Typhimurium-derived outer membrane vesicles delivering the pneumococcal protein PspA confers protection against challenge with *Streptococcus pneumoniae*. *Infect Immun* **79**, 887-894 (2011).
10 Schild, S., Nelson, E. J., Bischop, A. L., Camilli, A. Characterization of Vibrio cholerae outer membrane vesicles as a candidate vaccine for cholera. *Infect Immun* **77**, 472-84 (2009).
11 Schroeder, J. & Aebischer, T. Recombinant outer membrane vesicles to augment antigen-specific live vaccine responses. *Vaccine* **27**, 6748-6754 (2009).
12 Alaniz, R. C., Deatherage, B. L., Lara, J. C. & Cookson, B. T. Membrane vesicles are immunogenic facsimiles of Salmonella typhimurium that potently activate dendritic cells, prime B and T cell responses, and stimulate protective immunity in vivo. *Journal of immunology* **179**, 7692-7701 (2007).
13 Amuguni, H. & Tzipori, S. Bacillus subtilis: a temperature resistant and needle free delivery system of immunogens. *Hum Vaccin Immunother* **8**, 979-986, doi:10.4161/hv.20694 (2012).
14 Embry, A., Meng, X., Cantwell, A., Dube, P. H. & Xiang, Y. Enhancement of immune response to an antigen delivered by vaccinia virus by displaying the antigen on the surface of intracellular mature virion. *Vaccine* **29**, 5331-5339, doi:10.1016/j.vaccine.2011.05.088 (2011).
15 Hess, J. *et al.* Superior efficacy of secreted over somatic antigen display in recombinant Salmonella vaccine induced protection against listeriosis. *Proc Natl Acad Sci U S A* **93**, 1458-1463 (1996).
16 Kaufmann, S. H. & Hess, J. Impact of intracellular location of and antigen display by intracellular bacteria: implications for vaccine development. *Immunol Lett* **65**, 81-84 (1999).
17 Roose, K., De Baets, S., Schepens, B. & Saelens, X. Hepatitis B core-based virus-like particles to present heterologous epitopes. *Expert Rev Vaccines* **12**, 183-198, doi:10.1586/erv.12.150 (2013).
18 Jong, W. S. *et al.* A structurally informed autotransporter platform for efficient heterologous protein secretion and display. *Microb Cell Fact* **11**, 85 (2012).
19 Oloo, E. O., Yethon, J. A., Ochs, M. M., Carpick, B. & Oomen, R. Structure-guided antigen engineering yields pneumolysin mutants suitable for vaccination against pneumococcal disease. *The Journal of biological chemistry* **286**, 12133-12140 (2011).
20 Hjelm, A. *et al.* Autotransporter-based antigen display in bacterial ghosts. *Appl Environ Microbiol* **in press** (2014).
21 Daleke-Schermerhorn, M. H. *et al.* Decoration of outer membrane vesicles with multiple antigens by using an autotransporter approach. *Appl Environ Microbiol* **80**, 5854-5865 (2014).

22 van Ulsen, P., Rahman, S. U., Jong, W. S., Daleke-Schermerhorn, M. H. & Luirink, J. Type V secretion: From biogenesis to biotechnology. *Biochim Biophys Acta* **1843**, 1592-1611 (2014).
23 Otto, B. R. *et al.* Crystal structure of hemoglobin protease, a heme binding autotransporter protein from pathogenic Escherichia coli. *The Journal of biological chemistry* **280**, 17339-17345, doi:10.1074/jbc.M412885200 (2005).
24 Alexander, J. E. *et al.* Immunization of mice with pneumolysin toxoid confers a significant degree of protection against at least nine serotypes of *Streptococcus pneumoniae*. *Infect Immun* **62**, 5683-5688 (1994).
25 Briles, D. E. *et al.* PspA, a protection-eliciting pneumococcal protein: immunogenicity of isolated native PspA in mice. *Vaccine* **14**, 858-867 (1996).
26 Kadioglu, A., Weiser, J. N., Paton, J. C. & Andrew, P. W. The role of *Streptococcus pneumoniae* virulence factors in host respiratory colonization and disease. *Nat Rev Microbiol* **6**, 288-301 (2008).
27 Feldman, C. & Anderson, R. Review: current and new generation pneumococcal vaccines. *The Journal of infection* **69**, 309-325 (2014).
28 Hicks, L. A. *et al.* Incidence of pneumococcal disease due to non-pneumococcal conjugate vaccine (PCV7) serotypes in the United States during the era of widespread PCV7 vaccination, 1998-2004. *The Journal of infectious diseases* **196**, 1346-1354 (2007).
29 Lexau, C. A. *et al.* Changing epidemiology of invasive pneumococcal disease among older adults in the era of pediatric pneumococcal conjugate vaccine. *Jama* **294**, 2043-2051 (2005).
30 Miller, E., Andrews, N. J., Waight, P. A., Slack, M. P. & George, R. C. Herd immunity and serotype replacement 4 years after seven-valent pneumococcal conjugate vaccination in England and Wales: an observational cohort study. *The Lancet infectious diseases* **11**, 760-768 (2011).
31 Brueggemann, A. B., Pai, R., Crook, D. W. & Beall, B. Vaccine escape recombinants emerge after pneumococcal vaccination in the United States. *PLoS Pathog* **3**, e168 (2007).
32 Tettelin, H. *et al.* Complete genome sequence of a virulent isolate of *Streptococcus pneumoniae*. *Science* **293**, 498-506 (2001).
33 Cron, L. E. *et al.* Two DHH subfamily 1 proteins contribute to pneumococcal virulence and confer protection against pneumococcal disease. *Infect Immun* **79**, 3697-3710, doi:10.1128/IAI.01383-10 (2011).
34 Hashemzadeh-Bonehi, L. *et al.* Importance of using lac rather than ara promoter vectors for modulating the levels of toxic gene products in Escherichia coli. *Mol Microbiol* **30**, 676-678 (1998).
35 Berry, A. M., Ogunniyi, A. D., Miller, D. C. & Paton, J. C. Comparative virulence of *Streptococcus pneumoniae* strains with insertion-duplication, point, and deletion mutations in the pneumolysin gene. *Infect Immun* **67**, 981-985 (1999).
36 van Dooren, S. J., Tame, J. R., Luirink, J., Oudega, B. & Otto, B. R. Purification of the autotransporter protein Hbp of Escherichia coli. *FEMS Microbiol Lett* **205**, 147-150 (2001).
37 Wu, H. Y. *et al.* Establishment of a *Streptococcus pneumoniae* nasopharyngeal colonization model in adult mice. *Microb Pathog* **23**, 127-137 (1997).
38 Plumptre, C. D., Ogunniyi, A. D. & Paton, J. C. Vaccination against *Streptococcus pneumoniae* using truncated derivatives of polyhistidine triad protein D. *PLoS One* **8**, e78916 (2013).
39 Roche, H., Hakansson, A., Hollingshead, S. K. & Briles, D. E. Regions of PspA/EF3296 best able to elicit protection against *Streptococcus pneumoniae* in a murine infection model. *Infect Immun* **71**, 1033-1041 (2003).
40 Lu, Y. J. *et al.* Interleukin-17A mediates acquired immunity to pneumococcal colonization. *PLoS Pathog* **4**, e1000159 (2008).
41 Marques, J. M. *et al.* Protection against *Streptococcus pneumoniae* serotype 1 acute infection shows a signature of Th17- and IFN-gamma-mediated immunity. *Immunobiology* **217**, 420-429 (2012).
42 Moffitt, K. L. *et al.* T(H)17-based vaccine design for prevention of *Streptococcus pneumoniae* colonization. *Cell Host Microbe* **9**, 158-165 (2011).

43 Simell, B. *et al.* The fundamental link between pneumococcal carriage and disease. *Expert Rev Vaccines* **11**, 841-855 (2012).
44 Wang, S. *et al.* Immune responses to recombinant pneumococcal PsaA antigen delivered by a live attenuated Salmonella vaccine. *Infect Immun* **78**, 3258-3271 (2010).
45 Cohen, J. M. *et al.* Protective contributions against invasive *Streptococcus pneumoniae* pneumonia of antibody and Th17-cell responses to nasopharyngeal colonisation. *PLoS One* **6**, e25558 (2011).
46 Kim, O. Y. *et al.* Immunization with Escherichia coli outer membrane vesicles protects bacteria-induced lethality via Th1 and Th17 cell responses. *Journal of immunology (Baltimore, Md. : 1950)* **190**, 4092-4102 (2013).
47 Moffitt, K. *et al.* Toll-like receptor 2-dependent protection against pneumococcal carriage by immunization with lipidated pneumococcal proteins. *Infect Immun* **82**, 2079-2086 (2014).
48 Jong, W. S. *et al.* Limited tolerance towards folded elements during secretion of the autotransporter Hbp. *Mol Microbiol* **63**, 1524-1536, doi:10.1111/j.1365-2958.2007.05605.x (2007).

SUPPLEMENTARY MATERIALS AND METHODS

Plasmid construction

All reagents were purchased from Roche, except for Phusion DNA polymerase (Finnzymes) and SacI (New England Biolabs).All plasmids used for expression of Hbp (derivatives) have a pEH3 backbone[1]. Plasmids pHbpD(Δd1), pHbpD(Δd2) and pHbpD(d4in), in which sequences coding for side domains d1, d2 and d4 of the Hbp passenger were substituted for Gly/Ser-encoding linkers containing *SacI* and *BamHI* restriction sites have been described[2].

Fragments of *pspA* coding for the N-terminal and the C-terminal portions of the α-helical domain, the LFB domain and the Pro-rich region, and of *ply* encoding an N-terminal (F1; aa 1-156), a central (F2; aa 145-421) and a C-terminal fragment (F3; aa 357-471) were amplified with flanking *SacI/BamHI* sites using chromosomal DNA of *S. pneumoniae* TIGR4 as template and primers listed in Table S1. The resulting PCR amplicons were digested with SacI and BamHI and inserted into the *hbp orfs* of plasmids pHbpD(Δd1), pHbpD(Δd2) or pHbpD(d4in), which had been digested with the same restriction enzymes. This approach resulted in plasmids pHbpD(Δd1)-PspA(α1), pHbpD(Δd1)-PspA(LFBD), pHbpD(Δd1)-Ply(F1), pHbpD(Δd2)-PspA(α2), pHbpD(Δd2)-Ply(F3) and pHbpD(Δd4)-PspA(PRR).

To create a plasmid for expression of Hbp fused to both the α1 and the α2 fragments of PspA, the *NdeI/NsiI* fragment of pHbpD(Δd1)-PspA(α1) was substituted for that of pHbpD(Δd2)-PspA(α2), resulting in pHbpD-PspA(α1α2). Similarly, the *NdeI/NsiI* fragment of pHbpD(Δd1)-Ply(F1) was substituted for that of pHbpD(Δd2)-Ply(F3), yielding plasmid pHbpD-Ply(F1F3) for expression of a chimera containing both fragments F1 and F3 of pneumolysin. Finally, a plasmid was created for expression of Hbp fused to the LFBD and PRR fragments of PspA by replacing the NsiI/KpnI fragment of pHbpD(Δd1)-PspA(LFBD) for that of pHbpD(Δd4)-PspA(PRR).

Constructs for expression and purification of N-terminally His-tagged PspA and PdT[3] were created using the pET16b(+) vector (Novagen). For cloning of *pspA*, a fragment corresponding to aa 31 to 744 was amplified PCR using *S. pneumoniae* TIGR4 chromosomal DNA as template. The forward primer nHis-pspA(dN31)-fw was designed to contain a His_8-epitope encoding sequence and an *NcoI* restriction site, while the reverse primer pspA-rv contained an *NdeI* site. A synthetic *E. coli*-codon-optimized DNA fragment encoding PdT flanked with *NcoI* and *NdeI* restriction sites was ordered from Life Technologies. The fragments were digested with NcoI and NdeI and ligated into pET16b(+), digested with the same enzymes, resulting in pET16b(+)::PspA(31-744) and pET16b(+)::PdT. The nucleotide sequences of all constructs were confirmed by DNA sequencing.

Table S1 Primers used in this study

Name	Sequence (5' → 3')
PspA(PRR)-fw	cggggagctccgagttaggccctgatggag
PspA(PRR)-rv	tgccggatccttgtttccagcctgtttttgg
PspA (LFBD)-fw	cggggagctcccttgctggtgc**a**gatcctgatgatg
PspA (LFBD)-rv	tgccggatccagtttcttcttcatctccatcag
PspA(α2) fw	cggggagctccgtaagagcagttgtagttcc
PspA(α2) rv	tgccggatcctgtgccatcatcaggatctgcaccagc
PspA(α1) fw	cggggagctccgaagaatctccacaagttgtc
PspA(α1) rv	tgccggatccatttggttcaggaactacaactg
Ply(F1)-fw	cggggagctccatggcaaataaagcagtaaatgac
Ply(F1)-rv	tgccggatccgtgagccgtgatttttttcatac
Ply(F3)-fw	cggggagctccgcttacagaaacggagatttactg
Ply(F3)-rv	tgccggatccgtcattttctaccttatcttctac
nHis-pspA(dN31)-fw	aaaccatgggccatcatcatcatcatcatcatcacagcagcggcgaagaatctcca-caagttgtcg
pspA-rv	tttcatatgttaaacccattcaccattgg

Protein purification

Overnight cultures of *E. coli* BL21(DE3) harboring pET16b(+) plasmids for expression of PspA and PdT[3] were grown at 37°C in LB medium supplemented with ampicillin (100 µg/ml) and glucose (0.4%). The next morning, cultures were diluted to an OD_{660} of 0.05 in fresh medium and growth was continued under the same conditions. When the cultures had reached an OD_{660} of 0.6, recombinant protein production was induced by the addition of 100 µM IPTG for 2 h. Cells were harvested by low-speed centrifugation, resuspended in ice cold PBS (pH 7.4) containing 5 mM imidazole and 300 mM NaCl, and lysed in a One Shot cell disrupter (Constant Systems Ltd) at 1.72 kbar. Unbroken cells were removed by low-speed centrifugation. Thereafter, soluble proteins were obtained by high-speed centrifugation at 208.000×*g* at 4°C for 90 min. For PdT, His-tagged protein present in the high-speed supernatant was purified by affinity chromatography using HiTrap TALON crude columns (GE Healthcare). Bound PdT was eluted over a gradient of 5-500 mM imidazole in PBS (pH 7.4) containing 300 mM NaCl. Fractions containing His-tagged PdT were pooled and dialyzed against PBS containing 15% glycerol. The same procedure was followed

to isolate His-tagged PspA, except that the high-speed supernatant and the buffers used during HiTrap TALON affinity chromatography contained 8 M urea.

Detection of antibody responses by enzyme-linked immunosorbent assay analysis

Maxisorp high binding affinity plates (Nunc) were coated with 2 µg/mL purified PspA or PdT in carbonate coating buffer (0.1 M carbonate/bicarbonate pH 9.6) at 4°C overnight. The next day, wells were blocked with 1% BSA (Sigma) and subsequently incubated for 1 h at 37°C with serum or nasal samples from individual mice. Thereafter, the wells were incubated with primary anti-mouse IgG-alkaline phosphatase (Sigma) or primary anti-mouse IgA-alkaline phosphatase (Southern Biotech) for 1 h at 37°C. Between and after the incubations steps, all wells were washed with PBS containing 0.05% Tween-20 (Merck). Samples were developed using 1 mg/mL *p*-nitrophenylposphate in substrate buffer (1 M diethanolamine, 0.5 mM $MgCl_2$ pH 9.8) (Calbiochem, VWR) and the optical density was measured at 405 nm 10 and 30 minutes after substrate addition.

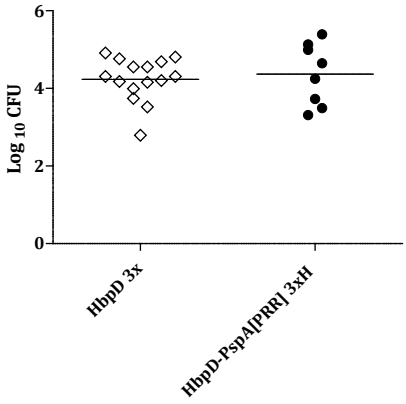

Figure S1 Bacterial recovery upon high expression of PRR.

Bacterial recovery of *S. pneumoniae* from nasal tissue three days post intranasal challenge of C57BL/6 mice that received three (3x) intranasal immunizations of OMVs displaying HbpD or high (H) levels of antigen fragment PRR. Each symbol represents an individual mouse, and bars represent mean per group. NB. The control samples (HbpD) are the same as shown in Figure 2B.

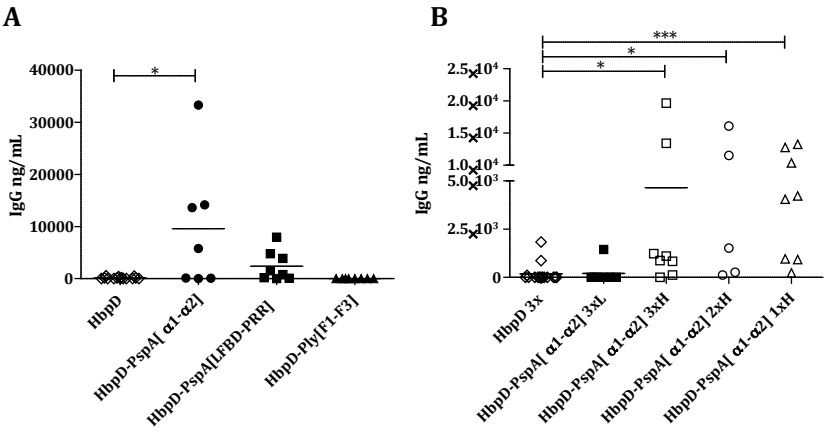

Figure S2 Systemic antigen-specific IgG levels.

(**A**) Systemic antigen-specific IgG responses directed against PspA or pneumolysin, respectively, in mice immunized with OMVs displaying *A*, indicated Hbp (derivatives) or (**B**) HbpD or HbpD-PspA[α1-α2] at high (H) or 5-fold lower (L) expression levels, and with varying immunization number (3x; 2x; 1x). Bars represent mean per group, and symbols represent samples from individual mice. *, $p < 0.05$; **, $p < 0.01$; *** $p < 0.001$.

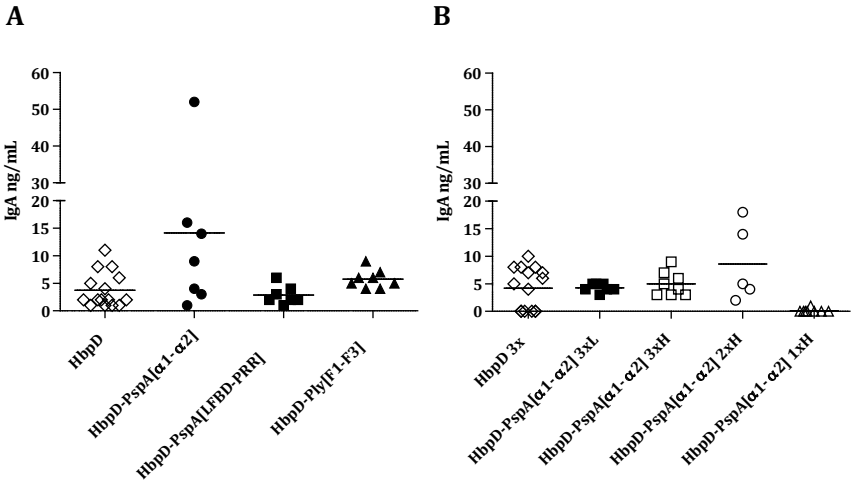

Figure S3 Nasal antigen-specific IgA levels.

Nasal antigen-specific IgA responses directed against PspA or pneumolysin, respectively, in mice immunized with OMVs displaying, (**A**) indicated Hbp (derivatives) or (**B**) HbpD or HbpD-PspA[α1α2] at high (H) or 5-fold lower (L) expression levels, and with varying immunization number (3x; 2x; 1x). Bars represent mean per group, and symbols represent samples from individual mice. *, $p < 0.05$; ** < 0.01; *** $p < 0.001$.

SUPPLEMENTARY REFERENCES

1 Hashemzadeh-Bonehi, L. *et al.* Importance of using lac rather than ara promoter vectors for modulating the levels of toxic gene products in Escherichia coli. *Mol Microbiol* **30**, 676-678 (1998).
2 Jong, W. S. *et al.* A structurally informed autotransporter platform for efficient heterologous protein secretion and display. *Microb Cell Fact* **11**, 85 (2012).
3 Berry, A. M., Ogunniyi, A. D., Miller, D. C. & Paton, J. C. Comparative virulence of *Streptococcus pneumoniae* strains with insertion-duplication, point, and deletion mutations in the pneumolysin gene. *Infect Immun* **67**, 981-985 (1999).

3

Highly conserved nucleotide phosphatase essential for membrane lipid homeostasis in *Streptococcus pneumoniae*

Kirsten Kuipers[*], Clement Gallay[*], Václav Martínek, Manfred Rohde, Markéta Martínková, Samantha L. van der Beek, Wouter S.P. Jong, Hanka Venselaar, Aldert Zomer, Hester Bootsma, Jan-Willem Veening[#], Marien I. de Jonge[#]

*Equal contribution
[#] Shared supervision

Mol Microbiol. 2016 Jul;101(1):12-26. doi: 10.1111/mmi.13312.

ABSTRACT

Proteins belonging to the DHH family, a member of the phosphoesterase superfamily, are produced by most bacterial species. While some of these proteins are well studied in *Bacillus subtilis* and *Escherichia coli*, their functions in *Streptococcus pneumoniae* remain unclear. Recently, the highly conserved DHH subfamily 1 protein PapP (SP1298) has been reported to play an important role in virulence. Here, we provide a plausible explanation for the attenuated virulence of the *papP* mutant. Recombinant PapP specifically hydrolyzed nucleotides 3'-phosphoadenosine-5'-phosphate (pAp) and 5'-phosphoadenylyl-(3'–>5')-adenosine (pApA). Deletion of *papP,* potentially leading to pAp/pApA accumulation, resulted in morphological defects and mis-localization of several cell division proteins. Incubation with both polar solvent and detergent led to robust killing of the *papP* mutant, indicating that membrane integrity is strongly affected. This is in line with previous studies showing that pAp inhibits the ACP synthase, an essential enzyme involved in lipid precursor production. Remarkably, partial inactivation of the lipid biosynthesis pathway, by inhibition of FabF or depletion of FabH, phenocopied the *papP* mutant. We conclude that pAp and pApA phosphatase activity of PapP is required for maintenance of membrane lipid homeostasis providing an explanation how inactivation of this protein may attenuate pneumococcal virulence.

INTRODUCTION

Streptococcus pneumoniae is a Gram-positive α-hemolytic bacterium and one of the leading causes of infection-related mortality worldwide[1]. This human-specific pathogen mainly resides on the mucosal surface of the upper respiratory tract generally resulting in asymptomatic carriage[2,3]. However, *S. pneumoniae* may transit to other tissues causing a broad range of diseases varying from non-invasive infections such as otitis media and sinusitis, to more severe invasive disease, including pneumonia, meningitis and sepsis[2,4].

Recently, the protein SP1298 of *S. pneumoniae* TIGR4 (here renamed to PapP for phosphoadenosine-5'-phosphate and 5'-phosphoadenylyl-(3'–>5')-adenosine phosphatase, see results) was discovered using GAF and Tn-Seq and appears to be a highly conserved protein across the different pneumococcal serotypes[5,6]. Inactivation of this gene strongly reduced virulence at different stages of pneumococcal disease, as studied in murine models of colonization, otitis media, pneumonia, and bacteremia[7,8], suggesting a critical role for PapP in pneumococcal virulence.

PapP is annotated as DHH subfamily 1 protein as it contains the two domains DHH and DHH1. The DHH subfamily 1 is part of the superfamily of phosphoesterases[9]. Within the phosphoesterases two subfamilies exist: the subfamily 2 found in eukaryotes, and the subfamily 1 found in archaea and bacteria. Although these proteins appear to be expressed by most bacteria, little is known about the function of DHH subfamily 1 proteins in *S. pneumoniae*.

PapP shares sequence homology with YtqI of *B. subtilis,* which has both oligonuclease and pAp-phosphatase activity[10]. Of note, most sequence homology is shared with SMU.1297, a *Streptococcus mutants* protein that was reported as pAp phosphatase *in vitro,* but which lacks an oligonuclease activity and is required for superoxide stress tolerance[11]. Recently, the PapP ortholog in strain D39 (SPD_1153) sharing 98% amino acid identity was annotated as Pde2 (PDE: phosphodiesterase)[8]. They showed that PapP synergizes with SP2205 (or Pde1) in a two-step *in vitro* process, converting c-di-AMP and pApA into AMP. Based on enzymatic assays, they hypothesized a role for PapP in cell wall maintenance and signaling[8], while the conversion of pAp, as previously found for other homologous proteins, was not described. Therefore, the function of this nucleotide phosphatase remains largely enigmatic, although most studies suggest that PapP homologs convert pAp, a byproduct of the panthotenate and CoA synthesis, into AMP[10-12]. More specifically, pAp is released upon generation of the acyl carrier protein (ACP), an essential precursor for the initiation of *de novo* fatty acid synthesis. Furthermore, it has been shown that ACP synthase activity can be inhibited by increased pAp concentrations[12].

In this study we demonstrate that PapP is a nucleotide phosphatase converting pAp and pApA into AMP *in vitro*. Deletion of *papP* directly influenced the cell morphology and the localization dynamics of several key cell division proteins in a temperature dependent manner. Furthermore, we discovered that the membrane integrity of the *papP* mutant was disrupted and that partial inactivation of the lipid biosynthesis process resulted in a similar Δ*papP* phenotype, thus providing a molecular explanation for reduced *S. pneumoniae* virulence.

MATERIALS AND METHODS

Pneumococcal strains, growth conditions and transformation

Pneumococcal strains were routinely grown at 37°C on Blood Agar (BA) or in liquid cultures of Todd Hewitt broth with 5 g L-1 yeast extract (THY). For microscopy analyses, strains were grown in C+Y medium at 37 °C, 30 °C or 25°C. For transformation, *S. pneumoniae* was grown in THY or C+Y medium pH = 6.8 until $O.D_{600nm}$ = 0.1; then 0.2 µg/mL of synthetic CSP-2 (Competence-Stimulating Peptide 2) was added and the cells were incubated at 37 °C for 12 min. After DNA addition, cells were incubated at 30 °C for 20 min, then diluted 10 times in THY or C+Y medium, followed by incubation for 1.5 h at 37 °C. Transformants were selected on Blood agar or Columbia agar supplemented with 3% (v/v) sheep blood and the appropriate antibiotic. For induction of the P_{Zn} promoter, 100 µM $ZnCl_2$ was added to liquid medium or agar plates. When required, the growth medium was supplemented with 150 µg/ml spectinomycin (Sp), 500 µg/ml kanamycin (Kan), 0.5 µg/mL tetracycline (Tc) or 0.25 µg/mL erythromycin (Ery). Strains and plasmids construction are detailed in *SI Methods*. Strains are listed in table 1, plasmids and primers are listed in tables S2-S3 respectively.

Bioinformatic protein conservation analyses and homology modeling

To study the conservation of SP1298 (PapP), the amino acid sequence was aligned with BLAST against the Concise Microbial Protein database with one orthologous sequence per species to avoid overrepresentation. 514 proteins (e-value <0.001) were selected and aligned using ClustalOmega[15]. PapP was located in a specific clade containing 127 proteins. Proteins in this clade were subsequently coupled to species and function using the batch retrieval option in the Protein Information Resource (PIR)[16] (Table S1).

A homology model for SP1298 was built using the experimentally solved 3D-structure of SH1221 protein from *Staphylococcus haemolyticus* as a template (PDB file 3DEV). These proteins share 43% sequence identity. A fast model

Table 1 *Streptococcus pneumoniae* strains used in this study

Strain	Relevant characteristics	Reference
TIGR4	Serotype 4 strain, TIGR4 wild type	[13]
papP-gfp	TIGR4, *bgaA*::P_{Zn}-*papP-gfp* (Tc^r)	This study
CG14	TIGR4, *ftsZ::ftsZ-mKate2* (Ery^r)	This study
CG16	TIGR4, *bgaA*::P_{Zn}-*gfp-ftsA* (Tc^r)	This study
Δ*papP*	TIGR4, *papP::spc* (Sp^r)	[7]
Δ*cps*	TIGR4, Deletion of the capsule operon	[14]
Δ*sp1479*	TIGR4, *sp1479::spc* (Sp^r)	This study
CG22	TIGR4, *papP::spc, ftsZ::ftsZ-mKate2* (Sp^r, Ery^r)	This study
CG18	TIGR4, *papP::spc, bgaA::*P_{Zn}*-gfp-ftsA* (Sp^r, Tc^r)	This study
Δ*papP**	TIGR4, *papP::spc, IS1167::pCEP-papP* (Sp^r Kan^r)	This study
Δ*fabH**	TIGR4, *fabH::ery, bgaA::*P_{Zn}*-fabH* (Ery^r, Tc^r)	This study

Sp^r : Spectinomycin resistant; Kan^r : Kanamycin resistant ; Tc^r: tetracycline resistant ; Ery^r: erythromycin resistant

algorithm with standard parameter settings in the YASARA & WHAT IF Twinset was used for model building and analysis[17,18].

Protein expression and purification

The expression and purification of PapP was performed as follows. BL21-pLC1298 [7] was grown at 37 ˚C in LB medium supplemented with 0.2% glucose and 100 µg/ml ampicillin. When the culture reached an OD_{660} of 1.0, the incubation temperature was shifted to 18 ˚C and growth was continued for 2h. The culture was then diluted into fresh medium with 0.2% glucose and 100 µg/ml ampicillin to an OD_{660} of 0.5. A concentration of 100 µM isopropyl-β-D-thiogalactopyranoside (IPTG) was added to induce the overexpression of PapP and the culture was grown overnight at 18 ˚C to prevent the formation of inclusion bodies.

The cells were harvested by centrifugation, re-suspended in ice-cold PBS containing 300 mM NaCl, 5 mM Imidazole and Complete protease inhibitor cocktail (Roche), and lysed by two passages through a One Shot cell disrupter (Constant systems). Cell debris and membrane material was removed by low-speed centrifugation at 8,000 x *g* for 20 min at 4 ˚C and subsequent ultracentrifigation of the low-speed supernatant at 208,500 x *g* for 90 min at 4 ˚C. The supernatant was loaded onto a 1 ml HiTrap TALON crude column (GE Healthcare) and PapP was eluted with a linear gradient of 5 - 500 nM Imidazole in PBS containing 300 nM NaCl at 125 mM Imidazole concentration. The elution peak

was collected and dialyzed at 4 ˚C against PBS containing 10% glycerol (w/v) using 12,000 – 14,000 MWCO SpectraPor4 dialysis membranes (Spectrumlabs). The protein was analyzed for purity with SDS-PAGE and Coomassie G250 staining and stored at -80 ˚C in glycerol-containing dialysis buffer to preserve the enzymatic activity.

Protein reconstitution with manganese

The concentration of purified PapP was determined spectroscopically at 280 nm using extinction coefficient 35870 $M^{-1}.cm^{-1}$. The molar extinction coefficient was predicted by ProtParam tool[19]. The Mn^{2+} concentration in PapP sample was determined using AA-spectrometer AAS3 (Carl Zeiss, Germany).

To ensure full saturation of the enzyme with Mn^{2+}, PapP was incubated with 1:2 molar excess of $MnCl_2$ for 20 min at room temperature. Unbound manganese ions were removed using gel filtration on Sephadex G-50 (2.5 cm, 5 ml column) in 50 mM phosphate buffer pH 7.4 in presence of 5% glycerol.

Enzymatic activity assays

Kinetic experiments with reconstituted enzyme were conducted in 80 mM phosphate buffer (pH 7.4) containing 1 µM $MnCl_2$ using 0.002 and 0.1 µM enzyme for 0-10000 µM 3'-phosphoadenosine-5'-phosphate (pAp, Santa Cruz Biotechnology, USA) and 0-300 µM 5'-phosphoadenylyl-(3' –> 5')-adenosine (pApA, Biolog, USA), respectively. The reaction was stopped after 3, 6, and 9 min incubation at 25 °C by immediate injection to the HPLC system. The reaction rate was determined as an increase of AMP product; different reaction stoichiometries for pApA and pAp hydrolysis were considered. The kinetic data were analyzed using non-linear Hill's fit (considering Hill's coefficient = 1) implemented in program Origin version 7.5 (OriginLab).

The AMP concentrations in incubation mixture were determined by ion-pair reversed-phase chromatography using method inspired by Nakajima et al. [20]. Fifteen µl aliquots of the incubation mixtures were injected into a monolithic C18 column (Chromolith RP-18e, 10 x 4.6 mm; Merck) and analyzed using Agilent 1200 HPLC System with detection at 260 nm. Mobile phase A contained 70 mM potassium phosphate buffer pH 6.0, with 4 mM Tetrabutylammonium hydrogen-sulphate (TBAS, Sigma-Aldrich, USA), as an ion-pair reagent; mobile phase B was methanol. The gradient was delivered at a flow rate of 2 ml/min according to the following program: 100% buffer A for 0.06 min; 0–50% linear gradient of B for 1.0 min; 50% B for 0.25 min; and 100% buffer A for 0.4 min. AMP (Sigma-Aldrich, USA), pAp and pApA standards were used for external calibration. Also ADP, ATP (Sigma-Aldrich, USA) and c-diAMP and c-diGMP (Biolog, USA) were analyzed as potential enzyme substrates using the same method.

Scanning electron microscopy

Bacteria were grown to early exponential growth phase (OD_{600nm} = 0.1) in C+Y medium and fixed with 2% formaldehyde. Scanning electron microscopy analyses were performed as described previously [21]. Briefly, for scanning electron microscopy (SEM) samples were dehydrated with a graded series of acetone on ice for 15 min for each step. Samples were subjected to critical-point drying with liquid CO_2 (CPD030; Balzers, Liechtenstein). The dried samples were covered with an approximately 10-nm-thick gold film by sputter coating (SCD040; Balzers Union, Liechtenstein) before examination with a field emission scanning electron microscope (Zeiss DSM 982 Gemini) using an Everhart Thornley SE detector and an in-lens detector at a 50:50 ratio at an acceleration voltage of 5 kV.

Phase contrast and epifluorescence microscopy

S. pneumoniae was grown in C+Y medium to early exponential growth phase (OD_{600nm} = 0.1), washed once in PBS and spotted onto a PBS-agarose slide. Microscopy pictures were acquired using a DV Elite microscope (Applied Precision) with either a sCMOS (PCO) or a CoolSNAP HQ^2 (Photometrics) camera, using Solid State Illumination (Applied Precision), with a 100x oil-immersion objective. Phase contrast images were acquired with 200 ms exposure time. To visualize the GFP fluorescence, a GFP filter (excitation 461/489 nm; emission 501/559 nm) was used. The mKate2 fluorescence was monitored using a mCherry filter (excitation 562/588 nm; emission 602/648 nm). The exposure time used for both GFP and mKate2 fluorescence was 600 ms. Pictures were acquired and deconvolved using Softworx (Applied Precision) and analyzed using Fiji (http://fiji.sc).

Membrane staining fluorescence microscopy

In order to visualize the membrane of *S. pneumoniae* with Nile Red, the cells were grown in C+Y medium to early exponential growth phase (OD_{600nm} = 0.1) and incubated with 5 µg/mL Nile red for 5 min. The cells were washed once in PBS and spotted onto a PBS-agarose slide. Fluorescence acquisition of Nile red was performed as described above using a TRITC filter (excitation 528/556 nm; emission 571/616 nm) with an exposure time of 300 ms. Pictures were acquired with Softworx and analyzed using Fiji.

Time-lapse fluorescence microscopy

S. pneumoniae was grown in C+Y medium to late log phase (OD_{600nm} = 0.3) and diluted 100 times in fresh C+Y medium supplemented (when appropriate) with 0.1 mM $ZnCl_2$ and incubated for 45 min. Cells were washed once in fresh C+Y

medium and spotted onto a polyacrylamide (10%) slide incubated with C+Y medium, if required complemented with $ZnCl_2$. Acrylamide pieces were placed inside a Gene Frame (Thermo Fisher Scientific) and sealed with the cover glass essentially as described [22]. Acquisition of fluorescence was performed on a DV Elite microscope with a sCMOS camera at 37°C or 30°C. The filters used to visualize the GFP or mKate2 fluorescence are the same as described above. Exposure time used was 500 ms with 32% excitation light. Movies were acquired and deconvolved using Softworx and analyzed using Fiji.

Immunofluorescence microscopy

For fluorescence analysis of the polysaccharide capsule of *S. pneumoniae*, the strains were grown in C+Y medium at 37 °C to exponential growth phase (OD_{600nm} = 0.1), then 1:1000 diluted serum anti-serotype 4 from rabbit (Neufeld antisera, Statens Serum Institut) was added for 5 min at 4 °C. Afterward, the cells were washed 3 times in pre-warmed C+Y medium and 1 µg/mL of secondary antibody anti-rabbit coupled to Alexa Fluor 555 (Invitrogen) was added for 5 min at 4 °C. The cells were then washed once again in pre-warmed C+Y medium and once with PBS before being spotted onto a PBS-agarose slide. Acquisition of the fluorescent signal was performed on Nikon Ti-E microscope (Nikon) equipped with a CoolSNAP HQ^2 camera, an Intensilight light source, with a 100x oil-immersion objective. To visualize the Alexa Fluor 555 fluorescence, a TRITC filter (excitation 528/556 nm; emission 571/616 nm) was used with an exposure time of 800 ms. Pictures were analyzed afterwards with Fiji.

Capsule quantification

Equal mid-log phase bacterial amounts were re-suspended in deionized water and chloroform and shaken for 5 min using TissueLyser LT (Qiagen). Subsequent centrifugation at 13,000 x *g* for 10 min resulted in layer separation of which the aqueous layer contained polysaccharides. These samples were subjected to plates coated with anti-serotype 4 (Statens Serum institute, Neufeld Antisera), followed by incubation with mouse anti-prevnar sera and subsequent alkaline-phosphatase-conjugated anti-mouse IgG (Sigma Aldrich). After each step the plates were washed with Phosphate Buffered Saline supplemented with 0.1% Tween-20 (PBST). Substrate solution (p-nitrophenyl phosphate in 10 mM diethanolamine and 0.5 mM magnesium chloride buffer pH 9.5) was added and absorbance was measured at 405 nm.

Quantitative analyses of cell wall phosphorylcholine

Equal amounts of mid-log phase grown pneumococci were resuspended in PBS and lysed in 0.5 gram acid-washed glass beads (150-212 µm) for 5 min at max

speed using a TissueLyser LT (Qiagen). Maxisorp high binding affinity plates (Nunc) were coated with bacterial lysates in carbonate coating buffer (0.1 M carbonate/bicarbonate pH 9.6) at 4 °C overnight. For choline detection, plates were incubated with mouse monoclonal TEPC-15 (Sigma) and secondary HRP-conjugated Rabbit anti-mouse antibody (DAKO). Signal was developed using 3,3',5,5'-Tetramethylbenzidine (TMB) phospho-citrate buffer and the reaction was stopped using 1.8 M sulfuric acid. Absorbance was measured at 450 nm. Detection of the choline migration pattern using Western Blot is described in the Supplementary Materials and Methods.

Lysozyme, ethanol, and Triton X-100 killing assays

Mid-log phase bacterial pellets were re-suspended in 1 mg/mL lysozyme (Merck), 25% ethanol (Merck), or 0.025% Triton X-100 (Sigma). Incubation with lysozyme was performed at 37 ˚C for 30 min and incubation with ethanol or Triton X-100 was done at room temperature for 10 min. At indicated time points (0, 10 or 30 min), samples were 10-fold serially diluted in PBS and spotted onto BA plates that were incubated at 37 ˚C overnight. The following day, single colonies were counted and percentage survival was calculated.

Growth curve assay

In order to follow the growth of *S. pneumoniae*, the strains were grown in C+Y medium at 37 °C to early exponential growth phase (OD_{600nm} = 0.1), then diluted to an $O.D_{600nm}$ = 0.001. The growth was monitored in a microtiter plate reader (TECAN Infinite F200 Pro) by measuring the OD_{600nm} every 10 min either at 37 °C or 30 °C. Each growth curve assay was performed in triplicate.

Statistical tests

All statistical analyses were performed using GraphPad Prism version 5.0 (Graphpad Software). Quantification of capsule and cell wall phosphorylcholine, and the killing assays were repeated in at least three independent experiments all performed in duplicate. Data were normalized to wild type assayed in the control condition (PBS), and illustrated as mean ± standard error of the mean (SEM). Groups were compared with one-way analysis of variance (ANOVA) and Tukey's multiple comparison post-test. A *P*-value of ≤ 0.05 was considered statistically significant.

RESULTS

Protein conservation and structure prediction

Protein sequence homology analyses revealed that PapP of *S. pneumoniae* TIGR4 (serotype 4) is a highly conserved phosphatase in Gram-positive bacteria, mycoplasmas and phytoplasmas. Of the 127 most conserved homologous proteins, two are well described in literature that are both 3'-phosphoadenosine-5'-phosphate (pAp) phosphatases: NrnA, also known as YtqI (*Bacillus spp.*), and SMU.1297 (*Streptococcus mutans*) (Table S1). The latter is 68% identical to PapP[10,11].

Homology-based structural modeling predicts PapP to be a homodimer (Figure 1A-C). The catalytic site is formed by Asp26, Asp28, Asp82, His105 and Asp155, containing a manganese (Mn^{2+}) ion as co-factor (Figure 1C). No transmembrane or membrane interacting domains were identified, which suggests that PapP is a cytoplasmic protein (Figure 1A-C). To confirm this localization, we fused a monomeric superfolder green fluorescent protein (GFP) to the C-terminal extremity of PapP. This genetic fusion was integrated at the non-essential *bgaA* locus, under the control of a zinc-inducible promoter (*papP-gfp*). As expected, the fluorescent signal was detected throughout the cell (Figure S1), confirming the cytoplasmic localization of PapP.

PapP converts both nucleotide substrates pAp and pApA into AMP

To confirm that PapP is a pAp phosphatase, the protein was purified, reconstituted with $Mn2^{+}$, incubated with its substrate and subjected to HPLC analysis to measure hydrolysis. Purified PapP was able to convert pAp to AMP and phosphate with a K_m value of 580 ± 70 µM and a K_m/K_{cat} of 19 ± 3 $s^{-1}.M^{-1}$ (Figure 1D). The enzymatic activity increased by adding manganese, but only slightly by magnesium ions (Figure S2), confirming that Mn^{2+} is indeed the co-factor as predicted by protein homology modeling (Figure 1A-C). Highly efficient hydrolysis of 5'-phosphoadenylyl-(3'–>5')-adenosine (pApA) by PapP was also detected K_m value of 67 ± 20 µM and a K_m/K_{cat} of 2100 ± 500 $s^{-1}.M^{-1}$ (Figure 1D). A similar K_m value (23.96 ± 7.78 µM) was reported for the PapP ortholog from *S. pneumoniae* D39 named SPD_1153 or Pde2[8]. No hydrolysis of ADP, ATP, c-di-AMP and c-di-GMP was found in the presence of PapP (Figure S3). This underlines the enzyme specificity for hydrolysis of 3'-phosphate group of linear adenine-containing nucleotides, but also indicates that it is more flexible regarding the size of the substrate, as the two substrates differ significantly in their length. In conclusion, these data confirm the 3'-phosphatase activity of PapP toward pAp and pApA substrates.

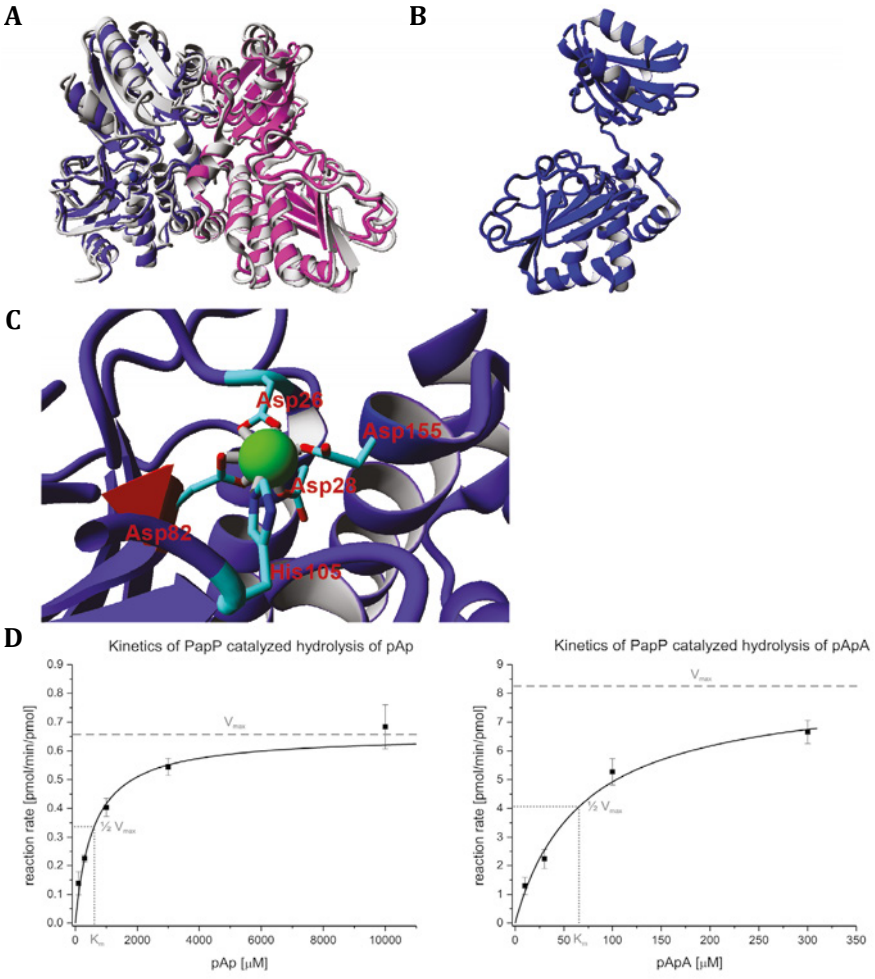

Figure 1 PapP structure and enzymatic activity.

The predicted structure of PapP is based on the crystal structure of SH1221 from *S. haemolyticus* (43% shared identity). (**A**) PapP is predicted to form a homodimer. The PapP model was structurally aligned with the SH1221 template (gray). PapP monomers are indicated in blue and pink. (**B**) Monomeric structure of PapP. (**C**) The catalytic site is predicted to contain a Mn^{2+} ion (green sphere) bound by Asp26, Asp28, Asp82, His105 and Asp155. (**D**) Steady-state kinetic analysis of PapP catalyzed hydrolysis of pAp (left) and pApA (right) with the corresponding Km and Vmax values. The reaction rates were determined from the AMP product formation and the kinetic parameters were obtained from non-linear Michaelis–Menten fits. AMP concentrations were analyzed using HPLC. All data are the mean ± SD (n = 3).

S. pneumoniae deficient for *papP* shows aberrant morphologies

It was established that deletion of *papP* leads to reduction of pneumococcal virulence at many stages of disease[7]. In order to understand the underlying mechanisms of virulence attenuation when the pAp phosphatase is absent, we investigated the cell morphology of a *S. pneumoniae* TIGR4 strain deficient for *papP* (Δ*papP*). Morphology analysis by phase contrast microscopy and membrane staining with Nile red revealed that the *papP* mutant only forms diplococci at early exponential growth phase, while the wild type forms long chains (Figure 2A). This is in line with the study of the PapP ortholog in *S. pneumoniae* D39 (serotype 2) where deletion *pde2* led to significantly shorter chains[8]. Another striking observation was that the cell-poles of the *papP* mutant were pointier compared to the wild type cells when measuring the pole-angles of the cells (Figure S4). Furthermore, cells of the *papP* mutant were significantly longer and had a wider cell diameter (Figure 2B). To characterize the cell morphology in higher resolution we performed scanning electron microscopy (SEM). The micrographs confirmed that the *papP* deficient strain displayed a substantial shorter chain length consisting of only few cocci with sharp cell-poles (Figure 2C). Protrusions on the cell surface appeared in all *S. pneumoniae* strains and could likely be capsule artifacts induced by the method[23]. Complementation of *papP* deletion by an ectopic version of *papP* (Δ*papP**) reversed the diplococcus phenotype, as this strain only forms long chains and possesses a wild type cell pole angularity (Figures 2A and S3). SEM pictures of this strain also confirmed that reversion of *papP* mutation restored the wild-type phenotype (Figure 2C). These observations suggest that *papP* deficiency affects the chain formation of *S. pneumoniae*. In addition to morphology defects, analysis of the growth rate in liquid culture at 37 °C revealed that the *papP* mutant demonstrates a reduced growth rate with a doubling time of 46 min (95% confidence interval 44.1 to 49.1 min) vs 34 min (95% confidence interval 35.5 to 37.4 min) for the wild type (Figure 2D). Taken together, these results indicate that absence of PapP directly influences the cell morphology and growth of *S. pneumoniae*.

The polysaccharide capsule is unaffected in the absence of PapP

It is known that the polysaccharide capsule plays a crucial role in virulence of *S. pneumoniae*. Indeed, the non-encapsulated S. *pneumoniae* R6 strain (derivate from D39 strain) is non-virulent. Interestingly, strain R6 only forms diplococci instead of chains[24]. Taking this into account, the phenotype observed in absence of PapP may be caused by perturbations in capsule production. To test this, we performed immunofluorescence microscopy using a serotype 4 specific capsule antibody. Interestingly, the signal illustrative for capsule presence appeared similar among wild type, mutant, and complemented strain (Figure 3A). This

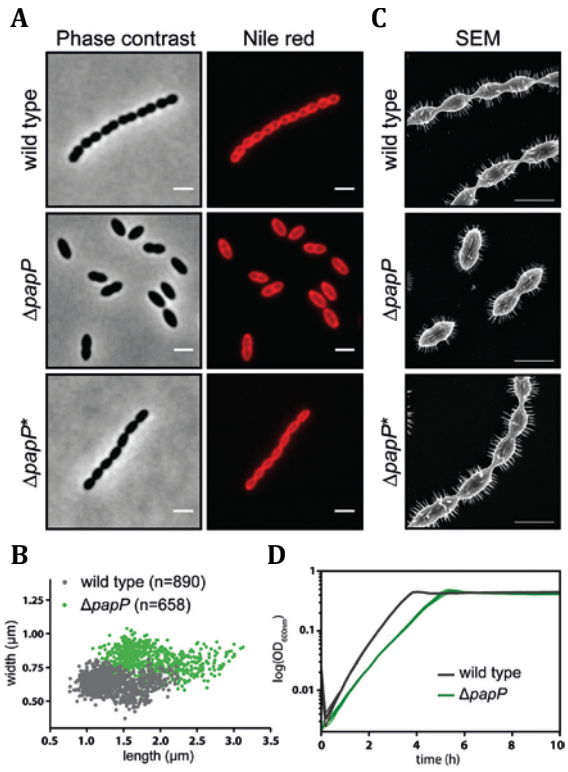

Figure 2 Morphological and growth defects of the *papP* mutant.

(**A**) Phase contrast microscopy (left panel) and Nile red staining (right panel) of TIGR4 wild type, Δ*papP* and Δ*papP**. Scale bar, 3 µm. (**B**) Cell width (p-value < 0.0001) and cell length (p-value < 0.0001) distribution of TIGR4 wild type (dark gray) and Δ*papP* (green). (**C**) Scanning electron micrographs (SEM) of TIGR4 wild type, Δ*papP* and Δ*papP**. Scale bar, 1,5 µm. (**D**) Growth curve of TIGR4 wild type (dark gray) and Δ*papP* (green) at 37 °C in liquid C+Y medium. SEM for TIGR4 wild type and Δ*papP* are shown in clear grey and clear green, respectively.

suggests that despite the morphological differences, the *papP* mutant displayed a normal polysaccharide capsule. To confirm that loss of PapP has no effect on capsule production, bacterial lysates were assayed for the amount of capsule. A non-encapsulated mutant of TIGR4, TIGR4Δ*cps*, was included as negative control (Figure 3B). Strikingly, all three TIGR4 strains, wild-type, mutant and complemented strain, showed similar capsule polysaccharide levels (Figure 3B). These data clearly indicate that the polysaccharide capsule remained intact in *S. pneumoniae* deficient for PapP. Hence, capsule alterations do not explain the atypical morphology of the mutant.

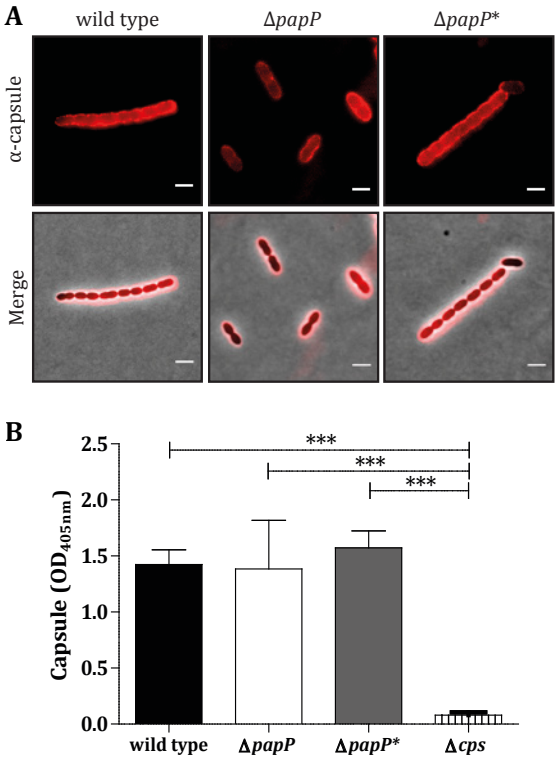

Figure 3 Intact polysaccharide capsule in *papP* deficient *S. pneumoniae*.

(**A**) Immunofluorescence staining (α-capsule) of the polysaccharide capsule of TIGR4 wild type, Δ*papP* and Δ*papP** using anti-serotype 4 antibodies. Scale bar, 3 µm. (**B**) All strains were screened for capsule expression in an ELISA-based assay, with an acapsular derivative (Δ*cps*) as negative control. Data are normalized from three independent experiments performed in duplicate. Results are illustrated at average ± SEM and compared by one-way ANOVA and Tukey's multiple comparison test. Significance is illustrated with ***, P< 0.001; **, P<0.01; *, P<0.05.

Effects of papP inactivation on the cell wall

To explore whether cell wall homeostasis may be influenced by inactivation of *papP*, qualitative and quantitative analyses were performed to probe the phosphorylcholine moieties of the pneumococcal teichoic acids. No differences were found in phosphorylcholine production between wild type, mutant, and complemented strain, as measured in a quantitative ELISA (Figure 4A). The phosphorylcholine migration pattern as determined by Western blotting appeared identical between the three variants (Figure 4B). These data indirectly indicate that lipoteichoic acid (LTA) and wall techoic acid (WTA) are unaffected in the

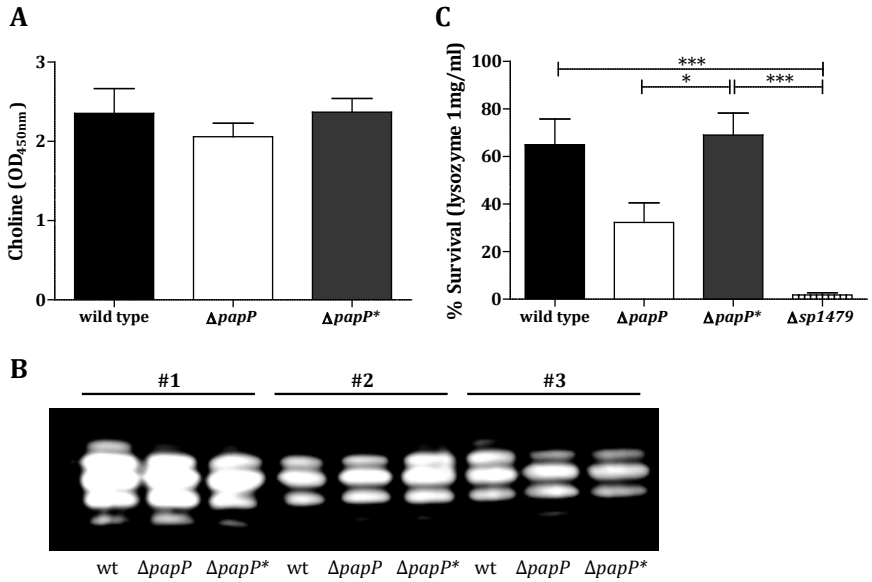

Figure 4 The effect of PapP absence on cell wall components.

(**A**) Cell-wall anchored choline levels of wild type, mutant (Δ*papP*) and complemented mutant strains (Δ*papP**) as measured by an ELISA-based assay. A higher OD_{450} indicates a higher choline content. (**B**) Analysis of phosphorylcholine in the cell wall by Western blotting. The phosphorylcholine migration pattern analyzed by SDS-PAGE and Western blotting in wild type (wt) , *papP* mutant (Δ*papP*) and complemented (Δ*papP**) strains. The results represent phosphorylcholine migration patterns from three independent experiments (#1, #2, #3). (**C**) Survival of pneumococcal strains in a lysozyme killing assay, with negative control Δ*sp1479*. Choline expression levels show normalized data from three independent experiments performed in duplicate. Lysozyme data are combined from four independent assays. Results are provided as average ± SEM and compared by one-way ANOVA and Tukey's multiple comparison test. Significance is illustrated with ***, P< 0.001; **, P<0.01; *, P<0.05.

papP mutant. Additionally, no significant differences in amount of lipoproteins were measured in Δ*papP*, Δ*papP**, and wild type (Figure S5).

Furthermore, the effect of absence of *papP* on peptidoglycan was studied in a lysozyme killing assay. Notably, the *papP* mutant was significantly more sensitive to lysozyme, exemplified by a 2-fold reduced survival, as compared to wild type and the complemented mutant strain (Figure 4C). Of note, survival of the Δ*papP* strain (mean survival of 32.3%) was over 15-fold higher than a Δ*sp1479* strain (mean survival of 1.8%), which lacks peptidoglycan N-acetylglucosamine deacetylase A (PgdA), an enzyme directly involved in peptidoglycan cross-linking (Figure 4C)[25]. The reduced sensitivity to lysozyme as compared to the Δ*sp1479* mutant implies that this may not be caused by a direct effect on peptidoglycan.

Loss of papP perturbs cell division protein dynamics

The cell division machinery *of S. pneumoniae* involves many important proteins that fine-tune the cell shape[26,27]. Deregulation of these proteins could therefore result in cell morphology defects. In order to determine whether the morphological changes of the Δ*papP* mutant could be attributed to a deregulation of the division process, we inserted an ectopic copy of a N-terminal GFP fusion of the early cell division protein FtsA under control of a zinc-inducible promoter in both wild type and Δ*papP* strains, resulting in strains CG16 and CG18, respectively. As expected, in the wild type cells, FtsA is recruited early at the new septum and thus localizes exclusively at mid-cell at early exponential growth phase (Figure 5A). However, the signal in the *papP* mutant appears to be at mid-cell but also at the old division site (Figure 5A). To exclude that addition of Zn^{2+} induced synthetic effects, we constructed a strain expressing a functional fusion of the early cell division protein FtsZ with the red fluorescent protein mKate2 (strains CG14 and CG22). This construct was inserted at the TIGR4 *ftsZ* locus, under the native promoter in order to keep the original FtsZ expression level. Fluorescence microscopy confirmed the localization of FtsZ at mid-cell in both wild type and Δ*papP* (Figure 5B). To better understand the localization dynamics of FtsZ, we performed time-lapse fluorescence microscopy at 37°C. Interestingly, while FtsZ was instantly disassembled from the old septum and re-assembled at the new septum in the wild type strain (Figure 5C, Movies S1 and S2), it slowly moved from the old septum to the new septum in the Δ*papP* mutant (Figure 5C, Movies S1 and S2). Similar results were obtained for GFP-FtsA (Movie S3). To further characterize the dynamics of these two cell division proteins, the distance between FtsA or FtsZ and the closest pole of the cell was measured. When plotted with the cell length, two different clusters are clearly visible for the wild type, indicating that FtsA and FtsZ are either at the old or the new division site, or at both positions (Figure 5D and E). However, the two distinct clusters disappeared for the mutant strain, giving way to a heterogeneous distribution (Fig. 5D and E). This indicates that FtsA and FtsZ are not only present at both the old and new septum, but also in between these two positions at one moment of the cell cycle (Figure 5F). Taken together, these results show that inactivation of *papP* results in mis-localization of FtsA and FtsZ.

Localization of cell division proteins is temperature dependent in the ΔpapP strain

To characterize the FtsZ dynamics of the *papP* mutant in more detail, we used time-lapse fluorescence microscopy to follow the cells on a semi-solid matrix at 30 °C, a temperature known to slow down the cell cycle compared to the previous experiments performed at 37 °C. Surprisingly, whereas FtsZ is well localized at

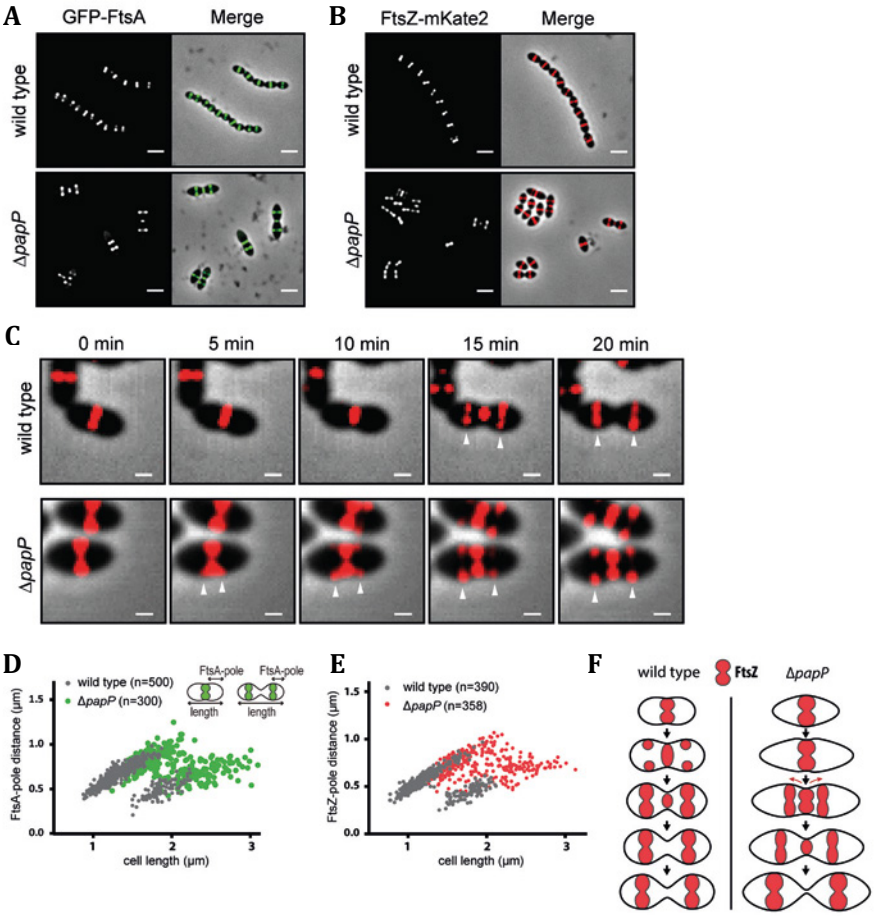

Figure 5 FtsA and FtsZ dynamics are impaired in Δ*papP*.

(**A**) Localization of GFP-FtsA in live TIGR4 wild type and Δ*papP*. The GFP fluorescent signal (left panel) is overlaid with the phase contrast image (right panel). Scale bar, 3 µm. (**B**) Localization of FtsZ-mKate2 in live TIGR4 wild type and Δ*papP*. The mKate2 signal (left panel) is overlaid with the phase contrast image (right panel). Scale bar, 3 µm. (**C**) Fluorescence time-lapse microscopy of FtsZ-mKate in TIGR4 wild type and Δ*papP* at 37 °C. The fluorescent signal is overlaid with the phase contrast. The white arrows indicate the localization of the newly formed Z-ring. Scale bar, 0.5 µm. (**D**) Distance between GFP-FtsA and the closest pole of TIGR4 wild type and Δ*papP* depending on cell size. (**E**) Distance between FtsZ-mKate2 and the closest pole of TIGR4 wild type and Δ*papP* depending on cell size. (**F**) Model of TIGR4 wild type and Δ*papP* cell division. Compared to the wild type situation where FtsZ (red) seems to be directly reassembled at the new division site, it seems to slowly slide from the old to the new septum in the *papP* mutant (green arrows) over the cell cycle. Cells of the *papP* mutant also appear bigger and pointier.

mid-cell in the wild type, it appears to be completely mis-localized in the Δ*papP* mutant after a few division cycles, followed by a quick death of the cells (Figure 6A and Movie S4). Identical results were obtained with GFP-FtsA (S5 Movie). Fluorescence microscopy of cells grown at 30 °C until early exponential growth phase in liquid medium confirmed the previous observations since many cells displayed abnormal morphologies and FtsZ was frequently mis-localized (Figure 6B). This excludes an indirect effect of the fluorescence time-lapse microscopy technique for FtsZ mis-localization. Growth in liquid C+Y medium at 30 °C also indicated a temperature sensitivity of the ΔpapP strain since it entered in stationary phase at lower cell density (Figure 6C). These data suggest that the *papP* mutant is cold sensitive, especially when also harboring a FtsZ-RFP fusion. To further characterize the temperature sensitivity, the mutant strain was grown at even lower temperatures (25 °C) and FtsZ localization was monitored. Despite a very slow growth at this temperature, FtsZ is still well localized in the wild type strain (Figure 6D). Surprisingly, the mutant strain shows many elongated cells displaying a helical pattern of FtsZ (Figure 6D). Thus, our data indicate that absence of the pAp phosphatase (PapP) leads to mis-localization of cell division proteins in a temperature-dependent manner.

Lack of PapP diminishes cell membrane integrity

Many cell division proteins are directly or indirectly anchored to the cell membrane. For instance, FtsA is a membrane-associated protein that anchors FtsZ[28]. A change in membrane properties can thus impact their localization. To assess whether membrane integrity may be reduced upon *papP* deletion, pneumococcal strains were screened for survival in both organic solvent and detergent killing assays. As hypothesized, the *papP* mutant appeared highly susceptible for ethanol (Figure 7A) and Triton X-100 in comparison with the wild type strain and the complemented mutant (Figure 7B). Survival in absence of *papP* was reduced approximately 5- and 4-fold in ethanol (13%) and Triton X-100 (20%) killing assays, respectively. These data clearly indicate an increased sensitivity of *S. pneumoniae* deficient for *papP* to both organic and solvent compounds that is likely caused by an unstable and more accessible membrane. This is supported by the increased sensitivity of the *papP* mutant against selected antibiotics (Table S4).

FabF or FabH inactivation phenocopy papP deletion

In order to investigate whether the phenotype of the *papP* mutant is the result of fatty acid biosynthesis perturbation, we sought to partially inactivate this process. Bacterial type II fatty-acid synthasis (FASII) inhibition seems a good strategy as these enzymes are involved in essential steps of the fatty acid

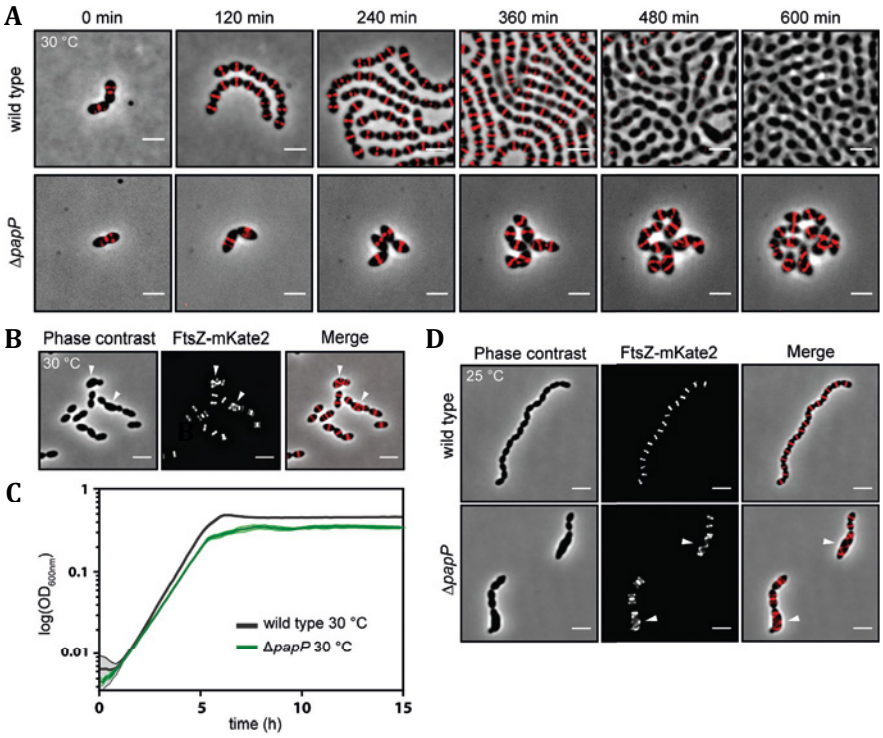

Figure 6 FtsZ localization is temperature dependent in Δ*papP*.

(**A**) Time lapse fluorescence microscopy of FtsZ-mKate2 in TIGR4 wild type and Δ*papP* at 30 °C. The fluorescent signal is overlaid with the phase contrast. Scale bar, 3 µm. (**B**) Localization of FtsZ-mKate2 in live TIGR4 wild type and Δ*papP* grown at 30 °C. Overlay between the phase contrast images (left panel) and the mKate2 signal (middle panel) is shown (right panel). The white arrows indicate the aberrant localization of FtsZ. Scale bar, 3 µm. (**C**) Growth curve of TIGR4 wild type (dark gray) and Δ*papP* (green) at 30 °C. SEM for TIGR4 wild type and Δ*papP* are shown in clear grey and clear green, respectively. (**D**) Localization of FtsZ-mKate2 in live TIGR4 wild type and Δ*papP* grown at 25 °C. Overlay between the phase contrast images (left panel) and the mKate2 signal (middle panel) is shown (right panel). The white arrows indicate the helical pattern of FtsZ. Scale bar, 3 µm.

biosynthesis[29]. For instance, the proteins FabH and FabF are respectively responsible for the initiation and elongation of the fatty acid chains. However, due to their essentiality, their inactivation by deleting the corresponding genes is not possible. On the other hand, it has been reported that FabF can by inactivated by a bacteriostatic drug, platensimycin[30]. To examine the effect of fatty acid synthesis inhibition by platensimycin on pneumococcal morphology, the wild type strain was grown in the presence of 0.75 µg.mL^{-1} platensimycin to early

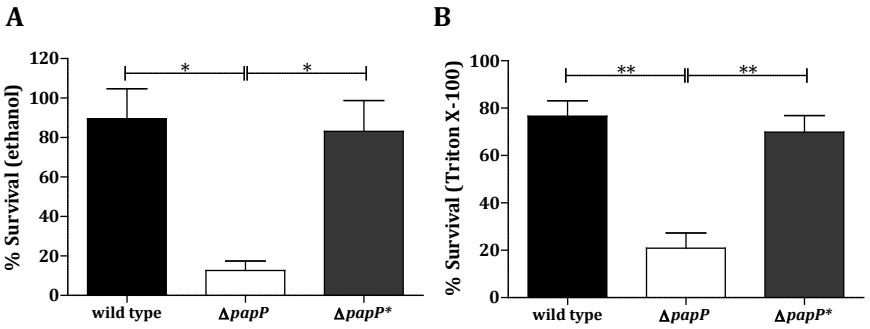

Figure 7 Loss of PapP increases susceptibility to organic solvent and detergent.

Survival of pneumococcal strains, wild type, mutant (Δ*papP*), and complemented mutant strain (Δ*papP**), in an (**A**) organic solvent ethanol and (**B**) detergent Triton X-100 killing assay. Ethanol and Triton X-100 killing show normalized data from three independent experiments performed in duplicate. Results are provided as average ± SEM and compared by one-way ANOVA and Tukey's multiple comparison test. Significance is illustrated with ***, P< 0.001; **, P<0.01; *, P<0.05.

exponential growth phase and cell morphology was assessed by phase contrast microscopy. A concentration was used at which the maximum optical density of *S. pneumoniae* was reduced by two-fold (MC50) (Figure S6)[31]. Strikingly, platensimycin treatment resulted in the formation of only diplococci (Figure 8A) and chains of cells were no longer observed. This shows that partial inactivation of the fatty acid biosynthesis by inactivation of FabF is able to phenocopy the *papP* mutant in this regard.

Next, we assessed the effect of FabH depletion on *S. pneumoniae* morphology by constructing a strain expressing an ectopic version of *fabH* under a zinc-inducible promoter and made a deletion of the native *fabH* gene in presence of Zn^{2+} (Δ*fabH**). Phase contrast microscopy revealed a wild type phenotype when grown in the presence of 0.1 mM Zn^{2+} (Figure 8B). Zinc absence is sufficient for minor expression of FabH, which is likely due to the leakage of the zinc-inducible promoter[32], Strikingly, when grown without zinc, chain formation was absent and cells display a diplococcus phenotype (Figure 8B). Apparently, reducing available FabH also phenocopies inactivation of *papP.* Taken together, these results strongly indicate that PapP deficiency affects the fatty acid biosynthesis resulting in the observed morphological defects.

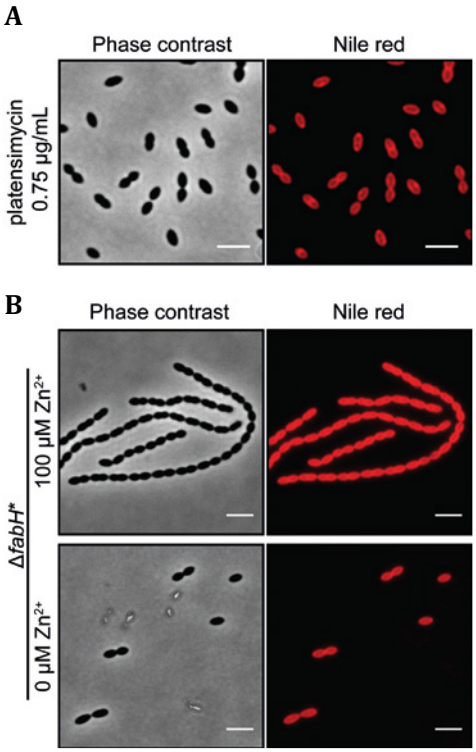

Figure 8 Partial inactivation of lipid synthesis phenocopies Δ*papP* morphology.

(**A**) Phase contrast microscopy (left panel) and Nile red staining (right panel) of TIGR4 wild type grown in presence of 0.75 µg/mL platensimycin. Scale bar, 3 µm. (**B**) Phase contrast microscopy (left panels) and Nile red staining (right panels) of Δ*fabH** grown in presence of 100 µM Zn^{2+} (upper panels) or without (lower panels). Scale bar, 3 µm.

DISCUSSION

The *papP* deletion mutant showed in a previous study decreased virulence in all stages of pneumococcal disease, which strongly indicates a critical role for *papP* in *S. pneumoniae* pathogenesis [7]. Remarkably, *S. pneumoniae* deficient for *papP* showed an abnormal morphology and was substantially weaker in various killing assays compared to wild type strains and the complemented mutant. Altogether, our data indicate that loss of *papP* results in a cell integrity defect, rather than loss of a specific virulence factor as suggested previously[7,8].

In this study we show that PapP is a phosphatase able to convert two adenine-nucleotide substrates, 3′-phosphoadenosine-5′-phosphate (pAp) and

5'-phosphoadenylyl-(3'–>5')-adenosine (pApA). Hydrolysis of pApA by *S. pneumoniae* D39 PapP ortholog (Pde2) was recently described and hypothesized to be implicated in c-di-AMP signaling and cell wall homeostasis, as pApA is a product of *in vitro* degradation of c-di-AMP[8,33]. However, it is unknown in which quantities and during which other metabolic processes pApA is produced in *S. pneumoniae*. More importantly, its biological role remains largely unknown. A possibility is that pApA is a metabolite generated during other *S. pneumoniae* metabolic processes, including lipid metabolism, which may be undetectable due to a fast degradation into end products like AMP. This theory is supported by our observation that PapP breakdown of pApA is remarkably rapid (Figure 1D).

In addition to pAp as substrate, Uemera and colleagues reported that Nrn degrades short RNAs, e.g. nanoRNAs. This dual preference for nanoRNA and pAp conversion has also been described for other DHH subfamily 1 proteins, including RecJ, Orn, and YtqI[10,34,35], suggesting a similar activity for PapP. Whether nanoRNA degradation contributes to the phenotype of *S. pneumoniae* deficient for PapP remains speculative. Namely, Mechold and colleagues reported that RNase activity is redundant[10], indicating that absence of a single RNase would not affect RNA metabolism. In addition, RNase activity has not been described for *S. mutans* protein SMU.1297, which shares 68% homology with PapP[11].

It is remarkable that PapP is highly conserved in Gram-positive bacteria, mycoplasmas and phytoplasmas, all containing a single membrane. In this regard, it is tempting to speculate that these single membrane-containing bacteria are more vulnerable for distortion of the lipid membrane homeostasis. Our findings demonstrate that loss of a single protein results in a weakened membrane integrity of *S. pneumoniae* (Figures 7A and B), which makes PapP an attractive target for therapeutic interventions for Gram-positive infections.

Perturbing the membrane altered the localization dynamics of key cell division proteins FtsA and FtsZ (Figures 5 and 6). A recent body of work has shown that cell division in *S. pneumoniae* is orchestrated by a complicated phosphorylation cascade via the eukaryotic-type serine-threonine kinase StkP[36]. It would be interesting to see what the effects of membrane perturbations, such as those caused by *papA* deletion, are on the signaling at the level of StkP and downstream proteins.

In conclusion, we hypothesize that in *S. pneumoniae* lacking the pAp phosphatase PapP, pAp and pApA levels will increase thereby inhibiting AcpS[12]. Subsequently, decreased enzyme activity may lead to reduced precursor formation, which is required to start fatty acid synthesis, thereby hampering *de novo* lipid production[12]. The resulting reduction in membrane integrity provides a plausible explanation for altered cell morphology and susceptibility and thereby reduced virulence of *papP* deficient *S. pneumoniae*[7]. Investigating newly

discovered conserved pneumococcal proteins will improve our understanding of pneumococcal physiology and pathogenesis. Gaining insight into *S. pneumoniae* membrane homeostasis and virulence may reveal potential targets that will aid the development of future therapeutics and vaccines to treat and prevent pneumococcal disease.

Acknowledgments

K.K. and M.d.J. were supported by Agentschap NL [PneumoVac, nr. OM111009]. Work in the Veening lab is supported by the EMBO Young Investigator Program, a VIDI fellowship (864.12.001) from the Netherlands Organisation for Scientific Research, Earth and Life Sciences (NWO-ALW) and ERC starting grant 337399-PneumoCell. The authors thank Dr. Jakub Hraníček from the Charles University in Prague, for assistance with determination of Mn^{2+} concentration in the PapP sample using AAS analysis, Prof. Sven Hammerschmidt and Dr. Franziska Voß for providing the α-enolase α-MetQ, α-PpmA, α-PsaA, and α-SlrA antibodies, and Dr. Jeroen Langereis for his helpful input.

REFERENCES

1 Walker, C. L. *et al.* Global burden of childhood pneumonia and diarrhoea. *Lancet* **381**, 1405-1416, doi:10.1016/s0140-6736(13)60222-6 (2013).

2 O'Brien, K. L. *et al.* Burden of disease caused by *Streptococcus pneumoniae* in children younger than 5 years: global estimates. *Lancet* **374**, 893-902 (2009).

3 Kadioglu, A., Weiser, J. N., Paton, J. C. & Andrew, P. W. The role of *Streptococcus pneumoniae* virulence factors in host respiratory colonization and disease. *Nat Rev Microbiol* **6**, 288-301, doi:10.1038/nrmicro1871 (2008).

4 Drijkoningen, J. J. & Rohde, G. G. Pneumococcal infection in adults: burden of disease. *Clin Microbiol Infect* **20 Suppl 5**, 45-51, doi:10.1111/1469-0691.12461 (2014).

5 Bijlsma, J. J. *et al.* Development of genomic array footprinting for identification of conditionally essential genes in *Streptococcus pneumoniae*. *Appl Environ Microbiol* **73**, 1514-1524, doi:10.1128/aem.01900-06 (2007).

6 van Opijnen, T. & Camilli, A. A fine scale phenotype-genotype virulence map of a bacterial pathogen. *Genome Res* **22**, 2541-2551, doi:10.1101/gr.137430.112 (2012).

7 Cron, L. E. *et al.* Two DHH subfamily 1 proteins contribute to pneumococcal virulence and confer protection against pneumococcal disease. *Infect Immun* **79**, 3697-3710, doi:10.1128/iai.01383-10 (2011).

8 Bai, Y. *et al.* Two DHH subfamily 1 proteins in *Streptococcus pneumoniae* possess cyclic di-AMP phosphodiesterase activity and affect bacterial growth and virulence. *J Bacteriol* **195**, 5123-5132, doi:10.1128/jb.00769-13 (2013).

9 Aravind, L. & Koonin, E. V. A novel family of predicted phosphoesterases includes Drosophila prune protein and bacterial RecJ exonuclease. *Trends Biochem Sci* **23**, 17-19 (1998).

10 Mechold, U., Fang, G., Ngo, S., Ogryzko, V. & Danchin, A. YtqI from Bacillus subtilis has both oligoribonuclease and pAp-phosphatase activity. *Nucleic Acids Res* **35**, 4552-4561, doi:10.1093/nar/gkm462 (2007).

11 Zhang, J. & Biswas, I. 3'-Phosphoadenosine-5'-phosphate phosphatase activity is required for superoxide stress tolerance in Streptococcus mutans. *J Bacteriol* **191**, 4330-4340, doi:10.1128/jb.00184-09 (2009).

12 McAllister, K. A., Peery, R. B., Meier, T. I., Fischl, A. S. & Zhao, G. Biochemical and molecular analyses of the *Streptococcus pneumoniae* acyl carrier protein synthase, an enzyme essential for fatty acid biosynthesis. *J Biol Chem* **275**, 30864-30872, doi:10.1074/jbc.M004475200 (2000).

13 Tettelin, H. *et al.* Complete genome sequence of a virulent isolate of *Streptococcus pneumoniae*. *Science (80-)* **293**, 498-506, doi:10.1126/science.1061217 (2001).

14 Cron, L. E. *et al.* Surface-associated lipoprotein PpmA of *Streptococcus pneumoniae* is involved in colonization in a strain-specific manner. *Microbiology* **155**, 2401-2410, doi:10.1099/mic.0.026765-0 (2009).

15 Sievers, F. *et al.* Fast, scalable generation of high-quality protein multiple sequence alignments using Clustal Omega. *Mol Syst Biol* **7**, 539, doi:10.1038/msb.2011.75 (2011).

16 Wu, C. H. *et al.* The Protein Information Resource. *Nucleic Acids Res* **31**, 345-347 (2003).

17 Krieger, E., Koraimann, G. & Vriend, G. Increasing the precision of comparative models with YASARA NOVA--a self-parameterizing force field. *Proteins* **47**, 393-402 (2002).

18 Vriend, G. WHAT IF: a molecular modeling and drug design program. *J Mol Graph* **8**, 52-56, 29 (1990).

19 Gasteiger E., H. C., Gattiker A., Duvaud S., Wilkins M.R., Appel R.D., Bairoch A. *Protein Identification and Analysis Tools on the ExPASy Server*. 571-607 (Humana Press, 2015).

20 Nakajima, K. *et al.* Simultaneous determination of nucleotide sugars with ion-pair reversed-phase HPLC. *Glycobiology* **20**, 865-871, doi:10.1093/glycob/cwq044 (2010).

21 Hammerschmidt, S. *et al.* Illustration of pneumococcal polysaccharide capsule during adherence and invasion of epithelial cells. *Infect Immun* **73**, 4653-4667, doi:10.1128/iai.73.8.4653-4667.2005 (2005).

22 de Jong, I. G., Beilharz, K., Kuipers, O. P. & Veening, J. W. Live Cell Imaging of Bacillus subtilis and *Streptococcus pneumoniae* using Automated Time-lapse Microscopy. *J Vis Exp*, doi:10.3791/3145 (2011).
23 Qin, L., Kida, Y., Imamura, Y., Kuwano, K. & Watanabe, H. Impaired capsular polysaccharide is relevant to enhanced biofilm formation and lower virulence in *Streptococcus pneumoniae*. *Journal of infection and chemotherapy : official journal of the Japan Society of Chemotherapy* **19**, 261-271 (2013).
24 Berg, K. H., Stamsas, G. A., Straume, D. & Havarstein, L. S. Effects of low PBP2b levels on cell morphology and peptidoglycan composition in *Streptococcus pneumoniae* R6. *J Bacteriol* **195**, 4342-4354, doi:10.1128/jb.00184-13 (2013).
25 Davis, K. M., Akinbi, H. T., Standish, A. J. & Weiser, J. N. Resistance to mucosal lysozyme compensates for the fitness deficit of peptidoglycan modifications by *Streptococcus pneumoniae*. *PLoS Pathog* **4**, e1000241, doi:10.1371/journal.ppat.1000241 (2008).
26 Massidda, O., Novakova, L. & Vollmer, W. From models to pathogens: how much have we learned about *Streptococcus pneumoniae* cell division? *Environ Microbiol* **15**, 3133-3157, doi:10.1111/1462-2920.12189 (2013).
27 Pinho, M. G., Kjos, M. & Veening, J. W. How to get (a)round: mechanisms controlling growth and division of coccoid bacteria. *Nat Rev Microbiol* **11**, 601-614 (2013).
28 Pichoff, S. & Lutkenhaus, J. Tethering the Z ring to the membrane through a conserved membrane targeting sequence in FtsA. *Mol Microbiol* **55**, 1722-1734, doi:10.1111/j.1365-2958.2005.04522.x (2005).
29 Parsons, J. B. & Rock, C. O. Bacterial lipids: metabolism and membrane homeostasis. *Prog Lipid Res* **52**, 249-276, doi:10.1016/j.plipres.2013.02.002 (2013).
30 Wang, J. *et al.* Platensimycin is a selective FabF inhibitor with potent antibiotic properties. *Nat New Biol* **441**, 358-361, doi:10.1038/nature04784 (2006).
31 Prudhomme, M., Attaiech, L., Sanchez, G., Martin, B. & Claverys, J. P. Antibiotic stress induces genetic transformability in the human pathogen *Streptococcus pneumoniae*. *Science (80-)* **313**, 89-92, doi:10.1126/science.1127912 (2006).
32 Sorg, R. A., Kuipers, O. P. & Veening, J. W. Gene expression platform for synthetic biology in the human pathogen *Streptococcus pneumoniae*. *ACS synthetic biology* **4**, 228-239, doi:10.1021/sb500229s (2015).
33 Corrigan, R. M., Abbott, J. C., Burhenne, H., Kaever, V. & Grundling, A. c-di-AMP is a new second messenger in Staphylococcus aureus with a role in controlling cell size and envelope stress. *PLoS Pathog* **7**, e1002217, doi:10.1371/journal.ppat.1002217 (2011).
34 Wakamatsu, T. *et al.* Role of RecJ-like protein with 5'-3' exonuclease activity in oligo(deoxy) nucleotide degradation. *J Biol Chem* **286**, 2807-2816, doi:10.1074/jbc.M110.161596 (2011).
35 Mechold, U., Ogryzko, V., Ngo, S. & Danchin, A. Oligoribonuclease is a common downstream target of lithium-induced pAp accumulation in Escherichia coli and human cells. *Nucleic Acids Res* **34**, 2364-2373, doi:10.1093/nar/gkl247 (2006).
36 Manuse, S., Fleurie, A., Zucchini, L., Lesterlin, C. & Grangeasse, C. Role of eukaryotic-like serine/threonine kinases in bacterial cell division and morphogenesis. *FEMS Microbiol Rev*, doi:10.1093/femsre/fuv041 (2015).

SUPPLEMENTARY EXPERIMENTAL PROCEDURES

Western blotting to determine phosphorylcholine in the cell wall

Bacterial lysates were obtained as described (see Materials & Methods: 'Quantitative analyses of cell wall phosphorylcholine'). Lysates were diluted in Tricine sample buffer (1M Tris-Cl pH 6.8), loaded on Tris acrylamide gels (29:1 acrylamide/bis, 0.3% SDS in 3M Tris-Cl pH 8.45, 80% glycerol), and ran at 100 V. Samples were transferred to a PVDF membrane using a semi-wet system (Bio-Rad) applied to 230 mA. Subsequently, the membrane was incubated with primary mAb TECP-15 (Sigma) followed by incubation with secondary HRP-conjugated rabbit anti-mouse antibody (DAKO). Signal was developed using ECL prime western blotting detection reagent (Amersham, GE Healthcare) and detected using enhanced chemiluminescence with a FluorChem E apparatus (Westburg).

Strain construction

Plasmids used in this study are listed in table S2, primers are listed in table S3. TIGR4 Δ*papP* and Δ*papP** were constructed as previously described[1]. Strain *papP-gfp* was constructed by transformation of *S. pneumoniae* TIGR4 wild type with plasmid pMK17-papP. This plasmid was constructed by amplifying *papP* on TIGR4 genomic DNA using oligos papP-FW-NotI and papP-RV-XbaI. The resulting PCR product was digested using NotI and XbaI and ligated in the corresponding sites of plasmid pMK17 (M. Kjos and J.-W. Veening, unpublished data) allowing insertion of a C-terminal fusion of *papP* with the monomeric super-folder GFP into the *bgaA* locus under control of the zinc-inducible promoter P_{czcD} (P_{Zn}). Transformants were selected on Columbia agar supplemented with tetracycline. Both strains CG16 (TIGR4, *bgaA*::P_{Zn}-*gfp-FtsA*) and CG18 (TIGR4, *papP::spc, bgaA*::P_{Zn}-*gfp-FtsA*) were constructed by transformation of *S. pneumoniae* TIGR4 wild type and Δ*papP*, respectively, with plasmid pJWV25-gfp-ftsA[2] in order to introduce a genetic fusion *gfp-ftsA* into the *bgaA* locus under control of the zinc inducible promoter P_{Zn}. In order to create the strains CG14 (*ftsZ::ftsZ-mKate2*) and CG22 (*papP::spc, ftsZ::ftsZ-mKate2*), *S. pneumoniae* TIGR4 wild type and Δ*papP*, were transformed with a DNA fragment *ftsZ-mKate2-ery* constructed as described by Beilharz *et al.*[3] and amplified with oligos ftsZ-up-FW and ftsZ-down-RV. This allows introduction of a genetic fusion *ftsZ-mKate2* in place of the native *ftsZ* gene under control of the native promoter. Transformants were selected on Columbia-agar with erythromycin. Strain Δ*fabH** was constructed in two steps. First, TIGR4 wild type was transformed with plasmid pMK11-fabH. This plasmid was obtained by amplifying the gene *fabH* on TIGR4 genomic DNA using oligos fabH-FW-EcorI and fabH-RV-SpeI and by ligating this product into

the plasmid pMK11 allowing insertion of an ectopic version of *fabH* under control of the zinc inducible promoter P_{Zn} into the *bgaA* locus. Afterwards, the resulting strain was transformed with a DNA fragment corresponding to the flanking region of *fabH* and an erythromycin marker. This latter construct was obtained by assembling the fragments corresponding to the upstream and the downstream region of *fabH* with the erythromycin marker using Gibson assembly. The upstream part was amplified from chromosomal DNA using primers fabH-up-FW and fabH-up-RV-ery and the downstream part using primers fabH-down-RV and fabH-down-FW-ery. The fragment corresponding to the erythromycin marker was amplified on plasmid pJWV502[2] using oligos ery-FW-fabH and ery-RV-fabH. Transformants were selected on Columbia agar supplemented with 0.25 µg/mL erythromycin.

Antibiotic susceptibility assay

Susceptibility to selected antibiotics was tested using the disc diffusion assay. Overnight cultures were suspended in PBS and used for inoculation of BA plates. Discs (SensiDisc, Becton Dickenson) were dispensed onto the plates after which 5 µL of the following antibiotics was applied: penicillin (0.25 µg/µL), erythromycin (3 µg/µL), trimethroprim (2.5 µg/µL), and ciprofloxacin (1 µg/µL) based on EUCAST standards. BA plates were placed at 37°C overnight and the diameter of bacteria-free zones were measured the next day.

Western blotting for detection of lipoproteins

Bacterial lysates were obtained as described (see Materials & Methods: 'Quantitative analyses of cell wall phosphorylcholine'). Lysates were diluted in sample buffer supplemented with 50 mM β-mercaptoethanol, loaded on pre-cast 4-15% gradient gels (Bio-Rad), and ran at 100 V. Samples were transferred to a PVDF membrane (Thermo Scientific) using a semi-wet blotting system (Bio-Rad) at 230 mA. Subsequently, the membrane was incubated with primary mAb against lipoproteins MetQ, PpmA, PsaA, and SlrA (mouse IgGs), and control protein enolase (Rabbit IgG) followed by incubation with secondary HRP-conjugated antibodies (DAKO). Signal was developed using ECL prime western blotting detection reagent (Amersham, GE Healthcare) and detected using enhanced chemiluminescence with a FluorChem E apparatus (Westburg). Densitometric analyses were performed with ImageJ software (Fiji)[4].

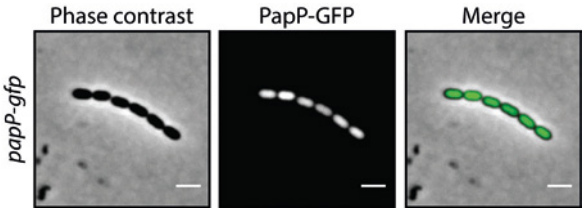

Figure S1 Cytoplasmic localization of PapP fused to the m(sf)GFP in live *S. pneumoniae* using fluorescence microscopy.

The GFP fluorescent signal (left panel) and the phase contrast image (middle panel) are overlaid in the right panel. Scale bar, 2 µm.

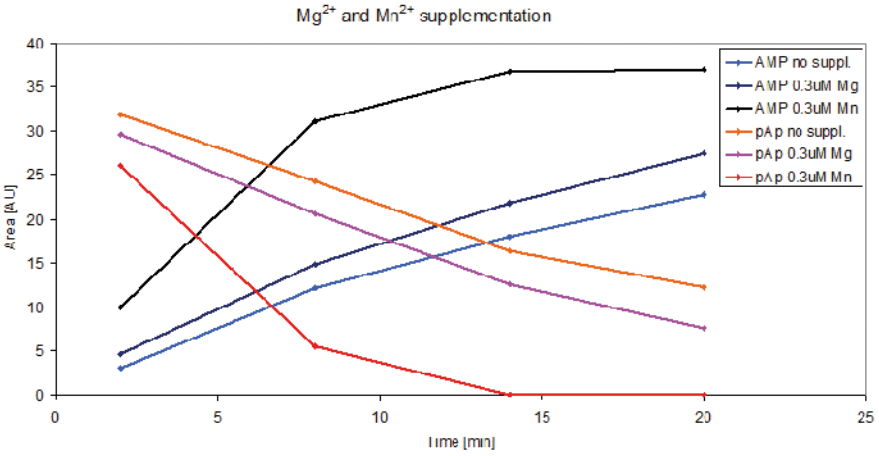

Figure S2 The effect of manganese (Mn^{2+}) and magnesium (Mg^{2+}) supplementation on PapP enzymatic activity towards substrate pAp.

0.1 µM PapP was incubated with 6 µM pAp in 30 mM potassium phosphate buffer pH 7. The stimulation effects of bivalent cations were observed as formation of the product (AMP) and decrease of the substrate (pAp) without or in presence of 0.3 µM $MgCl_2$ or $MnCl_2$.

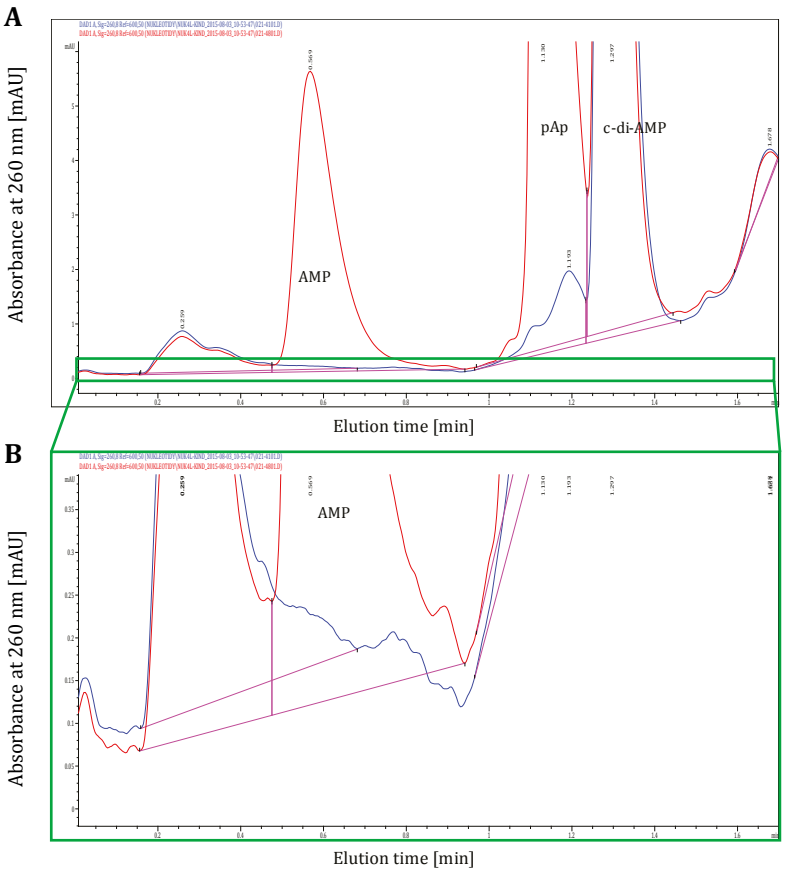

Figure S3 Comparison of *papP* mediated hydrolysis of c-di-AMP and pAp. 100 µM c-di-AMP was incubated at 25 °C in presence of 0.1 µM *papP*.

(**A**) After 10 min an aliquot of incubation mixture was analyzed for parental compound and AMP product using HPLC (blue line). Afterwards, pAp was added into the mixture (100 µM final concentration) and after 10 min incubation another aliquot was analyzed (red line). (**B**) A detailed view of the above shown chromatographic records with zoomed y-axis. No detectable presence of AMP (which should be eluted around 0.57 min) was found in presence of c-di-AMP substrate.

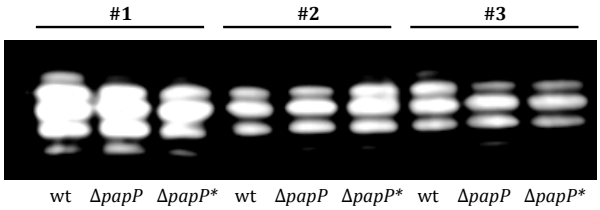

Figure S4 Cell-poles pointiness of the *papP* mutant.

Cell-poles angles were manually measured for > 200 cells for the wild type (black), Δ*papP* (white), Δ*papP** (grey) or the wild type subjected to 1 min chain disruption by bead beater (wild type BB). Results are illustrated at average ± SD and compared by one-way ANOVA and Tukey's multiple comparison test. Significance is illustrated with ****, P< 0.0001.

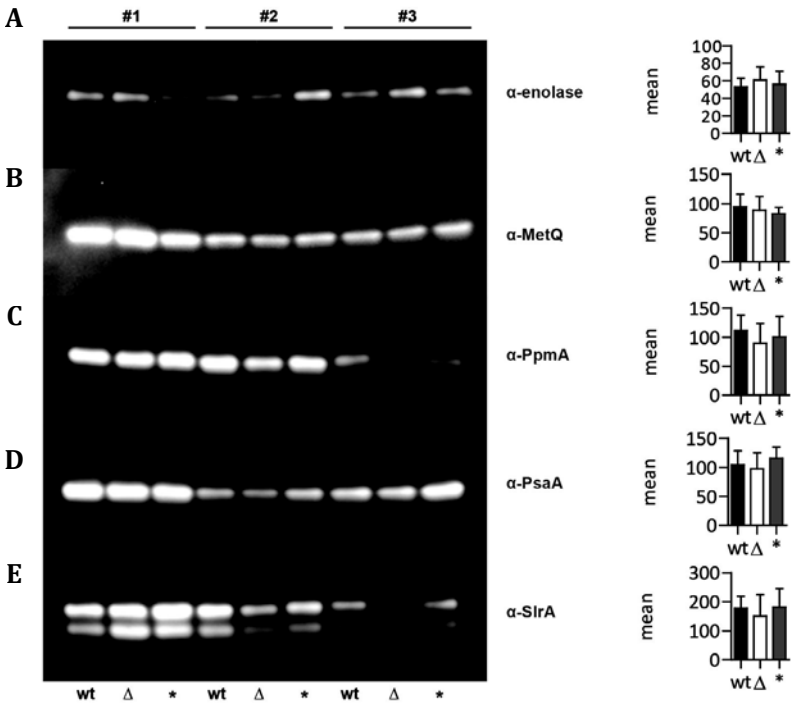

Figure S5 The influence of *papP* deletion on lipoprotein expression.

The presence of A. cytoplasmic protein enolase (control) and lipoproteins B. MetQ, C. PpmA, D. PsaA, and E. SlrA in wild type (wt), PapP mutant (Δ) and complemented (*) strains was analyzed by Western blotting. Results are illustrated from three independent experiments (#1, #2, #3). Graphs illustrate mean values from densitometric analysis of experiments #1, #2, and #3.

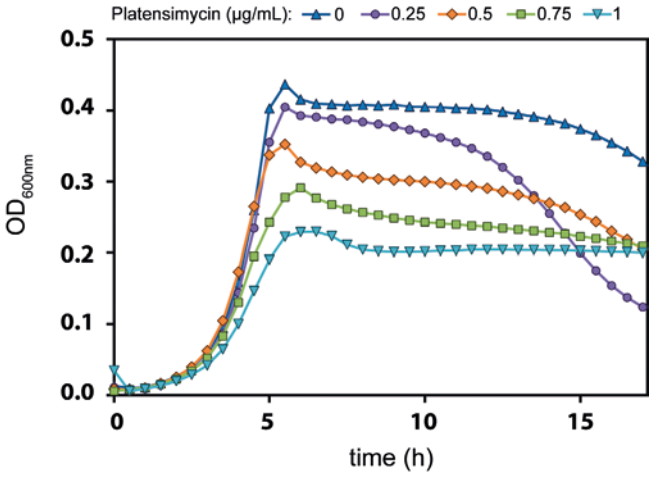

Figure S6 Determination of optimal platensimycin concentration.

Growth curve of TIGR4 wild type at 37 °C in liquid C+Y medium complemented with different platensimycin concentrations. An optimal concentration was used where the maximum optical density of *S. pneumoniae* was reduced by two-fold.

Remaining supporting information

Movies S1-5 can be found in the online version of this article at the publisher's website.

Table S1 Functional homologs (127) of PapP in other species

Protein ID	Protein Name	Length	Organism Name	GO Slim Func.
A0AJ24_LISW6	DHH family protein	311	Listeria welshimeri serovar 6b (strain ATCC 35897 / DSM 20650 / SLCC5334) []	0043167 : ion binding; 0003676 : nucleic acid binding; 0016787 : hydrolase activity
A4W2W3_STRS2	Putative uncharacterized protein	314	Streptococcus suis (strain 98HAH33) []	0043167 : ion binding; 0003676 : nucleic acid binding; 0016787 : hydrolase activity
A4VWL0_STRSY	Putative uncharacterized protein	253	Streptococcus suis (strain 05ZYH33) []	0043167 : ion binding; 0003676 : nucleic acid binding; 0016787 : hydrolase activity
A4IRR2_GEOTN	Phosphoesterase, DHH family protein	315	Geobacillus thermodenitrificans (strain NG80-2) []	0043167 : ion binding; 0003676 : nucleic acid binding; 0016787 : hydrolase activity
A3CNB8_STRSV	Conserved uncharacterized protein	311	Streptococcus sanguinis (strain SK36) []	0043167 : ion binding; 0016787 : hydrolase activity
A8YTI6_LACH4	Putative uncharacterized protein	318	Lactobacillus helveticus (strain DPC 4571) []	0043167 : ion binding; 0003676 : nucleic acid binding; 0016787 : hydrolase activity
A8FG63_BACP2	Putative uncharacterized protein ytqI	313	Bacillus pumilus (strain SAFR-032) []	0043167 : ion binding; 0003676 : nucleic acid binding; 0016787 : hydrolase activity
A8AWI8_STRGC	DHH subfamily 1 protein	314	Streptococcus gordonii (strain Challis / ATCC 35105 / CH1 / DL1 / V288) []	0043167 : ion binding; 0016787 : hydrolase activity
A7Z7L3_BACA2	YtqI	313	Bacillus amyloliquefaciens (strain FZB42) []	0043167 : ion binding; 0003676 : nucleic acid binding; 0016787 : hydrolase activity
A7GTQ2_BACCN	Phosphoesterase RecJ domain protein	310	Bacillus cereus subsp. cytotoxis (strain NVH 391-98) []	0043167 : ion binding; 0003676 : nucleic acid binding; 0016787 : hydrolase activity
A5VIX5_LACRD	Phosphoesterase, RecJ domain protein	319	Lactobacillus reuteri (strain DSM 20016) []	0043167 : ion binding; 0003676 : nucleic acid binding; 0016787 : hydrolase activity
A5IYN4_MYCAP	Putative uncharacterized protein	328	Mycoplasma agalactiae (strain PG2) []	0043167 : ion binding; 0016787 : hydrolase activity
A5IYN3_MYCAP	Putative uncharacterized protein	322	Mycoplasma agalactiae (strain PG2) []	0043167 : ion binding; 0003676 : nucleic acid binding; 0016787 : hydrolase activity
B1YKB7_EXIS2	Phosphoesterase RecJ domain protein	312	Exiguobacterium sibiricum (strain DSM 17290 / JCM 13490 / 255-15) []	0043167 : ion binding; 0003676 : nucleic acid binding; 0016787 : hydrolase activity
B1V8W9_PHYAS	Phosphoesterase family protein	326	Phytoplasma australiense []	0043167 : ion binding; 0003676 : nucleic acid binding; 0016787 : hydrolase activity
B1V8W7_PHYAS	Exopolyphosphatase-related protein	313	Phytoplasma australiense []	0043167 : ion binding; 0016787 : hydrolase activity
B1MZW6_LEUCK	Exopolyphosphatase-related protein	336	Leuconostoc citreum (strain KM20) []	0043167 : ion binding; 0003676 : nucleic acid binding; 0016787 : hydrolase activity
B1HX20_LYSSC	Putative uncharacterized protein	327	Lysinibacillus sphaericus (strain C3-41) []	0043167 : ion binding; 0003676 : nucleic acid binding; 0016787 : hydrolase activity
A9NE37_ACHLI	DHH domain protein	314	Acholeplasma laidlawii (strain PG-8A) []	0043167 : ion binding; 0003676 : nucleic acid binding; 0016787 : hydrolase activity
A9NE36_ACHLI	Putative uncharacterized protein	313	Acholeplasma laidlawii (strain PG-8A) []	0043167 : ion binding; 0003676 : nucleic acid binding; 0016787 : hydrolase activity
B2GB23_LACF3	Putative uncharacterized protein	319	Lactobacillus fermentum (strain NBRC 3956 / LMG 18251) []	0043167 : ion binding; 0003676 : nucleic acid binding; 0016787 : hydrolase activity
B7HFC1_BACC4	DHH subfamily 1 protein	356	Bacillus cereus (strain B4264) []	0043167 : ion binding; 0003676 : nucleic acid binding; 0016787 : hydrolase activity

B7GGS3_ANOFW	Bifunctional oligoRNAse and pAp phosphatase	315	Anoxybacillus flavithermus (strain DSM 21510 / WK1) []	0043167 : ion binding; 0003676 : nucleic acid binding; 0016787 : hydrolase activity
B5ZBR4_UREU1	DHH family protein	321	Ureaplasma urealyticum serovar 10 (strain ATCC 33699 / Western) []	0043167 : ion binding; 0003676 : nucleic acid binding; 0016787 : hydrolase activity
B4U293_STREM	DHH subfamily 1 protein	310	Streptococcus equi subsp. zooepidemicus (strain MGCS10565) []	0043167 : ion binding; 0003676 : nucleic acid binding; 0016787 : hydrolase activity
B3WC65_LACCB	Phosphoesterase, DHH family protein	318	Lactobacillus casei (strain BL23) []	0043167 : ion binding; 0003676 : nucleic acid binding; 0016787 : hydrolase activity
B3WBG0_LACCB	Exopolyphosphatase-related protein	310	Lactobacillus casei (strain BL23) []	0043167 : ion binding; 0003676 : nucleic acid binding; 0016787 : hydrolase activity
B3R0I6_PHYMT	Exopolyphosphatase-related protein	313	Phytoplasma mali (strain AT) []	0043167 : ion binding; 0003676 : nucleic acid binding; 0016787 : hydrolase activity
B3PNF5_MYCA5	DHH family phosphoesterase	325	Mycoplasma arthritidis (strain 158L3-1) []	0043167 : ion binding; 0003676 : nucleic acid binding; 0016787 : hydrolase activity
B3PNF4_MYCA5	DHH family phosphoesterase	329	Mycoplasma arthritidis (strain 158L3-1) []	0043167 : ion binding; 0003676 : nucleic acid binding; 0016787 : hydrolase activity
C0MHB3_STRS7	Putative uncharacterized protein	310	Streptococcus equi subsp. zooepidemicus (strain H70) []	0043167 : ion binding; 0003676 : nucleic acid binding; 0016787 : hydrolase activity
C0MC11_STRE4	Putative uncharacterized protein	310	Streptococcus equi subsp. equi (strain 4047) []	0043167 : ion binding; 0003676 : nucleic acid binding; 0016787 : hydrolase activity
B9E7A9_MACCJ	Putative uncharacterized protein	314	Macrococcus caseolyticus (strain JCSC5402) []	0043167 : ion binding; 0003676 : nucleic acid binding; 0016787 : hydrolase activity
B9DRQ1_STRU0	Putative uncharacterized protein	311	Streptococcus uberis (strain ATCC BAA-854 / 0140J) []	0043167 : ion binding; 0003676 : nucleic acid binding; 0016787 : hydrolase activity
B9DN99_STACT	Putative uncharacterized protein	313	Staphylococcus carnosus (strain TM300) []	0043167 : ion binding; 0003676 : nucleic acid binding; 0016787 : hydrolase activity
C6SPZ6_STRMN	Putative uncharacterized protein	310	Streptococcus mutans serotype c (strain NN2025) []	0043167 : ion binding; 0003676 : nucleic acid binding; 0016787 : hydrolase activity
C5WFM6_STRDG	Phosphoesterase, DHH family protein	313	Streptococcus dysgalactiae subsp. equisimilis (strain GGS_124) []	0043167 : ion binding; 0003676 : nucleic acid binding; 0016787 : hydrolase activity
C5J5G4_MYCCR	Mgp-operon protein 1	326	Mycoplasma conjunctivae (strain ATCC 25834 / HRC/581 / NCTC 10147) []	0043167 : ion binding; 0003676 : nucleic acid binding; 0016787 : hydrolase activity
C5J5G3_MYCCR	Mgp-operon protein 1	328	Mycoplasma conjunctivae (strain ATCC 25834 / HRC/581 / NCTC 10147) []	0043167 : ion binding; 0003676 : nucleic acid binding; 0016787 : hydrolase activity
C5D669_GEOSW	Phosphoesterase RecJ domain protein	315	Geobacillus sp. (strain WCH70) []	0043167 : ion binding; 0003676 : nucleic acid binding; 0016787 : hydrolase activity
C4L485_EXISA	Phosphoesterase RecJ domain protein	322	Exiguobacterium sp. (strain ATCC BAA-1283 / AT1b) []	0043167 : ion binding; 0003676 : nucleic acid binding; 0016787 : hydrolase activity
C1KVM2_LISMC	Putative uncharacterized protein	311	Listeria monocytogenes serotype 4b (strain Clip81459) []	0043167 : ion binding; 0003676 : nucleic acid binding; 0016787 : hydrolase activity
D2BPL5_LACLK	Phosphoesterase, DHH family	307	Lactococcus lactis subsp. lactis (strain KF147) []	0043167 : ion binding; 0016787 : hydrolase activity
D1J8W9_MYCHP	Putative uncharacterized protein	328	Mycoplasma hominis (strain ATCC 23114 / NBRC 14850 / NCTC 10111 / PG21) []	0043167 : ion binding; 0003676 : nucleic acid binding; 0016787 : hydrolase activity
D1J8W8_MYCHP	Putative uncharacterized protein	325	Mycoplasma hominis (strain ATCC 23114 / NBRC 14850 / NCTC 10111 / PG21) []	0043167 : ion binding; 0016787 : hydrolase activity

Table S1 Continued

Protein ID	Protein Name	Length	Organism Name	GO Slim Func.
C9RTI1_GEOSY	Phosphoesterase RecJ domain protein	315	Geobacillus sp. (strain Y412MC61) []	0043167 : ion binding; 0003676 : nucleic acid binding; 0016787 : hydrolase activity
C7TN24_LACRL	Phosphoesterase, DHH family protein	310	Lactobacillus rhamnosus (strain Lc 705) []	0043167 : ion binding; 0003676 : nucleic acid binding; 0016787 : hydrolase activity
C7THB2_LACRL	Phosphoesterase, DHH family protein	318	Lactobacillus rhamnosus (strain Lc 705) []	0043167 : ion binding; 0003676 : nucleic acid binding; 0016787 : hydrolase activity
C7TAL5_LACRG	Phosphoesterase; (SubName: Full=Phosphoesterase, DHH family protein)	318	Lactobacillus rhamnosus (strain ATCC 53103 / GG) []	0043167 : ion binding; 0003676 : nucleic acid binding; 0016787 : hydrolase activity
C7T7Z0_LACRG	Phosphoesterase, DHH family protein; (SubName: Full=Putative phosphoesterase)	310	Lactobacillus rhamnosus (strain ATCC 53103 / GG) []	0043167 : ion binding; 0003676 : nucleic acid binding; 0016787 : hydrolase activity
D5T587_LEUKI	Exopolyphosphatase-related protein (Putative)	330	Leuconostoc kimchii (strain IMSNU 11154 / KCTC 2386 / IH25) []	0043167 : ion binding; 0003676 : nucleic acid binding; 0016787 : hydrolase activity
D5H1H4_LACCS	Phosphoesterase, DHH family protein	318	Lactobacillus crispatus (strain ST1) []	0043167 : ion binding; 0016787 : hydrolase activity
D5E4R6_MYCCM	MgpA-like DHH family phosphoesterase	323	Mycoplasma crocodyli (strain ATCC 51981 / MP145) []	0043167 : ion binding; 0003676 : nucleic acid binding; 0016787 : hydrolase activity
D5E4R5_MYCCM	MgpA-like DHH family phosphoesterase	323	Mycoplasma crocodyli (strain ATCC 51981 / MP145) []	0043167 : ion binding; 0003676 : nucleic acid binding; 0016787 : hydrolase activity
D5DTV8_BACMQ	Oligoribonuclease (NanoRNAse); (EC=3.1.-.-)	312	Bacillus megaterium (strain ATCC 12872 / QMB1551) []	0043167 : ion binding; 0003676 : nucleic acid binding; 0016787 : hydrolase activity
D5DMX4_BACMD	Oligoribonuclease (NanoRNAse); (EC=3.1.-.-)	312	Bacillus megaterium (strain DSM 319) []	0043167 : ion binding; 0003676 : nucleic acid binding; 0016787 : hydrolase activity
D3VQT3_MYCA6	Putative uncharacterized protein	328	Mycoplasma agalactiae (strain 5632) []	0043167 : ion binding; 0016787 : hydrolase activity
D3VQT2_MYCA6	Putative uncharacterized protein	322	Mycoplasma agalactiae (strain 5632) []	0043167 : ion binding; 0003676 : nucleic acid binding; 0016787 : hydrolase activity
D3UNF8_LISSS	Phosphoesterase family protein	311	Listeria seeligeri serovar 1/2b (strain ATCC 35967 / DSM 20751 / CIP 100100 / SLCC 3954) []	0043167 : ion binding; 0003676 : nucleic acid binding; 0016787 : hydrolase activity
D3QC64_STALH	Phosphoesterase, DHH family protein	314	Staphylococcus lugdunensis (strain HKU09-01) []	0043167 : ion binding; 0003676 : nucleic acid binding; 0016787 : hydrolase activity
D3HCH7_STRG3	Putative uncharacterized protein	314	Streptococcus gallolyticus (strain UCN34) []	0043167 : ion binding; 0003676 : nucleic acid binding; 0016787 : hydrolase activity
D3FWZ7_BACPE	Phosphoesterase, DHH	317	Bacillus pseudofirmus (strain OF4) []	0043167 : ion binding; 0003676 : nucleic acid binding; 0016787 : hydrolase activity
D2P2K5_LISM1	Putative uncharacterized protein	312	Listeria monocytogenes serotype 1/2a (strain 08-5578) []	0043167 : ion binding; 0003676 : nucleic acid binding; 0016787 : hydrolase activity
NRNA_BACSU	Bifunctional oligoribonuclease and PAP phosphatase nrnA; (EC=3.1.-.-; AltName: Full=3'(2'),5'-bisphosphate nucleotidase; EC=3.1.3.7; AltName: Full=3'-phosphoadenosine 5'-phosphate phosphatase; Short=PAP phosphatase; AltName: Full=nanoRNAse)	313	Bacillus subtilis []	0016787 : hydrolase activity; 0043167 : ion binding; 0003676 : nucleic acid binding

MGP1_MYCPN	Mgp-operon protein 1; (Short=Mgp1; AltName: Full=ORF-1 protein)	324	Mycoplasma pneumoniae (strain ATCC 29342 / M129) []	0043167 : ion binding; 0003676 : nucleic acid binding; 0016787 : hydrolase activity
MGP1_MYCGE	Mgp-operon protein 1; (Short=Mgp1; AltName: Full=ORF-1 protein)	318	Mycoplasma genitalium (strain ATCC 33530 / G-37 / NCTC 10195) []	0043167 : ion binding; 0003676 : nucleic acid binding; 0016787 : hydrolase activity
Y549_MYCPN	Uncharacterized protein MG371 homolog	325	Mycoplasma pneumoniae (strain ATCC 29342 / M129) []	0043167 : ion binding; 0003676 : nucleic acid binding; 0016787 : hydrolase activity
D5TJZ3_BACT1	Phosphoesterase, DHH family protein	310	Bacillus thuringiensis (strain BMB171) []	0043167 : ion binding; 0003676 : nucleic acid binding; 0016787 : hydrolase activity
E0TWM6_BACPZ	Oligoribonuclease (NanoRNAse), 3',5'-bisphosphate nucleotidase	313	Bacillus subtilis subsp. spizizenii (strain ATCC 23059 / NRRL B-14472 / W23) []	0043167 : ion binding; 0003676 : nucleic acid binding; 0016787 : hydrolase activity
E0TJW2_MYCHH	MgpA-like DHH family phosphoesterase	321	Mycoplasma hyorhinis (strain HUB-1) []	0043167 : ion binding; 0016787 : hydrolase activity
E0TJW1_MYCHH	Putative MgpA-like protein	325	Mycoplasma hyorhinis (strain HUB-1) []	0043167 : ion binding; 0003676 : nucleic acid binding; 0016787 : hydrolase activity
D8MEQ1_LEUGT	Phosphoesterase, DHH family	338	Leuconostoc gasicomitatum (strain DSM 15947 / CECT 5767 / JCM 12535 / LMG 18811 / TB1-10) []	0043167 : ion binding; 0003676 : nucleic acid binding; 0016787 : hydrolase activity
D8GE84_LACCZ	Exopolyphosphatase-related protein	310	Lactobacillus casei (strain Zhang) []	0043167 : ion binding; 0003676 : nucleic acid binding; 0016787 : hydrolase activity
D7D206_GEOSC	3'(2'),5'-bisphosphate nucleotidase; (EC=3.1.3.7)	315	Geobacillus sp. (strain C56-T3) []	0016787 : hydrolase activity; 0043167 : ion binding; 0003676 : nucleic acid binding
D6XSR9_BACIE	Phosphoesterase RecJ domain protein	314	Bacillus selenitireducens (strain ATCC 700615 / DSM 15326 / MLS10) []	0043167 : ion binding; 0003676 : nucleic acid binding; 0016787 : hydrolase activity
E3IER1_GEOS0	3'(2'),5'-bisphosphate nucleotidase; (EC=3.1.3.7)	315	Geobacillus sp. (strain Y4.1MC1) []	0016787 : hydrolase activity; 0043167 : ion binding; 0003676 : nucleic acid binding
Q04EG3_OENOB	Phosphoesterase, DHH family protein	330	Oenococcus oeni (strain BAA-331 / PSU-1) []	0043167 : ion binding; 0003676 : nucleic acid binding; 0016787 : hydrolase activity
Q045P8_LACGA	Phosphoesterase, DHH family protein	339	Lactobacillus gasseri (strain ATCC 33323 / DSM 20243) []	0043167 : ion binding; 0003676 : nucleic acid binding; 0016787 : hydrolase activity
Q03VU5_LEUMM	Exopolyphosphatase-related protein	326	Leuconostoc mesenteroides subsp. mesenteroides (strain ATCC 8293 / NCDO 523) []	0043167 : ion binding; 0003676 : nucleic acid binding; 0016787 : hydrolase activity
Q03R41_LACBA	Phosphoesterase, DHH family protein	321	Lactobacillus brevis (strain ATCC 367 / JCM 1170) []	0043167 : ion binding; 0003676 : nucleic acid binding; 0016787 : hydrolase activity
Q03ER6_PEDPA	Phosphoesterase, DHH family protein	311	Pediococcus pentosaceus (strain ATCC 25745 / 183-1w) []	0043167 : ion binding; 0003676 : nucleic acid binding; 0016787 : hydrolase activity
F9UQJ8_LACPL	Phosphoesterase, DHH family	318	Lactobacillus plantarum (strain ATCC BAA-793 / NCIMB 8826 / WCFS1) []	0043167 : ion binding; 0003676 : nucleic acid binding; 0016787 : hydrolase activity
F9UND9_LACPL	Phosphoesterase, DHH family	325	Lactobacillus plantarum (strain ATCC BAA-793 / NCIMB 8826 / WCFS1) []	0043167 : ion binding; 0003676 : nucleic acid binding; 0016787 : hydrolase activity
Q1G945_LACDA	Phosphoesterase (DHH family)	319	Lactobacillus delbrueckii subsp. bulgaricus (strain ATCC 11842 / DSM 20081) []	0043167 : ion binding; 0003676 : nucleic acid binding; 0016787 : hydrolase activity
Y371_MYCGE	Uncharacterized protein MG371	324	Mycoplasma genitalium (strain ATCC 33530 / G-37 / NCTC 10195) []	0043167 : ion binding; 0003676 : nucleic acid binding; 0016787 : hydrolase activity
Q2NIG0_AYWBP	Exopolyphosphatase-related protein	316	Aster yellows witches'-broom phytoplasma (strain AYWB) []	0043167 : ion binding; 0003676 : nucleic acid binding; 0016787 : hydrolase activity
Q1WT30_LACS1	Phosphoesterase, DHH family protein	324	Lactobacillus salivarius (strain UCC118) []	0043167 : ion binding; 0003676 : nucleic acid binding; 0016787 : hydrolase activity

Table S1 Continued

Protein ID	Protein Name	Length	Organism Name	GO Slim Func.
Q1JCP8_STRPB	Phosphoesterase, DHH family protein	277	Streptococcus pyogenes serotype M12 (strain MGAS2096) []	0043167 : ion binding; 0003676 : nucleic acid binding; 0016787 : hydrolase activity
Q602E5_MYCH2	Putative uncharacterized protein	327	Mycoplasma hyopneumoniae (strain 232) []	0043167 : ion binding; 0003676 : nucleic acid binding; 0016787 : hydrolase activity
Q602E4_MYCH2	Putative uncharacterized protein	326	Mycoplasma hyopneumoniae (strain 232) []	0043167 : ion binding; 0003676 : nucleic acid binding; 0016787 : hydrolase activity
Q5WEE8_BACSK	Phosphoesterase	309	Bacillus clausii (strain KSM-K16) []	0043167 : ion binding; 0003676 : nucleic acid binding; 0016787 : hydrolase activity
Q5M4W8_STRT2	Putative uncharacterized protein	314	Streptococcus thermophilus (strain ATCC BAA-250 / LMG 18311) []	0043167 : ion binding; 0003676 : nucleic acid binding; 0016787 : hydrolase activity
Q4L745_STAHJ	Similar to unknown protein	312	Staphylococcus haemolyticus (strain JCSC1435) []	0043167 : ion binding; 0003676 : nucleic acid binding; 0016787 : hydrolase activity
Q4A6C5_MYCS5	Putative MgpA-like protein	318	Mycoplasma synoviae (strain 53) []	0043167 : ion binding; 0003676 : nucleic acid binding; 0016787 : hydrolase activity
Q4A673_MYCS5	Putative MgpA-like protein	322	Mycoplasma synoviae (strain 53) []	0043167 : ion binding; 0003676 : nucleic acid binding; 0016787 : hydrolase activity
Q4A672_MYCS5	Putative MgpA-like protein	322	Mycoplasma synoviae (strain 53) []	0043167 : ion binding; 0003676 : nucleic acid binding; 0016787 : hydrolase activity
Q49YD3_STAS1	Putative uncharacterized protein	311	Staphylococcus saprophyticus subsp. saprophyticus (strain ATCC 15305 / DSM 20229) []	0043167 : ion binding; 0003676 : nucleic acid binding; 0016787 : hydrolase activity
Q38YP2_LACSS	Putative phosphoesterase, DHH family	317	Lactobacillus sakei subsp. sakei (strain 23K) []	0043167 : ion binding; 0003676 : nucleic acid binding; 0016787 : hydrolase activity
Q2SSY0_MYCCT	DHH phosphoesterase family protein, putative	316	Mycoplasma capricolum subsp. capricolum (strain California kid / ATCC 27343 / NCTC 10154) []	0043167 : ion binding; 0003676 : nucleic acid binding; 0016787 : hydrolase activity
Q6YPH9_ONYPE	Exopolyphosphatase-related protein	322	Onion yellows phytoplasma (strain OY-M) []	0043167 : ion binding; 0003676 : nucleic acid binding; 0016787 : hydrolase activity
Q6MU91_MYCMS	DHH family protein (MgpA-like protein)	316	Mycoplasma mycoides subsp. mycoides SC (strain PG1) []	0043167 : ion binding; 0003676 : nucleic acid binding; 0016787 : hydrolase activity
Q6KIM3_MYCMO	Mgpa-like protein	329	Mycoplasma mobile (strain ATCC 43663 / 163K / NCTC 11711) []	0043167 : ion binding; 0003676 : nucleic acid binding; 0016787 : hydrolase activity
Q6F0X7_MESFL	Exopolyphosphatase-like	314	Mesoplasma florum (strain ATCC 33453 / NBRC 100688 / NCTC 11704 / L1) (Acholeplasma florum) []	0043167 : ion binding; 0003676 : nucleic acid binding; 0016787 : hydrolase activity
Q6F0I1_MESFL	Exopolyphosphatase-like	314	Mesoplasma florum (strain ATCC 33453 / NBRC 100688 / NCTC 11704 / L1) (Acholeplasma florum) []	0043167 : ion binding; 0003676 : nucleic acid binding; 0016787 : hydrolase activity
Q65G74_BACLD	YtqI	314	Bacillus licheniformis (strain DSM 13 / ATCC 14580) []	0043167 : ion binding; 0003676 : nucleic acid binding; 0016787 : hydrolase activity
Q8EVH9_MYCPE	Predicted phosphoesterase	323	Mycoplasma penetrans (strain HF-2) []	0043167 : ion binding; 0003676 : nucleic acid binding; 0016787 : hydrolase activity
Q8EPC9_OCEIH	Hypothetical conserved protein	315	Oceanobacillus iheyensis (strain DSM 14371 / JCM 11309 / KCTC 3954 / HTE831) []	0043167 : ion binding; 0003676 : nucleic acid binding; 0016787 : hydrolase activity
Q8E126_STRA5	DHH family protein	311	Streptococcus agalactiae serotype V []	0043167 : ion binding; 0003676 : nucleic acid binding; 0016787 : hydrolase activity

Q8DTN6_STRMU	Putative uncharacterized protein	310	Streptococcus mutans []	0043167 : ion binding; 0003676 : nucleic acid binding; 0016787 : hydrolase activity
Q8CS65_STAES	Putative uncharacterized protein	312	Staphylococcus epidermidis (strain ATCC 12228) []	0043167 : ion binding; 0003676 : nucleic acid binding; 0016787 : hydrolase activity
Q835K4_ENTFA	DHH family protein	317	Enterococcus faecalis (Streptococcus faecalis) []	0043167 : ion binding; 0003676 : nucleic acid binding; 0016787 : hydrolase activity
Q81KY2_BACAN	DHH subfamily 1 protein	310	Bacillus anthracis []	0043167 : ion binding; 0003676 : nucleic acid binding; 0016787 : hydrolase activity
Q817E6_BACCR	Phosphoesterase, DHH family protein	310	Bacillus cereus (strain ATCC 14579 / DSM 31) []	0043167 : ion binding; 0003676 : nucleic acid binding; 0016787 : hydrolase activity
Q7NC44_MYCGA	Exopolyphosphatase-related protein	322	Mycoplasma gallisepticum (strain R(low / passage 15 / clone 2)) []	0043167 : ion binding; 0003676 : nucleic acid binding; 0016787 : hydrolase activity
Q7NAY6_MYCGA	Phosphodiesterase	328	Mycoplasma gallisepticum (strain R(low / passage 15 / clone 2)) []	0043167 : ion binding; 0003676 : nucleic acid binding; 0016787 : hydrolase activity
Q74KV5_LACJO	Putative uncharacterized protein	321	Lactobacillus johnsonii (strain CNCM I-12250 / La1 / NCC 533) []	0043167 : ion binding; 0016787 : hydrolase activity
Q6YPI1_ONYPE	Putative uncharacterized protein	312	Onion yellows phytoplasma (strain OY-M) []	0043167 : ion binding; 0016787 : hydrolase activity
Q9K834_BACHD	BH3173 protein	314	Bacillus halodurans []	0043167 : ion binding; 0003676 : nucleic acid binding; 0016787 : hydrolase activity
Q9CHJ6_LACLA	Putative uncharacterized protein yheB	307	Lactococcus lactis subsp. lactis (strain IL1403) (Streptococcus lactis) []	0043167 : ion binding; 0016787 : hydrolase activity
Q9A0L5_STRP1	Phosphoesterase, DHH family protein	313	Streptococcus pyogenes serotype M1 []	0043167 : ion binding; 0003676 : nucleic acid binding; 0016787 : hydrolase activity
Q99TF9_STAAM	Putative uncharacterized protein	313	Staphylococcus aureus (strain Mu50 / ATCC 700699) []	0043167 : ion binding; 0003676 : nucleic acid binding; 0016787 : hydrolase activity
Q98RI7_MYCPU	MGPA-LIKE (Mycoplasma genitalium) PROTEIN	324	Mycoplasma pulmonis (strain UAB CTIP) []	0043167 : ion binding; 0003676 : nucleic acid binding; 0016787 : hydrolase activity
Q98PN0_MYCPU	MGPA-LIKE (Mycoplasma genitalium) PROTEIN	324	Mycoplasma pulmonis (strain UAB CTIP) []	0043167 : ion binding; 0003676 : nucleic acid binding; 0016787 : hydrolase activity
Q97QC1_STRPN	DHH subfamily 1 protein	311	Streptococcus pneumoniae []	0043167 : ion binding; 0003676 : nucleic acid binding; 0016787 : hydrolase activity
Q92BE0_LISIN	Lin1610 protein	311	Listeria innocua []	0043167 : ion binding; 0003676 : nucleic acid binding; 0016787 : hydrolase activity
Q8Y6V6_LISMO	Lmo1575 protein	311	Listeria monocytogenes []	0043167 : ion binding; 0003676 : nucleic acid binding; 0016787 : hydrolase activity
Q9PQ72_UREPA	Conserved hypothetical	321	Ureaplasma parvum serovar 3 (strain ATCC 700970) []	0043167 : ion binding; 0003676 : nucleic acid binding; 0016787 : hydrolase activity

Table S2 Plasmids used in this study

Plasmids	Relevant characteristics	Reference
pMK17-gfp-papP	*Amp, tet, bgaA,* P_{Zn}*-papP-gfp*	This study
pJWV25-gfp-ftsA	*Amp, tet, bgaA,* P_{Zn}*-gfp-ftsA*	[2]
pMK11-fabH	*Amp, tet, bgaA,* P_{Zn}*-fabH*	This study

Table S3 Primers used in this study

Name	Sequence
papP-FW-NotI	GCATGCGGCCGCAGAAAGAATTGAGGTTATTTATGGA
papP-RV-XbaI	CGCCTCTAGAGTTTTTAAGCAAGTTTTTTAACTTTTGG
fabH-FW-EcorI	CGATGGAATTCTTTTTGGAGGATTTGAAATAATGGC
fabH-RV-SpeI	GCGCACTAGTCTAAATTGTAAGAATGAGCGTGCC
fabH-up-FW	CTGGATGGTCAGGGTTGTTGGTATT
fabH-up-RV-ery	GTTCATATGAAAATTCCTCCGGGCGTTATTTCAAATCCTC-CAAAAATTGG
fabH-down-RV	TTCTCTGGCTTTCATCATCGGTTTC
fabH-down-FW-ery	TTTAACGGGAGGAAATAAGCTGGTAATCATGTGGTGAACACATTGTT
ery-FW-FabH	CCAATTTTTGGAGGATTTGAAATAACGCCCGGAGGAATTTTCATAT-GAAC
ery-RV-FabH	AACAATGTGTTCACCACATGATTACCAGCTTATTTCCTCCCGTTAAA
ftsZ-up-FW	CCTGTTATTGCTCGTATCGCCAAA
ftsZ-down-RV	ATCAAAACCGAACTCACCCTGTTGAT

Table S4 Antibiotic susceptibility using Disk Diffusion measured as inhibition zone (mm)

	Wild type	ΔPapP	ΔPapP*
penicillin	37 mm	48 mm	36 mm
erythromycin	26 mm	34 mm	24 mm
trimethroprim	12 mm	17 mm	10 mm

SUPPLEMENTARY REFERENCES

1 Cron, L. E. *et al.* Two DHH subfamily 1 proteins contribute to pneumococcal virulence and confer protection against pneumococcal disease. *Infect Immun* **79**, 3697-3710, doi:10.1128/iai.01383-10 (2011).

2 Beilharz, K. *et al.* Control of cell division in *Streptococcus pneumoniae* by the conserved Ser/Thr protein kinase StkP. *Proc Natl Acad Sci U S A* **109**, E905-913, doi:10.1073/pnas.1119172109 (2012).

3 Beilharz, K., van Raaphorst, R., Kjos, M. & Veening, J. W. Red Fluorescent Proteins for Gene Expression and Protein Localization Studies in *Streptococcus pneumoniae* and Efficient Transformation with DNA Assembled via the Gibson Assembly Method. *Appl Environ Microbiol* **81**, 7244-7252, doi:10.1128/aem.02033-15 (2015).

4 Schneider, C. A., Rasband, W. S. & Eliceiri, K. W. NIH Image to ImageJ: 25 years of image analysis. *Nat Methods* **9**, 671-675 (2012).

4

Cross-reactive Th17-mediated protection against pneumococcal carriage with a variable antigen

Kirsten Kuipers, Wouter S.P. Jong, Christa E. van der Gaast-de Jongh, Diane Houben, Fred van Opzeeland, Elles Simonetti, Saskia van Selm, Ronald de Groot, Marije I. Koenders, Taj Azarian, Elder Pupo, Peter van der Ley, Jeroen D. Langereis, Aldert Zomer, Joen Luirink, Marien I. de Jonge

Manuscript submitted

ABSTRACT

The current pneumococcal conjugate-based vaccines protect against severe disease, but only cover a limited number of serotypes. Furthermore, the efficacy of these vaccines is subject to serotype replacement, while polysaccharide conjugate valence has reached its maximum with regard to cost-efficiency. Hence, vaccines based on antigens other than polysaccharides are needed to protect against pneumococcal infection and to further improve current vaccination strategies. Pneumococcal protein antigens, such as pneumococcal surface protein A (PspA), have been shown to evoke strong protection. However, PspA is a variable protein and therefore less suitable as vaccine antigen. We have previously shown that outer membrane vesicles (OMV) displaying the N-terminal α1α2 fragment of PspA induce strong homologous protection against *Streptococcus pneumoniae* colonization, upon intranasal vaccination. Here, we sought to examine the cross-reactive potential of a variable antigen inducing Th17-mediated immunity. We show that LPS-inactivated OMVs expressing TIGR4 α1α2 still strongly protect against colonization in a Th17 dependent manner. Furthermore we set out to assess cross-reactivity of the OMV vaccine expressing TIGR4 α1α2 with other pneumococcal strains. By using sequences of 345 pneumococcal clinical isolates, we identified 35 groups based on the α1α2 fragment of PspA. Representative strains from each group were used to conduct an *ex vivo* screening to determine Th17 cross reactivity. These *ex vivo* recall responses were strongly predictive for *in vivo* IL17A levels in the nasal tissue of mice following heterologous challenge. This is turn was associated with a reduction in pneumococcal colonization. Although PspA is highly variable, the 35 groups accounted for 90% prevalence in a large carriage cohort and a single (TIGR4) α1α2 type would theoretically cover 19.1% of these strains. In conclusion, this work describes an easy tool to assess vaccine cross-reactivity and illustrates the extent to which a variable protein can offer cross-protection.

INTRODUCTION

Respiratory bacterial infections remain a major cause of severe morbidity and mortality worldwide, both in infants as well as in adults[1,2]. Vaccination is considered one of the most cost-effective strategies to reduce the global burden of disease, the associated healthcare costs and the risk of emerging antibiotic-resistant strains[3]. Vaccination against *Streptococcus pneumoniae* is implemented in different parts of the world. However, it is estimated that still about one million children die of pneumococcal disease every year (WHO)[1,2]. Pneumococcal polysaccharide conjugate vaccines (PCVs) are designed based on epidemiological data from the Western world. These protect against serotypes that are most prevalent and are most frequently associated with severe invasive disease. PCVs induce serotype specific protection against 13 of the 97 identified serotypes that are circulating world-wide[4]. This is an important limitation and during the last decade, non-vaccine variants of *S. pneumoniae* have emerged, causing severe invasive disease[5-7]. The phenomenon of strain or serotype replacement and the remaining high disease burden in developing countries highlight the need for broader protective vaccines against *S. pneumoniae*.

Currently, there is much attention for the development of novel, broadly protective, protein-based vaccines[8-13]. Vaccination with variable proteins, which are generally highly immunogenic, are known to offer strong protection[11,14-16]. Nevertheless, similar to capsule-based vaccines, immunization with protein antigens leads to antigen-specific antibody responses that protect only against a selection of strains[4]. Therefore, variable proteins have been considered less suitable antigens for a universal vaccine given their strong epitope heterogeneity. Whether variable proteins are suitable antigens when aiming at the induction of cellular immunity, e.g. Th17 memory, is still unclear.

In this study, we investigated the feasibility of inducing cross-protection against pneumococcal carriage using a variable protein antigen known to induce Th17 immunity. The best studied protein vaccine target in *S. pneumoniae* is Pneumococcal Surface Protein A (PspA), which is a virulence factor that binds lactoferrin and interferes with complement-mediated opsonization[17,18]. PspA is expressed by most pneumococcal strains and it consists of an N-terminal alpha-helical coiled coil domain, the most variable and most immunogenic part, a proline rich region and a choline binding domain. PspA is classified into three different families and six different clades based on the Clade Defining Region (CDR)[19]. It has been proposed that a vaccine combining family 1 and family 2 would provide universal protection against pneumococcal disease, but protection was not observed for all pneumococcal strains[20-26]. Previously, we generated recombinant *Salmonella* outer membrane vesicles (OMVs) exposing the coiled

coil domain of PspA, the α1α2 fragment, at the surface. We have shown that vaccination with this formulation confers strong protection against pneumococcal colonization[14].

Using bioinformatics analysis on the sequences of 345 invasive pneumococcal isolates we designed a novel PspA classification system based on the α1α2 domain of PspA. Vaccine cross-reactivity with these clinical strains was assessed in a Th17-based *ex vivo* screen, in which murine derived splenocytes were restimulated with whole pneumococcal cells. The IL17A levels, measured *ex vivo,* strongly correlated with the *in vivo* IL17A levels detected in the nasal cavity following infection with the clinical strains, which in turn highly correlated with protection against colonization. Moreover, based on the prevalence in a large carriage cohort, we estimated that the 35 α1α2 subtypes from our study accounted for 90% prevalence. Also, a vaccine consisting of this α1α2 subtype would cover approximately 19.1% of all circulating pneumococcal strains, which suggests that a universal vaccine, (partly) based on variable proteins is feasible.

MATERIALS AND METHODS

Bacterial strains and growth conditions

S. Typhimurium SL3261 Δ*tolRA*, *E. coli* TOP10F' and BL21(DE3) were grown at 37 °C in LB medium containing 0.2% glucose. When appropriate, kanamycin was used at a concentration of 25 μg/ml, tetracyclin at 6.25 ug/ml, and chloramphenicol at 30 μg/ml. SL3261Δ*tolRA*Δ*msbB* was grown at 30 °C in LB medium lacking NaCl (LB-0), supplemented with 2 mM $CaCl_2$, 2 mM $MgCl_2$ and 0.2% glucose. Pneumococcal laboratory strains and human clinical isolates, belonging to the Pneumococcal Bacteremia Collection Nijmegen (PBCN), were grown in Todd Hewitt Broth supplemented with yeast extract until mid-log phase and stored at -80°C until further usage[27,28]. Pneumococcal stocks, used for mouse challenge infections containing 10^6 colony forming units (CFU) in 10 μL phosphate buffered saline (PBS), were prepared as described previously[14].

Construction of the Δ*msbB* OMV production strain

A Δ*msbB* derivative of *S.* Typhimurium SL3261Δ*tolRA* was created by allelic exchange through double cross-over homologous recombination essentially as described by Kaniga *et al.* with some amendments[29]. Briefly, overlapping extension PCR was used to amplify a fragment representing an almost completely truncated form of *msbB* plus the ~1000 bp up- and downstream regions of *msbB* on the S. Typhimurium SL3261 genome. S. Typhimurium SL3261 genomic DNA was used as a template and the respective primer pairs used were msbB_a_XbaI

fw + msbB_b rv and msbB_c fw + msbB_d_XbaI rv (Table S1). The PCR product was digested with XbaI and cloned into XbaI-cut suicide vector pSB890 (Tetracyclin^R, Sucrose^S)[30]. The pSB890-Δ*msbB* suicide vector was transformed into the *E. coli* donor strain β2168Δnic35 that lacks the *asd* gene and can only grow in the presence of diaminopimelic acid (DAP). The resulting transformant was mated with Salmonella recipient strain SL3261Δ*tolRA* for 8 h on plate in the presence of DAP (50 µg/ml). Tetracyclin resistant Salmonella transconjugants were selected on plate in the absence DAP. Resolution of merodiploids and replacement of the wild-type locus with Δ*msbB* were achieved by selecting for resistance of the Salmonella mutants to sucrose (10%) on LB-0 plates. Positive clones were identified by PCR across the *msbB* locus using primers msbB_seq fw and msbB_seq rv (Table S1). In accordance with reports describing an altered sensitivity of *Salmonella* Δ*msbB* strains towards salts[31], SL3261Δ*tolRA*Δ*msbB* was maintained on LB-0 (agar) medium supplemented with 2 mM Mg^{2+} and 2 mM Ca^{2+} at 30 °C.

Mass spectrometry on lipopolysaccharides

The lipopolysaccharides (LPS) from *S.* Typhimurium SL3261 and mutant derivative SL3261Δ*tolRA*Δ*msbB* were isolated by a simplified hot-phenol water extraction followed by reversed phase solid phase LPS extraction (RP-SPE) using C4 ZipTips® micropipette tips (Millipore)[32]. Negative-ion electrospray ionization Fourier transform mass spectrometry (ESI-FT-MS) was performed on an LTQ Orbitrap XL instrument (Thermo Scientific). Typically, 5 µl of LPS in 50% (v/v) 2-propanol, 0.07 mM TEAA pH 8.5 were infused into the FT-MS by static nano-ESI[33,34]. The spray voltage was set to -1 kV and the capillary temperature to 200 °C. Under these ionization conditions, no appreciable fragmentation of LPS was produced. The MS instrument was calibrated with a Pierce Negative Ion Calibration Solution (Thermo Scientific) and internally with taurocholic acid following standard procedures provided by the manufacturer (Thermo Scientific). Fragmentation analysis of intact LPS was carried out by in-source collision-induced fragmentation (SID). Y- and B-type fragment ions, corresponding to the lipid A and oligosaccharide moieties of LPS, respectively, were generated by SID at a potential difference of 100 V**.** Fragment ions are annotated according to the nomenclature of Domon and Costello[35]. Mass spectra were charge-deconvoluted using the Xtract tool of Thermo Xcalibur 3.0 software (Thermo Scientific). All mass values given refer to monoisotopic molecular masses. Proposed LPS compositions are based on the chemical structure of the LPS from *S.* Typhimurium reported previously[36-39].

Plasmid construction

Plasmids used for expression of HbpD-α1α2 variants have a pEH3 backbone[40]. Plasmids pHbpD(Δd1) and pHbpD(Δd2) in which sequences coding for side domains d1 and d2 of the Hbp passenger were substituted for Gly/Ser-encoding linkers containing *SacI* and *BamHI* restriction sites have been described[41]. Plasmids for the expression of Hbp fused to the PspA α1α2 fragments of strain PBCN79 or PBCN87 were created as follows. First, fragments encoding the α1 regions of both strains were amplified by PCR with flanking *SacI/BamHI* sites and overhangs suitable for In-Fusion cloning. Chromosomal DNA of PBCN79 and PBCN87 was used as a template in combination with the primer pairs a1_PBCN79 fw + a1_PBCN79 rv and a1_PBCN87 fw + a1_PBCN87 rv, respectively (Table S1). The PCR products were cloned into SacI/BamHI digested pHbpD(Δd1) using In-Fusion technology according to manufacturer's protocols (Clontech Laboratories, Inc., Mountain view, CA, USA), yielding pHbpD(Δd1)-α1(PBCN79) and pHbpD(Δd1)-α1(PBCN87)[41]. Second, pHbpD(Δd2)-α2(PBCN79) and pHbpD(Δd2)-α2(PBCN87), encoding α2 fragments fused to the d2 position of Hbp, were generated making use of the same methodology. The respective primer pairs used for PCR were a2_PBCN79 fw + a2_PBCN79 rv and a2_PBCN87 fw + a2_PBCN87 rv, and SacI/BamHI-digested pHbpD(Δd2) was used as the accepting plasmid. Third, plasmids for expression of Hbp fused to both the α1 and the α2 fragments were created by substituting the *NdeI/NsiI* fragments of pHbpD(Δd1)-α1(PBCN79) and pHbpD(Δd1)-α1(PBCN87) for those of pHbpD(Δd2)-α2(PBCN79) and pHbpD(Δd2)-α2(PBCN87), respectively, resulting in pHbpD-α1α2(PBCN79) and pHbpD-α1α2(PBCN87). Sequences were confirmed by semi-automated DNA sequencing.

OMV vaccine production

Isolation procedure and design of *S.* Typhimurium OMVs displaying α1α2 from the *S. pneumoniae* TIGR4 background was previously described[14]. To isolate OMVs derived from SL3261Δ*tolRA*Δ*msbB* displaying α1α2 from either PBCN87 or 79 a modified growth and expression regime was used. SL3261Δ*tolRA*Δ*msbB* cells harboring HbpD-α1α2 expression vectors were grown until an OD_{660} of ~0.02, at which 50 μM of IPTG was added to the culture to induce expression of HbpD-α1α2. Growth was continued overnight after which OMVs were isolated from the culture medium and expression was confirmed as described previously[14,42].

Alignment and classification of α1α2 domains

Genome sequences and serotypes were obtained from Cremers *et al.*[27,28]. PspA coding genes were identified from the genome sequences by aligning the

conserved signal sequences, the CDRs and the conserved C-terminal domains against all protein coding sequences of the genomes using blastp[43]. Conserved protein domains in the α1α2 PspA coding sequence were detected by aligning the protein sequence between the signal sequence and the proline rich region (PRR) with MEME using default settings[44]. Variable domains were numbered according to their sequence conservation. Overrepresented peptides were detected by associating the number of unique amino acid 13mers in the α1α2 region with the level of IL17A production after splenocyte stimulation.

Mouse immunization and challenge

Seven week old female C57Bl/6 (Charles River Laboratories), C3H/HeJ (Jackson Laboratories), and IL17R$^{-/-}$ mice received three intranasal (i.n.) immunizations under anaesthetics (2.5% v/v isoflurane, AU Veterinary Services) of 10 µL containing 8 OD units of Δ*msbB* OMVs (corresponding to ~ 4 µg of total protein content) displaying PspA fragments α1α2 in PBS with 15% glycerol[14]. C3H/HeJ mice were immunized with OMVs derived from *S.* Typhimurium containing wild-type *msbB*. IL-17R−/− mice were obtained from Amgen Washington and bred in Louisiana State University Health Sciences Center Animal Care Facilities[45]. Three weeks after the final immunization, mice were i.n. challenged with *S. pneumoniae* and three days post-infection euthanized. Mice were terminally bled from which serum was obtained and stored for later analyses. Nasal tissue was harvested, homogenized using IKA T10 basic blender and used for inoculation of Gentamicin Blood Agar (Mediaproducts BV) plates to determine bacterial recovery (Log_{10} CFU). Remaining nasal tissue was stored and spleens were harvested for further analysis. All animal work was performed with approval of the Radboud University Medical Center Committee for Animal Ethics (RU-DEC2014-206).

Whole cell ELISA

Bacterial cultures were heat-killed at 56 °C for 1 h and taken up in an equal volume of PBS to coat Maxisorp high binding affinity plates (NUNC) at 4 °C overnight. Next day, the plates were blocked with 1% bovine serum albumin (Sigma), incubated with pooled serum from mice immunized with *S.* Typhimurium Δ*msbB* OMV expressing TIGR4 α1α2 and subsequently with IgG specific goat anti-mouse IgG conjugated horse radish peroxidase (eBioscience) at 37 °C for 1 h. Between incubation steps, wells were washed with PBS containing 0.05% Tween-20 (Merck). Development was done using 100 µg/mL 3,3',5,5'-Tetramethylbenzidine (Sigma-Aldrich) in 0.05 M phosphate-citrate substrate buffer (Sigma-Aldrich) and was stopped using 1.8 M H_2SO_4. Optical density was measured at 450 nm.

Human PBMC isolation & stimulation

Peripheral Blood Mononuclear Cells (PBMCs) were isolated from whole blood with density gradient centrifugation using Lymphoprep (Axis-Shield). The blood was diluted 1:1 with PBS and added on top of the Lymphoprep. Centrifugation was performed at 750 x *g* to separate PBMCs from the other blood components. PBCMs and CBMCs were harvested and washed two times with PBS and centrifuged at 500 x *g*. Subsequently, the cells were washed in RPMI-glutaMax© (Life Technologies) with 10% Fetal Calf Serum (FCS, Greiner Bio-One) and centrifuged at 250 x *g*. PBMCs were resuspended in RPMI+ 10% FCS and counted the cells using Türk's solution (Merck) and a haemocytometer (Bürker Bright-Line Labor Optik).

PBMCs ($5x10^5$ cells/well) were added to round-bottom 96 wells plates (Nunc) and incubated with an equal volume of the wild-type or Δ*msbB* OMVs expressing Hbp. PBMCs were incubated at 37 °C and 5% CO_2 for 24 h. Supernatant was harvested using centrifugation at 450 x *g* and stored at -20 °C until further analysis.

Mouse splenocyte isolation and stimulation

Harvested spleens were temporarily stored in RPMI-glutaMax© (Life Technologies) with 10% Fetal Calf Serum (FCS, Greiner Bio-One) and 1% penicillin streptomycin and transferred through a 70 µm cell strainer (BD Falcon) to obtain single cell suspensions. Erythrocytes were lysed using RBC lysis buffer (eBioscience), after which cells were thoroughly washed. Splenocytes ($5x10E^5$ cells/well) were added to round-bottom 96 wells plates (Nunc) and mixed with $5x10^5$ CFU of the pneumococcal cultures at MOI of 1 in an end volume of 200 µl. Cells were incubated at 37 °C and 5% CO_2 for 72 h. Supernatant was harvested by centrifugation at 450 x *g* and stored at -20 °C until further analysis.

Cytokine analyses

Human TNFα and IL1β concentrations were measured in human cell supernatants using ELISA kits (Pelpair reagent set, Sanquin, Amsterdam, The Netherlands). These kits were used according to the manufacturer's instructions. The detection limit for both TNFα and IL1β was 19.5 pg/ml.

Mouse IL17A concentrations were measured in the supernatants collected after restimulation of the splenocytes using the commercial Mouse IL-17A ELISA MAX™ Standard (Biolegend, ITK diagnostics) according to the manufacturer's instructions. The detection limit was 31.25 pg/ml.

IL17A production in mouse nasal samples was determined with Cytometric Bead Array (Becton Dickinson) according to manufacturer's instructions, using the Mouse Enhanced Sensitivity buffer kit in combination with the Enhanced

Sensitivity Flex set for IL-17A (Becton Dickinson). Concentrations were calculated using Soft Flow FCAP Array v1.0 (Becton Dickinson).

Vaccine coverage prediction

To determine the prevalence of PspA α1α2 variants, and therefore the projected vaccine coverage, available sequences from pneumococcal isolates collected in large carriage cohort were used. We assessed 614 previously reported pneumococcal carriage isolates from Massachusetts collected from 2001-2007. The details of this study population have previously been reported[46]. In addition, we extended this sample to include 738 carriage isolates collected from 2009-2014 from the same study population. In total, 1352 isolates including 33 serotypes were evaluated to determine their α1α2 genotype. The 35 *pspA* α1α2 variants were used to generate a custom database that was provided to SRST2 v0.2.0[47]. For each isolate, Illumnia MiSeq 2x150 bp sequencing reads were mapped to variants using default settings (90% minimum nucleotide identity and 10% maximum nucleotide divergence) to determine the variant genotype (Table S3).

Statistical analyses

All statistical analyses were performed using GraphPad Prism version 5.0 (Graphpad Software). Human cytokine data were analyzed using Wilcox-on-signed rank test. For bacterial recovery data, the Grubbs outlier test was used to test for significant outliers. The One-Way Anova Kruskall Wallis with Bonferroni post-test for multiple groups or Mann-Whitney t test for two groups were used for comparisons of vaccine-induced reduction in pneumococcal colonization and nasal IL17A immune responses. *Ex vivo* Th17 screening data were compared to RPMI using Univariate analysis of variance with Dunnet's post test in SPSS.

RESULTS

Protection upon immunization with LPS-detoxified OMVs

Outer membrane vesicles, decorated with the PspA fragment α1α2 using our Hbp-based antigen display platform, and produced by attenuated and hyper-vesiculating *S*. Typhimurium SL3261Δ*tolRA*, were previously used for intranasal vaccination[14]. This formulation conferred strong protection against pneumococcal colonization, illustrating the potential of an OMV/PspA-based vaccine[14]. Since a pneumococcal vaccine is intended for use in humans, we created a LPS-detoxified OMV production strain. To this end, we inactivated the *msbB* gene of strain SL3261Δ*tolRA* to produce OMVs with LPS carrying a penta-acylated lipid A

moiety, which is less immune reactive in humans compared to wild-type hexa-acylated lipid A due to reduced responses via Toll-like receptor (TLR)4 activation[48]. It was confirmed by ESI-FT mass spectrometry that the Δ*msbB* mutant has reduced hexacylated lipid A and increased pentacylated A (Figure S1A-B). Human PBMCs stimulated with OMVs produced by strain SL3261Δ*tolRA*Δ*msbB* produced significantly reduced TNFα and IL1β compared to OMVs produced by SL3261Δ*tolRA* harboring an intact *msbB* (Figure S1C-D), which confirmed its detoxified phenotype. Importantly, SDS-PAGE analysis showed that efficient Hbp-mediated display of the PspA fragment α1α2 was sustained in Δ*msbB* OMVs, to a similar level as in the Salmonella OMVs used in our previous studies carrying non-modified LPS (Figure S1E)[14]. Furthermore, a reduction in pneumococcal colonization was observed upon immunization with Δ*msbB* OMVs decorated with the PspA fragment α1α2, illustrating that OMVs derived from a Δ*msbB* Salmonella strain are still suitable for vaccination (Figure 1A). In agreement with this observation, reduction in pneumococcal load was independent of LPS-mediated signaling, which was confirmed by the use of C3H/HeJ mice, containing a point mutation in the *Tlr4* gene, resulting in reduced responses to LPS (Figure 1B)[49].

Mice vaccinated with OMVs expressing TIGR4 α1α2 showed strong levels of nasal IL17A (Figure 1C), indicating that the Δ*msbB* had no effect on the induction of IL-17A. Based on these and previous data we hypothesize that the Th17 response induced by our OMV-based vaccine contributes to a reduction in *S. pneumoniae*[14]. To confirm the role of IL17 in the reduction of colonization, IL17R deficient mice were vaccinated OMVs expressing TIGR4 α1α2 and received an infection with *S. pneumoniae*. Three days post-infection bacterial recovery resulted in absence of protection (i.e. no reduction of colonization) (Figure 1D)[45]. Therefore, we conclude that OMVs decorated with the PspA fragment α1α2 induce Th17-mediated protection against colonization.

Novel classification of PspA based on the α1α2 region

To determine Th17-mediated cross-protection of our OMV-based vaccine against other pneumococcal strains, we made use of a sequenced collection of 349 invasive clinical isolates obtained from patients with pneumococcal bacteremia, hospitalized in two hospitals in The Netherlands between 2001-2011[27,28]. PspA sequences were aligned and classified based on the α1α2 fragment (Figure 2A). This fragment was (partly) undetectable in 4 pneumococcal strains due to sequencing errors, and these strains were therefore excluded from further study.

To explore the variability of the α1α2 fragment between pneumococcal strains, sequences were aligned using MEME. This resulted in the division of the

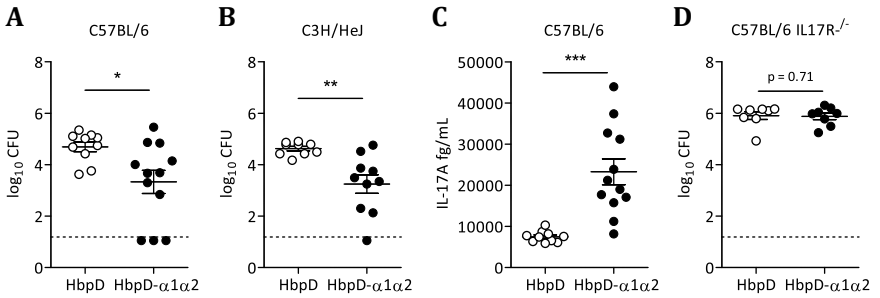

Figure 1 OMV-induced reduction in pneumococcal colonization is IL17-dependent.

Mice were vaccinated with control OMVs (HbpD; open circles) or OMVs displaying α1α2 (Hbp-α1α2; black circles) derived from (**A, C, D**) *Salmonella* Δ*msbB* or (**B**) wildtype (*msbB*$^{+}$) *Salmonella*. Intranasal infection was performed using TIGR4 (homologous challenge). Bacterial recovery (Log CFU) was calculated 3 days post-infection from the nasopharyanx of (**A**) C57BL/6, (**B**) C3H/HeJ, and (**D**) IL17R$^{-/-}$ mice. (**C**) IL17A measured in the nasal tissue of vaccinated C57BL/6 mice. Data represent individual mice and bars indicate group mean ± SEM. *, $p < 0.05$; **, $p < 0.01$.

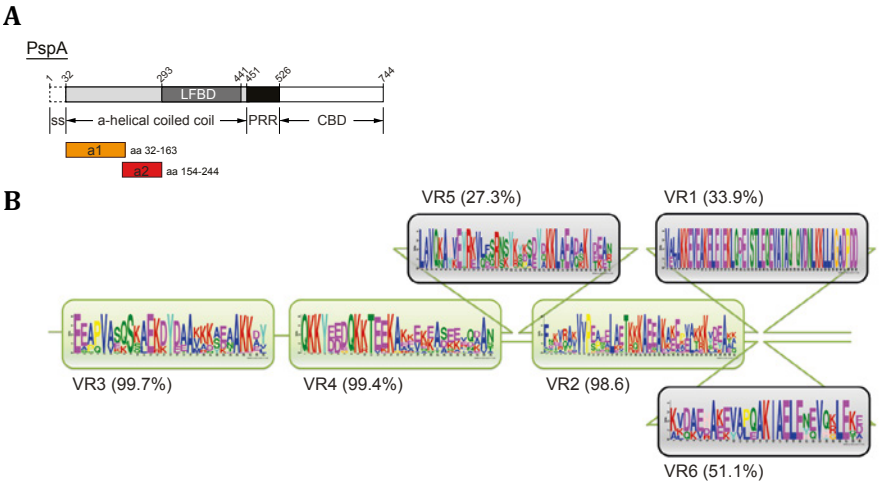

Figure 2 Vaccine α1α1 fragment.

(**A**) Schematic overview of TIGR4 PspA α1α2 adapted from Kuipers *et al.*[14]. The slightly overlapping fragments were selected to cover the α-helical coiled coil domain (α1 and α2. The lactoferrin-binding domain (LFBD), the Proline-rich region (PRR) and the choline-binding domain (CBD) of PspA were not included in the vaccine. (**B**) Alignment of the α1α2 regions derived from 345 sequenced pneumococcal invasive isolates. Based on amino acid identity, MIME analysis subdivided the α1α2 vaccine region into six Variable Regions (VR1-6). Some VRs appeared more conserved and were alternately expressed by the clinical isolates. Percentage of VR expression among pneumococcal isolates was calculated. Presence of the VR is shown in percentages.

α1α2 fragment into six variable regions (VRs), named VR1-6, respectively (Figure 2B; Table S2). Sequences in VR1 were the most conserved among pneumococcal strains, whereas sequences in VR6 were most variable. This means that sequence variation increased with increasing VR number. Also, these VRs were not present in all pneumococcal strains. The majority of clinical isolates expressed VR2 (98.6%), VR3 (99.7%) and VR4 (98.4%). A selection of strains had VR5 (27.3%) in between VR4 and VR2. Either VR1 (33.9%) or VR6 (51.1%) were present after VR2. Based on the α1α2 fragment homology, the 345 strains were divided into 35 different groups (Table S1). Interestingly, this novel α1α2 classification was associated with serotype distribution. Certain α1α2 types were present in specific serotypes, although occasionally multiple serotypes contain a similar α1α2 sequence (Table S2).

Vaccine-induced IgG and Th17 cross-reactivity with pneumococcal invasive isolates

To assess IgG and Th17 cross-reactivity, a representative strain from each of the 35 α1α2 groups was selected. The strain, TIGR4, was used as positive control (TIG) in these assays, as the α1α2 vaccine fragment displayed on our prototypic OMV/α1α2 vaccine was derived from this strain[14].

To test IgG cross-reactivity, ELISA plates were coated with whole pneumococcal cells and incubated with pooled sera from mice immunized with OMVs expressing TIGR4 α1α2. Cross-reactivity of IgG to the different strains was very limited. TIGR4 α1α2-specific IgG cross-reacted with PBCN268 and PBCN321, where PBCN268 is identical to TIGR4 α1α2 (Figure S2).

We developed an *ex vivo* Th17 screening assay using mouse splenocytes to measure cross-reactivity of vaccine-induced Th17 memory responses specific for TIGR4 α1α2. Spleens were isolated from mice that were immunized with control OMVs or OMVs displaying TIGR4 α1α2 three days after pneumococcal challenge. The cells were incubated with the 35 representative pneumococcal strains for three consecutive days, after which IL17A levels were measured in cell supernatants by ELISA. Splenocyte restimulation of control mice (immunized with OMV/HbpD but infected with TIGR4) showed extremely low to undetectable IL17A concentrations (Figure S3). In contrast, splenocyte restimulation of TIGR4 α1α2-immunized mice showed cross-reactivity with multiple pneumococcal strains. The TIGR4 strain and PBCN268 (containing an identical α1α2 fragment) resulted in high IL17A concentrations (Figure 3). Interestingly, restimulation with pneumococcal strains PBCN64, 461, 266, 321, and 16 also showed a significant increase in IL17A concentrations, to the same magnitude as with TIGR4. Peptide oligomer overrepresentation analysis of the α1α2 sequences yielding high IL17A concentrations revealed a sequence epitope of 42 amino

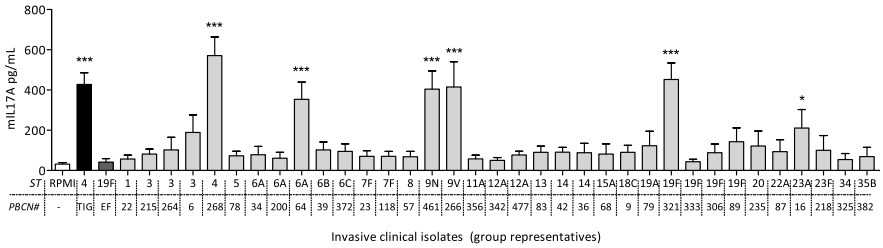

Figure 3 *Ex vivo* vaccine-induced Th17 memory cross-reactivity with clinical isolates.

Three days post-infection spleens were harvested from mice that were vaccinated with Δ*msbB* OMVs expressing α1α2 (Hbp-α1α2). Single cell suspensions were obtained and stimulated with selected pneumococcal isolates for three days. IL17A was measured in cell supernatant. IL17A levels represent n = 10 mice and were shown as mean ± SEM. Clinical strains were ordered based on serotype. ST: serotype; PBCN#: PBCN number; TIG: TIGR4; EF: EF3030.

acids shared by these pneumococcal isolates (Figure S4). This specific sequence was part of the α2 fragment. In addition, we found that re-activation of vaccine-induced Th17 memory responses was influenced by both capsule thickness and PspA expression levels, whereas serotype background had no significant effect on *ex vivo* IL17A levels (Figure S5).

Ex vivo Th17 responses predict *in vivo* nasal IL17A levels

Next, we assessed whether the IL17A levels measured in the *ex vivo* splenocyte assay predicted *in vivo* vaccine-induced IL17A responses in the nasal cavity. We determined whether infection with heterologous strains would activate the vaccine-induced Th17 memory response in the nasopharynx of animals vaccinated with TIGR4 α1α2. Based on the *ex vivo* Th17 screening (see Figure 3), we selected two groups of strains inducing high and low concentrations of IL17A after restimulation ('high IL17A': PBCN266 and 321 and 'low IL17A': PBCN200 and EF3030). Mice were immunized with either control OMVs (HbpD; control) or OMVs expressing TIGR4 α1α2 (Hbp-α1α2) and were subjected to challenge with homologous (TIGR4) or heterologous selected strains. Vaccination with OMVs without α1α2 induced higher levels of nasal IL17A than PBS controls (Figure S6A), indicating that empty OMVs induce IL17A to a low extend. Homologous challenge with TIGR4 significantly increased nasal IL17A in α1α2-vaccinated animals (Figure S6A). Likewise, heterologous challenge with 'high IL-17A' strains (PBCN266 and 321) showed a significantly higher level of IL17A in nasal tissue of α1α2-vaccinated mice as compared to the control vaccinated mice (Figure S6B-C). In contrast, heterologous challenge with 'low IL17A' strains (PBCN200

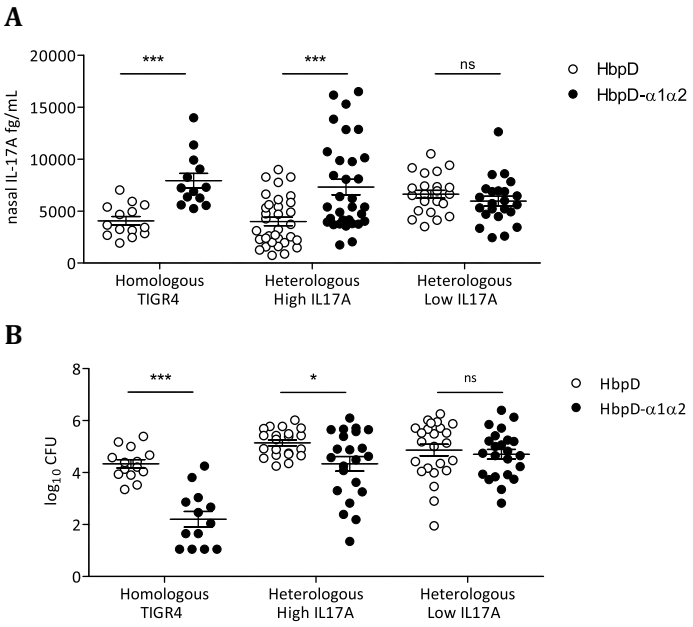

Figure 4 *Ex vivo* Th17 responses are predictive for *in vivo* nasal IL17A and a reduction in CFU.

Mice were vaccinated with PBS, Δ*msbB* empty OMVs (HbpD) or OMVs expressing α1α2 (Hbp-α1α2). Intranasal infection was performed using TIGR4 (homologous challenge), selected clinical strains (heterologous challenge), or laboratory strain EF3030 (heterologous challenge). (**A**) IL17A levels in nasal tissue and (**B**) bacterial recovery were assessed following infection with TIGR4, PBCN266, PBCN321, PBCN200, and EF3030. Results were pooled for heterologous high and low IL17A low strains respectively. Data represent individual mice and bars indicate group mean ± SEM. *, $p < 0.05$; **, $p < 0.01$; ***, $p < 0.001$.

and EF3030) showed similar nasal IL17A levels between α1α2-vaccinated and control vaccinated animals (Figure S6D-E). Combining the data of the individual strains shows that 'high IL17A' strains induce significantly increased levels of nasal IL17A following vaccination, unlike 'low IL17A' strains (Figure 4A).

Vaccine-induced nasal IL17A contributes to heterologous protection

All pneumococcal strains used in this study were first tested for their ability to colonize the murine nasopharynx without vaccination (Figure S7A, C, E, G, I). Mice were immunized with OMVs expressing TIGR4 α1α2 (Hbp-α1α2) or control OMVs (HbpD) and received a homologous (TIGR4) or a heterologous infection with 'IL-17A high' strains (PBCN266 and 321) and 'IL-17A low' strains (PBCN200

and EF3030). Vaccination with OMVs expressing α1α2 strongly protected against homologous challenge with TIGR4 (Figure S7B). The α1α2 vaccine led to a non-significant reduction in colonization by the 'IL-17A high' strains (PBCN266 and 321) (Figure S7D, F). Bacterial colonization was similar between α1α2-vaccinated and control animals following challenge with 'IL-17A low' strain PBCN200 (Figure S7H) , whereas a small but significant reduction in CFU counts was observed for 'IL-17A low' strain EF3030 (Figure S7J). Colonization of EF3030 was significantly reduced in α1α2-vaccinated mice, however the difference in CFU was less than one order of magnitude (Figure S7J). Interestingly, nasal IL17A levels were similar between α1α2-vaccinated and control animals following EF3030 infection (Figure 4E), suggesting that mucosal responses other than IL17A contributed to the vaccine-induced reduction in colonization[50]. Pooled CFU data demonstrated a significant reduction in pneumococcal colonization of the 'IL17A high' strains selected in the *ex vivo* screen (Figure 4B), which was not observed for the 'low IL17A' strains. Together, these results illustrate that IL17A contributes to protection against heterologous strains, while other types of mucosal responses may also play a role in reduction of colonization.

Prevalence of vaccine-induced cross-reactivity of TIGR4 α1α2 among clinical strains

Of the 1352 isolates derived from a large carriage study, genotypes were able to be determined for 89.3% (Table 1). Among those genotyped, the average mapping coverage was 99.6% with a mean nucleotide divergence of 0.4% (median 0.0). The most prevalent α1α2 variant was PBCN31 (10071_4#56_01432) (10%) followed by 7 (10050_2#21_00326) (9.0%). The PspA α1α2 was unable to be determined among 144 isolates (Table 2). Nineteen (25%) of the undeterminable PspA α1α2 variants were nontypeable pneumococci, which play a limited role in invasive disease[51]. However, almost half (46.2%) of serotype 23B isolates had undeterminable α1α2 variants, suggesting a subpopulation with a divergent α1α2 genotype. In all, we observed high coverage (90%) of our studied α1α2 variants in this large population carriage isolates.

To gain insight into the potential vaccine coverage of an α1α2-based OMV vaccine, we calculated the prevalence of pneumococcal strains that could be covered by a vaccine comprising the TIGR4 α1α2, assuming that measured *ex vivo* high IL17A concentrations in our study predict *in vivo* protection. For this, a cut-off of significantly higher IL17A measured in the *ex vivo* Th17 screening was used (Figure 3). This significant increase in IL17A was shown for the following strains PBCN268, 64, 461, 266, 321, and 16, suggesting high cross-reactivity with TIGR4 α1α2. When extended to the large carriage collection presented in

Table 1 Prevalence of PspA α1α2

Row Labels	PBCN ID	Protein	Total (n=1352)	Percent
ND	N/A	N/A	144	10.7%
Variant1	6	10050_2#2_00383	16	1.2%
Variant2	9	10050_2#4_00581	35	2.6%
Variant3	16	10050_2#8_00268	48	3.6%
Variant4	22	10050_2#11_00768	0	0.0%
Variant5	23	10050_2#12_01906	25	1.8%
Variant6	34	10050_2#20_01349	5	0.4%
Variant7	36	10050_2#21_00326	122	9.0%
Variant8	39	10050_2#22_01317	11	0.8%
Variant9	42	10050_2#24_00225	8	0.6%
Variant10	57	10050_2#30_00292	36	2.7%
Variant11	64	10050_2#35_00095	31	2.3%
Variant12	68	10050_2#37_01815	22	1.6%
Variant13	78	10050_2#41_00777	1	0.1%
Variant14	79	10050_2#42_00670	115	8.5%
Variant15	83	10050_2#45_00391	1	0.1%
Variant16	87	10050_2#48_00214	103	7.6%
Variant17	89	10050_2#50_00198	47	3.5%
Variant18	118	10050_2#71_00865	2	0.1%
Variant19	200	9953_7#38_01834	2	0.1%
Variant20	215	9953_7#47_00982	82	6.1%
Variant21	218	9953_7#49_01131	31	2.3%
Variant22	235	9953_7#58_00025	15	1.1%
Variant23	264	9953_7#79_01103	0	0.0%
Variant24	266	9953_7#81_00909	110	8.1%
Variant25	268	9953_7#82_01423	35	2.6%
Variant26	306	10071_4#18_00006	3	0.2%
Variant27	321	10071_4#30_00648	29	2.1%
Variant28	325	10071_4#32_00112	23	1.7%
Variant29	333	10071_4#40_00911	2	0.1%
Variant30	342	10071_4#46_00491	30	2.2%
Variant31	356	10071_4#56_01432	135	10.0%
Variant32	372	10071_4#71_00979	18	1.3%
Variant33	382	10071_4#80_00989	59	4.4%
Variant34	461	10208_2#57_01836	6	0.4%
Variant35	477	10396_8#26_00179	0	0.0%

Table 2 Serotype distribution of undetermined PspA α1α2 variants

Serotype	Count	Percent
23B	36	25.0%
NT	19	13.2%
23A	12	8.3%
35B	12	8.3%
15BC	10	6.9%
6C	10	6.9%
17F	8	5.6%
3	7	4.9%
21	6	4.2%
37	4	2.8%
19A	3	2.1%
23F	3	2.1%
35F	3	2.1%
10A	2	1.4%
11A	2	1.4%
19F	2	1.4%
34	1	0.7%
16F	1	0.7%
18C	1	0.7%
22F	1	0.7%
6B	1	0.7%
Total	**144**	**100.0%**

table 1, OMVs expressing a single type of α1α2 are estimated to cover 19.1% of more than 1350 carriage strains.

DISCUSSION

In most cases, immunizations with variable, often highly immunogenic proteins, offer strong protection upon homologous challenge[11,14-16]. Variable proteins show considerable surface epitope heterogeneity between subtypes and are therefore usually seen as unsuitable antigens to induce broad protection. However, whether variable proteins might induce a more broad Th17-mediated protection against bacterial carriage has, to our knowledge, not been investigated. In this study, we used PspA of *S. pneumoniae* as model antigen for the design of a universal vaccine to protect against carriage, an important prerequisite for

transmission and disease. LPS-detoxification of OMVs did not influence vaccine-induced protection by OMVs expressing TIGR4 α1α2. Furthermore, we developed an assay to determine Th17-based cross-reactivity that strongly predicted *in vivo* recall IL17A responses following vaccination. Vaccination with OMVs expressing TIGR4 α1α2 reduced pneumococcal colonization of strains that showed strong induction of IL17A upon *ex vivo* restimulation, illustrating the potency of such a vaccine to offer broader protection. Strikingly, the use of a single α1α2 type (TIGR4) at the basis of a Th17-mediated OMV-based vaccine could theoretically cover 19.1% of a large carriage cohort.

There is evidence that PspA could potentially offer universal protection against pneumococcal disease. It has been proposed that broad protection can be accomplished by a vaccine that combines family 1 and 2 PspA proteins[19]. Animal studies indeed showed that a vaccine combining the N-terminal part of family 1 and 2 PspA protected against infection with different pneumococcal strains, which was primarily attributed to protective antibodies specific for the conserved CDR and PRR region of PspA[20-25,52-54]. These broadly protective antibodies recognizing the PRR region of PspA pose a problem for human application as they were shown to cross-react with proteins from the human heart and skeletal muscles[55]. In this study we investigated the suitability of α1α2 fragment, part of the N-terminal region, for a broad vaccine that induces Th17-mediated protection. The use of sequenced clinical isolates allowed us to assess the effect of differences in the α1α2 sequence for IgG and Th17 cross-reactivity.

For antibody-based vaccines, it is difficult to assess vaccine cross-reactivity with pneumococcal strains in relation to actual *in vivo* protection. Even though cross-reactivity of colonization-induced IgG with heterologous pneumococcal strains in a whole cell ELISA was detected, no protection against disease was found[56]. Vaccine-induced IgG binding to the heterologous strains in the animal experiments may be hampered by differences in pneumococcal serotypes[57], which was also observed in our experiment. Although pneumococcal strains TIGR4 and PBCN268 express an identical α1α2, IgG binding to PBCN268 was reduced (Figure S2), which suggests that bacterial factors including capsule thickness and antigen expression levels might interfere with vaccine-induced IgG binding capacity. In a whole cell ELISA antigen-specific IgG does not discriminate between surface and subcapsular PspA, indicating ELISA is less predictive for *in vivo* antigen-specific binding of IgG as this is likely hindered by capsule expression[56].

Our study further points out that cross-reactivity of vaccine-induced responses specific for α1α2 with other pneumococcal strains was greatly increased for Th17 memory response as compared to the IgG response (Figures

3 and S2). This could be explained by the fact that the Th17 memory response is mediated by $CD4^+$ T cells and MHCII antigen presentation of linear peptides[58,59], whereas IgG binding often depends on conformational epitopes that can be masked by other components such as capsule and surface proteins and are therefore not always available. Similar to IgG binding capacity, reactivation of Th17 memory responses may, however, be influenced by antigen and capsule expression. In the *ex vivo* Th17 cross-reactivity screening, IL17A concentrations were reduced when splenocytes were exposed to lower PspA concentrations or to a highly encapsulated pneumococcal strain (Figure S5B-C). Similarly, others have shown that *ex vivo* splenocyte-derived IL17A by WCV-immunized animals slightly differed between different isogenic capsule-switch strains[57]. In the same study, vaccination with a whole cell vaccine followed by a homologous challenge induced Th17 memory responses in the spleens of mice[57]. Consistent with these data, in our study vaccination with a single α1α2 peptide of PspA promoted Th17 memory responses in mouse splenocytes, which we used to screen for heterologous cross-reactivity across 345 sequenced invasive isolates. This represented a simple method to screen for vaccine cross-reactivity among 35 α1α2 types instead of performing 35 heterologous challenges in animal studies. We showed that IL17A measured in the *ex vivo* assay was highly predictive for *in vivo* nasal IL17A levels induced by the OMV-based vaccine.

Vaccination with OMVs expressing TIGR4 α1α2 led to a clear reduction in pneumococcal colonization in homologous challenge infection, but was less pronounced after a heterologous challenge infection (Figure S7D and F). This demonstrates that although equal levels of *ex vivo* IL17A were measured for restimulation with TIGR4 (strain background vaccine) and the clinical 'high IL17A strains' (Figure 4 and S6), this does not result in a similar degree of protection. One explanation is that vaccine-induced IgG binding to conformational epitopes may play a role, which has a stronger effect on homologous challenge, contributing to a better reduction in pneumococcal colonization as compared to the reduction of the heterologous strains. Secondly, the concentration of nasal IL17A was slightly lower in mice infected with heterologous strains. Also, the kinetics of a nasal IL17A in response to pneumococcal infection may differ between homologous and heterologous strains, which could not be determined in this study as IL17A was only measured in the sacrificed mice three days post-infection. Interestingly, compared to laboratory strain TIGR4, PBCN266 and PBCN321 colonized the murine nasopharynx at higher densities (Figure S7D, F). The increased densities suggest that these clinical strains have an increased capacity to colonize the murine nasopharynx, compared to TIGR4. This may result in delayed clearance of these strains as measured at three days post-infection.

Nonspecific reduction in bacterial colonization observed following vaccination with empty OMVs was observed for TIGR4 and other clinical strains (Figures S7B and S8). This reduction in CFU was associated with increased nasal IL17A (Figure S6A), suggesting that IL17A may contribute to the nonspecific decrease in pneumococcal load. Mucosal adjuvants such as CTB and CT were also described to reduce pneumococcal colonization in a nonspecific manner, although the underlying mechanisms might differ[50,60]. IL17A might be derived from macrophages, NKT cells, ILC3 and γδ T cells in the nasal mucosa, which were shown to directly respond to *S. pneumoniae* infection upon recognition[61]. The current study did not investigate these cell types and their role in nonspecific protection. However, further study is needed to determine their role in a reduction in bacterial colonization.

The α1α2 fragment grafted onto the outer membrane vesicles represents the majority of the N-terminal region of PspA and is an interesting vaccine target based on existing literature in both mouse and human[14]. Importantly, the PRR region that potentially cross-reacts with human myosin is not part of the α1α2 fragment of PspA[55]. Multiple studies show that the coiled-coil N-terminal domain is implicated in cross-reactivity and cross-protection with pneumococcal strains[20-22,25,52,53,62]. In mouse and human, T-cell and antibody epitopes are localized to this particular fragment of PspA[62-67]. Since mucosal $CD4^{+}IL17^{+}$ T cells were detected in the human upper respiratory tract, it is possible that these cells play a role in protection against bacterial colonization in humans, like we have observed in our mouse studies[68]. Whether an OMV-based vaccine inducing Th17 immunity that reduces pneumococcal colonization will also prevent and/or reduce pneumococcal disease and transmission remains to be studied.

The classification based on the α1α2 types from 345 invasive clinical isolates from the Netherlands appears to be consistent in other regions of the world, as determined by using a large carriage cohort. Except for serotype 23B, which was not present in the invasive cohort of 345 clinical isolates. Importantly, protection conferred by such an α1α2 antigen variant should be tested, as for example not each α1α2 genotype promotes Th17 immunity and a reduction of pneumococcal colonization (Figure S9). The method for Th17 cross-reactivity screening, as described in the current study, can be applied to pneumococci collected in any region of the world, as well as for screening of cross-reactive Th17 responses by other variable proteins. This is particularly interesting as currently global efforts are undertaken to sequence thousands of pneumococcal strains before and after vaccine introduction in developing countries[69]. This allows for the measurement of vaccine-escape mutants and devise next-generation vaccines that are able to limit escape, such as an OMV-based protein vaccine.

In conclusion, our work illustrates the potential of a variable protein antigen

for cross-protection against pneumococcal carriage via a Th17-dependent clearance mechanism. Vaccine cross-reactivity and the capacity to evoke *in vivo* protection can easily be measured in an *ex vivo* Th17 screening, which allows for selection of a combination of variable protein antigens to increase vaccine coverage. The current study indicates that the use of variable proteins, inducing Th17 immunity, should be considered in future vaccine development programs when aiming at broad protection against bacterial carriage.

Acknowledgements
The work described in this manuscript was supported by Agentschap NL [PneumoVac, nr. 305 OM111009], Eurostars [PneumoNav, nr. E9285]), and the NIH (R01AI048935). We thank Dr. Amelieke Cremers for gathering the PBCN collection.

REFERENCES

1 Organization, W. H. *The top 10 causes of death*, <http://www.who.int/mediacentre/factsheets/fs310/en/> (2014).

2 Organization, W. H. *Children: Reducing mortality*, <http://www.who.int/mediacentre/factsheets/fs178/en/> (2014).

3 Lycke, N. Recent progress in mucosal vaccine development: potential and limitations. *Nat Rev Immunol* **12**, 592-605, doi:10.1038/nri3251 (2012).

4 Brown, J., Hammerschmidt, S., Orihuela, C. *Streptococcous pneumoniae molecular mechanisms of host-pathogen interactions*. (Elsevier, 2015).

5 Hicks, L. A. *et al.* Incidence of pneumococcal disease due to non-pneumococcal conjugate vaccine (PCV7) serotypes in the United States during the era of widespread PCV7 vaccination, 1998-2004. *J Infect Dis* **196**, 1346-1354, doi:10.1086/521626 (2007).

6 Lexau, C. A. *et al.* Changing epidemiology of invasive pneumococcal disease among older adults in the era of pediatric pneumococcal conjugate vaccine. *JAMA : the journal of the American Medical Association* **294**, 2043-2051, doi:10.1001/jama.294.16.2043 (2005).

7 Miller, E., Andrews, N. J., Waight, P. A., Slack, M. P. & George, R. C. Herd immunity and serotype replacement 4 years after seven-valent pneumococcal conjugate vaccination in England and Wales: an observational cohort study. *Lancet Infect Dis* **11**, 760-768, doi:10.1016/s1473-3099(11)70090-1 (2011).

8 Jambo, K. C., Sepako, E., Heyderman, R. S. & Gordon, S. B. Potential role for mucosally active vaccines against pneumococcal pneumonia. *Trends Microbiol* **18**, 81-89, doi:10.1016/j.tim.2009.12.001 (2010).

9 Malley, R. & Anderson, P. W. Serotype-independent pneumococcal experimental vaccines that induce cellular as well as humoral immunity. *Proc Natl Acad Sci U S A* **109**, 3623-3627, doi:10.1073/pnas.1121383109 (2012).

10 Dale, J. B. *et al.* in *Streptococcus pyogenes: Basic Biology to Clinical Manifestations* (eds J. J. Ferretti, D. L. Stevens, & V. A. Fischetti) (The University of Oklahoma Health Sciences Center., 2016).

11 Steer, A. C. *et al.* Status of research and development of vaccines for Streptococcus pyogenes. *Vaccine*, doi:10.1016/j.vaccine.2016.03.073 (2016).

12 Giersing, B. K., Dastgheyb, S. S., Modjarrad, K. & Moorthy, V. Status of vaccine research and development of vaccines for Staphylococcus aureus. *Vaccine*, doi:10.1016/j.vaccine.2016.03.110 (2016).

13 Proctor, R. A. Is there a future for a Staphylococcus aureus vaccine? *Vaccine* **30**, 2921-2927, doi:10.1016/j.vaccine.2011.11.006 (2012).

14 Kuipers, K. *et al.* Salmonella outer membrane vesicles displaying high densities of pneumococcal antigen at the surface offer protection against colonization. *Vaccine* **33**, 2022-2029, doi:10.1016/j.vaccine.2015.03.010 (2015).

15 Moffitt, K. L. *et al.* T(H)17-based vaccine design for prevention of *Streptococcus pneumoniae* colonization. *Cell Host Microbe* **9**, 158-165, doi:10.1016/j.chom.2011.01.007 (2011).

16 Ma, C. *et al.* FbaA- and M protein-based multi-epitope vaccine elicits strong protective immune responses against group A streptococcus in mouse model. *Microbes Infect* **16**, 409-418, doi:10.1016/j.micinf.2014.03.006 (2014).

17 Briles, D. E. *et al.* PspA, a protection-eliciting pneumococcal protein: immunogenicity of isolated native PspA in mice. *Vaccine* **14**, 858-867 (1996).

18 Kadioglu, A., Weiser, J. N., Paton, J. C. & Andrew, P. W. The role of *Streptococcus pneumoniae* virulence factors in host respiratory colonization and disease. *Nat Rev Microbiol* **6**, 288-301, doi:10.1038/nrmicro1871 (2008).

19 Hollingshead, S. K., Becker, R. & Briles, D. E. Diversity of PspA: mosaic genes and evidence for past recombination in *Streptococcus pneumoniae*. *Infect Immun* **68**, 5889-5900 (2000).

20 Darrieux, M. *et al.* Fusion proteins containing family 1 and family 2 PspA fragments elicit protection against *Streptococcus pneumoniae* that correlates with antibody-mediated enhancement of complement deposition. *Infect Immun* **75**, 5930-5938, doi:10.1128/iai.00940-07 (2007).

21 Piao, Z. *et al.* Protective properties of a fusion pneumococcal surface protein A (PspA) vaccine against pneumococcal challenge by five different PspA clades in mice. *Vaccine* **32**, 5607-5613, doi:10.1016/j.vaccine.2014.07.108 (2014).

22 Moreno, A. T. *et al.* Immunization of mice with single PspA fragments induces antibodies capable of mediating complement deposition on different pneumococcal strains and cross-protection. *Clin Vaccine Immunol* **17**, 439-446, doi:10.1128/cvi.00430-09 (2010).

23 Daniels, C. C. *et al.* The proline-rich region of pneumococcal surface proteins A and C contains surface-accessible epitopes common to all pneumococci and elicits antibody-mediated protection against sepsis. *Infect Immun* **78**, 2163-2172, doi:10.1128/iai.01199-09 (2010).

24 Campos, I. B. *et al.* Nasal immunization of mice with Lactobacillus casei expressing the Pneumococcal Surface Protein A: induction of antibodies, complement deposition and partial protection against *Streptococcus pneumoniae* challenge. *Microbes Infect* **10**, 481-488, doi:10.1016/j.micinf.2008.01.007 (2008).

25 Xin, W., Li, Y., Mo, H., Roland, K. L. & Curtiss, R., 3rd. PspA family fusion proteins delivered by attenuated Salmonella enterica serovar Typhimurium extend and enhance protection against *Streptococcus pneumoniae*. *Infect Immun* **77**, 4518-4528, doi:10.1128/iai.00486-09 (2009).

26 Roche, H., Ren, B., McDaniel, L. S., Hakansson, A. & Briles, D. E. Relative roles of genetic background and variation in PspA in the ability of antibodies to PspA to protect against capsular type 3 and 4 strains of *Streptococcus pneumoniae*. *Infect Immun* **71**, 4498-4505 (2003).

27 Cremers, A. J. *et al.* Effects of 7-valent pneumococcal conjugate 1 vaccine on the severity of adult 2 bacteremic pneumococcal pneumonia. *Vaccine* **32**, 3989-3994, doi:10.1016/j.vaccine.2014.04.089 (2014).

28 Cremers, A. J. *et al.* The post-vaccine microevolution of invasive *Streptococcus pneumoniae*. *Sci Rep* **5**, 14952, doi:10.1038/srep14952 (2015).

29 Kaniga, K., Bossio, J. C. & Galan, J. E. The Salmonella typhimurium invasion genes invF and invG encode homologues of the AraC and PulD family of proteins. *Mol Microbiol* **13**, 555-568 (1994).

30 Palmer, L. E., Hobbie, S., Galan, J. E. & Bliska, J. B. YopJ of Yersinia pseudotuberculosis is required for the inhibition of macrophage TNF-alpha production and downregulation of the MAP kinases p38 and JNK. *Mol Microbiol* **27**, 953-965 (1998).

31 Murray, S. R., Bermudes, D., de Felipe, K. S. & Low, K. B. Extragenic suppressors of growth defects in msbB Salmonella. *J Bacteriol* **183**, 5554-5561, doi:10.1128/jb.183.19.5554-5561.2001 (2001).

32 Westphal, O. J., K. in *Methods in Carbohydrate Chemistry* (ed R. L.; Wolfan Whistler, M. L.) p. 83-91 (Academic Press, Inc. , 1965).

33 Kondakov, A. & Lindner, B. Structural characterization of complex bacterial glycolipids by Fourier transform mass spectrometry. *Eur J Mass Spectrom (Chichester)* **11**, 535-546, doi:10.1255/ejms.721 (2005).

34 Wilm, M. S. M., M. . Electrospray and Taylor-Cone theory, Dole's beam of macromolecules at last? *Int J Mass Spectrom Ion Proc* **136(2-3)**, p. 167-180 (1994).

35 Domon, B. C., C. E. . A Systematic Nomenclature for Carbohydrate Fragmentations in FAB-MS/MS Spectra of Glycoconjugates. *Glycoconj J* **5**, 397-409 (1988).

36 Jansson, P. E., Lindberg, A. A., Lindberg, B. & Wollin, R. Structural studies on the hexose region of the core in lipopolysaccharides from Enterobacteriaceae. *Eur J Biochem* **115**, 571-577 (1981).

37 Holst, O. The structures of core regions from enterobacterial lipopolysaccharides - an update. *FEMS Microbiol Lett* **271**, 3-11, doi:10.1111/j.1574-6968.2007.00708.x (2007).

38 Olsthoorn, M. M. *et al.* The structure of the linkage between the O-specific polysaccharide and the core region of the lipopolysaccharide from Salmonella enterica serovar Typhimurium revisited. *Eur J Biochem* **267**, 2014-2027 (2000).

39 Hormaeche, C. E. *et al.* Protection against oral challenge three months after i.v. immunization of BALB/c mice with live Aro Salmonella typhimurium and Salmonella enteritidis vaccines is serotype (species)-dependent and only partially determined by the main LPS O antigen. *Vaccine* **14**, 251-259 (1996).

40 Hashemzadeh-Bonehi, L. *et al.* Importance of using lac rather than ara promoter vectors for modulating the levels of toxic gene products in Escherichia coli. *Mol Microbiol* **30**, 676-678 (1998).

41 Jong, W. S. *et al.* A structurally informed autotransporter platform for efficient heterologous protein secretion and display. *Microb Cell Fact* **11**, 85, doi:10.1186/1475-2859-11-85 (2012).
42 Jong, W. S. *et al.* An autotransporter display platform for the development of multivalent recombinant bacterial vector vaccines. *Microb Cell Fact* **13**, 162, doi:10.1186/s12934-014-0162-8 (2014).
43 Camacho, C. *et al.* BLAST+: architecture and applications. *BMC Bioinformatics* **10**, 421, doi:10.1186/1471-2105-10-421 (2009).
44 Bailey, T. L. *et al.* MEME SUITE: tools for motif discovery and searching. *Nucleic Acids Res* **37**, W202-208, doi:10.1093/nar/gkp335 (2009).
45 Ye, P. *et al.* Requirement of interleukin 17 receptor signaling for lung CXC chemokine and granulocyte colony-stimulating factor expression, neutrophil recruitment, and host defense. *J Exp Med* **194**, 519-527 (2001).
46 Croucher, N. J. *et al.* Population genomics of post-vaccine changes in pneumococcal epidemiology. *Nat Genet* **45**, 656-663, doi:10.1038/ng.2625 (2013).
47 Inouye, M. *et al.* SRST2: Rapid genomic surveillance for public health and hospital microbiology labs. *Genome Med* **6**, 90, doi:10.1186/s13073-014-0090-6 (2014).
48 Kong, Q. *et al.* Palmitoylation state impacts induction of innate and acquired immunity by the Salmonella enterica serovar typhimurium msbB mutant. *Infect Immun* **79**, 5027-5038, doi:10.1128/iai.05524-11 (2011).
49 Watson, J. & Riblet, R. Genetic control of responses to bacterial lipopolysaccharides in mice. I. Evidence for a single gene that influences mitogenic and immunogenic respones to lipopolysaccharides. *J Exp Med* **140**, 1147-1161 (1974).
50 Kuipers, K. *et al.* Antigen-Independent Restriction of Pneumococcal Density by Mucosal Adjuvant Cholera Toxin Subunit B. *J Infect Dis*, doi:10.1093/infdis/jiw160 (2016).
51 Park, I. H., Geno, K. A., Sherwood, L. K., Nahm, M. H. & Beall, B. Population-based analysis of invasive nontypeable pneumococci reveals that most have defective capsule synthesis genes. *PLoS One* **9**, e97825, doi:10.1371/journal.pone.0097825 (2014).
52 Ferreira, D. M. *et al.* Protection against nasal colonization with *Streptococcus pneumoniae* by parenteral immunization with a DNA vaccine encoding PspA (Pneumococcal surface protein A). *Microb Pathog* **48**, 205-213, doi:10.1016/j.micpath.2010.02.009 (2010).
53 Bosarge, J. R., Watt, J. M., McDaniel, D. O., Swiatlo, E. & McDaniel, L. S. Genetic immunization with the region encoding the alpha-helical domain of PspA elicits protective immunity against *Streptococcus pneumoniae*. *Infect Immun* **69**, 5456-5463 (2001).
54 Swiatlo, E., King, J., Nabors, G. S., Mathews, B. & Briles, D. E. Pneumococcal surface protein A is expressed in vivo, and antibodies to PspA are effective for therapy in a murine model of pneumococcal sepsis. *Infect Immun* **71**, 7149-7153 (2003).
55 Magyarics, Z. R., H.; Badarou, A.; Nielson, N.; Caccamo, M.; Weber, S.; Maierhofer, B.; Havlicek, K.; Dolezilkova, I.; Gross, K.; Nagy, E. in *European Meeting on the Molecular Biology of the Pneumococcus.*
56 Cohen, J. M., Wilson, R., Shah, P., Baxendale, H. E. & Brown, J. S. Lack of cross-protection against invasive pneumonia caused by heterologous strains following murine *Streptococcus pneumoniae* nasopharyngeal colonisation despite whole cell ELISAs showing significant cross-reactive IgG. *Vaccine* **31**, 2328-2332, doi:10.1016/j.vaccine.2013.03.013 (2013).
57 Moffitt, K. L., Yadav, P., Weinberger, D. M., Anderson, P. W. & Malley, R. Broad antibody and T cell reactivity induced by a pneumococcal whole-cell vaccine. *Vaccine* **30**, 4316-4322, doi:10.1016/j.vaccine.2012.01.034 (2012).
58 Lu, Y. J. *et al.* Interleukin-17A mediates acquired immunity to pneumococcal colonization. *PLoS Pathog* **4**, e1000159, doi:10.1371/journal.ppat.1000159 (2008).
59 Malley, R. *et al.* CD4+ T cells mediate antibody-independent acquired immunity to pneumococcal colonization. *Proc Natl Acad Sci U S A* **102**, 4848-4853, doi:10.1073/pnas.0501254102 (2005).
60 Malley, R. *et al.* Multiserotype protection of mice against pneumococcal colonization of the nasopharynx and middle ear by killed nonencapsulated cells given intranasally with a nontoxic adjuvant. *Infect Immun* **72**, 4290-4292, doi:10.1128/iai.72.7.4290-4292.2004 (2004).

61 Ivanov, S., Paget, C. & Trottein, F. Role of non-conventional T lymphocytes in respiratory infections: the case of the pneumococcus. *PLoS Pathog* **10**, e1004300, doi:10.1371/journal.ppat.1004300 (2014).
62 Nabors, G. S. *et al.* Immunization of healthy adults with a single recombinant pneumococcal surface protein A (PspA) variant stimulates broadly cross-reactive antibodies to heterologous PspA molecules. *Vaccine* **18**, 1743-1754 (2000).
63 Kolberg, J., Aase, A., Rodal, G., Littlejohn, J. E. & Jedrzejas, M. J. Epitope mapping of pneumococcal surface protein A of strain Rx1 using monoclonal antibodies and molecular structure modelling. *FEMS Immunol Med Microbiol* **39**, 265-273 (2003).
64 Vadesilho, C. F. *et al.* Mapping of epitopes recognized by antibodies induced by immunization of mice with PspA and PspC. *Clin Vaccine Immunol* **21**, 940-948, doi:10.1128/cvi.00239-14 (2014).
65 Vadesilho, C. F. *et al.* Characterization of the antibody response elicited by immunization with pneumococcal surface protein A (PspA) as recombinant protein or DNA vaccine and analysis of protection against an intranasal lethal challenge with *Streptococcus pneumoniae*. *Microb Pathog* **53**, 243-249, doi:10.1016/j.micpath.2012.08.007 (2012).
66 Singh, R. *et al.* Helper T cell epitope-mapping reveals MHC-peptide binding affinities that correlate with T helper cell responses to pneumococcal surface protein A. *PLoS One* **5**, e9432, doi:10.1371/journal.pone.0009432 (2010).
67 McDaniel, L. S., Ralph, B. A., McDaniel, D. O. & Briles, D. E. Localization of protection-eliciting epitopes on PspA of *Streptococcus pneumoniae* between amino acid residues 192 and 260. *Microb Pathog* **17**, 323-337, doi:10.1006/mpat.1994.1078 (1994).
68 Pido-Lopez, J., Kwok, W. W., Mitchell, T. J., Heyderman, R. S. & Williams, N. A. Acquisition of pneumococci specific effector and regulatory Cd4+ T cells localising within human upper respiratory-tract mucosal lymphoid tissue. *PLoS Pathog* **7**, e1002396, doi:10.1371/journal.ppat.1002396 (2011).
69 Geno, K. A. *et al.* Pneumococcal Capsules and Their Types: Past, Present, and Future. *Clin Microbiol Rev* **28**, 871-899, doi:10.1128/cmr.00024-15 (2015).

SUPPLEMENTARY TABLES AND FIGURES

Table S1 Primers used in this study

Name	Sequence (5' → 3')	Features
msbB_a_XbaI fw	cgcatctagaagcgtctgacatgggaagtc	*Xba*I site underlined
msbB_d_XbaI rv	cgcatctagaattgtggctaaggtcgaacg	*Xba*I site underlined
msbB_b rv	catgcttttccagggtctgc	
msbB_c_ fw	*gcagaccctggaaaagcatg*cgagattcagccgtataagc	overlap with msbB_b rv sequence in italics
msbB_seq fw	ggcacaggtgaaagaggttc	
msbB_seq rv	accgtcggttcaaccaatac	
a1_PBCN79 fw	**ggaagtcttgcggggagctcc**gaagaagcccccg-tagctag	overhang for In-Fusion cloning into pEH3-HbpD in bold
a1_PBCN79 rv	**taccgctgccggatcc**ttcaggaactacaactgctctta	overhang for In-Fusion cloning into pEH3-HbpD in bold
a1_PBCN87 fw	**ggaagtcttgcggggagctcc**gaagaagctcccg-tagctaag	overhang for In-Fusion cloning into pEH3-HbpD in bold
a1_PBCN87 rv	**taccgctgccggatcc**ttcaggaactacttttgcttgttc	overhang for In-Fusion cloning into pEH3-HbpD in bold
a2_PBCN79 fw	**tatgccggttctgggagctcc**gtaagagcagttg-tagttcctg	overhang for In-Fusion cloning into pEH3-HbpD in bold
a2_PBCN79 rv	**taccgctgccggatcc**atctttttcaagtttagcaacttc	overhang for In-Fusion cloning into pEH3-HbpD in bold
a2_PBCN87 fw	**tatgccggttctgggagctcc**aaggaacaagcaaaag-tagttcc	overhang for In-Fusion cloning into pEH3-HbpD in bold
a2_PBCN87 rv	**taccgctgccggatcc**ctctttttctagtccctgaac	overhang for In-Fusion cloning into pEH3-HbpD in bold

Table S2 Overview of sequenced human clinical invasive isolates

Available upon request

Table S3 Prevalence of 35 α1α2 types among strains of a large carriage cohort

Row Labels	PBCN ID	Protein	Total (n=1352)	Percent
ND	N/A	N/A	144	10,7%
Variant1	6	10050_2#2_00383	16	1,2%
Variant2	9	10050_2#4_00581	35	2,6%
Variant3	16	10050_2#8_00268	48	3,6%
Variant4	22	10050_2#11_00768	0	0,0%
Variant5	23	10050_2#12_01906	25	1,8%
Variant6	34	10050_2#20_01349	5	0,4%
Variant7	36	10050_2#21_00326	122	9,0%
Variant8	39	10050_2#22_01317	11	0,8%
Variant9	42	10050_2#24_00225	8	0,6%
Variant10	57	10050_2#30_00292	36	2,7%
Variant11	64	10050_2#35_00095	31	2,3%
Variant12	68	10050_2#37_01815	22	1,6%
Variant13	78	10050_2#41_00777	1	0,1%
Variant14	79	10050_2#42_00670	115	8,5%
Variant15	83	10050_2#45_00391	1	0,1%
Variant16	87	10050_2#48_00214	103	7,6%
Variant17	89	10050_2#50_00198	47	3,5%
Variant18	118	10050_2#71_00865	2	0,1%
Variant19	200	9953_7#38_01834	2	0,1%
Variant20	215	9953_7#47_00982	82	6,1%
Variant21	218	9953_7#49_01131	31	2,3%
Variant22	235	9953_7#58_00025	15	1,1%
Variant23	264	9953_7#79_01103	0	0,0%
Variant24	266	9953_7#81_00909	110	8,1%
Variant25	268	9953_7#82_01423	35	2,6%
Variant26	306	10071_4#18_00006	3	0,2%
Variant27	321	10071_4#30_00648	29	2,1%
Variant28	325	10071_4#32_00112	23	1,7%
Variant29	333	10071_4#40_00911	2	0,1%
Variant30	342	10071_4#46_00491	30	2,2%
Variant31	356	10071_4#56_01432	135	10,0%
Variant32	372	10071_4#71_00979	18	1,3%
Variant33	382	10071_4#80_00989	59	4,4%
Variant34	461	10208_2#57_01836	6	0,4%
Variant35	477	10396_8#26_00179	0	0,0%

The sequenced pneumococcal strains from the large carriage cohort were sequenced and aligned for the 35 α1α2 types after which prevalence was assessed.

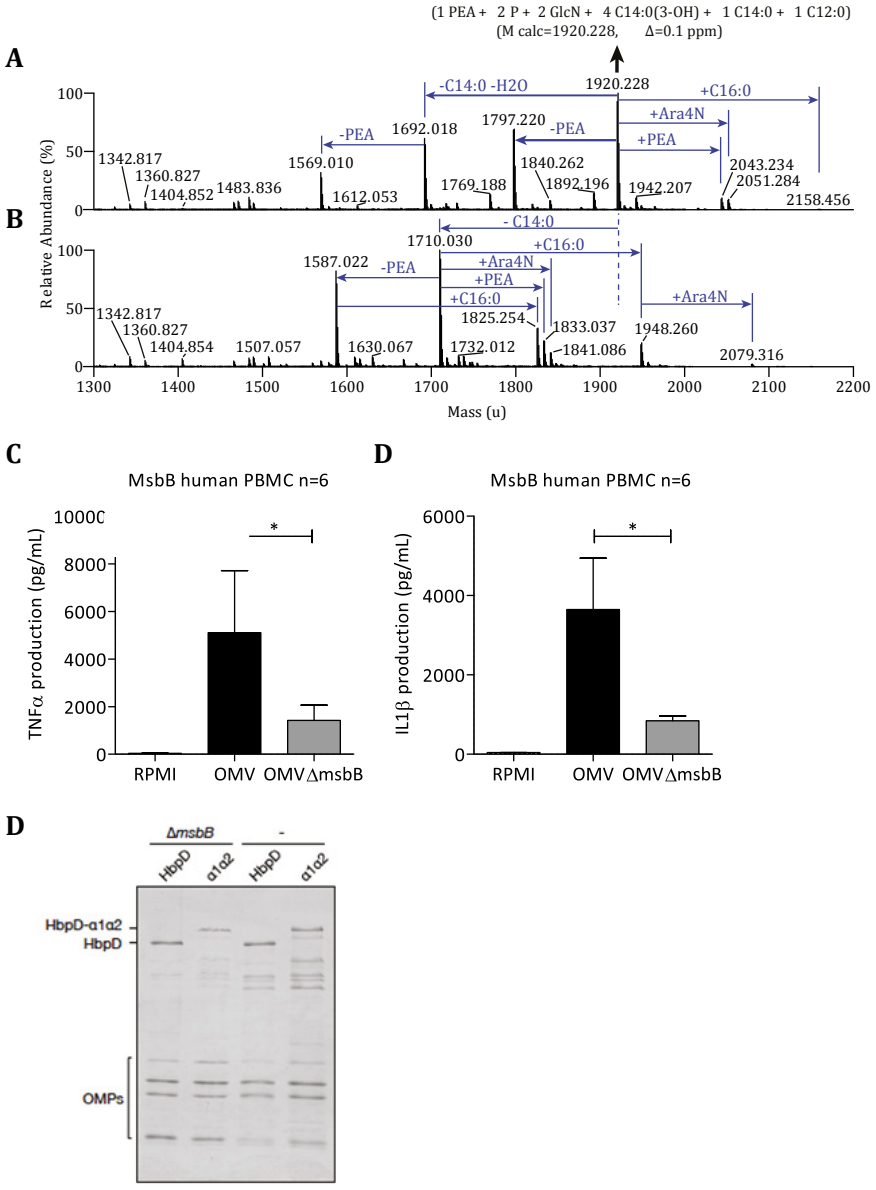

Figure S1 Salmonella Δ*msbB* OMVs reduced hexacylated LPS and cytokine production by human PBMCs.

(**A-B**) Sections of the charge-deconvoluted negative-ion (ESI-FT) SID mass spectra of LPS from *S. typhimurium* (**A**) SL3261 (delta-aroA) and mutant derivative (**B**) M1-1-31B are shown. LPS Y-type

fragment ions corresponding to lipid A moieties are depicted. Annotations refer to monoisotopic mass values. The ion peaks of masses 1797.220 and 1920.228 u obtained from the LPS of the parent strain correspond to hexa-acylated lipid A species carrying two phosphates (P) and two P plus a phosphoethanolamine (PEA) groups, respectively. In the Δ*msbB* mutant the main ion peaks of masses 1710.030 and 1587.022 u from the LPS correspond to penta-acylated lipid A species which lost a C14:0 fatty acid as compared to the main lipid A species of the parent strain. *PEA: phosphoethanolamine; P: phosphate; GlcN: glucosamine; C12:0: dodecanoic acid; C14:0: tetradecanoic acid; C14:0(3-OH): 3-hydroxy-tetradecanoic acid; C16:0: hexadecanoic acid; Ara4N: 4-amino-4-deoxy-L-arabinose.* (**C-D**) Human PBCMs were stimulated with equal amounts (1 ng/mL) of wildtype or Δ*msbB* Salmonella OMVs for 24h. (**C**) TNFα and (**D**) IL1β was measured in cell supernatant. Data was combined from n = 6 healthy donors and shown as mean ±SEM. *, $p < 0.05$. (**E**) SDS-PAGE/Coomassie protein profiles of LPS-detoxified (Δ*msbB*) and wild-type LPS (-) OMVs showing efficient display of HbpD or Hbp-α1α2.

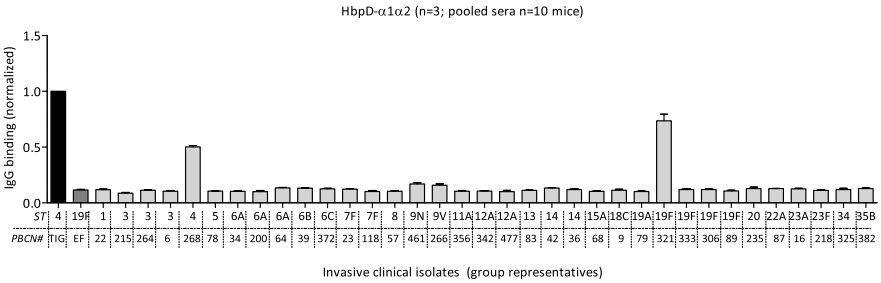

Figure S2 Vaccine-induced IgG cross-reactivity with clinical isolates.

Selected pneumococcal strains were grown to mid-log phase and used to coat ELISA plates. Cross-reactivity was determined using pooled serum derived from n = 10 mice vaccinated with Δ*msbB* OMVs expressing α1α2 (Hbp-α1α2). IgG binding was normalized to TIGR4 (vaccine background) and was shown as mean ± SEM (n = 3). Clinical strains were ordered based on serotype. *ST: serotype; PBCN#: PBCN number; TIG: TIGR4; EF: EF3030.*

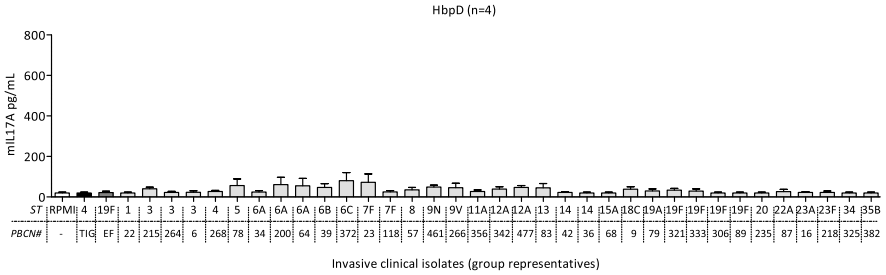

Figure S3 *Ex vivo* vaccine-induced Th17 memory cross-reactivity.

Three days post-infection spleens were harvested from mice that were vaccinated with Δ*msbB* OMVs expressing no pneumococcal antigen (HbpD; control). Single cell suspensions were obtained and stimulated with selected pneumococcal isolates for three days. IL17A was measured in cell supernatant. IL17A represent n = 4 mice and were shown as mean ± SEM. Clinical strains were ordered based on serotype. *ST: serotype; PBCN#: PBCN number; TIG: TIGR4; EF: EF3030.*

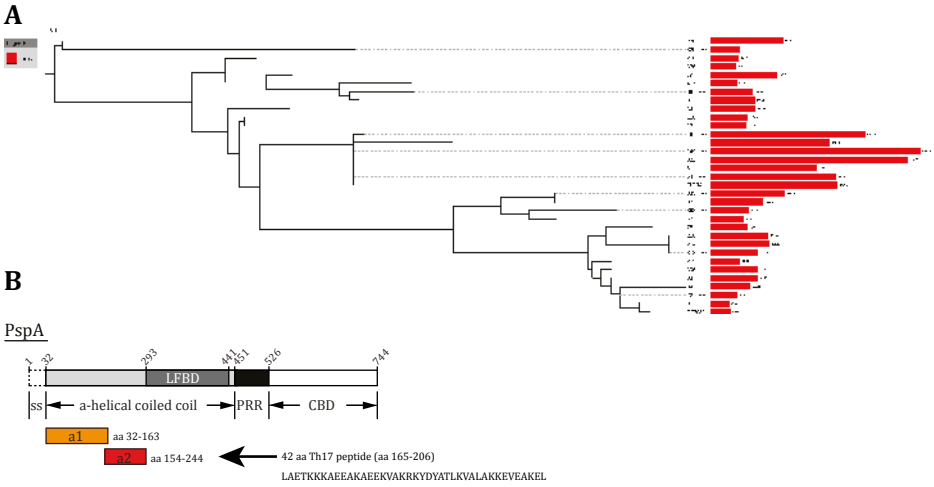

Figure S4 *Ex vivo* vaccine-induced Th17 memory cross-reactivity.

(**A**) Peptide tree analysis of α1α2 identity in relation to *ex vivo* IL17A levels among clinical isolates. Tree indicates that pneumococcal strains with an *ex vivo* high IL17A share a similar sequence in the α2 part of the α1α2 vaccine region. (**B**) Th17 peptide is located to the α2 region of PspA (aa 165-206) among the 42 amino acids.

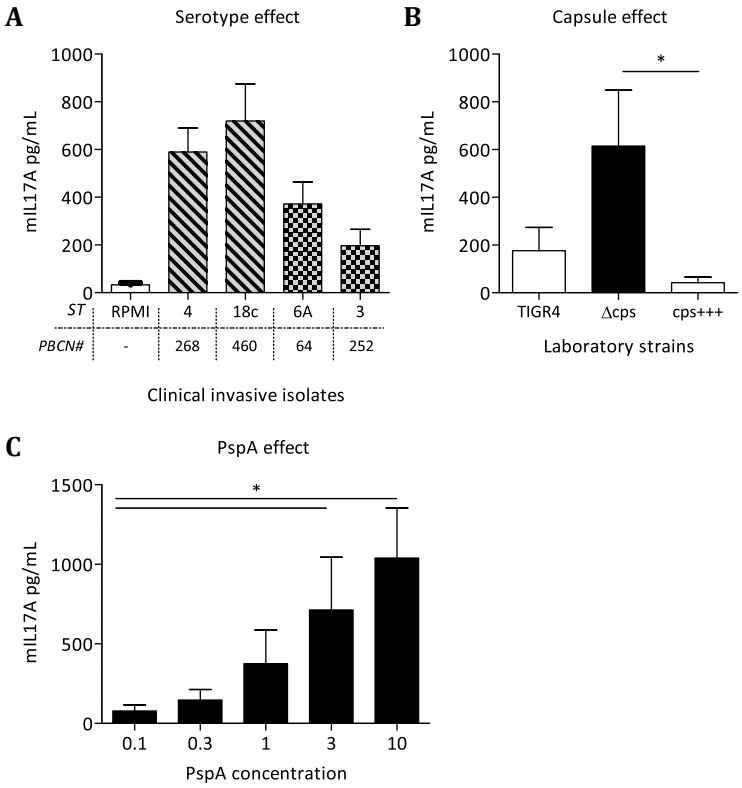

Figure S5 The influence of bacterial factors on *ex vivo* IL17A.

Three days post-infection spleens were harvested from mice that were vaccinated with Δ*msbB* OMVs expressing α1α2 (Hbp-α1α2). Splenocytes were stimulated with selected pneumococcal strains, TIGR4 isogenic strains, or purified PspA for three days to assess the effect of (**A**) serotype, (**B**) capsule, and (**C**) PspA antigen levels. (**A**) PBCN268 and PBCN360 share an identical α1α2 region, but belong to a different serotype. This is similar for PBCN64 and PBCN252. Splenocytes were exposed to (**B**) wildtype TIGR4, an acapsular TIGR4 (Δcps), and TIGR4 overexpressing capsule (cps+++), and (**C**) dose-dependent concentrations of PspA (0.1; 0.3; 1; 3; 10 μg/mL). IL17A was measured in cell supernatant. IL17A represent n = 5-9 mice and were shown as mean ± SEM. Clinical strains were ordered based on serotype. ST: serotype; PBCN#: PBCN number; TIG: TIGR4; EF: EF3030.

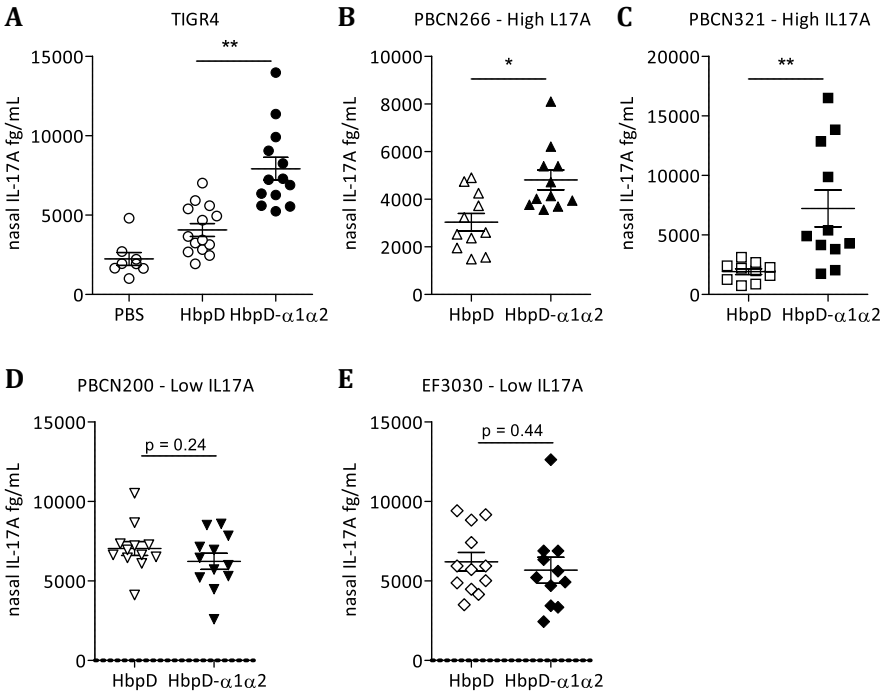

Figure S6 *Ex vivo* Th17 responses are predictive for *in vivo* nasal IL17A.

Mice were vaccinated with PBS, Δ*msbB* empty OMVs (HbpD) or OMVs expressing α1α2 (Hbp-α1α2). Intranasal infection was performed using TIGR4 (homologous challenge), selected clinical strains (heterologous challenge), or laboratory strain EF3030 (heterologous challenge). IL17A levels in nasal tissue were assessed following infection with (**A**) TIGR4, (**B**) PBCN266, (**C**), PBCN321, (**D**) PBCN200, and (**E**) EF3030. Data represent individual mice and bars indicate group mean ± SEM. *, $p < 0.05$; **, $p < 0.01$; ***, $p < 0.001$.

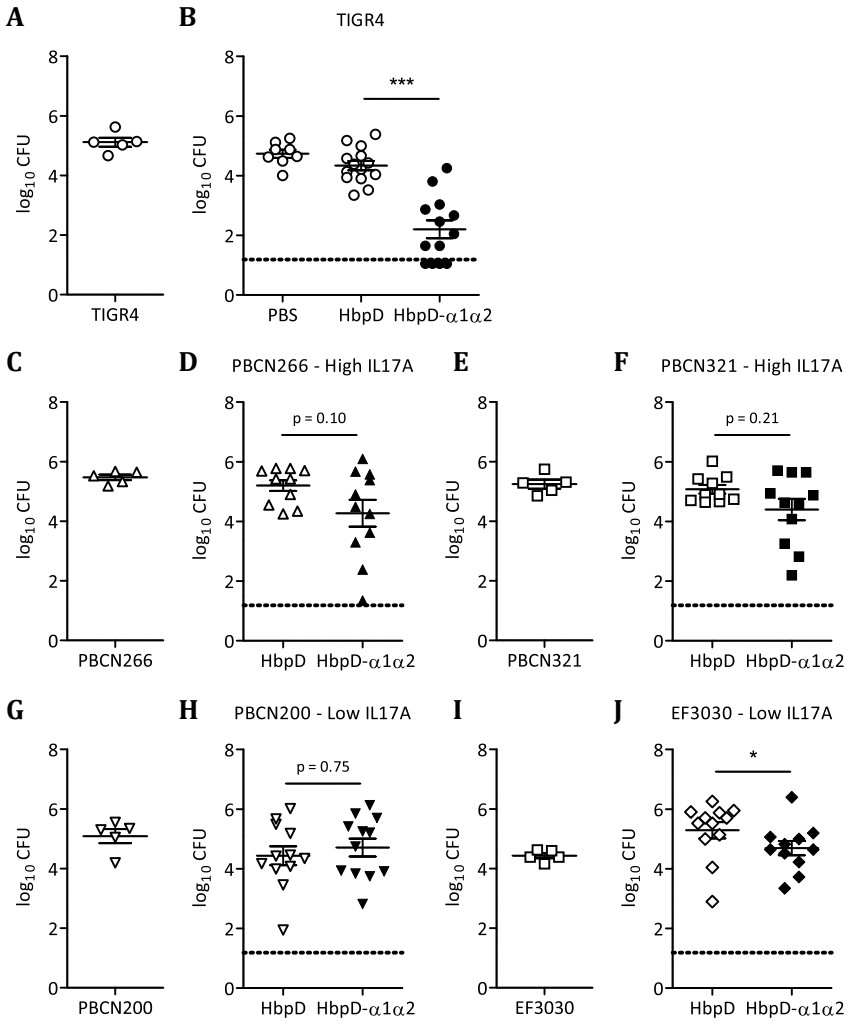

Figure S7 Vaccine-induced nasal IL17A reduces pneumococcal colonization.

Mice were vaccinated with PBS, Δ*msbB* empty OMVs (HbpD) or OMVs expressing α1α2 (Hbp-α1α2). Intranasal infection was performed using TIGR4 (homologous challenge), selected clinical strains (heterologous challenge), or laboratory strain EF3030 (heterologous challenge). (**A, C, E, G, I**) Clinical isolates were tested for colonization of the murine naspharynx. In vaccinated animals three days post-infection, bacterial recovery was assessed of (**B**) TIGR4, (**D**) PBCN266, (**F**) PBCN321, (**H**) PBCN200, and (**I**) EF3030. Data represent individual mice and bars indicate group mean ± SEM. *, $p < 0.05$; **, $p < 0.01$; ***, $p < 0.001$.

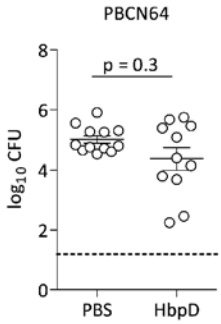

Figure S8 Non-specific effects of OMVs on pneumococcal colonization and nasal IL17A.

Mice were vaccinated with phosphate buffered saline (PBS) or Δ*msbB* empty OMVs (HbpD). Intranasal infection was performed using TIGR4 (homologous challenge). Three days following challenge bacterial CFU. **, $p < 0.01$.

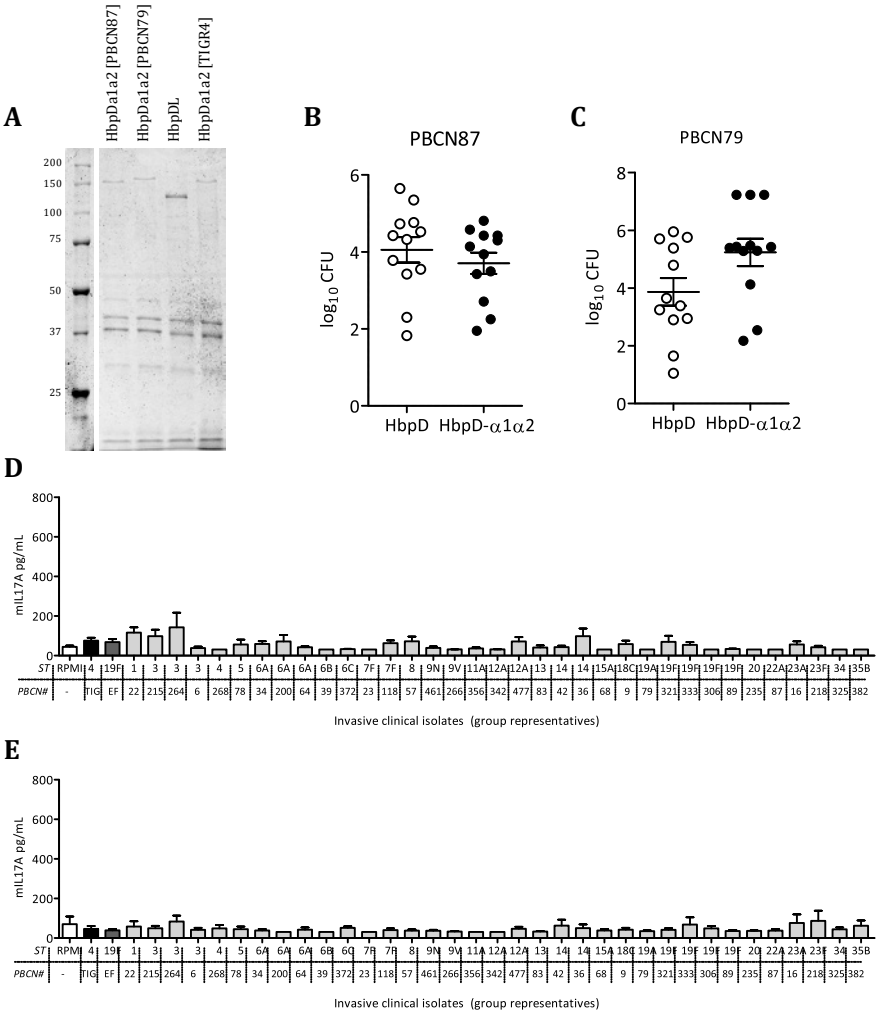

Figure S9 Distinct α1α2 vaccine regions: reduction in pneumococcal colonization & *ex vivo* vaccine-induced Th17 memory cross-reactivity.

(**A**) SDS-PAGE/Coomassie protein profiles of LPS-detoxified (Δ*msbB*) OMVs showing efficient display of HbpD or Hbp-α1α2 derived from TIGR4, PBCN87 or PBCN79. (**B-E**) Mice were vaccinated with empty OMVs (HbpD; open circles) or OMVs expressing α1α2 (Hbp-α1α2; black circles) either derived from (**B**) PBCN87 or (**C**) PBCN79. Bacterial recovery was assessed three days following homologous intranasal infection. Simultaneously spleens n = 5 were harvested and subjected to the *ex vivo* Th17 memory cross-reactivity assays. Vaccine-induced IL17A levels of the (**D**) PBCN87 and (**E**) PBCN79 α1α2 vaccine were measured in cell supernatants and indicative for cross-reactivity with clinical isolates.

15 November 2016
Volume 214
Number 10

The Journal of Infectious Diseases

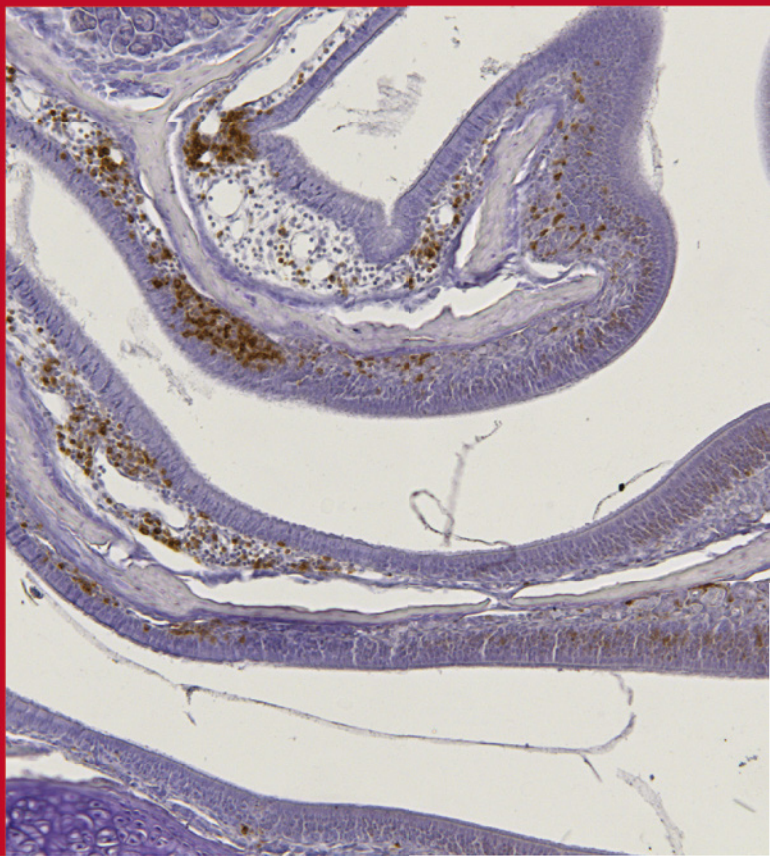

OXFORD
UNIVERSITY PRESS
jid.oxfordjournals.org

5

Antigen-independent restriction of pneumococcal density by mucosal adjuvant Cholera Toxin subunit B

Kirsten Kuipers, Dimitri A. Diavatopoulos, Fred van Opzeeland, Elles Simonetti, Corné H. van den Kieboom, Mariska Kerstholt, Malgortzata Borczyk, Dorette van Ingen Schenau, Eelke T. Brandsma, Mihai G. Netea, Marien I. de Jonge

J Infect Dis. 2016 Nov 15;214(10):1588-1596.

ABSTRACT

For many bacterial respiratory infections, development of (severe) disease is preceded by asymptomatic colonization of the upper airways. For *Streptococcus pneumoniae*, the transition to severe lower respiratory tract infection is associated with an increase in nasopharyngeal colonization density. Insight into how the mucosal immune system restricts colonization may provide new strategies to prevent clinical symptoms. Several studies have provided indirect evidence that the mucosal adjuvant Cholera Toxin subunit B (CTB) may confer non-specific protection against respiratory infections. Here, we show that CTB reduces pneumococcal load in the nasopharynx, which required activation of the caspase-1/11 inflammasome, mucosal T cells and macrophages. Our findings suggest that CTB-dependent activation of the local innate response synergizes with non-cognate T cells to restrict bacterial load. Our study not only provides insight into the immunological components required for containment and clearance of pneumococcal carriage, but also highlight an important yet often understudied aspect of adjuvants.

INTRODUCTION

Bacterial respiratory tract infections are a major cause of severe morbidity and mortality worldwide, both in infants as well as in adults[1,2]. The gram-positive pathogen *Streptococcus pneumoniae* (the pneumococcus) in particular remains an important bacterial pathogen, despite the availability of effective vaccines. The pneumococcus colonizes the mucosal surfaces of the upper respiratory tract for weeks to months, typically in the absence of clinical symptoms. However, under certain conditions, pneumococcal colonization may progress to disease, ranging from mucosal infections such as sinusitis and otitis media to potentially life-threatening invasive infections such as pneumococcal pneumonia, meningitis and sepsis. Progression to disease has been associated with a concomitant increase in bacterial density in the nasopharynx[3-6]. Increased insight into, not only the acquired immune response, but also in the early (innate) mechanisms that may limit the density and duration of nasopharyngeal colonization with *S. pneumoniae* is of significant interest and may lead to the development of new preventive or therapeutic strategies to reduce the burden of pneumococcal disease. In this study, we make use of the observation that certain adjuvants can confer protection against respiratory infections, independent of co-adminstered specific antigens, which we define as 'non-specific' protection. One of these adjuvants is Cholera Toxin (CT), which is produced by *Vibrio cholerae,* the causative agent for severe cholera in humans[7]. CT is comprised of an enzymatically active subunit A (CTA) and a non-toxic subunit B (CTB), the latter of which has previously been shown to bind to the GM-1 ganglioside. GM-1 is present on all nucleated cells, resulting in uptake of the toxin. For decades, both cholera toxin (CT) and its A or pentameric B subunits (CTA and CTB, respectively) have been used as a highly effective mucosal adjuvant, mostly in experimental preclinical models[8]. The versatility and potency of CTB in particular is illustrated in many studies, including against pneumococcal colonization[9-12]. An interesting yet often overlooked finding of these studies is the observation that vaccination with CTB alone, thus without additional antigens, can also reduce pathogen load, e.g. against *S. pneumoniae* and influenza virus[9,13]. These findings suggest that CTB may be able to confer mucosal protection in a non-cognate manner. Here, we examine the effects of CTB on pneumococcal density, using a mouse model of nasopharyngeal colonization. We studied the role of CTB in pneumococcal clearance, with a particular focus on caspase-1/11, mucosal T cells and macrophages. Perturbed mucosal immune homeostasis through CTB administration resulted in a significant reduction of pneumococcal load in the nasopharynx.

MATERIALS AND METHODS

Ethics statement

This study was conducted according to the national guidelines. The protocol was reviewed and approved by Institutional Animal Care and Use Committee Radboud University Medical Center ('Dierexperimentencommissie van de Radboud Universiteit') (DEC number 2011-107, 2011-259, 2013-055, and 2014-188).

Mice experiments

Outbred CD-1, C57BL/6 (Charles River Laboratories, France), C57BL/6 *Ccr2*$^{-/-}$, *Scid*$^{-/-}$ (Jackson Laboratories, ME, USA) and *Casp-1/11*$^{-/-}$ mice[14] were housed under SPF conditions. Mice were immunized intranasally (i.n.) with one or three doses of 4 µg CTB (Sigma, MO, USA) in 10 µL PBS, or an equivalent volume of PBS alone, under isoflurane anesthetics (Pharmachemie BV, The Netherlands)[13]. Where stated, mice received 100 µg clodronate i.n. to deplete nasal macrophages[15], or an equivalent dose of empty liposomes. For challenge, mice were infected i.n. with 10^6 CFU of strain BHN100 (serotype 19F) or with PBS seven days after CTB treatment. Two to four days after infection, mice were sacrificed and nasal tissue was harvested and homogenized (IKA T10 blender). For bacterial enumeration, samples were serially diluted on blood agar plates containing gentamicin (Mediaproducts BV, The Netherlands) and incubated at 37°C overnight.

Immunohistochemistry

For immunohistochemistry experiments, mouse heads were obtained seven and ten days post CTB treatment. The skin, ears and whiskers were removed and heads were fixed in EAFS fixative containing 40% ethanol, 5% acetic acid, 3.7% formaldehyde and 45% of 0.9% sodium chloride solution for three days[16]. Decalcification was performed in 6.5% formic acid at 40°C for four days after which the mouse heads were cut in three transversal slices of 2 mm thick. After 24 hours of post-decalcification in 5% formic acid, samples were dehydrated with increasing concentrations of ethanol (70%, 90%, 96%, 100%) followed by immersion in xylene. Specimens were embedded in paraffin and 4 µm sections were prepared. Prior to immunohistochemical staining, slides were dewaxed and rehydrated followed by blocking with 2% bovine serum albumin, 2% normal goat serum, and 2% normal mouse serum in 0.05% PBS-Tween 20. Slides were then stained overnight at 4 °C with antibodies against CD3 (A0452, DAKO, Belgium) and F4/80 (MCA497G, AbD serotec, United Kingdom). Biotinylated antibodies (Vector Laboratories, CA, USA) were used as secondary antibody, followed by incubation with metal-enhanced diaminobenzidine in Stable Peroxide Substrate Buffer (Thermo Fisher Scientific Inc., MA, USA). Slides were

then counterstained with haemotoxylin (1:3), dehydrated and coverslipped using Entellan (Merck, The Netherlands). Digital images were obtained using a VisionTek© digital microscope (Sakura FineTek, CA, USA). Quantification of positively stained cells in selected regions in the murine nasopharynx, as indicated in Supplementary Figure 1*A* (F4/80) and 1*B* (Ly6G and CD3), was performed with FIJI software[17].

Nasal samples and qPCR

For gene expression analysis, Trizol (Invitrogen, Life Technologies, The Netherlands) was added to homogenized nasal tissue samples and 1:5 diluted with chloroform. After centrifugation, the upper phase was harvested and mixed with an equal amount of 70% ethanol. RNA isolation was performed using the Qiagen RNeasy mini kit according to the manufacturer's instructions. To remove contaminating DNA, the Turbo DNAfree kit was used (Ambion, Life technologies, The Netherlands), after which cDNA was generated using iScript (Bio-Rad, The Netherlands) according to the manufacturer's protocol. Realtime gene expression was performed using Taqman with the following primer-probe combinations: *Il1b* (Mm00434228_m1), *Cd19* (Mm00515420_m1), *Cd3* (Mm00599684_g1), *Foxp3* (Mm00475162_m1), *Il17a* (Mm00439618_m1), *Infg* (Mm01168134_m1), *Il10* (Mm01288386_m1), and *Gapdh* (Mm99999915_g1) (all from Life Technologies, The Netherlands). Reaction mixes contained cDNA, Taqman probes Sso Advanced Universal probe Mastermix (Bio-Rad). In total, 45 cycles were ran using a CFX96 Touch™ Real-Time PCR detection system (Bio-Rad) with the following program: 95°C for 3 minutes, 95°C for 15 seconds, 60°C for 30 seconds.

Statistical analyses

RNA expression and bacterial counts were analyzed using GraphPad Prism version 5.0 (Graphpad Software, CA, USA). Comparisons of CFU counts between groups were performed using the one-way analysis of variance (ANOVA), followed by a Bonferroni post test.

Nasal gene expression for all genes was first normalized to *Gapdh* and illustrated as fold-change according to the Livak method [18]. The non-parametric unpaired T test and One-Way ANOVA with Bonferroni post test was applied for analysis of differences in gene expression and immunohistochemistry analysis between CTB and mock-treated mice. Differences were considered significant at p values < 0.05, results were indicated as follows: *, $p < 0.05$; **, $p < 0.01$; and *** $p < 0.001$; ns, not significant.

RESULTS

CTB transiently reduces the nasopharyngeal pneumococcal load

We first investigated whether three i.n. vaccinations with CTB affected pneumococcal density in a murine model of nasopharyngeal colonization. To this end, outbred CD-1 mice were treated i.n. with CTB or PBS (mock) for three times with 2-week intervals. Seven days after the final treatment, mice were challenged i.n. with *S. pneumoniae*. At two and four days after challenge, mucosal nasal tissue, consisting of nasal associated lymphoid tissue (NALT) and epithelial cells, was obtained and the pneumococcal load in the nasopharynx was determined. CTB-treated mice consistently showed a significant reduction in pneumococcal load in comparison with mock-treated mice, both at day 2 and 4 post-challenge (Figure 1A and B). These results demonstrate that CTB reduces pneumococcal colonization in the absence of prior exposure to pneumococcal antigens. To examine whether this reduction in bacterial load was specific for CTB, mice were treated with Immune Stimulating complexes (ISCOMs). ISCOMs represent an alternative mucosal adjuvant, which for instance is used in a currently licensed i.n. equine influenza vaccine[19,20]. In contrast to CTB, we found no reduction in pneumococcal load in ISCOMs-treated mice following challenge as compared to mock-treated mice (Figures 1A and B). This implies that the observed effect on pneumococcal load is not a universal trait of all mucosal adjuvants.

To examine the duration of the CTB-mediated effects on pneumococcal load, we repeated the experiment described above, but challenged the mice two weeks after the final treatment instead of one week. Two days after infection, we found a reduction in pneumococcal load (Figure 1C), similar to our previous findings. However, this effect was no longer observed at the 4-day time point (Figure 1D).

Thereafter, we investigated whether a single vaccination with CTB would result in the same level of reduction of pneumococcal density. Groups of naïve 6-8 week old C57BL/6 mice (n=10/group) were treated i.n. once with CTB or PBS (mock) and subsequently were infected seven days later with *S. pneumoniae*. Enumeration of bacterial load, three days post-infection, indicated that treatment with a single dose of CTB induced a similar reduction as compared to mice that had received three doses (Figure 2A). Collectively, the protection observed in both inbred and outbred mice supports the ability of CTB to transiently reduce *S. pneumoniae* load in the nasal cavity.

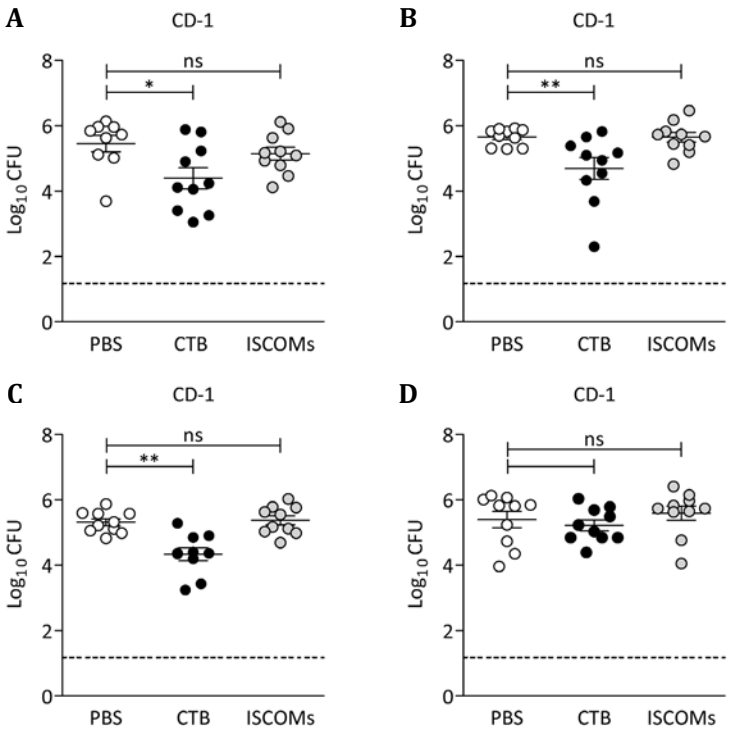

Figure 1 CTB induces a transient reduction in pneumococcal colonization.

CD-1 mice received three i.n. treatments with CTB, PBS (mock), or ISCOMs with a two-week interval. Bacterial recovery in mice challenged with *S. pneumoniae* one week after the final immunization and were sacrificed (**A**) 2 and (**B**) 4 days post-infection to assess bacterial load in the nasal tissue. Bacterial recovery in mice that received *S. pneumoniae* infection two weeks post-immunization and were sacrificed (**C**) 2 and (**D**) 4 days after challenge. Bacterial recovery was assessed in nasal tissue and presented as Log_{10} CFU values, every dot represents individual mice (n = 9-10 per group) and bars indicate group mean ± SEM. The dotted line represents the lower limit of detection. One-way ANOVA with Bonferroni post test was performed for comparison between CTB-, PBS-, ISCOMs-treated mice.*, $p < 0.05$; **, $p < 0.01$; ns, not significant.

Role of inflammasome in CTB-induced reduction in pneumococcal load

CTB has previously been shown to activate the inflammasome in LPS-primed bone marrow derived macrophages[14]. To investigate whether the inflammasome is also activated by CTB *in vivo,* in the nasopharynx, we performed qPCR analysis on *Il1b* expression in nasal tissue of mice treated with a single i.n. dose of CTB or PBS. Groups of mice were either challenged i.n. with *S. pneumoniae* or with mock.

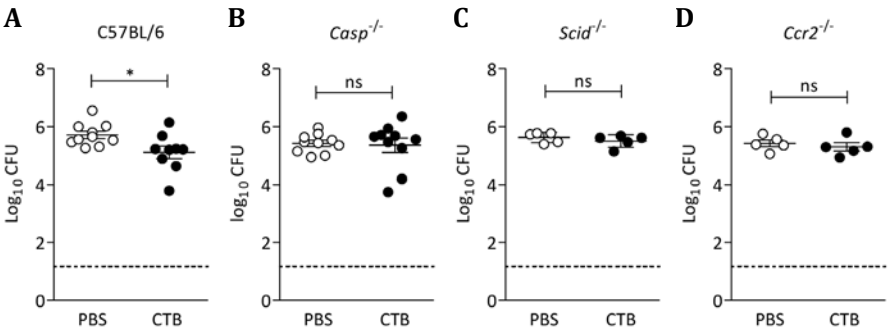

Figure 2 CTB required caspase-1/11, T cells and macrophages for reduction in pneumococcal load.

Mice received a single i.n. treatment with CTB or PBS (mock) and were challenged with *S. pneumoniae* seven days post-treatment. Mice were euthanized 3 days post-infection, e.g. 10 days post-treatment and nasal tissue was harvested to assess bacterial load. Bacterial recovery in (**A**) C57BL/6 mice, (**B**) C57BL/6 *Casp-1/11*$^{-/-}$ (*Casp*$^{-/-}$) mice, (**C**) C57BL/6 *Ccr2-/-* mice, and (**D**) C57BL/6 *Scid*$^{-/-}$ mice. Bacterial recovery is illustrated as Log_{10} CFU values, every dot represents individual mice (n = 5-10 per group) and bars indicate group mean ± SEM. The dotted line represents the lower limit of detection Mann Whitney T test was performed for comparison between CTB- and PBS-immunized mice. *, $p < 0.05$; ns, not significant.

On day 10 after CTB treatment (i.e. three days after infection), significantly elevated *Il1b* expression was measured in the nasal tissue (3.9 ± 2.4 fold, Figure 3A). Subsequent challenge with *S. pneumoniae* further increased *Il1b* expression (Figure 3A).

Macrophages are an important source of IL1β. To assess the presence of macrophages in the nasopharynx, immunohistochemistry (IHC) was performed on the nasal tissue seven days after CTB- or mock-treatment. Although macrophages (F4/80+ cells) were already relatively abundant in mock-treated mice, the number of macrophages increased significantly after CTB treatment (Figure 3B and C). Next, we determined the presence of neutrophils (Ly6G) in the nasal tissue derived from the same mice, using IHC. More neutrophils were detected in CTB treated mice, but was not significantly different compared to mock treated mice at seven days post-infection (Figure 3D).

As the CTB-induced increase in *Il1b* expression suggests a role for the inflammasome, we further explored this using *Casp1/11*$^{-/-}$ mice. *Casp1/11*$^{-/-}$ mice are deficient in caspase-1 and caspase-11-dependent cleavage of pro-IL1β and pro-IL18 into their biologically active forms[14]. *Casp-1/11*$^{-/-}$ mice were treated and infected as described above and the bacterial load in the nasopharynx was

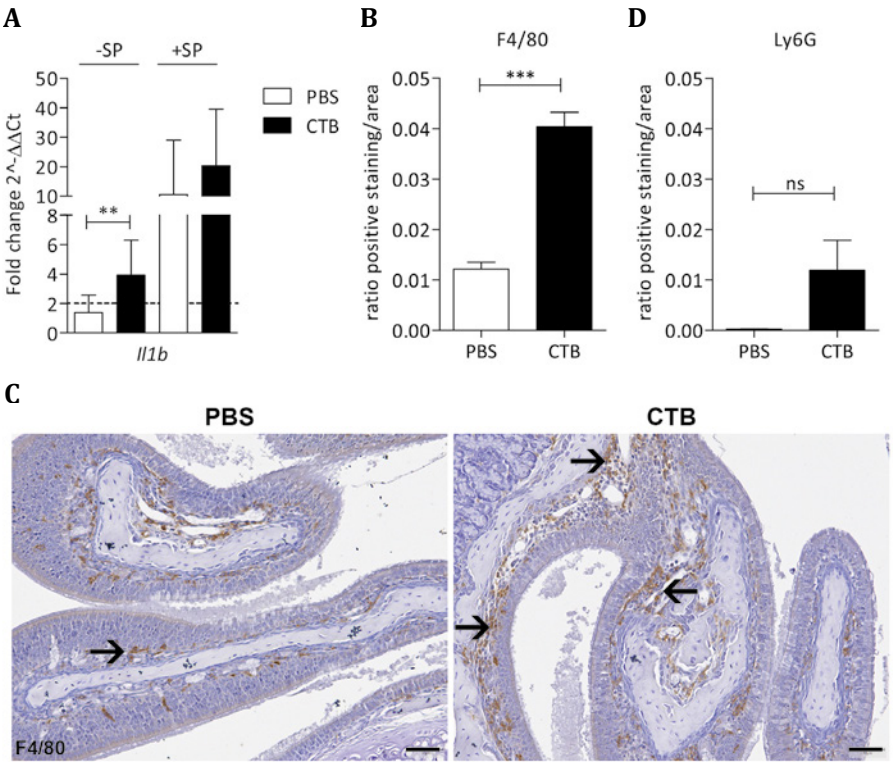

Figure 3 CTB upregulates *Il1b* and recruits macrophages to the nasal mucosa.

(**A**) C57BL/6 mice received a single i.n. dose of CTB or PBS (mock), which were either challenged with *S. pneumoniae* (+SP) or mock-infected (-SP) and sacrificed 10 days post-treatment, e.g. 3 days post-infection. Nasal tissue was harvested 10 days post-treatment and analyzed for local expression of *Il1b*. RNA expression represents n = 5-8 mice from two independent experiments. Results are illustrated as ΔΔCt fold change and represent group mean ± SD. An increase above 2-fold was considered biologically relevant (dotted line). (**B-C**) C57BL/6 mice received a single i.n. CTB or PBS (mock) treatment. At seven days post-immunization the heads of the mice were collected and processed for subsequent immunohistochemistry analysis to specifically detect F4/80-positive macrophages. Arrows indicate positively stained cells and scale bar of 50µm µm. (**B**) Pictures are representative examples from CTB- (n = 4) and mock-treated mice (n = 4). (**C**) Quantification of macrophages (F4/80) from CTB- (n = 4) and mock-treated mice (n = 4) using FIJI software. (**D**) Quantification of neutrophils (Ly6G) from CTB- (n = 4) and mock-treated mice (n = 4) using FIJI software. Data are illustrated as the positive stained area divided by the total area measured with SEM. Unpaired T test was applied to fold-change data and immunohistochemistry quantification for comparison between CTB and PBS-treated mice. **, $p < 0.01$; *** $p < 0.001$.

determined at three days post-infection. In contrast to wildtype C57BL/6 mice, no reduction in pathogen load was observed in the *Casp-1/11* deficient mice (Figure 2A and B), thus pointing to an important role for the inflammasome.

CTB polarizes mucosal T cells

T cells, in particular $CD4^+$ IL17-producing T cells, are thought to be an important component of the mucosal immune response to *S. pneumoniae*[21]. We therefore used IHC to evaluate the presence of T cells ($CD3^+$) in mice treated with CTB or PBS, similar to the macrophages described above. Whilst mock-treated mice showed only low numbers of $CD3^+$ T cells in the lamina propria, treatment with CTB resulted in a strong increase in T cells in the sub-epithelial layer (Figure 4A and B). To confirm this, we examined the expression of *Cd3*, using the pan-B cell marker *Cd19* as a control. Whilst no changes were observed in *Cd19* expression in CTB-treated mice, expression patterns of *Cd3* were in line with IHC observations, demonstrating a 4.8-fold increase (± 2.3) in nasal *Cd3* gene expression in CTB-treated mice compared to mock-treated controls mice (Figure 4C and D). This effect was even more pronounced following *S. pneumoniae* infection (6.7 ± 3.6 fold, Figure 4D).

To further understand whether CTB affected the polarization of T cells into Th17, Th1 or Treg cells, we determined the nasal gene expression of *Il17a*, *Ifng* and *Il10*, respectively. Although IL17 has previously been implicated in mucosal protection against *S. pneumonia*[21,22], we could not detect *Il17a* in the nasopharynx of either CTB immunized or control mice (Figure 5A). Although low expression of *Il17a* was observed in some mice following i.n. infection with *S. pneumoniae,* the majority of mice still did not produce detectable *Il17a* (Figure 5A). This suggests that the reduction in pneumococcal load is independent of IL17. In contrast, nasal expression of *Ifng* and *Il10* was significantly increased in CTB-treated mice compared to controls (15.8 ± 7 fold and 6.1 ± 3 fold respectively, Figures 5B and C). This increase was augmented in the presence of *S. pneumoniae* infection (38.9 ± 29 fold and 9.9 ± 4 fold respectively, Figures 5B and C). Taken together, these findings suggest that CTB promotes local Th1/Treg, but not Th17, responses in the nasal mucosa.

Reduction of pneumococcal load is dependent on both T cells and macrophages

To further investigate the contribution of T cells and macrophages to CTB-mediated reduction in pneumococcal density, $Scid^{+/-}$ and $Ccr2^{-/-}$ mice were used. $Scid^{+/-}$ mice are deficient for T, B and NK cells mice and are frequently used to examine the role of cells involved in the adaptive immune response, such as T cells. $Ccr2^{-/-}$ mice have a deficiency in the chemokine receptor CCR2, resulting in

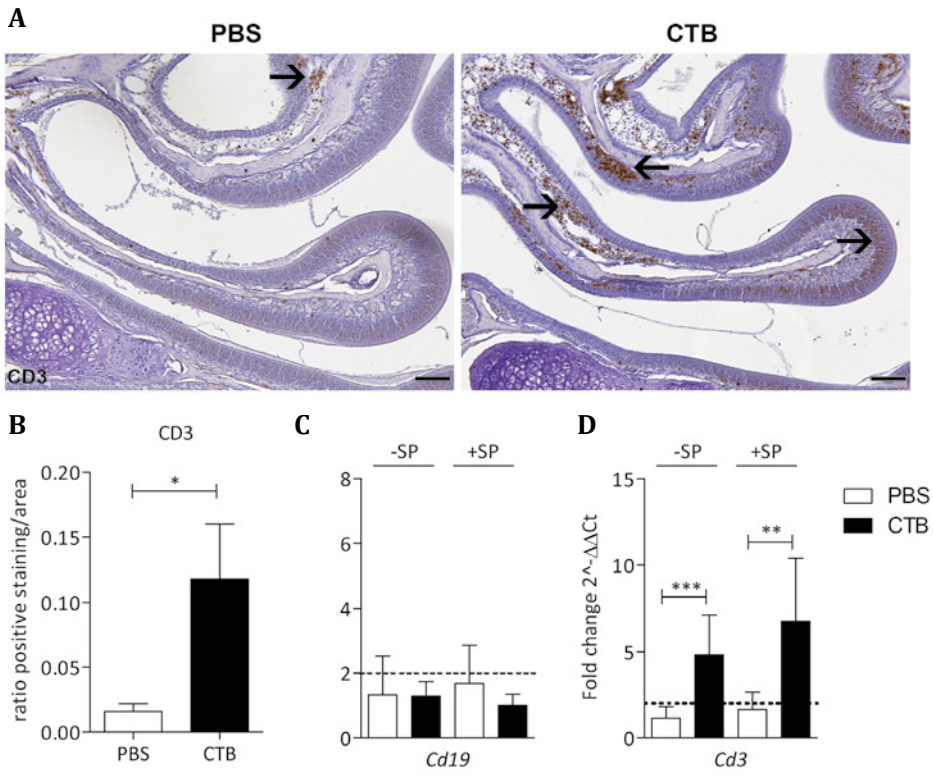

Figure 4 CTB increases *Cd3* expression and recruits T cells to the nasal mucosa.

C57BL/6 mice received a single i.n. CTB or PBS (mock) treatment. At seven days post-immunization the heads of the mice were collected and processed for subsequent immunohistochemistry analysis to specifically detect CD3-positive T cells. Arrows indicate positively stained cells and scale bar of 100µm µm. (**A**) Pictures are representative examples from CTB- (n = 4) and mock-treated mice (n = 4). (**B**) Quantification of T cells (CD3) from CTB- (n = 4) and mock-treated mice (n = 4) using FIJI software. Data are illustrated as the positive stained area divided by the total area measured with SEM. (**C-D**) C57BL/6 mice received a single i.n. dose of CTB or PBS (mock), which were either challenged with *S. pneumoniae* (+SP) or mock-infected (-SP) and sacrificed 10 days post-treatment, e.g. 3 days post-infection. Nasal tissue was harvested 10 days post-treatment and analyzed for local expression of B-cell and T- cell markers (**C**) *Cd19*, (**D**) *Cd3*. RNA expression represents n = 5-8 mice from two independent experiments. Results are illustrated as ΔΔCt fold change and represent group mean ± SD. An increase above 2-fold was considered biologically relevant (dotted line). Unpaired T test was applied to fold-change data and immunohistochemistry quantification for comparison between CTB and PBS-treated mice. *, $p < 0.05$; **, $p < 0.01$; *** $p < 0.001$.

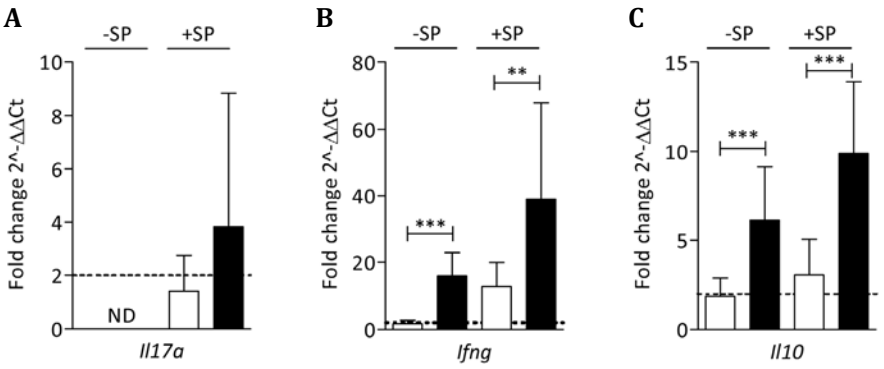

Figure 5 CTB influences T-cell polarization in the nasal mucosa.

C57BL/6 mice received a single i.n. dose of CTB or PBS (mock), which were either challenged with *S. pneumoniae* (+SP) or mock-infected (-SP) and sacrificed 10 days post-treatment, e.g. 3 days post-infection. Nasal tissue was harvested 10 days post-treatment and analyzed for local expression of T cell cytokines (**A**) *Il17a*, (**B**) I*fng*, and (**C**) *Il10*. RNA expression represents n = 13, mice from three independent experiments. Results are illustrated as ΔΔCt fold change and represent group mean ± SD. An increase above 2-fold was considered biologically relevant (dotted line). Unpaired T test was applied to fold-change data for comparison between CTB and PBS-treated mice. **, $p < 0.01$; *** $p < 0.001$; ND, not detectable.

reduced monocyte infiltration upon inflammation[23]. *Scid*$^{-/-}$ and *Ccr2*$^{-/-}$ mice were treated with a single dose of CTB or PBS and infected seven days later. Bacterial load was determined three days after challenge. In contrast to the B6 controls, CTB-mediated protection was absent in both *Scid*$^{-/-}$ and *Ccr2*$^{-/-}$ mice (Figure 2A, C and D). These findings not only suggest that recruitment of inflammatory monocytes is an important component of the CTB-mediated clearance of *S. pneumoniae,* but also that the reduction in pneumococcal load is likely dependent on T cells.

Macrophages are essential for the CTB-mediated effects

Macrophages can play a role early after CTB treatment by priming the local immune response to pneumococcal infection. Alternatively, they can also play a role as (recruited) effector cells in pneumococcal clearance, i.e. at a later stage. To distinguish between these two possibilities, we used clodronate-loaded liposomes to deplete nasal macrophages at two different time points[15]. Depletion was first confirmed by flow cytometry (Supplementary Figure S2*A-B*). Macrophages were either depleted in mice one day before (-1d) or six days (+6d) after CTB treatment in other mice, followed by infectious challenge seven days after CTB treatment. Three days after CTB treatment, pneumococcal load was

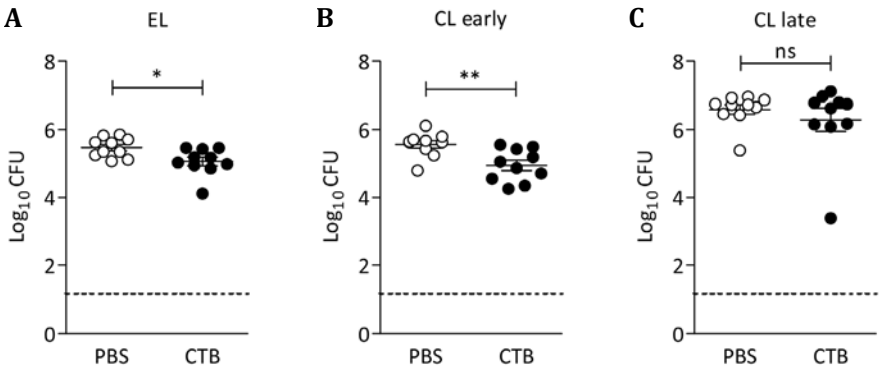

Figure 6 Reduction in pneumococcal colonization is directly mediated by macrophages.

C57BL/6 mice received i.n. CTB or PBS (mock), *S. pneumoniae* infection and bacterial recovery was assessed in nasal tissue 3 days post-infection. (**A**) Bacterial recovery in mice additionally treated with empty liposomes (EL). Bacterial recovery in mice receiving additional treatment with clodronate-loaded liposomes (CL) to deplete nasal macrophages (**B**) early (1 day before CTB treatment) or (**C**) late (6 days post-treament, 1 day prior to challenge infection). Bacterial recovery is illustrated as Log_{10} CFU, values indicate individual mice (n = 5-10 per group) and bars represent group mean ± SEM. The dotted line represents the lower limit of detection. Mann Whitney T test was performed for comparison between CTB- and PBS-immunized mice. *, $p < 0.05$; **, $p < 0.01$; ns, not significant.

determined. Protection was still observed at both time points following treatment with empty liposomes (Figure 6A). Whilst early depletion of macrophages (-1d; CL early) did not abrogate protection (Figure 6B), protection was lost in mice that had received clodronate liposomes at the +6d (CL late) time point (Figure 6C). These results strongly suggest that the CTB-mediated reduction in pneumococcal load is dependent on the recruitment of macrophages. Of note, in all clodronate-treated mice, an increased bacterial load was observed as compared to mice treated with empty liposomes, which highlights the critical role for macrophages in the control of primary pneumococcal infection[24].

DISCUSSION

Previous studies have shown indirect evidence that the mucosal adjuvant CTB is able to reduce pathogen density after challenge with respiratory pathogen, independent of specific antigens. Because increased pneumococcal colonization densities have been associated with progression to disease and/or transmission[3-6], insight into the mechanisms that restrict pneumococcal load in the nasopharynx is important. Here, we demonstrate that CTB reduces nasopharyngeal density in

a murine model of pneumococcal colonization, a process that critically required caspase-1/11 activation, T-cells, and macrophages.

When we challenged mice 14 days after CTB treatment, the reduction in bacterial density was not observed anymore at the 4-day time point, suggesting that the effect of CTB is transient. This coincides with the observation that the CTB-dependent increase in macrophage numbers has waned to non significant levels at 10 days after treatment (Figure S3). Others have also observed complete clearance of pneumococcal carriage in mice up to four weeks after CTB-treatment[13], showing CTB-mediated reduction in pneumococcal density can sustain for a prolonged period. The fact that a reduction in bacterial load was observed in both outbred (CD-1) and inbred mice (CD57BL/6) increases the likelihood that the phenotype is independent of genetic background. The effects of CTB on pathogen load appear not to be limited to *S. pneumoniae* (this paper), but were also observed for influenza A virus[9]. It is unclear whether the mechanisms by which CTB restricts bacterial and viral infection are identical. However, both macrophages and the inflammasome (NLRP3) have a critical role in protection against influenza A infection[25,26].

CTB has previously been shown to activate the inflammasome *in vitro*. Kayagaki *et al*. reported that CTB specifically activated NLRP3 in LPS-primed bone marrow-derived macrophages, resulting in the production of IL-1β[14]. NLRP3 is also highly expressed by respiratory epithelial cells in both mice and men[27]. Of note, inflammasome activation typically requires co-activation of other innate pattern recognition receptor for production of biologically active IL-1β and IL-18[28]. This is in line with other studies showing that the CTB-mediated response is dependent on TLR co-signaling[14,29]. In our model, it is possible that the effects of CTB are dependent on the presence of microbiota-derived co-signals[30]. Alternatively, Phongsisay recently reported that CTB is able to activate TLR4 by itself, as shown by the reduction in cytokine expression of *ex vivo* CTB-treated bone marrow-derived macrophages and peritoneal cells from TLR4$^{-/-}$ mice[31].

We found that macrophages play an important role later after CTB treatment, i.e. just prior to pneumococcal challenge. This is in line with studies demonstrating that the secondary influx of macrophages is essential for the elimination of a primary pneumococcal infection[24]. At present, it is unclear what the primary mechanism is that drives the recruitment of these macrophages, as protection was still observed when macrophages were depleted early after CTB administration. We also observed increased numbers of neutrophils after CTB treatment, although it was not found for all CTB treated mice.

The role of T cells in our model is less clear. Pneumococcal antigen-specific T cells, in particular CD4^{+} IL17-producing cells, have been shown to be important

for effective clearance of pneumococcal colonization[21,22]. However, these memory cells are normally only induced by previous exposure to pneumococcal antigens, which is lacking in our experimental setup. Notably, IFNγ and IL10 could also be produced by other immune cells including NK cells and γδ T cells. The latter have been described to be among the first responders upon *S. pneumoniae* infection[32]. There is increasing attention to tissue resident memory cells (T_{RM}), which have also been described to respond in an innate manner. CTB has previously been shown to polarize T cells into Th1 and Treg[33-35]. Indeed, we show that administration of CTB results in the production of IL10 and IFNγ. Although the source of these cytokines remains unknown, recent literature has shown that T_{RM} cells can indeed produce IFNγ without T-cell receptor signaling in response to *in vivo* inflammasome activation[36-39]. This would fit with our observation that 1. CTB promoted *Ifng* expression, 2. CTB induced a strong T-cell influx, and 3. the reduction in pneumococcal density was dependent on caspase-1/11 activation.
To the best of our knowledge, this is the first report describing that CTB is able to restrict bacterial density in the nasopharynx in a model of pneumococcal colonization. Our study not only provides further insight into the biological mechanisms for containment of pneumococcal density in the nasopharynx, but also improves our understanding of the underlying mechanisms through which certain adjuvants, including the mucosal adjuvant CTB, may beneficially influence infections independently of specific antigenic stimulation.

Acknowledgements

We thank Dr. Josbert M. Metselaar (Enceladus, The Netherlands) and Dr. Laurens van der Meer (Department Pediatrics, Radboud UMC, The Netherlands) for kindly providing the clodronate and empty liposomes. We thank Prof. Dr. Leo Joosten (Internal medicine, Radboud UMC, The Netherlands) and Prof. Dr. Marten Hofker (Department of Molecular Genetics, Groningen UMC, The Netherlands) for kindly providing the *Casp-1/11*$^{-/-}$ mice, and Dr. Gerben Ferwerda for the active discussions. The work described in this manuscript was supported by Agentschap NL (PneumoVac, nr. OM111009). MGN was supported by an ERC Consolidator Grant (#310372). We thank Dr. Merijn van Erp from the Microscopic Imaging Center of the Radboud UMC, The Netherlands for help in developing the FIJI plugin. The authors declared no conflict of interest.

REFERENCES

1 Organization, W. H. *The top 10 causes of death*, <http://www.who.int/mediacentre/factsheets/fs310/en/> (2014).
2 Organization, W. H. *Children: reducing mortality*, <http://www.who.int/mediacentre/factsheets/fs178/en/> (2014).
3 Diavatopoulos, D. A. *et al.* Influenza A virus facilitates *Streptococcus pneumoniae* transmission and disease. *FASEB J* **24**, 1789-1798, doi:10.1096/fj.09-146779 (2010).
4 Mina, M. J., Klugman, K. P. & McCullers, J. A. Live attenuated influenza vaccine, but not pneumococcal conjugate vaccine, protects against increased density and duration of pneumococcal carriage after influenza infection in pneumococcal colonized mice. *J Infect Dis* **208**, 1281-1285, doi:10.1093/infdis/jit317 (2013).
5 Short, K. R., Reading, P. C., Wang, N., Diavatopoulos, D. A. & Wijburg, O. L. Increased nasopharyngeal bacterial titers and local inflammation facilitate transmission of *Streptococcus pneumoniae*. *MBio* **3**, doi:10.1128/mBio.00255-12 (2012).
6 Vu, H. T. *et al.* Association between nasopharyngeal load of *Streptococcus pneumoniae*, viral coinfection, and radiologically confirmed pneumonia in Vietnamese children. *Pediatr Infect Dis J* **30**, 11-18, doi:10.1097/INF.0b013e3181f111a2 (2011).
7 Holmgren, J. Actions of cholera toxin and the prevention and treatment of cholera. *Nat New Biol* **292**, 413-417 (1981).
8 Lycke, N. Recent progress in mucosal vaccine development: potential and limitations. *Nat Rev Immunol* **12**, 592-605 (2012).
9 Matsuo, K. *et al.* Induction of innate immunity by nasal influenza vaccine administered in combination with an adjuvant (cholera toxin). *Vaccine* **18**, 2713-2722 (2000).
10 Areas, A. P. *et al.* Expression and characterization of cholera toxin B-pneumococcal surface adhesin A fusion protein in Escherichia coli: ability of CTB-PsaA to induce humoral immune response in mice. *Biochem Biophys Res Commun* **321**, 192-196 (2004).
11 Qiu, S. *et al.* Fusion-expressed CTB improves both systemic and mucosal T-cell responses elicited by an intranasal DNA priming/intramuscular recombinant vaccinia boosting regimen. *J Immunol Res* **2014**, 308732 (2014).
12 Kono, M., Hotomi, M., Hollingshead, S. K., Briles, D. E. & Yamanaka, N. Maternal immunization with pneumococcal surface protein A protects against pneumococcal infections among derived offspring. *PLoS One* **6**, e27102 (2011).
13 Malley, R. *et al.* Multiserotype protection of mice against pneumococcal colonization of the nasopharynx and middle ear by killed nonencapsulated cells given intranasally with a nontoxic adjuvant. *Infect Immun* **72**, 4290-4292, doi:10.1128/iai.72.7.4290-4292.2004 (2004).
14 Kayagaki, N. *et al.* Non-canonical inflammasome activation targets caspase-11. *Nat New Biol* **479**, 117-121 (2011).
15 van Rooijen, N. & Hendrikx, E. Liposomes for specific depletion of macrophages from organs and tissues. *Methods Mol Biol* **605**, 189-203, doi:10.1007/978-1-60327-360-2_13 (2010).
16 Harrison, P. T. An ethanol-acetic acid-formol saline fixative for routine use with special application to the fixation of non-perfused rat lung. *Lab Anim* **18**, 325-331 (1984).
17 Schindelin, J. *et al.* Fiji: an open-source platform for biological-image analysis. *Nat Methods* **9**, 676-682, doi:10.1038/nmeth.2019 (2012).
18 Livak, K. J. & Schmittgen, T. D. Analysis of relative gene expression data using real-time quantitative PCR and the 2(-Delta Delta C(T)) Method. *Methods* **25**, 402-408 (2001).
19 Paillot, R. & Prowse, L. ISCOM-matrix-based equine influenza (EIV) vaccine stimulates cell-mediated immunity in the horse. *Vet Immunol Immunopathol* **145**, 516-521 (2012).
20 Hu, K. F., Lovgren-Bengtsson, K. & Morein, B. Immunostimulating complexes (ISCOMs) for nasal vaccination. *Adv Drug Deliv Rev* **51**, 149-159 (2001).
21 Malley, R. *et al.* CD4+ T cells mediate antibody-independent acquired immunity to pneumococcal colonization. *Proc Natl Acad Sci U S A* **102**, 4848-4853 (2005).

22 Lu, Y. J. *et al.* Interleukin-17A mediates acquired immunity to pneumococcal colonization. *PLoS Pathog* **4**, e1000159, doi:10.1371/journal.ppat.1000159 (2008).
23 Kurihara, T., Warr, G., Loy, J. & Bravo, R. Defects in macrophage recruitment and host defense in mice lacking the CCR2 chemokine receptor. *J Exp Med* **186**, 1757-1762 (1997).
24 Zhang, Z., Clarke, T. B. & Weiser, J. N. Cellular effectors mediating Th17-dependent clearance of pneumococcal colonization in mice. *The Journal of clinical investigation* **119**, 1899-1909 (2009).
25 Schneider, C. *et al.* Alveolar macrophages are essential for protection from respiratory failure and associated morbidity following influenza virus infection. *PLoS Pathog* **10**, e1004053, doi:10.1371/journal.ppat.1004053 (2014).
26 Owen, D. M. & Gale, M., Jr. Fighting the flu with inflammasome signaling. *Immunity* **30**, 476-478, doi:10.1016/j.immuni.2009.03.011 (2009).
27 Santana, P. *et al.* Is the inflammasome relevant for epithelial cell function? *Microbes Infect*, doi:10.1016/j.micinf.2015.10.007 (2015).
28 Latz, E., Xiao, T. S. & Stutz, A. Activation and regulation of the inflammasomes. *Nat Rev Immunol* **13**, 397-411 (2013).
29 Gloudemans, A. K. *et al.* The mucosal adjuvant cholera toxin B instructs non-mucosal dendritic cells to promote IgA production via retinoic acid and TGF-beta. *PLoS One* **8**, e59822 (2013).
30 Clarke, T. B. *et al.* Recognition of peptidoglycan from the microbiota by Nod1 enhances systemic innate immunity. *Nat Med* **16**, 228-231 (2010).
31 Phongsisay, V., Iizasa, E., Hara, H. & Yoshida, H. Evidence for TLR4 and FcRgamma-CARD9 activation by cholera toxin B subunit and its direct bindings to TREM2 and LMIR5 receptors. *Mol Immunol* **66**, 463-471, doi:10.1016/j.molimm.2015.05.008 (2015).
32 Ivanov, S., Paget, C. & Trottein, F. Role of non-conventional T lymphocytes in respiratory infections: the case of the pneumococcus. *PLoS Pathog* **10**, e1004300, doi:10.1371/journal.ppat.1004300 (2014).
33 Eriksson, K., Fredriksson, M., Nordstrom, I. & Holmgren, J. Cholera toxin and its B subunit promote dendritic cell vaccination with different influences on Th1 and Th2 development. *Infect Immun* **71**, 1740-1747 (2003).
34 Sun, J. B., Czerkinsky, C. & Holmgren, J. Mucosally induced immunological tolerance, regulatory T cells and the adjuvant effect by cholera toxin B subunit. *Scand J Immunol* **71**, 1-11 (2010).
35 Anjuere, F. *et al.* Transcutaneous immunization with cholera toxin B subunit adjuvant suppresses IgE antibody responses via selective induction of Th1 immune responses. *J Immunol* **170**, 1586-1592 (2003).
36 Carbone, F. R. Tissue-Resident Memory T Cells and Fixed Immune Surveillance in Nonlymphoid Organs. *J Immunol* **195**, 17-22, doi:10.4049/jimmunol.1500515 (2015).
37 Pham, O. H. & McSorley, S. J. Divergent behavior of mucosal memory T cells. *Mucosal Immunol* **8**, 731-734, doi:10.1038/mi.2015.52 (2015).
38 Holmkvist, P. *et al.* A major population of mucosal memory CD4+ T cells, coexpressing IL-18Ralpha and DR3, display innate lymphocyte functionality. *Mucosal Immunol* **8**, 545-558, doi:10.1038/mi.2014.87 (2015).
39 Kupz, A. *et al.* NLRC4 inflammasomes in dendritic cells regulate noncognate effector function by memory CD8(+) T cells. *Nat Immunol* **13**, 162-169, doi:10.1038/ni.2195 (2012).

SUPPLEMENTARY MATERIALS AND METHODS

Flow cytometry

To confirm macrophage depletion in the nasopharyngeal area, blood was taken and mice were intracardially perfused with PBS. Nasal tissue was collected in RPMI supplemented with 5% fetal calf serum (FCS), 1 mg/ml collagenase type 2 (Sigma, MO, USA), and 20 U DNase I (Roche, MO, USA), and incubated at 37°C for 30 min after which single cells were treated with RBC lysis buffer (eBioscience, CA, USA). Nonspecific binding was blocked with FcγII/III (BD Biosciences) and cells were stained with macrophage marker F4/80 APC (AbD Serotec, United Kingdom) in PBS + 1% bovine serum albumin (BSA) in the dark on ice for 30 min. Cells were fixed in 1% paraformaldehyde for 20 min and data were acquired using a BD LSR II flow cytometer. Data were analyzed using FlowJO (Tree Star, Inc, OR, USA). For gating, lymphocytes were selected using FSC and SSC and F4/80 positive cells were selected based on the SSC and F4/80 expression.

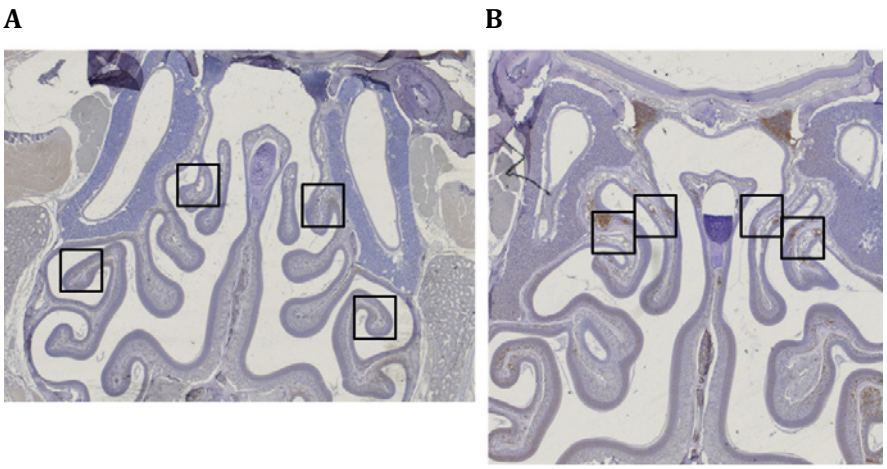

Figure S1 Overview of nasopharyngeal regions used for IHC quantification.

Four selected regions (indicated by rectangles) per slide were used for IHC quantification of (**A**) macrophages (F480) and (**B**) neutrophils (Ly6G) and T cells (CD3).

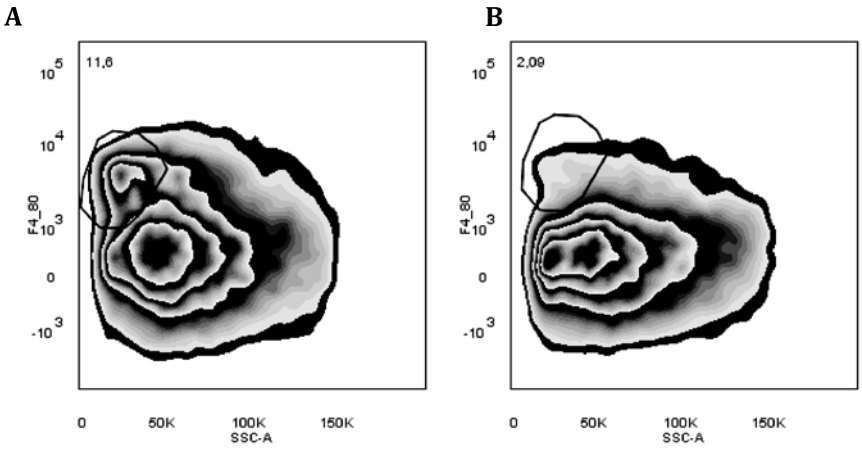

Figure S2 Intranasal clodronate-loaded liposomes treatment depletes nasal macrophages.

C57BL/6 mice were i.n. treated with empty liposomes (EL; control) or clodronate-loaded liposomes (CL) to deplete nasal macrophages. Macrophage were detected with F4/80 in nasal tissue by flow cytometry. Gating was performed on the F4/80 positive cells within the lymphocyte population and numbers show the percentage F4/80 positive cells. (**A**) Baseline macrophage levels in nasal tissue from mice treated with EL (control). (**B**) Lower percentage of macrophages in nasal tissue after CL treatment. Results show representative flow cytometry analyses from nasal tissue of mice treated with empty liposomes (n = 3) and clodronate liposomes (n = 3).

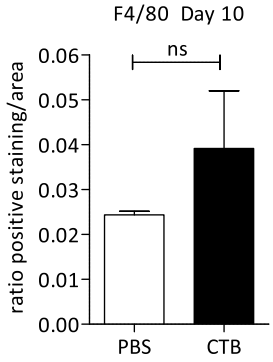

Figure S3 Quantification of CTB-mediated macrophage recruitment at 10 days post treatment.

C57BL/6 mice received a single i.n. CTB or PBS (mock) treatment. At ten days post-immunization the heads of the mice were collected and processed for subsequent immunohistochemistry analysis to specifically detect F4/80-positive macrophages. Data show quantification of macrophages (F4/80) from CTB- (n = 4) and mock-treated mice (n = 4) using FIJI software.

6

Genetic background impacts vaccine-induced reduction of pneumococcal colonization

Kirsten Kuipers, Saskia van Selm, Fred van Opzeeland, Jeroen D. Langereis, Lilly M. Verhagen, Dimitri A. Diavatopoulos, Marien I. de Jonge

Manuscript submitted

ABSTRACT

Vaccination has been one of the most successful strategies to reduce morbidity and mortality caused by respiratory infections. Differences in the host genetic background and environmental factors can contribute to heterogeneity in the immune response to vaccination. Here we examined the influence of host genetics on vaccine-induced protection against pneumococcal colonization, using two commonly used inbred mouse strains, i.e. C57BL/6 and BALB/c, as well as the F1 cross of these two strains. Groups of mice were vaccinated intranasally with a vaccine formulation containing the model antigen, pneumococcal surface protein A (PspA), with the well-known mucosal adjuvant, cholera toxin subunit B (CTB). Baseline colonization varied between mouse strains with high pneumococcal load observed in BALB/c. Vaccination with PspA significantly reduced pneumococcal density in all mouse genetic backgrounds, however, strong differences were observed in the magnitude of protection. We examined immunological parameters known to be involved in vaccine-induced mucosal clearance, including PspA-specific antibodies and cytokines associated with cellular immunity to *S. pneumoniae.* PspA-specific IgG levels in nasal tissue significantly correlated with a reduction in colonization. Also, the concentration of nasal IL17A, but not IFNγ, IL10, or IL4, was found to be mouse strain specific. This suggests that a reduction of bacterial load in different genetic backgrounds can be achieved in a similar way, likely via a Th17 response. Increased insight into the different immune mechanisms that affect pneumococcal carriage will contribute to development of future vaccines against *S. pneumoniae*.

INTRODUCTION

The human immune system is capable to respond to highly diverse and constantly evolving pathogens[1,2]. From both experimental animal studies as well as human studies it is known that the genetic background is an important determinant of pathogen susceptibility[3-9]. Host genetic components are also known to affect vaccine-induced responses[10-12]. Importantly, a vaccine is made to protect all individuals within the vaccinated population and an effect of individual genetic makeup on the establishment of vaccine-induced protection may thus lead to inadequate protection.

In this study we focus on *Streptococcus pneumoniae,* a human-specific pathogen ranking among the top 10 of infection-related mortality and causing severe diseases, including pneumonia and sepsis[13-15]. Since colonization is a prerequisite for both transmission and invasive disease, targeting pneumococcal carriage by vaccination has led to a significant reduction of invasive pneumococcal disease[16]. Pre-clinical evaluation of experimental human vaccines is typically performed in single inbred mouse strains, such as C57BL/6 and BALB/c. Considering that these vaccines are intended to work in a heterogenic population, this may complicate successful translation of findings in the mouse model. C57BL/6 and BALB/c mice are known to induce Th1 and Th2-prone responses, respectively. Conversely, vaccine-induced reduction of pneumococcal colonization was previously shown to be dependent on a Th17 response[17,18].

In this study, we investigated the effect of mouse strain genetic background on the efficacy of mucosal vaccination against *S. pneumoniae*, using the model antigen pneumococcal surface protein A (PspA). Protection outcomes were then correlated to differences in cellular and humoral immune markers.

MATERIALS AND METHODS

Mouse vaccination and infection studies

Seven week-old female C57BL/6J (inbred), BALB/c (inbred), and CB6F1 (outbred) mice, a cross between BALB/c × C57BL/6J (Charles River Laboratories), received three intranasal (i.n.) immunizations with 10 µg purified recombinant PspA from TIGR4 (kindly provided by Mucosis B.V., Groningen, The Netherlands) with 4 µg CTB (Sigma) or 4 µg CTB alone (control) in a volume of 10 µL, at two-week intervals, under anesthetics (2.5% v/v isoflurane, AU Veterinary Services)[19]. Three weeks after the final immunization mice received a homologous infection i.n. with 10^6 CFU of *S. pneumoniae* TIGR4[20]. Mice were euthanized five days after challenge, after which both nasal lavage was obtained and mucosal nasal tissue was harvested. Nasal lavage was taken using 1 mL PBS and serially diluted onto

Colombia Agar with Gentamicin (Mediaproducts BV) to determine bacterial recovery (log CFU/organ). Nasal tissue was homogenized in 1 mL PBS using an IKA T10 basic blender and used for later analyses. All animal experimentation was performed in accordance with and approved by the Radboud University Medical Center Committee for Animal Ethics (DEC2013-266).

Detection of nasal antibody responses

Maxisorp high binding affinity plates (Nunc) were coated with 2 µg/mL of purified PspA in carbonate coating buffer (0.1 M carbonate/bicarbonate pH 9.6) at 4°C overnight[20]. The following day, wells were washed with PBS containing 0.05% Tween-20 (PBST; Merck), blocked with 1% BSA (Sigma) and incubated with individual mouse serum samples for 1 h at 37 °C. Wells were washed with PBST and incubated with anti-mouse IgG-alkaline phosphatase (Sigma) for 1 h at 37 °C. After washing, samples were developed using 1 mg/mL *p*-nitrophenyl-posphate in substrate buffer, 1 M diethanolamine, 0.5 mM $MgCl_2$ pH 9.8, (Calbiochem, VWR) and optical density was measured at 405 nm 10 and 30 minutes after substrate addition.

Measurement of nasal IFNγ, IL4, IL17A and IL10

IFNγ, IL4, IL17A and IL10 concentrations in nasal tissue were determined using the Cytometric Bead Array kit. The Mouse Enhanced Sensitivity buffer kit (Becton Dickinson) in combination with the IFNγ, IL4, IL17A and IL10 Enhanced Sensitivity Flex sets (Becton Dickinson) was used according to manufacturer's instructions. Concentrations were calculated using Soft Flow FCAP Array v1.0 (Becton Dickinson) with 274 fg/mL as the lower limit of detection.

Statistical analyses

The Mann-Whitney *t* test was applied to CFU numbers and cytokine levels for comparison between vaccinated and control mice. Antibody and cytokine concentrations, and bacterial load were analyzed using Spearman rank correlations. All statistical analyses were performed using GraphPad Prism version 5.0 (Graphpad Software) and SPSS (IBM SPSS Statistics 22). Differences were considered significant at p-values < 0.05 and were indicated as follows: *, $p < 0.05$; **, $p < 0.01$; and *** $p < 0.001$; ns, not significant.

RESULTS

Baseline pneumococcal colonization densities differ between genetically distinct mouse strains

To determine the influence of the genetic background on pneumococcal colonization, we used three different mouse strains: C57BL/6 (inbred), BALB/c (inbred) and CB6F1 (outbred, BALB/c × C57BL/6). The mice received three intranasal immunizations with CTB only (mock) or PspA plus CTB at two-week intervals and were challenged intranasally with *S. pneumoniae* at three weeks post-vaccination. Five days after infection, bacterial colonization was determined in the nasal cavity.

Remarkably, infection in mock-immunized mice led to clear differences in baseline pneumococcal densities between the different genetic backgrounds (Figure 1). At day 5 post-infection, BALB/c mice showed significantly higher CFU recovered from the nasopharynx compared C57BL/6 and CB6F1 mice. The intra-group variation is relatively small for BALB/c mice (Log CFU 1.56), but larger in both C57BL/6 and CB6F1 mice (Log CFU 2.43 and 4.00, respectively). This variation in initial colonization between the strains suggests that the kinetics of pneumococcal clearance differ per mouse strain.

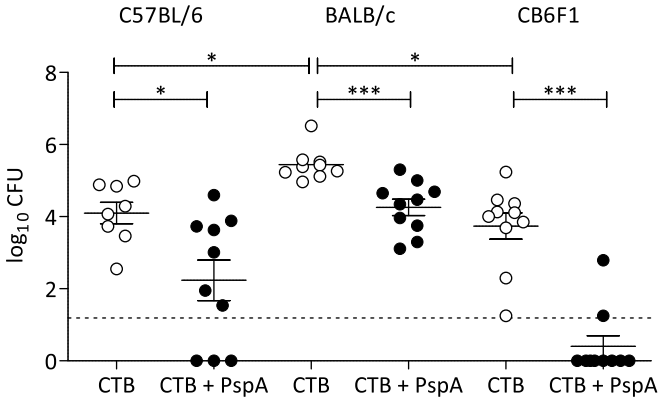

Figure 1 Baseline pneumococcal colonization and vaccine-induced protection against pneumococcal colonization in C57BL/6, BALB/c, and CB6F1 mice.

Mice were 3x i.n. immunized with PspA + CTB, or CTB only (control mice) and challenged i.n. at three weeks post-immunization with 10^6 CFU of *S. pneumoniae*. Bacterial recovery was determined in two independent studies at 5 days post-infection in C57BL/6, BALB/c, and CB6F1 mice. Symbols represent individual mice receiving CTB (open circles) or PspA + CTB (black circles) and show group mean ±SEM from n = 8-10 mice. *, $p < 0.05$; **, $p < 0.01$; ***, $p < 0.001$.

Vaccine-induced reduction of *S. pneumoniae* colonization in genetically distinct mouse strains

Furthermore, we determined the influence of the genetic background on the reduction in *S. pneumoniae* colonization following vaccination with PspA. In all PspA-vaccinated mice, pneumococcal load was significantly reduced compared to mock-vaccinated mice at five days after infection (Figure 1). In PspA-vaccinated mice, the degree of intra-strain variation in colonization densities, and thus clearance capacity following vaccination, differed per mouse strain. At day 5 post-infection, BALB/c mice showed overall minor variation (Log CFU 2.19), in contrast to C57BL/6 and CB6F1 mice that illustrate higher intra-strain variations (Log CFU 4.60 and 2.79, respectively) (Figure 1). The results suggest that the initial magnitude of colonization is indicative for intra-group variation in PspA-vaccinated animals. Notably, the variation within mock-vaccinated (CTB) mice might also be caused by antigen-independent effects of CTB on pneumococcal density[21]. Together this illustrates that PspA vaccine-induced reduction in pneumococcal colonization can be achieved in distinct genetic backgrounds, although the actual reduction in pneumococcal load seems to be influenced by the initial magnitude of colonization, which is mouse strain dependent.

Levels of PspA-specific IgG in all mouse strains

It has previously been described that antibodies can contribute to prevention or clearance of pneumococcal colonization[22-26]. To examine the antibody response in these mice, we measured PspA-specific IgG concentrations in nasal washes at five days post-infection. Although all mouse strains showed significantly increased nasal PspA-specific IgG levels (Figures 2A-C) compared to the CTB-treated control mice, the total level of PspA-specific IgG differs between mouse strains. High PspA-specific IgG concentrations were measured in both C57BL/6 and CB6F1 mice, i.e. mean levels of 181 ng/mL and 325 ng/mL respectively, while in BALB/c mice mean levels of 45 ng/mL were measured. In all mouse backgrounds, increased nasal IgG significantly correlates with a reduction in colonization (Figures 2D-F).

Nasal T helper signature cytokine levels in distinct mouse strains

Cellular responses have also been associated with clearance of pneumococcal colonization[17,18]. To investigate the contribution of cellular immunity, hallmark T helper cytokines IFNγ (Th1), IL17A (Th17), IL4 (Th2), and IL10 (Treg) were measured in nasal tissue at five days post-infection. In none of the samples IL4 was detected. IFNγ concentrations were very low to undetectable, and similar in C57BL/6, BALB/c and CB6F1 mice. All three mouse strains showed increased

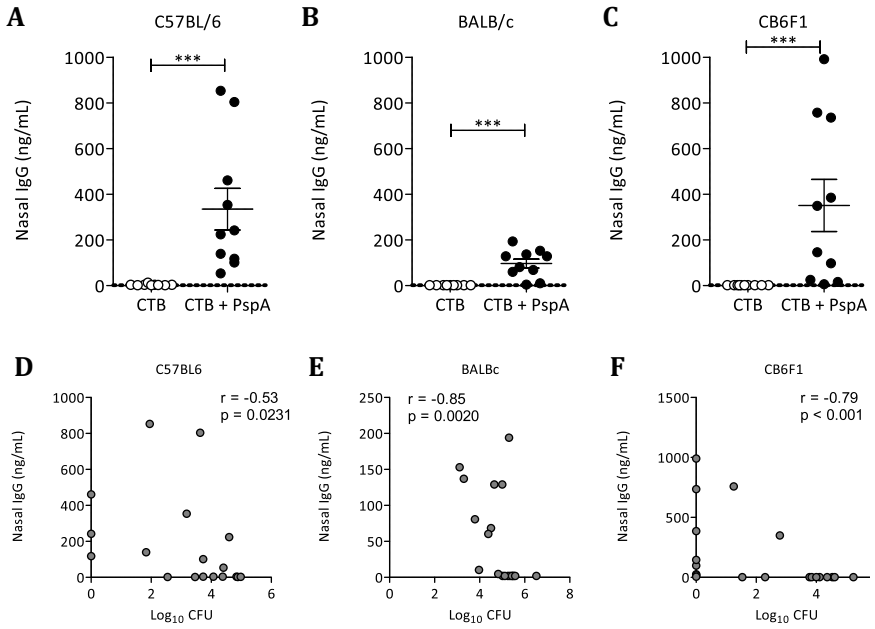

Figure 2 Nasal antigen-specific IgG significantly correlates with protection.

Mice received three i.n. immunizations with PspA + CTB, or CTB only (control mice) and i.n. infection with 10^6 *S. pneumoniae* three weeks post-immunization. Nasal lavages obtained five days post-infection from two independent studies were assessed for PspA-specific IgG in (**A**) C57BL/6, (**B**) BALB/c, and (**C**) CB6F1 mice. Symbols represent individual mice receiving CTB (open circles) or PspA + CTB (black circles) and show group mean ±SEM from n = 8-10 mice. Results show group mean ±SEM and significance is indicated with *, $p < 0.05$; **, $p < 0.01$. Antigen-specific IgG concentrations were correlated with bacterial density recovered from the nasal lavage of (**D**) C57BL/6, (**E**) BALB/c, and (**F**) CB6F1 mice using Spear man rank test. Spearman's correlation coefficient (r) and p-value are indicated.

IL17A levels after vaccination with PspA, compared to mock-vaccinated animals (Figures 3A-C). Interestingly, a non-significant trend was observed in C57BL/6 and CB6F1 mice, while this increase was highly significant in BALB/c mice. IL10 was detectable in nasal tissue of all mice. However, no differences were observed between mice immunized with PspA as compared to their respective mock-treated controls (Figures 3D-F). Taken together, increased concentrations of nasal IL17A were measured in all three mouse genetic backgrounds following PspA vaccination.

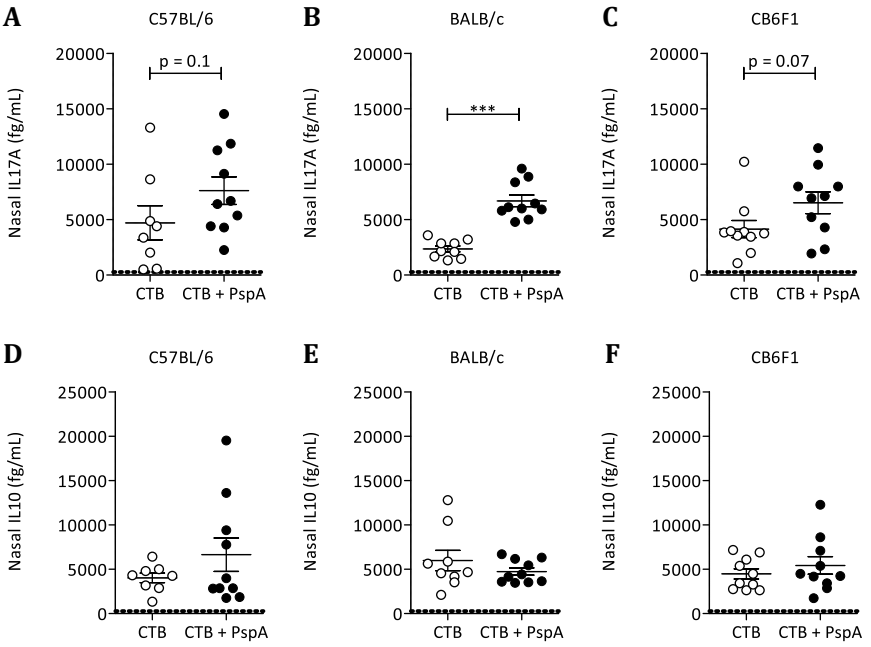

Figure 3 Increase in nasal IL17A, but not IL10, in C57BL/6, BALB/c, and CB6F1 mice.

T helper cytokines were assessed in nasal tissue, from i.n. immunized mice, at five days after homologous pneumococcal infection. Concentrations (**A-C**) IL17A and (**D-F**) IL10 were measured using flow cytometry in C57BL/6, BALB/c, and CB6F1 mice respectively. Data show individual mice with group mean ±SEM from n = 8-10 mice and significance was accepted at p-value 0.05 with *, $p < 0.05$.

Nasal IL17A correlates with vaccine-induced reduction in *S. pneumoniae* colonization

To identify relations between T helper cytokines and vaccine-induced reduction of colonization of *S. pneumoniae*, we correlated the nasal cytokine concentrations of individual mice with their respective pneumococcal load, as determined at five days post-infection. Nasal IL17A correlated with reduced colonization for C57BL/6, BALB/c and CB6F1 mice (Figures 4A-C). A strong negative correlation was observed between nasal IL17A and bacterial load in the noses of BALB/c mice (Figure 4B), with a p-value of 0.0006. Nasal IL10 did not correlate with bacterial load in the three mouse strains (Figures 4D-F). In conclusion, only IL17A, and not IL10, was associated with vaccine-induced protection against pneumococcal colonization.

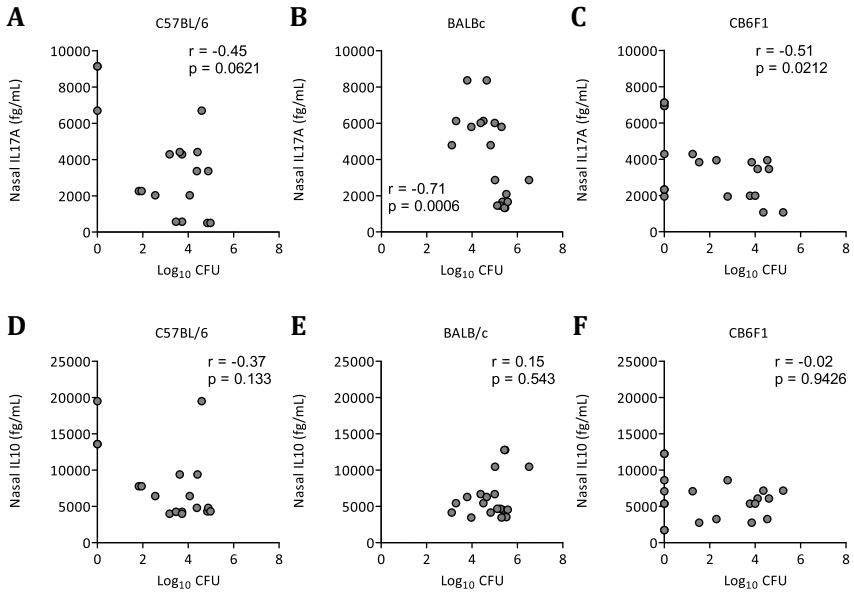

Figure 4 IL17A correlates with pneumococcal density in the nasopharynx.

T helper cytokines were correlated with bacterial recovery derived from the nasal tissue of mice that received three i.n. immunizations, five days after homologous pneumococcal infection. Single cytokines concentrations of (**A-C**) IL17A and (**D-F**) IL10 in C57BL/6, BALB/c and CB6F1 mice respectively were correlated with pneumococcal load illustrated as CFU. Spearman rank test was applied for analysis from n = 8-10 mice and Spearman's correlation coefficient (r) and p-value are indicated. Significance was accepted at a p-value of 0.05

DISCUSSION

It is widely accepted that the genetic makeup of the host is a critical determinant for susceptibility to infection[1,2,8]. Although genetic variation also affects the quantity, persistence and type of immune responses[10], its effect on vaccine efficacy remains largely unclear. Here, we studied whether the mouse genetic background influences vaccine-induced reduction of pneumococcal colonization. Immunization with PspA in combination with an adjuvant has previously shown to confer protection against pneumococcal colonization in a range of different mouse strains[20,27]. In our study, we found significant differences in pneumococcal load between C57BL/6, BALB/c and CB6F1, following mock-vaccination and vaccination with PspA. The lower pneumococcal densities in C57BL/6 and CB6F1 suggest that these strains are intrinsically more resistant to pneumococcal

colonization than BALB/c mice. Pneumococcal densities were correlated to nasal cytokine profiles following vaccination and illustrated the importance of nasal IL17A as common mechanism for clearance in C57BL/6, BALB/c and CB6F1 mice.

Murine studies of pneumococcal carriage have demonstrated that protection against colonization is critically dependent on a Th17 response. This response is induced by colonization, but also by intranasal vaccination with e.g. inactivated whole pneumococci[17,18,20,28]. Notably, these studies were performed only in the C57BL/6 background. In the current study, an increased IL17A response was observed in C57BL/6, BALB/c, CB6F1 mice vaccinated with PspA. Also in all three mouse genetic backgrounds, nasal IL17A correlated with a reduction in colonization load. It should be noted that nasal IL17A may also be a reflection of the bacterial load present in the nasopharynx. It has previously been demonstrated by our group that IL17A in nasal tissue correlates with a reduction in pneumococcal load[20]. Surprisingly, BALB/c mice showed the highest increase in nasal IL17A (Figure 3B). This might suggest that the kinetics of IL17A are different between mouse strains and could mean that in our study the time point to measure IL17A in BALB/c and CB6F1 is suboptimal. In our study, BALB/c mice appear to be more susceptible to pneumococcal colonization than C57BL/6 and CB6F1, based on the initial magnitude of pneumococcal load in the nasopharynx of mock-vaccinated mice. This led us to question whether BALB/c mice potentially have a slower IL17A response, as protection was less pronounced in these mice. We hypothesize that IL17A is of great importance for reduction of pneumococcal colonization, but that the height and kinetics are determined by the mouse genetic background. Notably, differences observed between genetic backgrounds in colonization density and mucosal immune responses could also be influenced by the type of microbiota present in the different mouse strains[29]. Protection against pneumococcal colonization in mice by pneumococcal specific IgG is mediated by agglutination[22]. In this process, antibodies agglutinate bacterial cells and accelerate clearance from the nasopharyngeal mucosa. Recently, our group observed that incubation of PspA-specific antibodies with pneumococci leads to agglutination (Unpublished data). In our study, we observed that the mice from all three mouse strains vaccinated with PspA showed a significantly higher level of PspA-specific antibodies in the nasal mucosa (Figure 2A-C). These antibodies together with the increase in nasal IL17A induced by vaccination may synergistically cause a reduction in pneumococcal load.

In conclusion, the current study demonstrates that vaccine-induced reduction of *S. pneumoniae* colonization was independent of the mouse strain used. However, the level of reduction strongly varied between the different mouse strains. The nasal T helper cytokine profiles post-challenge infection suggest that

similar immune mechanisms measured as IL17A and antigen-specific IgG lead to reduction of pneumococcal load. Altogether, improved understanding of the immune mechanisms underlying vaccine-induced protection against pneumococcal colonization will contribute to the development of future mucosal pneumococcal vaccines.

Acknowledgements
The authors thank Dr. Kees Leenhouts and Dr. Maarten van Roosmalen (Mucosis B.V., Groningen, The Netherlands) for providing purified recombinant PspA.

REFERENCES

1 Chapman, S. J. & Hill, A. V. Human genetic susceptibility to infectious disease. *Nat Rev Genet* **13**, 175-188, doi:10.1038/nrg3114 (2012).
2 Lazzaro, B. P. & Schneider, D. S. The genetics of immunity. *Genetics* **197**, 467-470, doi:10.1534/genetics.114.165449 (2014).
3 Chiavolini, D., Pozzi, G. & Ricci, S. Animal models of *Streptococcus pneumoniae* disease. *Clin Microbiol Rev* **21**, 666-685, doi:10.1128/cmr.00012-08 (2008).
4 Gingles, N. A. *et al.* Role of genetic resistance in invasive pneumococcal infection: identification and study of susceptibility and resistance in inbred mouse strains. *Infect Immun* **69**, 426-434, doi:10.1128/iai.69.1.426-434.2001 (2001).
5 McCool, T. L. & Weiser, J. N. Limited role of antibody in clearance of *Streptococcus pneumoniae* in a murine model of colonization. *Infect Immun* **72**, 5807-5813, doi:10.1128/iai.72.10.5807-5813.2004 (2004).
6 Mizrachi-Nebenzahl, Y. *et al.* Differential activation of the immune system by virulent *Streptococcus pneumoniae* strains determines recovery or death of the host. *Clin Exp Immunol* **134**, 23-31 (2003).
7 Lundbo, L. F. *et al.* Genetic Variation in NFKBIE Is Associated With Increased Risk of Pneumococcal Meningitis in Children. *EBioMedicine* **3**, 93-99, doi:10.1016/j.ebiom.2015.11.048 (2016).
8 Sellers, R. S., Clifford, C. B., Treuting, P. M. & Brayton, C. Immunological variation between inbred laboratory mouse strains: points to consider in phenotyping genetically immunomodified mice. *Vet Pathol* **49**, 32-43, doi:10.1177/0300985811429314 (2012).
9 van der Maten, E. *et al.* Complement Factor H Serum Levels Determine Resistance to Pneumococcal Invasive Disease. *J Infect Dis* **213**, 1820-1827, doi:10.1093/infdis/jiw029 (2016).
10 Newport, M. J. The genetic regulation of infant immune responses to vaccination. *Front Immunol* **6**, 18, doi:10.3389/fimmu.2015.00018 (2015).
11 Fine, P. E. Variation in protection by BCG: implications of and for heterologous immunity. *Lancet* **346**, 1339-1345 (1995).
12 Wiertsema, S. P. *et al.* Impact of genetic variants in IL-4, IL-4 RA and IL-13 on the anti-pneumococcal antibody response. *Vaccine* **25**, 306-313, doi:10.1016/j.vaccine.2006.07.024 (2007).
13 Kadioglu, A., Weiser, J. N., Paton, J. C. & Andrew, P. W. The role of *Streptococcus pneumoniae* virulence factors in host respiratory colonization and disease. *Nat Rev Microbiol* **6**, 288-301, doi:10.1038/nrmicro1871 (2008).
14 O'Brien, K. L. *et al.* Burden of disease caused by *Streptococcus pneumoniae* in children younger than 5 years: global estimates. *Lancet* **374**, 893-902, doi:10.1016/s0140-6736(09)61204-6 (2009).
15 Drijkoningen, J. J. & Rohde, G. G. Pneumococcal infection in adults: burden of disease. *Clin Microbiol Infect* **20 Suppl 5**, 45-51, doi:10.1111/1469-0691.12461 (2014).
16 Myint, T. T. *et al.* The impact of 7-valent pneumococcal conjugate vaccine on invasive pneumococcal disease: a literature review. *Adv Ther* **30**, 127-151, doi:10.1007/s12325-013-0007-6 (2013).
17 Malley, R. *et al.* CD4+ T cells mediate antibody-independent acquired immunity to pneumococcal colonization. *Proc Natl Acad Sci U S A* **102**, 4848-4853, doi:10.1073/pnas.0501254102 (2005).
18 Lu, Y. J. *et al.* Interleukin-17A mediates acquired immunity to pneumococcal colonization. *PLoS Pathog* **4**, e1000159, doi:10.1371/journal.ppat.1000159 (2008).
19 Tettelin, H. *et al.* Complete genome sequence of a virulent isolate of *Streptococcus pneumoniae*. *Science (80-)* **293**, 498-506, doi:10.1126/science.1061217 (2001).
20 Kuipers, K. *et al.* Salmonella outer membrane vesicles displaying high densities of pneumococcal antigen at the surface offer protection against colonization. *Vaccine* **33**, 2022-2029, doi:10.1016/j.vaccine.2015.03.010 (2015).
21 Kuipers, K. *et al.* Antigen-Independent Restriction of Pneumococcal Density by Mucosal Adjuvant Cholera Toxin Subunit B. *J Infect Dis* **214**, 1588-1596, doi:10.1093/infdis/jiw160 (2016).

22 Roche, A. M., Richard, A. L., Rahkola, J. T., Janoff, E. N. & Weiser, J. N. Antibody blocks acquisition of bacterial colonization through agglutination. *Mucosal Immunol* **8**, 176-185, doi:10.1038/mi.2014.55 (2015).
23 Prevaes, S. M. *et al.* Nasopharyngeal colonization elicits antibody responses to staphylococcal and pneumococcal proteins that are not associated with a reduced risk of subsequent carriage. *Infect Immun* **80**, 2186-2193, doi:10.1128/iai.00037-12 (2012).
24 Xu, Q., Casey, J. R. & Pichichero, M. E. Higher levels of mucosal antibody to pneumococcal vaccine candidate proteins are associated with reduced acute otitis media caused by *Streptococcus pneumoniae* in young children. *Mucosal Immunol* **8**, 1110-1117, doi:10.1038/mi.2015.1 (2015).
25 Holmlund, E. *et al.* Antibodies to pneumococcal proteins PhtD, CbpA, and LytC in Filipino pregnant women and their infants in relation to pneumococcal carriage. *Clin Vaccine Immunol* **16**, 916-923, doi:10.1128/cvi.00050-09 (2009).
26 Lebon, A. *et al.* Natural antibodies against several pneumococcal virulence proteins in children during the pre-pneumococcal-vaccine era: the generation R study. *Infect Immun* **79**, 1680-1687, doi:10.1128/iai.01379-10 (2011).
27 Ferreira, D. M. *et al.* Protection against nasal colonization with *Streptococcus pneumoniae* by parenteral immunization with a DNA vaccine encoding PspA (Pneumococcal surface protein A). *Microb Pathog* **48**, 205-213, doi:10.1016/j.micpath.2010.02.009 (2010).
28 Zhang, Z., Clarke, T. B. & Weiser, J. N. Cellular effectors mediating Th17-dependent clearance of pneumococcal colonization in mice. *J Clin Invest* **119**, 1899-1909, doi:10.1172/jci36731 (2009).
29 Ivanov, II *et al.* Induction of intestinal Th17 cells by segmented filamentous bacteria. *Cell* **139**, 485-498, doi:10.1016/j.cell.2009.09.033 (2009).

7

Altered macrophage biology drives age-related susceptibility to infection – lessons from pneumococcal colonization

Kirsten Kuipers, Marien I. de Jonge

Manuscript in preparation

ABSTRACT

Many infectious diseases primarily strike the very young and very old. Although members of both age groups are often targeted by the same infectious agent, a mechanistic understanding of this age-related susceptibility is generally lacking. One such example is infection caused by *Streptococcus pneumoniae* (the pneumococcus), which was recently investigated in infant and aged mice in two independent studies that demonstrated prolonged carriage in both age groups. A common theme in these studies involved altered macrophage responses that delay pneumococcal clearance from the respiratory mucosa. Herein, we discuss age-related defects in macrophage biology that contribute to susceptibility to infection. At both extremes of age, an elevated basal level of inflammation leads to suboptimal macrophage recruitment, although regulated differently in the young and old. Collectively, these studies provide insight into the underlying susceptibility of infants and elderly and why infections occur at the extreme ages of life.

INTRODUCTION

Young children have an elevated risk of infection, which remains a leading source of morbidity and mortality in this age group[1-3]. With increasing age, the susceptibility to infection gradually decreases[4]. However, the risk for infection increases again later in life and is a major contributor to morbidity and mortality among the elderly[5]. The very young and very old are often struck by the same infectious disease due to a similar array of infectious agents. An example is pneumonia, which is a leading cause of death in both the first and last years of life[6,7]. Our understanding of the underlying mechanisms that drive this age-related susceptibility to pneumonia remains incomplete, and, in particular, it is unknown whether there might be common themes among the young and old. The age-related susceptibility to infection as occurs in humans can be recapitulated in various animal models[8]. One such model involves the study of pneumococcal carriage. Colonization along the mucosal surfaces of the nasopharynx is the source of organisms aspirated into the lower airways and, thus, the first step in the pathogenesis of this leading etiologic agent of bacterial pneumonia. The susceptibility to pneumococcal infection in both infant and aged mice correlates with prolonged carriage similar to humans[9-11]. This murine model has been used to dissect the host responses that explain why infants and the elderly have an increased risk for pneumococcal infection compared to normal adults[8,12,13].

Factors affecting the clearance of pneumococcal colonization were recently investigated in both infant and old mice respectively by two independent studies[9,10]. Indeed, these reports demonstrate that similar mechanisms, including altered macrophage responses and increased levels of mucosal inflammation, mediate prolonged pneumococcal carriage in both the young and old. Herein, we discuss the age-related defects in macrophage responses in both these age groups. Furthermore, we elaborate on how high baseline inflammation in the very young and very old may drive suboptimal macrophage responses. Together, these common themes may provide insight into the susceptibility to infection at the extreme ages of life.

An age-related defect in monocyte recruitment following infection

Prolonged carriage in both age groups is associated with a reduced capacity to eliminate the infectious threat[9,14,10,15,16]. Mucosal clearance requires a sustained influx of F4/80$^+$ macrophages derived from the monocyte pool to the airways at sites of pneumococcal colonization of epithelial surfaces, although once within the airway lumen these no longer display markers typical of monocytes[13,17,18]. Evidence that these macrophages are derived from monocytes includes the

requirement for expression of the chemokine receptor CCR2, involved in monocyte migration[13]. Since infant and aged mice both show delayed pneumococcal clearance, the dynamics of monocyte/macrophages effectors have been the focus of investigation (Figure 1)[9,10,13,18-28]. During infection, circulating blood monocytes are recruited to the site of infection upon recognition of an infectious threat, in particular via pattern recognition receptors such as TLR2[18,29]. These macrophage responses are critical for restriction and elimination of the infection, either directly by engulfing microbes or indirectly by activating adaptive immunity[29]. The importance of TLR2 was illustrated by a delayed macrophage influx and clearance of *S. pneumoniae* from the nasopharynx in adult *tlr2*$^{-/-}$ mice[9,12]. There are differences in TLR2 responses between the young and adults, however, these do not account for the susceptibility to colonization observed in infant mice as *tlr2* deficiency showed no additional delay in colonization, unless TLR2 expression is very low infant mice[9,14]. Importantly, the delayed clearance of the infection in the infant coincided with reduced macrophage numbers in the nasopharynx as compared to adult mice[9]. When monocyte influx was restored by exogenous CCL2 expression in infant mice to numbers equivalent to those in adults, pneumococcal clearance was accelerated[9]. This confirms that the prolonged colonization in infants mice was attributed to a delayed monocyte influx into the nasopharynx.

In contrast, in aged mice an increased rather than decreased monocyte influx into the nasal tissue was associated with delayed clearance of pneumococcal infection[10]. This observation, however, is in conflict with the study of Krone *et al.* which demonstrated reduced macrophage numbers in the nasopharynx of aged mice following pneumococcal infection[15]. A possible explanation for these conflicting findings is that they used F4/80 markers to detect macrophages. This may give an underestimation of the macrophages present in the nasopharynx, as the study by Puchta and colleagues demonstrated that F4/80 expression was strongly reduced on the macrophages recruited following infection[10,15]. How increased monocyte numbers in the very old hamper clearance of infection is currently unclear, but these observations suggest that monocyte function in the aged is impaired. Similar to the human infant, aged human monocytes and aged mouse lungs demonstrated reduced PRR responses, including sensing through TLR2, resulting in reduced cytokine expression[4,16]. Although there is conflicting literature with regard to the effect of aging on monocyte function, multiple studies demonstrated impaired phagocytosis of human monocytes derived from aged individuals[30-32]. In this regard, it has also been shown that excessive monocyte influx exacerbates mycobacterial infection and delays its clearance, which correlated with increased inflammation measured by increased CCL2 and CCR2 expression[29,33]. Possibly, the excessive

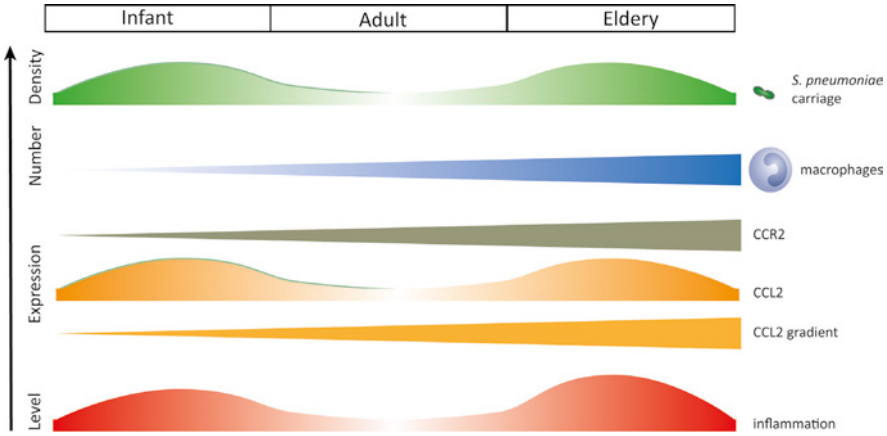

Figure 1 Overview of altered macrophage biology in the very young and the very old.

Monocyte responses vary at different ages and correlate with susceptibility to pneumococcal infection. With increasing age, monocyte recruitment becomes more pronounced and monocyte CCR2 expression increases. In contrast, baseline CCL2 levels decrease with increasing age, allowing for establishment of a stronger CCL2 gradient to drive monocyte recruitment during infection.

macrophage recruitment observed in aged mice may further enhance pneumococcal infection and thereby delay elimination. This is supported by the observation that partial restoration of monocyte influx by anti-TNF treatment in aged mice to normal levels improved pneumococcal clearance[10]. In summary, a defective, although opposing, monocyte influx following infection appears to account for increased susceptibility in both young and aged mice.

Age-related alterations in CCL2 and CCR2 determine susceptibility to infection

How is this opposing monocyte influx following infection regulated in infants and the elderly? Monocyte recruitment to the site of infection is mediated by local upregulation of CCL2, the major chemokine stimulating the recruitment of monocytes[17,29,34]. CCL2 is produced by epithelial and immune cells in response to TLR activation by detection of bacterial components at the site of infection[9,10,17,29,35]. Recruited myeloid cells then become an additional source of CCL2 creating a positive feedback loop. The establishment of a concentration gradient of CCL2 between the mucosal surface and circulation allows for the influx of monocytes that express CCR2 into the inflamed tissues. Alterations in any of these molecules will affect monocyte recruitment to the site of infection. The two recent studies

of pneumococcal infection in infant and aged mice demonstrated alterations in expression of CCL2 and CCR2 in both age groups (Figure 1)[9,10]. The net effect of these perturbations in CCL2 and CCR2 expression is dysfunction of monocyte recruitment into infected tissues that results in delayed clearance and exacerbated infection[29,33].

Under normal physiologic conditions, infant mice express higher levels of CCL2 in the nasopharynx compared to adults[9]. CCL2 expression may already be at maximum levels in infants, as it was not further upregulated following infection. While this would be expected to promote a strong signal for monocyte recruitment, baseline CCL2 levels were also high in infant sera, thus no concentration gradient can be established by the local response to infection[9]. This gradient could be restored by exogenous expression of CCL2 to generate supra-physiologic levels sufficient to increase monocyte recruitment and thereby promote pneumococcal clearance[9,36]. As would be expected from the high levels of its ligand, murine CCR2 expression on infant monocytes was reduced as compared to adult cells[9]. This reduced level of CCR2 on monocytes, however, could be a factor in defective trafficking into inflamed tissues[17,29].

In contrast to infant mice, baseline CCL2 levels in aged mice were not different from normal adults[10]. Additionally, during infection, CCL2 expression showed significant upregulation in aged mice compared to younger adults. Baseline levels of CCR2 expression were increased on aged murine monocytes and monocyte efflux from the bone marrow into the circulation was increased in aged mice[10]. Together, the stronger CCL2 gradient and increased expression of CCR2 during aging potentially contribute to a more robust monocyte recruitment to the site of inflammation. Hinojosa and colleagues also proposed that aged mice have an initial delayed response to infection due to an incapacity to respond to infections, which results eventually in increased inflammation accompanied by a stronger monocyte influx[10,16].

In sum, these data demonstrate that tight regulation of CCL2 and CCR2 expression is required for optimal monocyte recruitment in order to clear an infection. The very young and elderly show altered regulation of the CCL2 and CCR2 axis, although these manifest differently, that underlies their defective monocyte recruitment leading to increased susceptibility to infection.

The age-related elevated baseline inflammation drives suboptimal monocyte influx

Evidence suggests that in both the young and the old it is high levels of mucosal inflammation that drive these alterations in CCL2 and CCR2 expression (Figure 1). However, as the inflammation status in both studies was assessed differently, it is difficult to make direct comparisons between infant and aged mice[9,10].

In each instance, high inflammation and, thus, suboptimal monocyte influx was attributed to environmental factors associated with age.

In infant mice, analyses of proinflammatory responses in both sera and the nasopharyngeal mucosa showed elevated inflammation at baseline without infection. In the infant nasopharyngeal mucosa this was characterized by increased expression of CCL2, CCL7 and IL6 compared to adults[9]. Furthermore, the observation of increased levels of CCL2 in infant sera indicated systemic inflammation. The high levels of the increased mucosal expression of CCL2 and CCL7 appeared to be a consequence of nasopharyngeal microbiome acquisition during the newborn period since microbiome depletion by maintaining the dams on broad-spectrum antibiotics restored baseline CCL2 and CCL7 expression to adult levels[9]. It was proposed that systemic inflammation in the infant was due to leakage of bacterial products at colonized surfaces into otherwise sterile sites, an event previously linked to the newborn period[37]. Pneumococcal infection of pups of formerly antibiotic-treated mothers led to adult-like numbers of mucosal macrophages, which corresponded with reduced bacterial density. These data provided key support for the conclusion that high baseline inflammation is driven by the nasopharyngeal microbiome, and, therefore, responsible for the delayed monocyte influx and clearance of infection[9]. How this affected CCR2 expression was not studied, but the infant microbiome could play a role, since it has been shown that stimulation of human monocytes with pathogen-associated molecular patterns like LPS reduced CCR2 expression[38]. That increased inflammation in infants underlies their susceptibility to infection as shown by the study of Siegel *et al.* may come as a surprise, since young children are generally considered to be non- or low-immune responders, both in their mucosa as well as in their circulation[4,39]. Therefore, these recent findings shed new light on our view of inflammation status during the period when colonization of mucosal surfaces is first established.

In contrast, chronic inflammation in the elderly is a generally accepted hallmark of aging and contributing factor underlying their increased mortality due to infectious and immune-related diseases[4,16,40]. In both aged mice and humans, increased inflammation is characterized by heightened serum TNFα levels at baseline[4,10,16,40]. That chronic inflammation due to high TNFα levels drives suboptimal macrophage responses during aging was proven through two lines of experimental evidence. Both aged TNFα-deficient mice and anti-TNFα treatment of aged wild type mice restored monocyte numbers to normal young adult levels and promoted pneumococcal clearance[10]. This chronic inflammatory state in aged mice, which appears to be similar to 'inflamm-aging' as observed in the elderly, was linked to increased CCR2 expression on monocytes[10]. This would promote a stronger recruitment of monocytes as observed in aged mice that,

however, may increase local inflammation levels that exacerbate infection[33]. Whether the elevated state of inflammation also drives a stronger CCL2 gradient was not directly investigated. Baseline inflammation measured by TNFα and IL6 levels in the nasopharyngeal mucosa of aged mice was similar to young adult animals[10]. However, these proinflammatory cytokines were strongly increased following infection[10]. What is causing these high levels of inflammation in aged mice is unclear. Observations from Puchta and colleagues hint that these cytokines may be produced by macrophages, as the increased mucosal inflammation coincided with the influx of monocytes into the nasopharynx[10]. Importantly, anti-TNF treatment did not restore monocyte production in the bone marrow of aged mice, suggesting an intrinsic cell defect rather than chronic inflammatory environment fueling monocyte production and efflux from the bone marrow during aging. It would be interesting to assess whether this increased monocyte production is also responsible for the increased chronic inflammation in the very old. Alternatively, the altered microbiome composition of the aged may increase inflammation, as observed for infant mice[9].

It is evident that heightened inflammation in both extremes of age drive altered macrophage biology and affects susceptibility to infection. How this is regulated and how it negatively impacts immune responses, including those determined by macrophages, should be a topic of future research. A further question is how the inflammatory state has distinct effects on CCL2 and CCR2 in both age groups, although to our knowledge the mechanisms by which the CCL2/CCR2 axis is regulated have only been partly deciphered[17,29]. This is an important topic since monocytes and their recruitment have a pivotal role during infection, as demonstrated in the case of pneumococcal colonization, as well as other immune-related diseases[17,19].

Conclusions

Individuals early and late in life are at increased risk for infections. However, the mechanisms by which this is established are not fully understood. Recent work illustrated that susceptibility to infection in the young and very old maybe more similar than initially believed. One such shared mechanism involves defects in monocyte/macrophage responses, which are critical for infection biology, and are driven by a heighted level of inflammation in both age groups. Chronic inflammation is not novel in the elderly. However, the concept of heightened inflammation in the very young is new and thus intriguing. Understanding how increased inflammation, early and late in life, alters macrophage biology and promotes susceptibility to infection will require further study.

REFERENCES

1 Organization, W. H. Children: reducing mortality. (2015).
2 Lawn, J. E., Cousens, S. & Zupan, J. 4 million neonatal deaths: when? Where? Why? *Lancet* **365**, 891-900, doi:10.1016/s0140-6736(05)71048-5 (2005).
3 Goldenberg, R. L., McClure, E. M., Saleem, S. & Reddy, U. M. Infection-related stillbirths. *Lancet* **375**, 1482-1490, doi:10.1016/s0140-6736(09)61712-8 (2010).
4 Kollmann, T. R., Levy, O., Montgomery, R. R. & Goriely, S. Innate immune function by Toll-like receptors: distinct responses in newborns and the elderly. *Immunity* **37**, 771-783, doi:10.1016/j.immuni.2012.10.014 (2012).
5 McElhaney, J. E. & Effros, R. B. Immunosenescence: what does it mean to health outcomes in older adults? *Curr Opin Immunol* **21**, 418-424, doi:10.1016/j.coi.2009.05.023 (2009).
6 Janssens, J. P. Pneumonia in the elderly (geriatric) population. *Curr Opin Pulm Med* **11**, 226-230 (2005).
7 O'Brien, K. L. *et al.* Burden of disease caused by *Streptococcus pneumoniae* in children younger than 5 years: global estimates. *Lancet* **374**, 893-902, doi:10.1016/s0140-6736(09)61204-6 (2009).
8 Kadioglu, A., Weiser, J. N., Paton, J. C. & Andrew, P. W. The role of *Streptococcus pneumoniae* virulence factors in host respiratory colonization and disease. *Nat Rev Microbiol* **6**, 288-301, doi:10.1038/nrmicro1871 (2008).
9 Siegel, S. J., Tamashiro, E. & Weiser, J. N. Clearance of Pneumococcal Colonization in Infants Is Delayed through Altered Macrophage Trafficking. *PLoS Pathog* **11**, e1005004, doi:10.1371/journal.ppat.1005004 (2015).
10 Puchta, A. *et al.* TNF Drives Monocyte Dysfunction with Age and Results in Impaired Anti-pneumococcal Immunity. *PLoS Pathog* **12**, e1005368, doi:10.1371/journal.ppat.1005368 (2016).
11 Bogaert, D., Hermans, P. W., Adrian, P. V., Rumke, H. C. & de Groot, R. Pneumococcal vaccines: an update on current strategies. *Vaccine* **22**, 2209-2220, doi:10.1016/j.vaccine.2003.11.038 (2004).
12 van Rossum, A. M., Lysenko, E. S. & Weiser, J. N. Host and bacterial factors contributing to the clearance of colonization by *Streptococcus pneumoniae* in a murine model. *Infect Immun* **73**, 7718-7726, doi:10.1128/iai.73.11.7718-7726.2005 (2005).
13 Zhang, Z., Clarke, T. B. & Weiser, J. N. Cellular effectors mediating Th17-dependent clearance of pneumococcal colonization in mice. *J Clin Invest* **119**, 1899-1909, doi:10.1172/jci36731 (2009).
14 Bogaert, D., Weinberger, D., Thompson, C., Lipsitch, M. & Malley, R. Impaired innate and adaptive immunity to *Streptococcus pneumoniae* and its effect on colonization in an infant mouse model. *Infect Immun* **77**, 1613-1622, doi:10.1128/iai.00871-08 (2009).
15 Krone, C. L., Trzcinski, K., Zborowski, T., Sanders, E. A. & Bogaert, D. Impaired innate mucosal immunity in aged mice permits prolonged *Streptococcus pneumoniae* colonization. *Infect Immun* **81**, 4615-4625, doi:10.1128/iai.00618-13 (2013).
16 Hinojosa, E., Boyd, A. R. & Orihuela, C. J. Age-associated inflammation and toll-like receptor dysfunction prime the lungs for pneumococcal pneumonia. *J Infect Dis* **200**, 546-554, doi:10.1086/600870 (2009).
17 Deshmane, S. L., Kremlev, S., Amini, S. & Sawaya, B. E. Monocyte chemoattractant protein-1 (MCP-1): an overview. *J Interferon Cytokine Res* **29**, 313-326, doi:10.1089/jir.2008.0027 (2009).
18 Serbina, N. V., Jia, T., Hohl, T. M. & Pamer, E. G. Monocyte-mediated defense against microbial pathogens. *Annu Rev Immunol* **26**, 421-452, doi:10.1146/annurev.immunol.26.021607.090326 (2008).
19 Torraca, V., Masud, S., Spaink, H. P. & Meijer, A. H. Macrophage-pathogen interactions in infectious diseases: new therapeutic insights from the zebrafish host model. *Dis Model Mech* **7**, 785-797, doi:10.1242/dmm.015594 (2014).
20 Barin, J. G. *et al.* Collaborative Interferon-gamma and Interleukin-17 Signaling Protects the Oral Mucosa from Staphylococcus aureus. *Am J Pathol* **186**, 2337-2352, doi:10.1016/j.ajpath.2016.07.001 (2016).

21 Goldmann, O., Rohde, M., Chhatwal, G. S. & Medina, E. Role of macrophages in host resistance to group A streptococci. *Infect Immun* **72**, 2956-2963 (2004).

22 Marti-Lliteras, P. *et al.* Nontypeable Haemophilus influenzae clearance by alveolar macrophages is impaired by exposure to cigarette smoke. *Infect Immun* **77**, 4232-4242, doi:10.1128/iai.00305-09 (2009).

23 Berenson, C. S., Murphy, T. F., Wrona, C. T. & Sethi, S. Outer membrane protein P6 of nontypeable Haemophilus influenzae is a potent and selective inducer of human macrophage proinflammatory cytokines. *Infect Immun* **73**, 2728-2735, doi:10.1128/iai.73.5.2728-2735.2005 (2005).

24 Fink, J. *et al.* Moraxella catarrhalis stimulates the release of proinflammatory cytokines and prostaglandin E from human respiratory epithelial cells and monocyte-derived macrophages. *FEMS Immunol Med Microbiol* **46**, 198-208, doi:10.1111/j.1574-695X.2005.00022.x (2006).

25 Galdiero, M. *et al.* Haemophilus influenzae porin induces Toll-like receptor 2-mediated cytokine production in human monocytes and mouse macrophages. *Infect Immun* **72**, 1204-1209 (2004).

26 Pahlman, L. I. *et al.* Streptococcal M protein: a multipotent and powerful inducer of inflammation. *J Immunol* **177**, 1221-1228 (2006).

27 Rosseau, S. *et al.* Moraxella catarrhalis--infected alveolar epithelium induced monocyte recruitment and oxidative burst. *Am J Respir Cell Mol Biol* **32**, 157-166, doi:10.1165/rcmb.2004-0091OC (2005).

28 Slevogt, H. *et al.* Moraxella catarrhalis is internalized in respiratory epithelial cells by a trigger-like mechanism and initiates a TLR2- and partly NOD1-dependent inflammatory immune response. *Cell Microbiol* **9**, 694-707, doi:10.1111/j.1462-5822.2006.00821.x (2007).

29 Shi, C. & Pamer, E. G. Monocyte recruitment during infection and inflammation. *Nat Rev Immunol* **11**, 762-774, doi:10.1038/nri3070 (2011).

30 Plowden, J., Renshaw-Hoelscher, M., Engleman, C., Katz, J. & Sambhara, S. Innate immunity in aging: impact on macrophage function. *Aging Cell* **3**, 161-167, doi:10.1111/j.1474-9728.2004.00102.x (2004).

31 Linehan, E. & Fitzgerald, D. C. Ageing and the immune system: focus on macrophages. *Eur J Microbiol Immunol (Bp)* **5**, 14-24, doi:10.1556/eujmi-d-14-00035 (2015).

32 Hearps, A. C. *et al.* Aging is associated with chronic innate immune activation and dysregulation of monocyte phenotype and function. *Aging Cell* **11**, 867-875, doi:10.1111/j.1474-9726.2012.00851.x (2012).

33 Antonelli, L. R. *et al.* Intranasal Poly-IC treatment exacerbates tuberculosis in mice through the pulmonary recruitment of a pathogen-permissive monocyte/macrophage population. *J Clin Invest* **120**, 1674-1682, doi:10.1172/jci40817 (2010).

34 Rutledge, B. J. *et al.* High level monocyte chemoattractant protein-1 expression in transgenic mice increases their susceptibility to intracellular pathogens. *J Immunol* **155**, 4838-4843 (1995).

35 Hoff, J. S., DeWald, M., Moseley, S. L., Collins, C. M. & Voyich, J. M. SpyA, a C3-like ADP-ribosyltransferase, contributes to virulence in a mouse subcutaneous model of Streptococcus pyogenes infection. *Infect Immun* **79**, 2404-2411, doi:10.1128/iai.01191-10 (2011).

36 Winter, C. *et al.* Lung-specific overexpression of CC chemokine ligand (CCL) 2 enhances the host defense to *Streptococcus pneumoniae* infection in mice: role of the CCL2-CCR2 axis. *J Immunol* **178**, 5828-5838 (2007).

37 Stockinger, S., Hornef, M. W. & Chassin, C. Establishment of intestinal homeostasis during the neonatal period. *Cell Mol Life Sci* **68**, 3699-3712, doi:10.1007/s00018-011-0831-2 (2011).

38 Sica, A. *et al.* Bacterial lipopolysaccharide rapidly inhibits expression of C-C chemokine receptors in human monocytes. *J Exp Med* **185**, 969-974 (1997).

39 Dowling, D. J. & Levy, O. Ontogeny of early life immunity. *Trends Immunol* **35**, 299-310, doi:10.1016/j.it.2014.04.007 (2014).

40 Krone, C. L., van de Groep, K., Trzcinski, K., Sanders, E. A. & Bogaert, D. Immunosenescence and pneumococcal disease: an imbalance in host-pathogen interactions. *The Lancet. Respiratory medicine* **2**, 141-153, doi:10.1016/s2213-2600(13)70165-6 (2014).

8

General Discussion and Future Perspectives

GENERAL DISCUSSION AND FUTURE PERSPECTIVES

Novel strategies to improve the protection against *Streptococcus pneumoniae*

Streptococcus pneumoniae is a resident of the human upper respiratory tract. *S. pneumoniae* carriage is asymptomatic and occurs multiple times throughout life[1]. Despite its commensal lifestyle the pneumococcus is a major cause of infection-related mortality worldwide[1-4]. Widespread PCV vaccination of infants has greatly reduced the incidence of pneumococcal disease in all age groups[1,4-6]. However, a major burden of disease remains, especially in developing countries[1-3] where PCVs are not universally available for all young children[7]. Even when a high vaccine coverage will be achieved in those countries, PCV may not be as effective as in the Western world. This is due to the observation that pneumococcal serotypes other than those most prevalent in Western countries and in the current PCVs, are widely circulating and causing disease in endemic settings[1]. It is therefore conceivable that PCV coverage will be lower leading to accelerated serotype replacement[8-10].

In order to increase the broadness of protection, PCVs with an increasing number of capsular polysaccharides have been developed, including a 15-valent PCV that has been tested in clinical studies[11,12]. However, inclusion of more polysaccharide variants may not be the solution, since head-to-head comparison of the PCVs showed that inclusion of more capsular polysaccharides reduces serotype-specific antibody responses[13,14]. Also production costs will increase as a consequence of the addition of more capsular polysaccharides[1]. These limitations in the use of multicapsular containing PCVs have accelerated the development of protein-based vaccines aiming at serotype-independent protection[1,15,16].

Pneumococcal carriage in the young and elderly

The large reduction in pneumococcal disease by PCV is partly caused by direct effects on pneumococcal carriage and transmission[1,8,9,17]. Reduction of colonization will be an important primary endpoint for studies with future vaccines. The immunological pressure by PCV vaccination has resulted in serotype replacement, which limits long-term efficacy of the vaccine[1,8-10].

Infants are highly susceptible to pneumococcal carriage as compared to adults. Studies demonstrate prolonged carriage events in infants with increased pneumococcal densities[1,18]. The first carriage event in children in the Western world generally occurs around the age of 6 months[1,19]. In contrast, practically all children in developing countries are carriers within three months of age. Young children are considered to be the natural reservoir of *S. pneumoniae* and primarily responsible for transmission within the community. Recent studies

show that the percentage of carriage in adults may be underestimated due to the method used for detection[20]. Carriage in the elderly has hardly been studied. Knowledge about the duration of carriage and pneumococcal density in this specific age group is lacking. Interestingly, the characteristics of pneumococcal carriage are similar in young and old mice, e.g. both show prolonged colonization at higher densities as compared to adult mice[21-23].

The mechanisms underlying the increased susceptibility for infections by *S. pneumoniae* in the age extremes of life are only partly understood, but much ascribed to immaturity (infants) and senescence (elderly) of the immune system[24]. Interestingly, recent evidence indicates that prolonged colonization in both age groups can be attributed to increased baseline inflammation that drives macrophage dysfunction, although regulated differently in the young and old (**Chapter 7**)[21-23]. A critical hallmark in this respect is the increased chronic inflammation in elderly, also referred to as inflamm-aging[22,24]. Young children are generally considered less responsive to infections and vaccines, but there is increasing evidence that also infants are characterized by elevated inflammation at baseline (**Chapter 7**)[23].

Prolonged colonization in the young and the old can possibly be attributed to differences in Th17 and Treg immunity. A skewed Th17 and Treg balance with relatively lower Th17 and higher Treg responses is observed in the nasopharynx of young children with lower IL17A and higher IL10 levels compared to adults[25,26]. This is in agreement with the observation that carriage positive children have a lower Th17/Treg ratio, e.g. reduced IL17A and elevated IL10, compared to carriage negative children[26]. Similar studies following pneumococcal carriage in the elderly are lacking. However, increased Treg and reduced Th17 responses are also characteristic of the very old since during aging Th17 immunity wanes and Treg responses increase[24]. We therefore hypothesize that Treg responses may limit Th17-mediated immunity. A direct inhibitory effect of IL10 addition on IL17A production has been observed in mouse macrophages that were re-stimulated with WCV[27]. However, none of these studies coupled altered Th17/Treg ratio's to bacterial killing by macrophages or neutrophils, cells that are both essential for clearance of pneumococcal carriage[28-30].

Together, susceptibility to pneumococcal carriage of infants and elderly may be caused by similar mechanisms, steered by increased levels of baseline inflammation (**Chapter 7**)[25,26]. Therefore, improved knowledge about mucosal immune responses may help to understand the mechanisms that increase susceptibility for infection by *S. pneumoniae*.

Although data from animal studies indicate that the very young and very old are similarly colonized by *S. pneumoniae* (prolonged colonization and increased densities), the percentage of human individuals which is colonized differs

between both extremes of age[22,23]. In industrialized countries, 20-50% of the children below the age of three years is carrier of *S. pneumoniae*, whereas the elderly are colonized at a steady level of 10-20% similar to adults[1,19,31,32]. Importantly, in young children pneumococcal invasive disease rates are associated with carriage frequency: more and longer carriage events increase the chance of progression to disease[33]. Pneumococcal carriage density and duration should therefore be reduced in children in order to prevent progression to disease[33]. In contrast, each single carriage event in elderly has a high likelihood to progress into pneumococcal disease[34,35]. Therefore, pneumococcal acquisition should be prevented in the elderly[36]. Overall, both age groups would benefit from a reduction in pneumococcal transmission by reducing pneumococcal colonization at the population level.

Selection of antigens and adjuvants for a protein-based vaccine against *S. pneumoniae* carriage

Several protein-based vaccines have been designed to target pneumococcal carriage. Selection of the antigens combined with the right type of adjuvant is critical for vaccine efficacy. Protection against pneumococcal colonization can be accomplished by two distinct vaccine-induced immune mechanisms: 1) an antibody response that prevents pneumococcal acquisition via agglutination and thus blocks colonization[37,38], or 2) a Th17 response that reduces the density and duration of pneumococcal colonization which is likely due to the recruitment of neutrophils leading to uptake and killing of the pneumococcus (Figure 1)[28-30].

These two vaccine-induced responses and their distinct modes of action determine the selection of the type of antigen. For example, antibody-mediated immunity requires surface exposed antigens accessible for antibody binding despite the presence of a polysaccharide capsule[1]. Antigen surface exposure is not a requirement for a vaccine with Th17-mediated immunity. Following bacterial engulfment by phagocytic cells, both intracellular and surface exposed pneumococcal protein peptides are loaded onto MHCII and presented to Th17 cells[28-30,39]. This in turn leads to the recruitment of neutrophils and macrophages to the site of infection and engulfment of pneumococci without the need of specific antigens.

The type of vaccine-induced immunity is critical for the choice of a suitable adjuvant. Aluminum salts are licensed for human use. These generate high antibody levels following parental administration[1]. Pneumococcal specific antibodies that are systemically generated are actively transported over the mucosal epithelium resulting in bacterial agglutination[37,38,40]. Intranasal vaccination is preferred in order to establish vaccine-induced Th17 memory in the nasopharynx. This requires the use of mucosal adjuvants. Intranasal

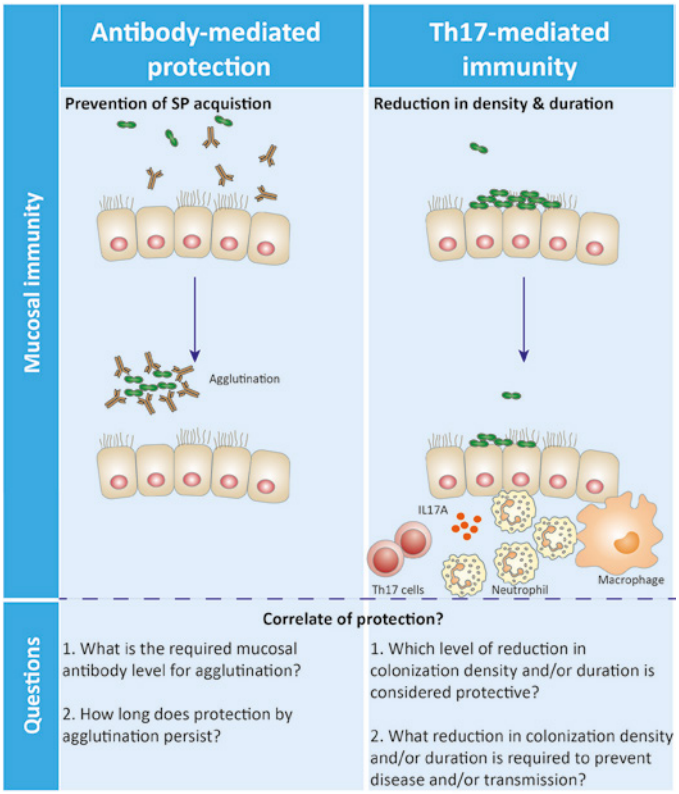

Figure 1 Overview of vaccine-mediated effects of antibody- and Th17-immunity on pneumococcal carriage.

Vaccine-induced immunity mediated by serotype-specific antibodies (PCV) or a Th17-inducing intranasal vaccine have distinct effects on pneumococcal carriage. Vaccine-induced antibodies prevent pneumococcal colonization, whereas a Th17-mediated vaccine response reduces pneumococcal colonization by decreasing density and duration. Therefore, the mucosal immune responses that impact on pneumococcal carriage differ between vaccines that mediate antibody- and Th17-immunity. Importantly, both vaccine strategies lack a correlate of protection. *SP: S. pneumoniae; NP: nasopharynx.*

vaccines tested in animal studies often use cholera toxin (CT) and derivatives (including CTB - **Chapter 5**), which may not be suitable for human use[41]. The lack of suitable mucosal adjuvants for human application is an important challenge for intranasal vaccination[41].

Salmonella OMVs are attractive delivery vehicles for mucosal delivery of vaccine antigens with intrinsic adjuvant activity (**Chapters 2 and 4**)[42-46]. We demonstrated that *Salmonella* OMVs are strong mucosal adjuvants which

allow for vaccine-induced reduction of pneumococcal colonization in an IL17 receptor dependent manner (**Chapters 2 and 4**)[46,47]. Our studies further illustrate the potency of *Salmonella* OMVs for mucosal application and the induction of vaccine-induced Th17 memory responses. Although *Salmonella* OMVs have not yet been tested for human application, a Neisseria OMV-based vaccine (Bexsero) has recently been licensed[48]. Future studies will elucidate whether *Salmonella* OMVs are a suitable adjuvant for human intranasal administration. *Salmonella* OMVs with surface exposed pneumococcal antigens will be tested for their impact on pneumococcal carriage (acquisition and density), preferably in the human challenge model. Mucosal adjuvants may also have antigen-independent effects on pneumococcal carriage, which is described for CTB (**Chapter 5**) and also observed for *Salmonella* OMVs (**Chapter 4**). Nonspecific effects of adjuvants on respiratory infection represent an understudied area, which requires more attention. In conclusion, the selection of the right antigens and adjuvant can only be based when the mechanisms of protection in humans are understood.

Towards universal protection using protein-based vaccines

Several experimental protein-based vaccines have been developed. These consist of whole pneumococcal cells or purified proteins. The best example of a whole pneumococcal cell vaccine is WCV, a killed unencapsulated pneumococcal strain. In animal studies WCV offers strong protection against pneumococcal colonization. This vaccine is currently studied in a phase II clinical trial, but the results remain to be seen[15,28,30,49].

Many purified protein antigens (both variable and conserved proteins) have been tested in intranasal vaccination studies aiming to reduce *S. pneumoniae* carriage. In general, variable proteins offer strong protection against pneumococcal colonization following vaccination[46,50,51]. However, conserved proteins are preferred because their low level of variation will likely result in universal protection against all circulating pneumococcal strains. In multiple intranasal vaccination studies a reduction in pneumococcal colonization following mucosal vaccination with conserved proteins was demonstrated[52,53].
An important limitation of subunit vaccines is that vaccination may result in the emergence of bacteria deficient for the vaccine antigen, e.g. vaccine escape mutants[54]. PspA deficient pneumococci, although very rare, have previously been described[5,55]. This implies that PspA is not essential for pneumococcal colonization or disease. Proteins with a critical role in cell function are less likely to emerge as vaccine escape mutants. We found that conserved protein PapP has a critical role in pneumococcal lipid metabolism and can therefore be a potential vaccine candidate (**Chapter 3**). Future studies in mice in our laboratory

will test the efficacy of intranasal vaccination with PapP to protect against pneumococcal colonization.

Novel protein-based vaccines need to offer broad protection and thus ideally cover all circulating pneumococcal strains[1,15,16]. Prediction of broad protection is based on immunological assays that address cross-reactivity of vaccine-induced responses with other pneumococcal strains. Our studies indicate that the degree of cross-reactivity is dependent on the type of immune response. For example the α1α2-specific IgG raised by our OMV-based vaccine showed limited binding to whole pneumococcal strains (**Chapter 4**). The low level of antibody-mediated cross-reactivity could be the result of the use of a variable protein fragment from PspA as vaccine antigen.

Variable proteins often show surface epitope heterogeneity, as is known for the α1α2 N-terminal region of PspA[1]. However, surprisingly, sharing identical antigens does not always guarantee cross-reactive antibody responses, as demonstrated in our study in which different clinical isolates with an identical α1α2 region did not show similar levels of antibody binding (**Chapter 4**). This may be due to different levels of capsule expression or to different type of capsules. Nevertheless, we observed, using an *ex vivo* restimulation assay, strong vaccine-induced Th17 cross-reactivity (**Chapter 4**). Furthermore, this was highly predictive for *in vivo* re-reactivation of vaccine-induced Th17 memory responses in the murine nasopharynx following infection with other pneumococcal strains (**Chapter 4**). We demonstrated that Th17-based cross-reactivity with pneumococcal strains is influenced by both capsule and antigen expression levels. More importantly, *in vivo* reactivation of these responses protected against some, but not all pneumococcal strains (**Chapter 4**). This demonstrates that *ex vivo* cross-reactivity does not equal *in vivo* protection.

Cross-reactivity of WCV has been primarily addressed in *ex vivo* immunological assays of both IgG and Th17. Based on these results WCV was predicted to induce broad protection[15,56,57]. This is supported by the fact that WCV contains all (conserved) proteins of a pneumococcal cell. It has been shown that WCV offers *in vivo* protection against serotype 3, 5 and 6B strains[56,58]. However, the evaluation of *in vivo* cross-reactivity was limited to three strains. Establishment of broad protection may also be limited by the fact that WCV consists of a single strain and may therefore induce strain-specific rather than strain-independent responses[15,53,57]. In animal studies it was demonstrated that a single colonization event protected against re-infection by the same strain, e.g. strain-specific protection[28,30]. However, humans become repeatedly colonized by different pneumococcal strains throughout their life, showing previous carriage events do not offer strain-independent protection against colonization by other circulating pneumococci.

Prediction of the degree of coverage induced by WCV is also complicated by the fact that it is not completely understood which proteins are driving WCV-induced protection. A study in mice indicated that specific conserved proteins that are part of WCV elicited IL17A in an *ex vivo* splenocyte restimulation assay[52]. This is suggestive of the contribution of these proteins to WCV-induced immune responses. This is promising, since conserved proteins are thought to increase strain-independent protection. However, vaccination with these conserved antigens evoking an IL17A response did not protect against pneumococcal colonization[52]. This illustrates how difficult it is to determine which proteins are driving vaccine-induced protection of WCV thus hampering the prediction of vaccine coverage.

Based on our current knowledge of pneumococcal carriage in humans and animal studies, variable proteins may dominate immune responses causing strain-dependent rather than strain-independent protection. This is supported by studies in children showing high natural antibody levels which are directed against variable proteins including PspA following natural exposure to *S. pneumoniae*[59,60]. A possible explanation is that variable proteins may outcompete other (conserved) proteins, because of their higher affinity for intracellular processing and peptide loading on MHCII thereby dominating MHC presentation[39]. We hypothesize that serotype-independent protection may be improved by WCV which is deficient for variable proteins (PspA and others). This may skew vaccine-induced protection towards conserved antigens, shared by all circulating pneumococci, and thus promote increased coverage.

Together, our studies suggest that the highest cross-reactivity with pneumococcal strains is achieved by a vaccine that induces Th17-mediated, rather than antibody-mediated immunity. Our work further points out that prediction of vaccine coverage should not be limited to *ex vivo* immunological assays and requires confirmation by *in vivo* vaccination studies using heterologous challenge strains. Also, in case of a whole cell vaccine or a vaccine combining multiple proteins, knowledge about the proteins that drive vaccine-induced protection will facilitate prediction of vaccine coverage. Alternatively, insight into why some (in particular variable) proteins dominate immune responses over other (more conserved) proteins will help to select the best vaccine antigens.

Novel protein-based vaccines in clinical trials

To date, effects on colonization as primary end point were only studied in two vaccine trials with protein-based vaccines. However, both vaccines were designed to protect against disease and not against carriage. These vaccines, studied by Sanofi and GSK, incorporated similar pneumococcal proteins (Table 1). Pneumolysoid (Pld) and conserved histidine triad protein (PhtD) were combined

in the GSK vaccine[61]. Sanofi incorporated Pld, PhTD, and choline binding protein PcpA in the formulation[62]. The choice for these proteins was based on: i) increased mucosal and serum antibody levels against these proteins are associated with pneumococcal colonization and otitis media in young children; ii) protein-specific antibodies decrease pneumococcal adherence to human epithelial cells; and iii) passive transfer of anti-Ply and anti-PhtD, but not anti-PcpA, reduces pneumococcal colonization in mice[63,64].

In the clinical trials vaccination with the GSK or Sanofi vaccine showed no impact on pneumococcal carriage[61]. Notably, both vaccines are parenterally administered and adjuvanted with aluminum thus generating an antibody-mediated response (Table 1). A possible explanation for these findings is that the protein antigens are not expressed or accessible during pneumococcal colonization. Alternatively anti-protein IgG levels may not be present at sufficient levels on the mucosa to prevent acquisition, since high concentrations are essential for agglutination to occur[37]. We propose that these vaccine formulations are not optimal in regard with their antigen and adjuvant choice, nor administered via the proper route to have an impact on carriage.

Another vaccine that has been studied in humans is the GEN-004 vaccine developed by Genocea (Table 1)[65]. This vaccine was designed to have an impact on pneumococcal carriage, based on T-cell stimulation of three universal lipoproteins: SP2108, SP0148, and SP1912. This vaccine was administered to subjects followed by an intranasal challenge infection with *S. pneumoniae*. The primary end point of this study was a reduction in or prevention of colonization[66,67]. The results show that GEN-004 prevented pneumococcal colonization in healthy volunteers[65]. However, GEN-004 did not affect carriage density measured at different time points in the carriage-positive individuals. This latter observation is particular interesting and intriguing, as GEN-004 was proposed to be a vaccine that induces Th17-mediated immunity. Such a vaccine should therefore reduce pneumococcal carriage density as shown by us (**Chapter 2, 4 and 6**) and by others[53,68].

Intranasally administered GEN-004 adjuvanted with CT reduced pneumococcal colonization in an IL17A-dependent manner in pre-clinical animal studies (Table 1)[68]. In the same study, the investigators showed that parenteral administration of GEN-004, adjuvanted with aluminum hydroxide, decreases pneumococcal carriage. This was associated with an increased level of IL17A in blood. However, they did not study whether this reduction was IL17A dependent. The underlying mechanism for the reduction in carriage by GEN-004 remains therefore unclear[68]. It would have been interesting if mucosal Th17 responses had been measured during different time points in the carriage positive individuals. The observation that carriage, but not density, was prevented in

Table 1 Overview of experimental vaccine formulations in the pre-clinical and clinical testing phase

Vaccine	*Pre-clinical testing*		*Clinical testing*	
	Adjuvant	**Administration route**	**Adjuvant**	**Administration route**
Pld – PhtD –PcpA Subunit purified proteins (Sanofi)[61,63,64,70]	Alum	Parenteral	Alum	Parenteral
Pld – PhtD Subunit purified proteins (GSK)[62-64,71]	Oil/water emulsion plus MPL	Parenteral	Alum	Parenteral
GEN-004 Subunit purified proteins (Genocea)[65,68]	CT	Intranasal	Alum	Parenteral
WCV Heat-killed whole cell vaccine (PATH, Boston Children's Hospital)[15,28,30,49,69]	CT	Intranasal	Alum	Parenteral

In pre-clinical testing in animals, experimental vaccines are often formulated with a mucosal vaccines and applied mucosally (intranasal) to impact on pneumococcal carriage. For clinical trials, experimental vaccines are switched to a formulation with aluminum as adjuvant following parenteral application. *WCV: whole cell vaccine; NA: Not applicable; CT: Cholera Toxin; Alum: aluminum hydroxide.*

some individuals receiving GEN-004, suggests an antibody-based vaccine mechanism of action that prevents pneumococcal acquisition. This is in agreement with the fact that the vaccine contained aluminum hydroxide and was administered via the parenteral route.

A common theme in the studies described above is that all three protein-based vaccines are supplemented with aluminum salts and parenterally administered thus promoting strong antibody responses (Table 1). The choice of adjuvant and route of administration for the human studies is not supported by the experimental set-up of the pre-clinical studies in animal studies, in which these vaccine formulations were often tested intranasally using CT as adjuvant (Table 1). The selection is probably determined by the regulatory authorities, whose authorization is needed for approval of novel vaccines. However, this approach

strongly impacts the development of novel vaccines against pneumococcal colonization, because of their different mode of actions (antibody- vs. Th17-mediated). Similarly, in pre-clinical animal studies WCV was intranasally applied and adjuvanted with CT, but for human application WCV is supplemented with aluminum hydroxide and administered parenterally (Table 1)[15,28,30,49,69]. We therefore suggest that future clinical studies should evaluate the effects of intranasal application of protein-based vaccines with a mucosal adjuvant for their impact on pneumococcal colonization.

Mucosal immunity restricting pneumococcal density in the nasopharynx

Vaccine-induced reduction in pneumococcal colonization critically requires a Th17 memory response. Depletion of Th17 responses eliminates these protective effects[28,30]. Therefore vaccines that aim to reduce pneumococcal carriage are generally designed to generate Th17 immunity[15,53,72]. **Chapters 2, 4 and 6** support the important role of Th17 memory responses to protect against *S. pneumoniae* colonization. Interestingly, humans with a IL17 deficiency are prone to develop diseases caused by *Staphylococcus aureus* and *Candida albicans*, but not by *S. pneumoniae*[73]. This suggests that other immune responses than Th17 can maintain the pneumococcus in the nasopharynx and prevent disease progression. Bacterial carriage has not been studied in these individuals. A recent study indicates that individuals with a IL17 G-152A polymorphism, associated with reduced serum IL17 levels, showed increased rates of pneumococcal colonization[74,75]. Importantly, our observations and those of others suggest that mucosal immune responses, other than Th17, may contribute to a reduction in pneumococcal carriage (**Chapters 4 and 5**).

For example, agglutination is proposed to be an important mechanism underlying PCV-mediated reduction of *S. pneumoniae* carriage (Figure 1)[37,38]. To optimize the process of agglutination, in order to prevent acquisition, high antibody levels are required. The critical threshold for these levels is not achieved during natural carriage events[37,76]. Thus far it is unknown how long vaccine-induced protection by agglutination is maintained, e.g. how long the high antibody levels and resident plasma cells are retained in the nasal mucosa (Figure 1). A recent report demonstrated that PCV7-mediated IgG responses do not persist above natural serotype antibody levels in time, suggesting that agglutination is waning and requires serotype re-exposure to maintain sufficient antibody levels[77]. In addition, there is increasing evidence from our work and that of others that IFNγ and IL10 may also impact on pneumococcal colonization[28-30].

In **Chapter 5** we describe that an increased IFNγ response was associated with a reduction in pneumococcal colonization following vaccination. The increased IFNγ levels coincided with an influx of inflammatory macrophages that were critical for the reduction in pneumococcal colonization (**Chapter 5**). Together, this suggests that IFNγ may impact on pneumococcal colonization by recruitment and/or by promoting macrophage activation[78-80]. That macrophages are critical for clearance of pneumococcal colonization has been shown by others and is supported by our studies in **Chapters 5 and 7**[29]. The studies described in **Chapter 7** demonstrate that susceptibility to pneumococcal carriage is caused by defective macrophage responses in both infant and old mice[22,23]. Both age groups are characterized by reduced Th1 responses[24,81]. Whether IFNγ indeed affects pneumococcal density and duration requires further and more detailed investigation.

There is also increasing evidence from our and other studies that IL10 responses have an influence on pneumococcal colonization, either in a positive or negative manner[1,19,25,26,82-85]. In **Chapter 5** we describe a reduction in pneumococcal colonization following vaccination, which was associated with elevated levels of IL10 in the nasopharynx. To our knowledge direct effects of IL10 on reduction in pneumococcal colonization have not yet been described. Hypothetically, IL10 is an inhibitor of inflammation and may impact on pneumococcal carriage by inhibiting local inflammation that prevents further bacterial outgrowth. This is based on reports which show that increased pneumococcal densities are associated with increased inflammation as observed for co-infection with influenza A[82,83]. Alternatively, Treg responses are associated with overall higher pneumococcal densities and prolonged carriage in mice and men as by other studies[1,19,25,26,84]. This (partly) contradicts with our findings. One explanation for this contradiction is that vaccine-induced IL10, may prevent pneumococcal outgrowth in the nasopharynx. Simultaneously, increased IL10 levels may hamper Th17- and/or Th1-mediated responses causing prolonged colonization[85].

All together, we speculate that the combination of nasal T helper cell responses (Treg, Th17 and Th1) and their kinetics determine pneumococcal carriage density and duration (**Chapters 4, 5 and 6**)[1,19,24,27,81,85]. A plausible hypothesis is that IL17A and IFNγ activate cellular responses (macrophages and neutrophils) that reduce pneumococcal carriage, whereas IL10 simultaneously limits pneumococcal outgrowth by dampening inflammation (increased inflammation during influenza co-infection). Evidence for this hypothesis is lacking. However, our work suggests that a combination of IL17A and IFNγ with IL10 may act synergistically leading to reduction of pneumococcal colonization (**Chapter 5**). Support for this hypothesis is offered by a recent report

demonstrating that IL17A and IFNy collaboratively drive neutrophil and macrophage responses for protection against mucosal infection by *Staphylococcus aureus*[86].

Evidence that combined T helper responses have an impact on pneumococcal carriage is limited to association studies. Therefore, future studies should focus on unraveling the role of mucosal T helper responses in restriction of pneumococcal carriage. Importantly, these type of immune responses are not limited to recruited $CD4^+$ T cells, but are produced by resident innate and adaptive cells present in the nasal mucosa in response to bacterial infection[87-89]. These studies should further analyze the influence on pneumococcal killing by effector cells, including macrophages and neutrophils. Experimental endpoints, such as pneumococcal densities, duration of carriage and transmission, should be monitored over time to understand causal relations between the cytokine dynamics and the stage of carriage.

Effects of pneumococcal vaccination on the nasopharyngeal ecology

Immediately after birth, the human respiratory tract becomes populated by a variety of microorganisms[90,91]. This composition is thought to change throughout life. In the mucosa, viral and bacterial co-infections may alter host responses and influence disease progression and outcome.[90] Important bacterial pathogens in the nasopharyngeal mucosa are: *S. pneumoniae*, *Haemophilus influenzae*, and *Staphylococcus aureus*[90]. High carriage rates of *S. pneumoniae* and *H. influenzae* in healthy children suggest that co-carriage of these species is common[90,92,93].

In an animal model, co-infection with *H. influenzae* accelerated clearance of pneumococcal colonization by recruiting neutrophils that subsequently opsonized pneumococci[94]. The accelerated clearance of *S. pneumoniae* involved synergistic innate immune co-stimulation by pneumococcal and Haemophilus components[90,95]. Therefore, co-carriage with *H. influenzae* is only occurring with serotypes that are resistant towards opsonophagocytosis by neutrophils[90,96]. On the other hand, an inverse relation exists between *S. pneumoniae* and *S. aureus* carriage. Children carrying the pneumococcus will likely not be colonized by *S. aureus*[90]. It was shown in an animal model that cross-reactive pneumococcal antibodies against a conserved dehydrogenase prevented *S. aureus* acquisition, probably via agglutination[90,97].

Respiratory viruses inhabiting the nasal mucosa, including influenza A and RSV, are thought to influence pneumococcal carriage[1,98]. Animal studies have demonstrated that co-infection with influenza A enhances pneumococcal carriage density and duration, and thereby promotes progression to disease and transmission[82,83]. So far, there is little understanding of how influenza A promotes pneumococcal carriage, disease, and transmission, but a reduction in

influenza A may indirectly impact on pneumococcal disease burden. This hypothesis is supported by the observation that the influenza vaccine is protective against pneumococcal disease[99]. Targeting influenza A may thus indirectly impact on pneumococcal carriage, a non-classical approach that requires further consideration.

Given these microbial interactions, a future vaccine that impacts on pneumococcal carriage may alter the microbiome composition in the nasopharynx[100]. It is important to note that the PCVs also strongly affect pneumococcal carriage in a serotype specific manner. PCV introduction significantly reduced pneumococcal carriage and circulation of vaccine types (VTs)[8-10,33,101]. Therefore the major concern is replacement of VTs by non-vaccine types (NVTs) that more frequently cause disease[8,9,101-104]. The effects of the introduction of PCV on bacterial carriage of other bacterial species colonizing the nasopharyngeal cavity, such as *H. influenzae* and *S. aureus*, were also studied. These epidemiological studies were done in distinct human populations show opposing results[10,93,101,105-107]. Studies in The Netherlands and the US demonstrate that PCV led to increased carriage of both *H. influenzae* and *S. aureus*[101,105,107]. In contrast, in African and Israeli study populations carriage of *H. influenzae* and *S. aureus* remained unaltered following PCV vaccination[10,93,106]. Whether a future vaccine that targets pneumococcal carriage will affect prevalence of *H. influenzae* and *S. aureus* carriage seems to be dependent on the genetic background as well as on environmental factors.

Targeting a 'certain carriage state' (acquisition, density or duration) via vaccination likely results in distinct effects on the nasopharyngeal microbiome composition within the human population[19]. PCVs with antibody-immunity and mucosal vaccines with Th17 immunity employ distinct mechanisms for a reduction in pneumococcal carriage (Figure 1). PCVs prevent pneumococcal acquisition by agglutination, and thus completely prevent pneumococcal carriage thereby creating an open niche in the nasopharyngeal microbiome[37]. In contrast, a vaccine with Th17 immunity is unlikely to prevent pneumococcal acquisition, because the neutrophils that clear the pneumococcus do not reside in the nasopharynx but are recruited following pneumococcal colonization[28,29]. For that reason Th17-mediated immunity is proposed to prevent pneumococcal outgrowth and progression to disease and simultaneously reduce transmission[19,72,108]. How and to what extent a mucosal vaccine with Th17 immunity will disturb the ecological niche remains currently unclear, but the effect will not be directly comparable to the PCV-mediated effects on the nasopharyngeal microbiome.

Concluding remarks

It is evident that alternative vaccination strategies are required to stop the continuing burden of disease caused by *S. pneumoniae*. The increasing serotype

replacement due to PCV vaccination emphasizes the need for development of novel protein-based vaccines to target pneumococcal carriage. Such a vaccine is attractive as it prevents disease progression and simultaneously reduces transmission, providing herd immunity within the human population. The latter may be particularly important for the protection of the elderly. Major changes in nasopharyngeal carriage rates of pneumococci may be undesired since they may result in unwanted alterations in the nasopharyngeal microbiome. However, an altered microbiome and herd immunity offered by reduced transmission likely represent two sides of the same coin. Also, a vaccine that targets pneumococcal carriage will reduce further selection of antimicrobial resistance, as prolonged carriage promotes horizontal gene transfer[109-111].

In our opinion, the best strategy to impact on pneumococcal colonization is a protein-based vaccine that induces cell-mediated protection, including Th17 memory responses. Mucosal application and the use of a strong mucosal adjuvant are essential for strong reduction of colonization. Also a novel vaccine should meet the criteria of low manufacturing costs and increased vaccine coverage. Approaches that indirectly impact on pneumococcal colonization should also be considered. These include studies that involve the influence of viral infection on pneumococcal carriage and transmission. Improved understanding of the interaction between influenza A, *S. pneumoniae*, and host immunity on pneumococcal carriage (density and duration) and transmission will facilitate novel vaccine strategies to decrease the residual disease burden.

A major challenge for a vaccine that impacts on pneumococcal carriage, is the lack of a correlate of protection (Figure 1). How can we measure vaccine efficacy with pneumococcal colonization as clinical endpoint? This question cannot be answered since it is currently unclear what level of reduction of pneumococcal carriage is required to prevent disease progression and reduce transmission. Therefore, future studies should address the impact of a vaccine that reduces density and duration of colonization rather than only blocking acquisition. These studies should also include vaccine-induced effects on protection against pneumococcal disease and reduction in transmission. Finally, critical for pneumococcal vaccine development is the need for increased insight into the mechanisms that drive pneumococcal carriage densities and duration in relation to pneumococcal disease and transmission within the human population. This can be accomplished by improvements in the understanding of the (vaccine-induced) host, bacterial and viral factors that affect pneumococcal carriage (density and duration) and transmission.

REFERENCES

1 Brown, J., Hammerschmidt, S. & Orihuela, C. *Streptococcous pneumoniae molecular mechanisms of host-pathogen interactions*. (Elsevier, 2015).

2 O'Brien, K. L. *et al.* Burden of disease caused by *Streptococcus pneumoniae* in children younger than 5 years: global estimates. *Lancet* **374**, 893-902, doi:10.1016/s0140-6736(09)61204-6 (2009).

3 Walker, C. L. *et al.* Global burden of childhood pneumonia and diarrhoea. *Lancet* **381**, 1405-1416, doi:10.1016/s0140-6736(13)60222-6 (2013).

4 Drijkoningen, J. J. & Rohde, G. G. Pneumococcal infection in adults: burden of disease. *Clin Microbiol Infect* **20 Suppl 5**, 45-51, doi:10.1111/1469-0691.12461 (2014).

5 Keller, L. E., Robinson, D. A. & McDaniel, L. S. Nonencapsulated *Streptococcus pneumoniae*: Emergence and Pathogenesis. *MBio* **7**, doi:10.1128/mBio.01792-15 (2016).

6 Feldman, C. & Anderson, R. Review: current and new generation pneumococcal vaccines. *J Infect* **69**, 309-325, doi:10.1016/j.jinf.2014.06.006 (2014).

7 <view-hub.org 3/10/2016: PCV introduction/planned & children coverage> (

8 Weinberger, D. M., Malley, R. & Lipsitch, M. Serotype replacement in disease after pneumococcal vaccination. *Lancet* **378**, 1962-1973, doi:10.1016/s0140-6736(10)62225-8 (2011).

9 Hanage, W. P. *et al.* Evidence that pneumococcal serotype replacement in Massachusetts following conjugate vaccination is now complete. *Epidemics* **2**, 80-84, doi:10.1016/j.epidem.2010.03.005 (2010).

10 Nzenze, S. A. *et al.* Temporal association of infant immunisation with pneumococcal conjugate vaccine on the ecology of *Streptococcus pneumoniae*, Haemophilus influenzae and Staphylococcus aureus nasopharyngeal colonisation in a rural South African community. *Vaccine* **32**, 5520-5530, doi:10.1016/j.vaccine.2014.06.091 (2014).

11 Skinner, J. M. *et al.* Pre-clinical evaluation of a 15-valent pneumococcal conjugate vaccine (PCV15-CRM197) in an infant-rhesus monkey immunogenicity model. *Vaccine* **29**, 8870-8876, doi:10.1016/j.vaccine.2011.09.078 (2011).

12 McFetridge, R. *et al.* Safety, tolerability, and immunogenicity of 15-valent pneumococcal conjugate vaccine in healthy adults. *Vaccine* **33**, 2793-2799, doi:10.1016/j.vaccine.2015.04.025 (2015).

13 Wijmenga-Monsuur, A. J. *et al.* Direct Comparison of Immunogenicity Induced by 10- or 13-Valent Pneumococcal Conjugate Vaccine around the 11-Month Booster in Dutch Infants. *PLoS One* **10**, e0144739, doi:10.1371/journal.pone.0144739 (2015).

14 Siber, G. in *International Symposium on Pneumococci and Pneumococcal Diseases.*

15 Malley, R. & Anderson, P. W. Serotype-independent pneumococcal experimental vaccines that induce cellular as well as humoral immunity. *Proc Natl Acad Sci U S A* **109**, 3623-3627, doi:10.1073/pnas.1121383109 (2012).

16 Jefferies, J. M., Clarke, S. C., Webb, J. S. & Kraaijeveld, A. R. Risk of red queen dynamics in pneumococcal vaccine strategy. *Trends Microbiol* **19**, 377-381, doi:10.1016/j.tim.2011.06.001 (2011).

17 Dagan, R. *et al.* Comparative immunogenicity and efficacy of 13-valent and 7-valent pneumococcal conjugate vaccines in reducing nasopharyngeal colonization: a randomized double-blind trial. *Clin Infect Dis* **57**, 952-962, doi:10.1093/cid/cit428 (2013).

18 Bogaert, D., De Groot, R. & Hermans, P. W. *Streptococcus pneumoniae* colonisation: the key to pneumococcal disease. *Lancet Infect Dis* **4**, 144-154, doi:10.1016/s1473-3099(04)00938-7 (2004).

19 Simell, B. *et al.* The fundamental link between pneumococcal carriage and disease. *Expert Rev Vaccines* **11**, 841-855, doi:10.1586/erv.12.53 (2012).

20 Trzcinski, K. *et al.* Superiority of trans-oral over trans-nasal sampling in detecting *Streptococcus pneumoniae* colonization in adults. *PLoS One* **8**, e60520, doi:10.1371/journal.pone.0060520 (2013).

21 Krone, C. L., Trzcinski, K., Zborowski, T., Sanders, E. A. & Bogaert, D. Impaired innate mucosal immunity in aged mice permits prolonged *Streptococcus pneumoniae* colonization. *Infect Immun* **81**, 4615-4625, doi:10.1128/iai.00618-13 (2013).

22 Puchta, A. *et al.* TNF Drives Monocyte Dysfunction with Age and Results in Impaired Anti-pneumococcal Immunity. *PLoS Pathog* **12**, e1005368, doi:10.1371/journal.ppat.1005368 (2016).
23 Siegel, S. J., Tamashiro, E. & Weiser, J. N. Clearance of Pneumococcal Colonization in Infants Is Delayed through Altered Macrophage Trafficking. *PLoS Pathog* **11**, e1005004, doi:10.1371/journal.ppat.1005004 (2015).
24 Kollmann, T. R., Levy, O., Montgomery, R. R. & Goriely, S. Innate immune function by Toll-like receptors: distinct responses in newborns and the elderly. *Immunity* **37**, 771-783, doi:10.1016/j.immuni.2012.10.014 (2012).
25 Zhang, Q. *et al.* Characterisation of regulatory T cells in nasal associated lymphoid tissue in children: relationships with pneumococcal colonization. *PLoS Pathog* **7**, e1002175, doi:10.1371/journal.ppat.1002175 (2011).
26 Mubarak, A. *et al.* A dynamic relationship between mucosal T helper type 17 and regulatory T-cell populations in nasopharynx evolves with age and associates with the clearance of pneumococcal carriage in humans. *Clin Microbiol Infect*, doi:10.1016/j.cmi.2016.05.017 (2016).
27 Bogaert, D., Weinberger, D., Thompson, C., Lipsitch, M. & Malley, R. Impaired innate and adaptive immunity to *Streptococcus pneumoniae* and its effect on colonization in an infant mouse model. *Infect Immun* **77**, 1613-1622, doi:10.1128/iai.00871-08 (2009).
28 Lu, Y. J. *et al.* Interleukin-17A mediates acquired immunity to pneumococcal colonization. *PLoS Pathog* **4**, e1000159, doi:10.1371/journal.ppat.1000159 (2008).
29 Zhang, Z., Clarke, T. B. & Weiser, J. N. Cellular effectors mediating Th17-dependent clearance of pneumococcal colonization in mice. *J Clin Invest* **119**, 1899-1909, doi:10.1172/jci36731 (2009).
30 Malley, R. *et al.* CD4+ T cells mediate antibody-independent acquired immunity to pneumococcal colonization. *Proc Natl Acad Sci U S A* **102**, 4848-4853, doi:10.1073/pnas.0501254102 (2005).
31 Sleeman, K. L. *et al.* Capsular serotype-specific attack rates and duration of carriage of *Streptococcus pneumoniae* in a population of children. *J Infect Dis* **194**, 682-688, doi:10.1086/505710 (2006).
32 Esposito, S. *et al.* Pneumococcal colonization in older adults. *Immun Ageing* **13**, 2, doi:10.1186/s12979-016-0057-0 (2016).
33 van Gils, E. J. *et al.* Effect of reduced-dose schedules with 7-valent pneumococcal conjugate vaccine on nasopharyngeal pneumococcal carriage in children: a randomized controlled trial. *Jama* **302**, 159-167, doi:10.1001/jama.2009.975 (2009).
34 Krone, C. L. *et al.* Carriage of *Streptococcus pneumoniae* in aged adults with influenza-like-illness. *PLoS One* **10**, e0119875, doi:10.1371/journal.pone.0119875 (2015).
35 Perez-Trallero, E., Marimon, J. M., Larruskain, J., Alonso, M. & Ercibengoa, M. Antimicrobial susceptibilities and serotypes of *Streptococcus pneumoniae* isolates from elderly patients with pneumonia and acute exacerbation of chronic obstructive pulmonary disease. *Antimicrob Agents Chemother* **55**, 2729-2734, doi:10.1128/aac.01546-10 (2011).
36 Grau, I. *et al.* Declining mortality from adult pneumococcal infections linked to children's vaccination. *J Infect* **72**, 439-449, doi:10.1016/j.jinf.2016.01.011 (2016).
37 Roche, A. M., Richard, A. L., Rahkola, J. T., Janoff, E. N. & Weiser, J. N. Antibody blocks acquisition of bacterial colonization through agglutination. *Mucosal Immunol* **8**, 176-185, doi:10.1038/mi.2014.55 (2015).
38 Collins, A. M. *et al.* First human challenge testing of a pneumococcal vaccine. Double-blind randomized controlled trial. *Am J Respir Crit Care Med* **192**, 853-858, doi:10.1164/rccm.201503-0542OC (2015).
39 Miller, M. A., Ganesan, A. P. & Eisenlohr, L. C. Toward a Network Model of MHC Class II-Restricted Antigen Processing. *Front Immunol* **4**, 464, doi:10.3389/fimmu.2013.00464 (2013).
40 Yoshida, M. *et al.* Neonatal Fc receptor for IgG regulates mucosal immune responses to luminal bacteria. *J Clin Invest* **116**, 2142-2151, doi:10.1172/jci27821 (2006).
41 Lycke, N. Recent progress in mucosal vaccine development: potential and limitations. *Nat Rev Immunol* **12**, 592-605, doi:10.1038/nri3251 (2012).

42 Bergman, M. A. *et al.* CD4+ T cells and toll-like receptors recognize Salmonella antigens expressed in bacterial surface organelles. *Infect Immun* **73**, 1350-1356, doi:10.1128/iai.73.3.1350-1356.2005 (2005).

43 Ellis, T. N. & Kuehn, M. J. Virulence and immunomodulatory roles of bacterial outer membrane vesicles. *Microbiol Mol Biol Rev* **74**, 81-94, doi:10.1128/mmbr.00031-09 (2010).

44 Underhill, D. M. & Goodridge, H. S. Information processing during phagocytosis. *Nat Rev Immunol* **12**, 492-502, doi:10.1038/nri3244 (2012).

45 Pritsch, M. *et al.* Comparison of Intranasal Outer Membrane Vesicles with Cholera Toxin and Injected MF59C.1 as Adjuvants for Malaria Transmission Blocking Antigens AnAPN1 and Pfs48/45. *Journal of immunology research* **2016**, 3576028, doi:10.1155/2016/3576028 (2016).

46 Kuipers, K. *et al.* Salmonella outer membrane vesicles displaying high densities of pneumococcal antigen at the surface offer protection against colonization. *Vaccine* **33**, 2022-2029, doi:10.1016/j.vaccine.2015.03.010 (2015).

47 Kuipers, K. J., W. S. P.; van der Gaast-de Jongh, C. E.; Houben, D.; van Opzeeland, F.; Simonetti, E.; van Selm, S.; de Groot, R.; Koenders, M. I., Azarian, T.; Langereis, J. D.; Zomer, A.; Luirink, J.; de Jonge, M. I. *A highly variable protein at the basis of a universal vaccine against pneumococcal carriage* (2016).

48 Andrews, S. M. & Pollard, A. J. A vaccine against serogroup B Neisseria meningitidis: dealing with uncertainty. *Lancet Infect Dis* **14**, 426-434, doi:10.1016/s1473-3099(13)70341-4 (2014).

49 Goncalves, V. M. *et al.* Development of a whole cell pneumococcal vaccine: BPL inactivation, cGMP production, and stability. *Vaccine* **32**, 1113-1120, doi:10.1016/j.vaccine.2013.10.091 (2014).

50 Steer, A. C. *et al.* Status of research and development of vaccines for Streptococcus pyogenes. *Vaccine*, doi:10.1016/j.vaccine.2016.03.073 (2016).

51 Ma, C. *et al.* FbaA- and M protein-based multi-epitope vaccine elicits strong protective immune responses against group A streptococcus in mouse model. *Microbes Infect* **16**, 409-418, doi:10.1016/j.micinf.2014.03.006 (2014).

52 Moffitt, K. L., Malley, R. & Lu, Y. J. Identification of protective pneumococcal T(H)17 antigens from the soluble fraction of a killed whole cell vaccine. *PLoS One* **7**, e43445, doi:10.1371/journal.pone.0043445 (2012).

53 Moffitt, K. L. *et al.* T(H)17-based vaccine design for prevention of *Streptococcus pneumoniae* colonization. *Cell Host Microbe* **9**, 158-165, doi:10.1016/j.chom.2011.01.007 (2011).

54 Li, Y. *et al.* Distinct effects on diversifying selection by two mechanisms of immunity against *Streptococcus pneumoniae*. *PLoS Pathog* **8**, e1002989, doi:10.1371/journal.ppat.1002989 (2012).

55 Schachern, P. A. *et al.* Pneumococcal PspA and PspC proteins: potential vaccine candidates for experimental otitis media. *Int J Pediatr Otorhinolaryngol* **78**, 1517-1521, doi:10.1016/j.ijporl.2014.06.024 (2014).

56 Lu, Y. J. *et al.* GMP-grade pneumococcal whole-cell vaccine injected subcutaneously protects mice from nasopharyngeal colonization and fatal aspiration-sepsis. *Vaccine* **28**, 7468-7475, doi:10.1016/j.vaccine.2010.09.031 (2010).

57 Moffitt, K. L., Yadav, P., Weinberger, D. M., Anderson, P. W. & Malley, R. Broad antibody and T cell reactivity induced by a pneumococcal whole-cell vaccine. *Vaccine* **30**, 4316-4322, doi:10.1016/j.vaccine.2012.01.034 (2012).

58 Malley, R. *et al.* Intranasal immunization with killed unencapsulated whole cells prevents colonization and invasive disease by capsulated pneumococci. *Infect Immun* **69**, 4870-4873, doi:10.1128/iai.69.8.4870-4873.2001 (2001).

59 Lebon, A. *et al.* Natural antibodies against several pneumococcal virulence proteins in children during the pre-pneumococcal-vaccine era: the generation R study. *Infect Immun* **79**, 1680-1687, doi:10.1128/iai.01379-10 (2011).

60 Prevaes, S. M. *et al.* Nasopharyngeal colonization elicits antibody responses to staphylococcal and pneumococcal proteins that are not associated with a reduced risk of subsequent carriage. *Infect Immun* **80**, 2186-2193, doi:10.1128/iai.00037-12 (2012).

61 Alderson, M. in *International Symposium on Pneumococci and Pneumococcal Diseases.*
62 Brooks, W. A., Chang, L. J., Sheng, X. & Hopfer, R. Safety and immunogenicity of a trivalent recombinant PcpA, PhtD, and PlyD1 pneumococcal protein vaccine in adults, toddlers, and infants: A phase I randomized controlled study. *Vaccine* **33**, 4610-4617, doi:10.1016/j.vaccine.2015.06.078 (2015).
63 Pichichero, M. E. *et al.* Antibody response to *Streptococcus pneumoniae* proteins PhtD, LytB, PcpA, PhtE and Ply after nasopharyngeal colonization and acute otitis media in children. *Hum Vaccin Immunother* **8**, 799-805, doi:10.4161/hv.19820 (2012).
64 Kaur, R., Surendran, N., Ochs, M. & Pichichero, M. E. Human antibodies to PhtD, PcpA, and Ply reduce adherence to human lung epithelial cells and murine nasopharyngeal colonization by *Streptococcus pneumoniae*. *Infect Immun* **82**, 5069-5075, doi:10.1128/iai.02124-14 (2014).
65 Gordon, S. B. in *10th International Symposium on Pneumococci & Pneumococcal Diseases.*
66 Ferreira, D. M. *et al.* Controlled human infection and rechallenge with *Streptococcus pneumoniae* reveals the protective efficacy of carriage in healthy adults. *Am J Respir Crit Care Med* **187**, 855-864, doi:10.1164/rccm.201212-2277OC (2013).
67 *clinical trials.gov*, <https://clinicaltrials.gov/ct2/show/study/NCT02116998-->accessed> (
68 Moffitt, K. *et al.* Toll-like receptor 2-dependent protection against pneumococcal carriage by immunization with lipidated pneumococcal proteins. *Infect Immun* **82**, 2079-2086, doi:10.1128/iai.01632-13 (2014).
69 Goncalves, V. M. in *10th International Symposium on Pneumococci and Pneumococcal Diseases* (Glasgow, UK, 2016).
70 Verhoeven, D., Perry, S. & Pichichero, M. E. Contributions to protection from *Streptococcus pneumoniae* infection using the monovalent recombinant protein vaccine candidates PcpA, PhtD, and PlyD1 in an infant murine model during challenge. *Clin Vaccine Immunol* **21**, 1037-1045, doi:10.1128/cvi.00052-14 (2014).
71 Godfroid, F., Hermand, P., Verlant, V., Denoel, P. & Poolman, J. T. Preclinical evaluation of the Pht proteins as potential cross-protective pneumococcal vaccine antigens. *Infect Immun* **79**, 238-245, doi:10.1128/iai.00378-10 (2011).
72 Paton, J. C. & Ogunniyi, A. D. Evicting the pneumococcus from its nasopharyngeal lodgings. *Cell Host Microbe* **9**, 89-91, doi:10.1016/j.chom.2011.01.013 (2011).
73 Puel, A. *et al.* Inborn errors of human IL-17 immunity underlie chronic mucocutaneous candidiasis. *Curr Opin Allergy Clin Immunol* **12**, 616-622, doi:10.1097/ACI.0b013e328358cc0b (2012).
74 Vuononvirta, J., Peltola, V., Ilonen, J., Mertsola, J. & He, Q. The Gene Polymorphism of IL-17 G-152A is Associated with Increased Colonization of *Streptococcus pneumoniae* in Young Finnish Children. *Pediatr Infect Dis J* **34**, 928-932, doi:10.1097/inf.0000000000000691 (2015).
75 Hoe, E. *et al.* Reduced IL-17A Secretion Is Associated with High Levels of Pneumococcal Nasopharyngeal Carriage in Fijian Children. *PLoS One* **10**, e0129199, doi:10.1371/journal.pone.0129199 (2015).
76 Grant, L. in *10th International Symposium on Pneumococci and Pneumococcal Diseases* (Glasgow, UK, 2016).
77 Grant, L. R. *et al.* Persistence of IgG antibody following routine infant immunization with the 7-valent pneumococcal conjugate vaccine. *Pediatr Infect Dis J* **34**, e138-142, doi:10.1097/inf.0000000000000655 (2015).
78 Rubins, J. B. & Pomeroy, C. Role of gamma interferon in the pathogenesis of bacteremic pneumococcal pneumonia. *Infect Immun* **65**, 2975-2977 (1997).
79 Yamamoto, N. *et al.* Essential role for the p40 subunit of interleukin-12 in neutrophil-mediated early host defense against pulmonary infection with *Streptococcus pneumoniae*: involvement of interferon-gamma. *Microbes Infect* **6**, 1241-1249, doi:10.1016/j.micinf.2004.08.007 (2004).
80 Palaniappan, R. *et al.* CCL5 modulates pneumococcal immunity and carriage. *J Immunol* **176**, 2346-2356 (2006).
81 Dowling, D. J. & Levy, O. Ontogeny of early life immunity. *Trends Immunol* **35**, 299-310, doi:10.1016/j.it.2014.04.007 (2014).

82 Richard, A. L., Siegel, S. J., Erikson, J. & Weiser, J. N. TLR2 signaling decreases transmission of *Streptococcus pneumoniae* by limiting bacterial shedding in an infant mouse Influenza A co-infection model. *PLoS Pathog* **10**, e1004339, doi:10.1371/journal.ppat.1004339 (2014).

83 Siegel, S. J., Roche, A. M. & Weiser, J. N. Influenza promotes pneumococcal growth during coinfection by providing host sialylated substrates as a nutrient source. *Cell Host Microbe* **16**, 55-67, doi:10.1016/j.chom.2014.06.005 (2014).

84 Neill, D. R. *et al.* Density and duration of pneumococcal carriage is maintained by transforming growth factor beta1 and T regulatory cells. *Am J Respir Crit Care Med* **189**, 1250-1259, doi:10.1164/rccm.201401-0128OC (2014).

85 McCool, T. L. & Weiser, J. N. Limited role of antibody in clearance of *Streptococcus pneumoniae* in a murine model of colonization. *Infect Immun* **72**, 5807-5813, doi:10.1128/iai.72.10.5807-5813.2004 (2004).

86 Barin, J. G. *et al.* Collaborative Interferon-gamma and Interleukin-17 Signaling Protects the Oral Mucosa from Staphylococcus aureus. *Am J Pathol* **186**, 2337-2352, doi:10.1016/j.ajpath.2016.07.001 (2016).

87 Ivanov, S., Paget, C. & Trottein, F. Role of non-conventional T lymphocytes in respiratory infections: the case of the pneumococcus. *PLoS Pathog* **10**, e1004300, doi:10.1371/journal.ppat.1004300 (2014).

88 Carbone, F. R. Tissue-Resident Memory T Cells and Fixed Immune Surveillance in Nonlymphoid Organs. *J Immunol* **195**, 17-22, doi:10.4049/jimmunol.1500515 (2015).

89 Pham, O. H. & McSorley, S. J. Divergent behavior of mucosal memory T cells. *Mucosal Immunol* **8**, 731-734, doi:10.1038/mi.2015.52 (2015).

90 Lijek, R. S. & Weiser, J. N. Co-infection subverts mucosal immunity in the upper respiratory tract. *Curr Opin Immunol* **24**, 417-423, doi:10.1016/j.coi.2012.05.005 (2012).

91 Shak, J. R., Vidal, J. E. & Klugman, K. P. Influence of bacterial interactions on pneumococcal colonization of the nasopharynx. *Trends Microbiol* **21**, 129-135, doi:10.1016/j.tim.2012.11.005 (2013).

92 Neto, A. S. *et al.* Risk factors for the nasopharyngeal carriage of respiratory pathogens by Portuguese children: phenotype and antimicrobial susceptibility of Haemophilus influenzae and *Streptococcus pneumoniae. Microb Drug Resist* **9**, 99-108, doi:10.1089/107662903764736409 (2003).

93 Lewnard, J. A. *et al.* Epidemiological Markers for Interactions Among *Streptococcus pneumoniae*, Haemophilus influenzae, and Staphylococcus aureus in Upper Respiratory Tract Carriage. *J Infect Dis* **213**, 1596-1605, doi:10.1093/infdis/jiv761 (2016).

94 Lysenko, E. S., Ratner, A. J., Nelson, A. L. & Weiser, J. N. The role of innate immune responses in the outcome of interspecies competition for colonization of mucosal surfaces. *PLoS Pathog* **1**, e1, doi:10.1371/journal.ppat.0010001 (2005).

95 Ratner, A. J., Lysenko, E. S., Paul, M. N. & Weiser, J. N. Synergistic proinflammatory responses induced by polymicrobial colonization of epithelial surfaces. *Proc Natl Acad Sci U S A* **102**, 3429-3434, doi:10.1073/pnas.0500599102 (2005).

96 Lysenko, E. S., Lijek, R. S., Brown, S. P. & Weiser, J. N. Within-host competition drives selection for the capsule virulence determinant of *Streptococcus pneumoniae*. *Curr Biol* **20**, 1222-1226, doi:10.1016/j.cub.2010.05.051 (2010).

97 Lijek, R. S. *et al.* Protection from the acquisition of Staphylococcus aureus nasal carriage by cross-reactive antibody to a pneumococcal dehydrogenase. *Proc Natl Acad Sci U S A* **109**, 13823-13828, doi:10.1073/pnas.1208075109 (2012).

98 Short, K. R., Habets, M. N., Hermans, P. W. & Diavatopoulos, D. A. Interactions between *Streptococcus pneumoniae* and influenza virus: a mutually beneficial relationship? *Future Microbiol* **7**, 609-624, doi:10.2217/fmb.12.29 (2012).

99 Mina, M. J., Klugman, K. P. & McCullers, J. A. Live attenuated influenza vaccine, but not pneumococcal conjugate vaccine, protects against increased density and duration of pneumococcal carriage after influenza infection in pneumococcal colonized mice. *J Infect Dis* **208**, 1281-1285, doi:10.1093/infdis/jit317 (2013).

100 McDaniel, L. S. & Swiatlo, E. Should Pneumococcal Vaccines Eliminate Nasopharyngeal Colonization? *MBio* **7**, doi:10.1128/mBio.00545-16 (2016).
101 Biesbroek, G. *et al.* Seven-valent pneumococcal conjugate vaccine and nasopharyngeal microbiota in healthy children. *Emerg Infect Dis* **20**, 201-210, doi:10.3201/eid2002.131220 (2014).
102 Hicks, L. A. *et al.* Incidence of pneumococcal disease due to non-pneumococcal conjugate vaccine (PCV7) serotypes in the United States during the era of widespread PCV7 vaccination, 1998-2004. *J Infect Dis* **196**, 1346-1354, doi:10.1086/521626 (2007).
103 Lexau, C. A. *et al.* Changing epidemiology of invasive pneumococcal disease among older adults in the era of pediatric pneumococcal conjugate vaccine. *Jama* **294**, 2043-2051, doi:10.1001/jama.294.16.2043 (2005).
104 Miller, E., Andrews, N. J., Waight, P. A., Slack, M. P. & George, R. C. Herd immunity and serotype replacement 4 years after seven-valent pneumococcal conjugate vaccination in England and Wales: an observational cohort study. *Lancet Infect Dis* **11**, 760-768, doi:10.1016/s1473-3099(11)70090-1 (2011).
105 Xu, Q., Almudervar, A., Casey, J. R. & Pichichero, M. E. Nasopharyngeal bacterial interactions in children. *Emerg Infect Dis* **18**, 1738-1745, doi:10.3201/eid1811.111904 (2012).
106 Madhi, S. A. *et al.* Long-term effect of pneumococcal conjugate vaccine on nasopharyngeal colonization by *Streptococcus pneumoniae*--and associated interactions with Staphylococcus aureus and Haemophilus influenzae colonization--in HIV-Infected and HIV-uninfected children. *J Infect Dis* **196**, 1662-1666, doi:10.1086/522164 (2007).
107 Spijkerman, J. *et al.* Long-term effects of pneumococcal conjugate vaccine on nasopharyngeal carriage of S. pneumoniae, S. aureus, H. influenzae and M. catarrhalis. *PLoS One* **7**, e39730, doi:10.1371/journal.pone.0039730 (2012).
108 Griffin, M. R. & Grijalva, C. G. Restraining the pneumococcus. *Lancet Infect Dis* **15**, 491-492, doi:10.1016/s1473-3099(15)70085-x (2015).
109 Marks, L. R., Reddinger, R. M. & Hakansson, A. P. High levels of genetic recombination during nasopharyngeal carriage and biofilm formation in *Streptococcus pneumoniae*. *MBio* **3**, doi:10.1128/mBio.00200-12 (2012).
110 Chaguza, C. *et al.* Recombination in *Streptococcus pneumoniae* Lineages Increase with Carriage Duration and Size of the Polysaccharide Capsule. *MBio* **7**, doi:10.1128/mBio.01053-16 (2016).
111 Lipsitch, M. & Siber, G. R. How Can Vaccines Contribute to Solving the Antimicrobial Resistance Problem? *MBio* **7**, doi:10.1128/mBio.00428-16 (2016).

9

Closing pages

Nederlandse samenvatting
Dankwoord
List of publications
Curriculum Vitae

NEDERLANDSE SAMENVATTING

Introductie

De pneumokok (of *Streptococcus pneumoniae*) is een bacterie die aanwezig kan zijn in bovenste luchtwegen van kinderen en volwassen zonder dat deze hiervan ziek worden. Dit fenomeen wordt ook wel dragerschap of kolonisatie genoemd. Dragers van de pneumokok kunnen deze bacterie via direct contact met andere personen en inademing van kleine druppeltjes die ontstaan bij het uitademen, niezen of hoesten, overdragen naar anderen in hun omgeving. In een beperkt aantal gevallen kan kolonisatie gevolgd worden door ernstige, levensbedreigende ziekten, zoals sepsis, hersenvliesontsteking en longontsteking. Infecties door pneumokokken vormen wereldwijd een belangrijke oorzaak van ziekte en overlijden. Vooral jonge kinderen en ouderen zijn extra vatbaar voor deze infecties. De huidige vaccins beschermen zeer effectief tegen ziekte door pneumokokken. In landen waar deze vaccins (nog) niet beschikbaar zijn overlijden echter nog steeds veel mensen aan de gevolgen van infectie.

Pneumokokken vaccins worden met een naald toegediend en beschermen uitstekend tegen ziekte, maar in mindere mate tegen kolonisatie. Dit betekent dat pneumokokken, ook bij een goede vaccinatiegraad, nog steeds kunnen worden verspreid binnen de populatie. In dit proefschrift wordt onderzoek gedaan om te bestuderen of vaccinatie via de neus leidt tot vermindering van kolonisatie door pneumokokken. Vermindering van kolonisatie wordt bewerkstelligd door activatie van het afweersysteem (immuunsysteem) dat het lichaam beschermt tegen ziekmakende organismen, zoals bacteriën en virussen. Met behulp van vaccinatie worden specifieke afweerreacties geactiveerd die leiden tot bescherming. In onze studies hebben wij voornamelijk de immuunreacties in de neus nader bestudeerd en het effect hiervan op vermindering van kolonisatie door pneumokokken. Omdat kolonisatie van de pneumokok een essentiële stap is voor ontstaan van ziekte en voor verdere verspreiding van de bacterie (transmissie), zal een vaccin dat kolonisatie vermindert een reductie geven in het aantal infecties veroorzaakt door pneumokokken.

Pneumokokken kolonisatie, verspreiding en ziekte

Ieder kind en volwassene wordt tijdens het leven meerdere malen gekoloniseerd door pneumokokken. Dragerschap van de pneumokok vindt voornamelijk plaats in onze neus-keelholte (nasopharynx). De duur van het dragerschap varieert van een week tot enkele maanden en is afhankelijk van de suikermantel (kapsel) die de meeste pneumokokken maken om zich te beschermen tegen afweerreacties. Deze kapsels worden ook wel serotypes genoemd omdat de verschillen tussen de suikers bepaald worden aan de hand van antistoffen die verschillende

suikergroepen herkennen (serologie). Er zijn inmiddels 90 verschillende serotypes geïdentificeerd. Vooral jonge kinderen dragen pneumokokken in hun neus-keelholte. In de westerse wereld zijn 20 tot 50% van de kinderen, jonger dan 3 jaar, gekoloniseerd. Dit percentage ligt vele malen hoger in ontwikkelingslanden. Jonge kinderen vormen dus een belangrijk reservoir voor pneumokokken en bepalen voor een groot deel de verspreiding van de bacterie in de bevolking.

Kolonisatie met pneumokokken in de nasopharynx gaat ongemerkt voorbij, maar in sommige gevallen kan kolonisatie leiden tot ziekte. Hierbij kan een onderscheid gemaakt worden tussen relatief minder ernstige aandoeningen, zoals keelontsteking (pharyngitis) of middenoorontsteking (otitis media) en ernstige, soms levensbedreigende ziekten zoals longontsteking (pneumonie), hersenvliesonsteking (meningitis) of bloedvergiftiging (sepsis). Jaarlijks overlijden wereldwijd meer dan 800.000 kinderen jonger dan 5 jaar ten gevolge van infecties door pneumokokken.

Pneumokokken vaccins en verbetering van bescherming

De pneumokokken vaccins die momenteel opgenomen zijn in rijksvaccinatie programma's (RVP) in verschillende landen zijn tot nu toe zeer effectief. Een belangrijke beperking van deze vaccins is dat ze (sero)type-specifieke bescherming opwekken. Dit betekent dat het vaccin alleen werkzaam is tegen een beperkt aantal (sero)types, die onderdeel zijn van het vaccin. Synflorix dat onder andere in Nederland en Finland opgenomen is in het RVP, bestaat uit 10 verschillende suikers afkomstig van 10 verschillende serotypes en beschermt derhalve alleen tegen deze 10 varianten. Invoering van dit vaccin in het RVP heeft geleid tot een enorme vermindering van pneumokokken infecties in kinderen en ouderen. In de laatste 10 jaar wordt echter steeds duidelijker dat andere serotypes, dan degenen die opgenomen zijn in de huidige vaccins, kolonisatie veroorzaken en in toenemende mate ook milde en ernstige infecties. Dit benadrukt de noodzaak voor de ontwikkeling van vaccins die een bredere bescherming opwekken.

Om deze bredere bescherming op te wekken moeten nieuwe vaccins ontwikkeld worden waarin andere onderdelen van pneumokokken, zoals eiwitten, opgenomen zijn. Deze andere antigenen (onderdelen van de bacterie die een beschermende immuunreactie opwekken) moeten een alternatief bieden voor vaccinatie waar alleen gebruik gemaakt wordt van kapsel suikers. Een op eiwit-antigeen-gebaseerd vaccin heeft als voordeel dat het potentieel bredere bescherming opwekt terwijl het ook goedkoper is om te produceren. Dit is een groot voordeel in vergelijking met de huidige pneumokokken vaccins, die voor ontwikkelingslanden veel te duur zijn. De belangrijkste vereiste van een nieuw, op eiwit-gebaseerd, vaccin is dat het geen serotype-specifieke bescherming moet geven, maar juist brede bescherming moet bieden tegen alle circulerende

pneumokokken varianten. Dit kan worden bereikt door een pneumokokken eiwit te selecteren dat voorkomt in alle pneumokokken, of door gebruik te maken van een combinatie van eiwitten.

Het op eiwit-gebaseerde vaccin zal intranasaal toegediend moeten worden om een maximale vermindering van kolonisatie te bewerkstelligen. Intranasale toediening ligt voor de hand om bescherming tegen kolonisatie op te wekken maar toediening via deze route leidt ook tot een sterke systemische reactie van het afweersysteem dat in het bloed gemeten kan worden. Een bijkomend voordeel van deze manier van vaccineren is het gemak (neusspray) en de hogere kans op acceptatie (geen naalden). Aangezien de neusholte continu blootgesteld wordt aan lichaamsvreemde stoffen die worden ingeademd, is er een zekere mate van tolerantie ontwikkeld, waardoor het moeilijker is om met een vaccin een immuunreactie op te wekken. Aan bijna alle vaccins wordt een helperstof of adjuvant toegevoegd om de immuunrespons te versterken. Een belangrijke uitdaging voor de ontwikkeling van een intranasaal vaccin is de noodzaak om een krachtig werkend adjuvant toe te voegen om een sterke en beschermende immuunreactie in de neus op te wekken. Op dit moment zijn er nog geen adjuvantia in gebruik voor intranasale vaccins voor mensen.

In dit proefschrift

De samenstelling of formulering van een vaccin, bestaande uit antigenen en, in veel gevallen ook van een adjuvant, zijn bepalend voor de effectiviteit. In **hoofdstuk 2** van dit proefschrift hebben wij de toepasbaarheid van een nieuw vaccin getest voor bescherming tegen kolonisatie door pneumokokken. Dit vaccin bestaat uit kleine vetblaasjes, ook wel outer membrane vesicles (OMVs) genoemd, die afkomstig zijn van een andere bacterie (Salmonella). Deze OMVs worden gevormd tijdens de groei van Salmonella, maar zijn zelf niet infectieus. In samenwerking met andere onderzoekers zijn we er in geslaagd om pneumokokken eiwitten (antigenen) op het oppervlak van de OMVs te zetten. Omdat de OMVs het immuunsysteem stimuleren (adjuvant werking) hebben we op deze manier een eenvoudig vaccin geproduceerd waarbij zowel antigeen als adjuvant aanwezig zijn in eenzelfde deeltje. In deze studie hebben we gebruik gemaakt van een bekend pneumokokken eiwit, namelijk PspA.

In **hoofdstuk 2** laten we zien dat intranasale vaccinatie met OMVs en PspA in muizen leidt tot vermindering van kolonisatie door pneumokokken. Verder hebben we aangetoond dat de bescherming tegen kolonisatie sterk geassocieerd is met een specifiek type immuunrespons, die gekenmerkt wordt door de aanwezigheid van een bepaald type witte bloedcel, ook wel de T helper 17 (Th17) cel genoemd. Deze cellen produceren stoffen die weer andere immuun cellen (macrofagen en neutrofielen) stimuleren om te migreren naar de nasopharynx

waar deze cellen betrokken worden bij het opruimen van de pneumokok. Het is bekend dat de Th17 respons een kritische rol speelt in vermindering van kolonisatie door pneumokokken. De resultaten van deze studies tonen aan dat OMVs geschikt zijn om gebruikt te worden voor toepassing in een intranasaal vaccin dat kolonisatie door pneumokokken beoogt te verminderen.

De bescherming tegen infecties door pneumokokken kan verbreed worden door in nieuwe vaccins gebruik te maken van eiwit antigenen die in alle varianten van de pneumokok voorkomen en identiek (geconserveerd) zijn. In **hoofdstuk 3** hebben we de functie bestudeerd van een sterk geconserveerd pneumokokken eiwit, PapP genoemd. We hebben aangetoond dat PapP essentieel is voor de structuur en het metabolisme van de pneumokok. Deze essentiële functie en het feit dat PapP geconserveerd is maken het een interessant antigeen voor introductie in vaccins tegen kolonisatie door pneumokokken. Wij zullen hier in de toekomst nader onderzoek naar doen.

In hoofdstuk 2 hebben we aangetoond dat intranasale vaccinatie met OMVs, welke PspA bevatten, leidt tot bescherming, i.e. vermindering van kolonisatie door pneumokokken. In **hoofdstuk 4** wordt onderzocht of dit vaccin ook brede bescherming opwekt tegen verschillende pneumokokken varianten. We hebben onderzoek gedaan met levende milt cellen uit gevaccineerde muizen welke we buiten het lichaam (*ex vivo*) hebben blootgesteld aan verschillende pneumokokken stammen om te bepalen of er een Th17 respons te meten was. Uit deze *ex vivo* gemeten respons konden we opmaken dat er sprake was van kruis bescherming. Ook hebben we kunnen bepalen dat de Th17 respons die we *ex vivo* gemeten hadden overeenkwam met de *in vivo* Th17 respons in de neus van de muis. De Th17 respons in de miltcellen en in de neus bleek ook goed te correleren met bescherming tegen kolonisatie door pneumokokken. Samenvattend hebben we een goed werkende laboratorium test ontwikkeld die op een relatief eenvoudige manier de vaccin gestimuleerde beschermende responsen en het effect op de vermindering van kolonisatie na pneumokokken infecties kan voorspellen.

In **hoofdstuk 5** belichten we een ander aspect van vaccins dat tot nu toe weinig aandacht heeft gekregen. Het principe van vaccinatie is dat bescherming wordt verkregen door het immuunsysteem in contact te brengen met onderdelen van een ziekmakend micro-organisme (vaccin antigenen). Deze antigenen betreffen in ons geval pneumokokken eiwitten. Antigenen worden in veel vaccins gecombineerd met een adjuvant om het immuunsysteem te activeren. Gebruik van een vaccin met alleen een adjuvant zou normaliter geen bescherming moeten bieden. Interessant genoeg laten wij in **hoofdstuk 5** op basis van een aantal studies zien dat intranasale vaccinatie met alleen een adjuvant (CTB genoemd), zonder toevoeging van een pneumokokken eiwit, gedeeltelijk

beschermt tegen kolonisatie door pneumokokken. We hebben in deze studie aangetoond dat bescherming wordt veroorzaakt door een specifiek type immuuncel (de macrofaag), en niet door een Th17 geïnduceerde immuunreactie. Dit suggereert dat toekomstige studies naar mechanismen van bescherming tegen kolonisatie door pneumokokken niet alleen de Th17 immuunrespons moeten bestuderen, maar ook andere celtype gemedieerde immuunreacties.

De genetische achtergrond van de gevaccineerde individuen beïnvloedt eveneens de door het vaccin gestimuleerde immuunrespons en daarmee de mate van bescherming. Mensen zijn genetisch immers erg verschillend, ook in de manier waarop het immuunsysteem op ziekmakende organismen, zoals bacteriën en virussen, reageert. Het doel van vaccinatie is om de hele bevolking te beschermen. De vaccins die geproduceerd worden moeten dus ondanks deze individuele verschillen in alle individuele gevallen werken. In **hoofdstuk 6** hebben wij onderzocht of de genetische achtergrond invloed heeft op de bescherming tegen kolonisatie door pneumokokken door gebruik te maken van een experimenteel vaccin. Dit vaccin bestaat uit PspA en CTB en wordt veelvuldig gebruikt in dierstudies. We hebben door experimenten in verschillende muis stammen aangetoond dat dit type vaccin bescherming biedt tegen kolonisatie door pneumokokken ondanks de evidente verschillen in genetische achtergrond bij deze muizen.

Met name jonge kinderen en ouderen zijn kwetsbaar voor infecties door pneumokokken. Waarom deze leeftijdsgroepen extra gevoelig zijn is niet duidelijk. **Hoofdstuk 7** beschrijft ons perspectief over de gevoeligheid van jonge kinderen en ouderen voor kolonisatie door pneumokokken, gebaseerd op twee onafhankelijk dierstudies in jonge en oude muizen. Interessant genoeg blijkt uit beide studies dat zowel jonge als oude muizen een vergelijkbare gevoeligheid laten zien tegen kolonisatie door pneumokokken, hetgeen zich in beide gevallen uit door een langere duur van dragerschap. In **hoofdstuk 7** bediscussiëren we dat de gevoeligheid van jonge en oude muizen voor kolonisatie door pneumokokken veroorzaakt wordt door eenzelfde afweermechanisme. Onafhankelijk uitgevoerde studies door verschillende onderzoeksgroepen laten zien, dat een defect in de macrofaag ten grondslag ligt aan de verhoogde kolonisatie in zowel jonge als oude muizen. De aanwezigheid van een vergelijkbaar defect in de macrofaag in zowel jonge als oude muizen is een interessante bevinding gezien de enorme verschillen die bestaan in het afweersysteem tussen deze leeftijdsgroepen.

In **hoofdstuk 8** worden de resultaten van dit proefschrift bediscussieerd in de bredere context van toekomstige ontwikkelingen op het gebied van vaccinatie tegen pneumokokken. Ons inziens is intranasale vaccinatie, om pneumokokken dragerschap te verminderen, een goede strategie om de totale ziektelast

veroorzaakt door pneumokokken te verminderen, met name in de leeftijdsgroepen die een verhoogd risico hebben voor infectie door pneumokken. Verder laat ons werk zien dat een Th17 immuunrespons belangrijk is om kolonisatie te verminderen, maar dat de immuunmechanismen van bescherming complexer zijn en er ook andere type immuunreacties en immuuncellen bij betrokken zijn. Daarom zouden toekomstige studies zich niet alleen moeten focussen op een analyse van de Th17 immuunrespons, maar eveneens op onderzoek gericht op andere typen afweer reacties. Er zijn op het moment drie pneumokokken vaccins die worden getest in klinische studies voor evaluatie van bescherming tegen kolonisatie. Deze vaccins worden allen via een naald (in de spier) en niet intranasaal toegediend. Dit is in tegenstelling tot de pre-klinische dierstudies waar deze geadjuveerde vaccins intranasaal werden toegediend. Vaccineren via een naald leidt tot een ander type immuunrespons en zal minder tot mogelijk zelfs geen effect hebben op kolonisatie. Wij achten het van groot belang, dat in de toekomst klinische studies met een geadjuveerd intranasaal vaccin uitgevoerd gaan worden en te bestuderen of hierbij inderdaad een sterkere reductie van kolonisatie en ziekte bewerkstelligd kan worden, dan door intramusculair toegediende conjugaat vaccins. Er zijn nog veel vragen die in dit proefschrift onbeantwoord zijn gebleven. Voorbeelden hiervan zijn: welke mate van bescherming tegen kolonisatie is noodzakelijk om ziekte te voorkomen? en hoe kunnen we de effectiviteit van een intranasaal vaccin meten in toekomstige klinische trials? Om antwoorden op deze vragen te krijgen zullen we een beter inzicht moeten krijgen in welke factoren, zowel bacteriële als immunologische, de overgang van kolonisatie naar ziekte bepalen. Dit is essentieel voor de ontwikkeling van een intranasaal vaccin dat niet alleen beschermt tegen verspreiding van de pneumokok maar ook tegen ziekte veroorzaakt door pneumokokken.

DANKWOORD

Daar zit ik dan in New York. Begonnen als postdoc afgelopen januari, terwijl ik me absoluut nog geen postdoc voel. De afgelopen maanden, het einde van mijn PhD en de start hier, zijn in een vogelvlucht voorbijgegaan en hebben veel impact op mij gemaakt. Dit in combinatie met de herinneringen aan mijn PhD maken me wat gevoelig. Natuurlijk het beste moment om het dankwoord voor mijn PhD te schrijven! Wat heb ik een geweldige tijd gehad. Wetenschappelijk heb ik ontzettend veel geleerd en ben ik gegroeid, maar zeker ook als persoon. Ik ben dankbaar dat ik omgeven word door zulke fijne mensen, van wie ik veel heb geleerd, ontzettend veel mee heb gelachen (heel erg veel!), maar zeker ook frustraties bij heb geuit en gevoeligheden mee heb gedeeld. Ik denk al een tijdje na over het schrijven van mijn dankwoord, waarin ik in mijn gedachten elke keer tegen hetzelfde probleem aanloop. Hoe kan ik iedereen die belangrijk voor mij is geweest tijdens mijn promotietraject voldoende bedanken en erkennen in een paar pagina's dankwoord? Ik ben tot de conclusie gekomen dat dat onmogelijk is, dus zal ik het kort maar hopelijk toch persoonlijk houden. Degenen die mij goed kennen weten dat dat laatste, iets kort houden wanneer het persoonlijk voelt, voor mij een behoorlijke uitdaging is. Daar ga ik dan…

Als ik naar andere dankwoorden kijk, zie ik dat deze meestal beginnen met het bedanken van de promotor. Toch doe ik dat niet. Waarom niet? Omdat jij **Marien**, mijn co-promotor, de reden was dat ik dit PhD traject binnen Laboratorium Kindergeneeskunde Infectieziekten aan wilde gaan. Ik herinner me nog mijn sollicitatiegesprek met jou (en **Fred**) dat door ons beider enthousiasme, als ik het me goed herinner, bijna 2 uur heeft geduurd! Door onze goede klik verdwenen de paar initiële twijfels als sneeuw voor de zon. Dat we een team zijn is wel gebleken tijdens deze 4 jaar. Mijn PhD was een gezamelijke missie en dit proefschrift voelt daarom als ons werk (en natuurlijk dat van vele anderen) waar ik erg trots op ben. Verder heb ik veel van je geleerd, vooral van jouw politieke management skills, iets wat erg handig was gezien mijn eigen (Overijsselse?) directheid. **Marien**, ik ken werkelijk niemand die zo betrokken is bij zijn mensen als jij. Je deur stond altijd voor mij open en je was (en bent dat nog steeds) bereid om mij met alles te helpen en te ondersteunen. Ik heb er bewondering voor dat ondanks alles wat je op je bordje hebt, je het belangrijk vindt dat jouw mensen zich goed voelen en vooral ook goed terecht komen. Bedankt voor alles en ik hoop dat we dit in de toekomst voorzetten!

Ronald, jij behoort tot het type promotoren dat erg betrokken is bij zijn promovendi. Je wilt immers dat ze het beste uit zichzelf halen. Daarbij hebben

jouw visie en jouw passie voor de wetenschap en pediatrie specifiek mij enorm gemotiveerd. Je was altijd benaderbaar en ik vond het erg verfrissend wanneer je ondanks je eigen drukte af en toe een zoete inval deed in de PhD kamer, of in was voor een kort koffie momentje of een lunch buiten. Gewoon om eens te horen hoe het met de promovendi was of voor een leuk verhaal, waardoor je ons daardoor toch wel een beetje van ons werk afhield. Tijdens onze gesprekken vond ik jouw directheid verfrissend. Jouw duidelijke tips voor het schrijven, maar zeker ook jouw advies voor de toekomst waardeer ik zeer en hebben me al heel wat gebracht. Bedankt hiervoor!

Dear members of the manuscript committee, **Prof. dr. André van der Ven**, **Prof. dr. Heiman Wertheim**, and **Prof. dr. Jeffrey Weiser**, thank you for your time to read and evaluate my thesis. **Jeff** and **Daniela**, I really appreciate the effort you are taking to come all the way from New York and Liverpool to attend my defense. **Nina**, ik wil jou toch zeker ook bedanken, maar niet alleen omdat je zitting neemt in mijn corona. Ons contact begon tijdens mijn masterstage bij Victor in San Diego, waarvoor jij mijn Nederlandse supervisor was. Tijdens deze periode ben ik door jou in contact gekomen met het LKI, dank hiervoor, en sindsdien, zijn we altijd betrokken bij elkaar geweest. Door onze bijzondere klik heb ik jouw advies erg hoog staan. Ik hoop dan ook dat we dit zullen voortzetten in de toekomst.

To all of the corona members, I am looking forward to our discussions on the 29th of May!

Tijdens mijn PhD heb ik met veel mensen buiten het LKI mogen samenwerken. **Joen**, **Wouter**, en **Diane**, onze samenwerking begon bij de start van mijn PhD door het Pneumovac consortium. In het begin was het misschien samen even zoeken, maar ik heb echt genoten van onze samenwerking. Qua werk stonden onze neuzen dezelfde kant op en voor mijn gevoel hebben we samen het maximaal haalbare uit ons project gehaald in deze jaren. Wat ik geweldig vond was jullie humor. God wat heb ik gelachen met **Marien** om de grappige en droge opmerkingen tijdens de teleconferenties of de consortium meetings! Wanneer de andere consortium leden veel te serieus verder gingen en wij blijkbaar de enigen waren die elkaars humor begrepen, kwam ik soms niet meer bij van het lachen. Heerlijk! Bedankt voor de fijne en gezellige samenwerking. Ik hoop dat het einde van mijn PhD niet het einde voor ons contact betekent. **Wouter** en **Diane**, ook bedankt voor jullie tips m.b.t. mijn postdoc. **Joen**, ik hoop jou nog een keer te zien hier in New York. Je begrijpt natuurlijk wel dat ik je aan het beloofde etentje zal houden!

Mihai, ook onze samenwerking begon met de aanvang van mijn PhD. Je interesse voor ons CTB project en jouw kennis waren erg motiverend. Dank voor

de meetings en bovenal voor je waardevolle input. Ik denk dat we ons werk mooi hebben weggezet in *The Journal of Infectious Diseases*. **Leo**, jouw additionele input en connecties hebben zeker een bijdrage geleverd aan dit werk. Ook dank voor de acceptatie als mijn mentor binnen het RIMLS. Jouw advies voor de toekomst, qua baan en funding aanvragen, hebben me doen nadenken en invloed gehad op de keuzes die ik heb gemaakt en op dit moment nog maak. **Eelke**, hartelijk dank voor de hulp met de proeven die uitgevoerd zijn in Groningen. **Marije** and **Taj**, thank you for all your efforts. I enjoyed our fruitfull collaboration.

Jan-Willem and **Clement**, and **Markéta** and **Vaclàv**, thanks for your major contributions to our PapP project. Your input and perseverance led to the acceptance of this beautiful work for publication in *Molecular Microbiology.*

Pieter, **Roel** en **Miriam**, onze proefdierdeskundigen binnen het Radboud. Ik durf grif toe te geven dat jullie een aandeel hebben gehad in het grootste deel van mijn proefschrift. Wat heb ik jullie vaak gebeld voor advies (echt vaak) over hoe wij het beste onze aanvragen konden indienen. Wat de meest optimale weg was. Maar vaak toch ook wel wat de snelste route was. Jullie waren altijd vriendelijk, toegankelijk en deden jullie best om mij verder te helpen. Het was prettig te voelen dat we in 'hetzelfde team' zaten. Hartelijk dank!

Stefanie en **Mike**, ook jullie heb ik vaak benaderd voor hulp. Het was zo prettig voor ons wanneer er onverwachte dingen gebeurden waarvoor actie nodig was, dat jullie er waren om ons te ondersteunen. Hartelijk dank! Daarbij kan ik niet ontkennen dat ik onze korte momenten samen in de flow erg gezellig vond. **Mike**, ik moest zo hard lachen toen je zei, mede door het gezicht van **Fred**: 'He Dushi, je hebt blote benen, dat mag helemaal niet!' **Stefanie**, ik kijk er naaruit om je hier in New York te zien, dan gaan we gezellig een hapje eten en drinken en rondwandelen in de stad.

Lieve **Christa**, **Marc**, **Elles**, en **Fred**, jullie vormen toch echt wel de ruggengraat van het lab. Behalve jullie experimentele ervaringen vond ik het geweldig fijn en gezellig met jullie. Wat heb ik veel tijd in jullie kamer door gebracht. We wisten ook allemaal dat als ik over de drempel van jullie deur stapte, ik minstens een kwartier bleef, waardoor de drempel een toch wat symbolische waarde kreeg. Meestal kwam ik gewoon even om te kletsen om te horen hoe het was, maar toch ook wel eens om mijn frustratie te uiten als een proef geheel andere uitkomsten gaf (ik kan me nog herinneren dat we met dingen gegooid hebben…). **Chrisje**, wat hebben wij fijn samen gewerkt voor ons PspA project waarvoor je kennis erg waardevol was. Door deze intensievere samenwerking hebben we elkaar erg goed leren kennen. Wat hebben we ook veel gelachen, onze grappen en dansjes in het lab (hilarisch!), die misschien niet door iedereen werden begrepen maar zeker door ons. Ook onze diepere gesprekken, waarin je positiviteit een groot

aandeel had. Ik ben blij dat je mijn paranimf wilt zijn op mijn belangrijke dag, dank! **Elles** en **Fred**, met jullie heb ik veel lange dagen gemaakt in het CDL, bedankt voor jullie geduld, hulp en goede humeur! Meestal waren deze dagen toch ook wel een klein feestje. Wat was het leuk om elkaar te plagen! Lieve **Elles**, wij hebben elkaar ook op een andere manier leren kennen tijdens mijn PhD. Ik kan mijn gevoel niet goed op papier zetten zonder te veel in details te treden. Ik wil je heel erg bedanken voor onze gesprekken, je openheid en steun. Dat is van grote waarde voor mijn 2e leven. **Fred**, Fredje, Fredretteketet, Fred ….(4 letters!) plet. Haha ik moet al meteen lachen. Waar te beginnen? Wat hebben wij veel momenten beleefd in het CDL! Het was duidelijk dat er meteen synergie was tussen ons en we elkaars grappen (heel!) erg konden waarderen. Wat hebben wij gelachen zeg! Onze step momenten naar en van het CDL, door de kelder, of soms zelfs buitenom. Ik herinner me nog een moment specifiek in het CDL waardoor ik niet meer bij kwam van het lachen en de gedachte alleen al tranen in mijn ogen doet komen! Dit zal ik maar niet op papier zetten, maar je weet heel goed wat ik bedoel. Behalve humor zochten we zeker ook de diepte op in onze gesprekken. Je was altijd erg betrokken (soms zelfs bezorgd) en het was fijn je te horen zeggen wanneer ik iets goed deed wanneer ik dat nodig had. Labpapa, zo noem ik je niet voor niets, bedankt voor werkelijk alles.

Ik wil ook zeker mijn kamergenoten bedanken. **Ria**, jij bent de enige met wie ik vanaf het begin tot het eind het kantoor heb gedeeld. Je was een fijne kamergenoot, we hadden immers altijd interesse in elkaar en dingen die speelden in ons leven. De nieuwe PhD'ers, die nu eigenlijk niet meer zo nieuw zijn, **Inge** en **Esther**. We zochten elkaar vaak op, ook zeker buiten werk om, voor gezellige, grappige en diepgaandere gesprekken, die voor mij erg waardevol waren. Ik heb het harstikke fijn met jullie gehad en onze outings waren super, vooral wanneer er een drankje in ging gevolgd door een dansje! Ik hoop dan ook dat we in contact zullen blijven. To the really new PhD'ers **Liz, Josh**, **Lucille,** and **Evi**, I wish you the best of luck with your PhD in this terrific group of people. Also thanks to my students, **Michelle**, **Mariska**, and **Gosia**, it was great to supervise you and thank you for all your work!

Ook de andere kamergenoten **Erika**, **Hanneke**, **Corné**, **Fredrick**, en de onco's **Dorette**, **Liesbeth**, **Kirsten**, **Laurens**, **René**, **Frank**, **Miriam** en andere oud LKI'ers en onco's bedankt voor de leuke klets en dansmomentjes en alle andere gezelligheid. **Dorette**, het was hartstikke leuk om met je samen te werken en LKI en LKO wat dichter bij elkaar te brengen. Ik herinner me nog goed onze poging om samen op één step naar de microscopie afdeling te gaan. Dat ging toch eigenlijk best goed?!

Gerben, **Dimitri**, **Saskia**, **Jeroen**, de ervaren science mensen in het lab, bedankt voor jullie ondersteuning tijdens mijn traject. **Gerben**, jouw enthousiaste creatieve geest en het stellen van de juiste vragen heeft ons onderzoek zeker voortgeholpen. Je liet me met een andere blik naar ons onderzoek kijken. Ook dank voor de brainstormsessie over mijn toekomst. **Dimitri**, ik heb veel geleerd van jouw kennnis m.b.t. immunologie en jouw kritische blik op vraagstellingen, de daarbij horende proeven, maar zeker ook het schrijven. **Saskia**, jouw expertise en ervaring omtrent dierproeven waren erg waardevol, vooral wanneer het anders liep dan gedacht. **Jeroen**, onze samenwerking kwam iets later op gang toen je aan pneumokokken ging werken, jaja wie had dat gedacht! Onze discussies over ons project en jouw gedrevenheid motiveerde me enorm en werkte aanstekelijk. Daarbij was je ook zeker niet vies van een biertje en een feestje (KNVM), waarop ook jij de dansvloer onveilig hebt gemaakt!

Aldert en **Hester**, het was fijn samenwerken met jullie wat tot een mooie publicatie heeft geleid en hopelijk binnenkort nog een. Ook al werkten jullie al een tijdje elders, toch zochten we elkaar veel op tijdens congressen voor een aantal drankjes en wanneer er de mogelijkheid was, toch ook zeker op de dansvloer voor een aantal dansjes. Tijdens de KNVM, behoorden we dan ook vaak tot de laatsten op de dansvloer en gingen we swingend door tot de D.J. stopte!

Sandra, bedankt voor al je hulp mbt organisatorische dingen. Je was altijd benaderbaar en zeker ook in voor een grapje op zijn tijd! Lieve **Ada**, ook al ben je niet meer onder ons, jouw ondersteuning tijdens mijn PhD waardeer ik zeer. Je zult gemist worden.

Pittige dames **Lilly**, **Amelieke**, en **Marloes**, we klikken erg goed en konden werkelijk over van alles met elkaar praten. Volgens mij zit er geen limiet aan hoeveel wij met elkaar kunnen kletsen, waarin we zelfs af en toe uitspraken deden voor de toekomst. Gezellige koffie momentjes, etentjes en congressen, zelfs toen jullie al elders werkten. Wat ben ik blij dat ik jullie heb leren kennen en ik weet zeker dat we in contact zullen blijven.

Dear **Jeff**, how grateful I am that you gave me the opportunity to work as a postdoc in your group. I know I will learn a great deal from the way you perform science and know you will be a great mentor to me. You are genuinely involved in all the lab work and during my first days, I was positively surprised to see you look at pneumococci under the microscope (lab member quote: 'he likes to do that every day'). The rest of the lab members, **Jen**, **Pam**, **Alex**, **Shigeto**, **Mila**, **Kristen**, and **Ammar**, thank you for being so welcoming! **Jen**, it is so nice to hang out with you, I love your jokes and your catchy personality. **Pam**, thanks for the

ginger tea and the painkillers for **Toni** and me after our wine outing the night before. **Toni**, how could anyone be more welcoming than you were! I cannot express my gratitude enough. You helped me with literally everything. It is so comforting to have you, I have not felt alone since the minute I came to NY. How I loved shopping with you at Ikea to choose 'our' furniture. How I love to hang out with you. I cannot wait to experience our list of plans with all the cool things we have in mind!

Evelien en **Michiel**, jullie hebben me erg geholpen tijdens deze toch wel grote stap. Het is fijn dat er andere top Dutchies 'to the rescue' komen en begrijpen waar je in zit. Bedankt voor jullie hulp, de gezelligheid, de uitjes en alvast voor alle uitjes en gezelligheid die nog gaan volgen!

En dan mijn vriendinnen voor het leven! De **BMW chickies**, bedankt voor alle gezellige etentjes drankjes en dansjes tijdens deze periode! **Eline**, **Anne**, **Janneke** en **Judith**, we zagen elkaar niet zo frequent als we zouden willen maar als we elkaar zagen was het altijd als vanouds. Zulke vriendinnen zijn goud waard! We praatten dan honderduit over werkelijk alles en qua PhD konden we elkaar met veel (nerden!) humor goed laten relativeren. Heerlijk met lekker eten en wijn&cocktails op de bank en zelfs een sleepover (blijkbaar kun je daar toch echt nooit te oud voor zijn). Lieve **Juud**, jij in het bijzonder bedankt voor de chille en fijne momenten. Het was erg waardevol dat je mij op essentiële momenten eens goed een spiegel voor hield.

Lieve **Leonie**, **Eva** en **Majorie**, we kennen elkaar al sinds de middelbare school en hebben al heel wat belangrijke momenten in onze levens samen mogen ervaren (wat zijn we al oud geworden!). Ik geniet van onze afspraakjes waarin we altijd te weinig tijd hebben om elkaar volledig op de hoogte te brengen. Onze vriendschap is belangrijk voor mij en ik ben blij dat ik ook dit belangrijke moment met jullie mag delen.

Vrienden uit Rijssen, bedankt voor alle borrels, feestjes en gezelligheid! **Annelies**, bedankt voor de gezellig borrels en de goede verhalen. Lieve **Linda**, bedankt voor de fijne en relaxte weekenden, vooral die in Alkmaar omgeving. Lieve **Tamara** en **Melanie**, jullie hebben mij het meest ervaren van iedereen en daarom ook al mijn 'colors' mogen zien, de leuke en zeker ook de minder leuke. Bedankt dat jullie mij wegtrokken uit mijn sleur en serieusheid wanneer dat het meest nodig was. Onze borrels, spelletjesmiddagen en feesten waren memorabel en ik hoop dat we dat in de toekomst nog heel veel gaan doen (want ja ik kom nu immers terug naar NL). **Mel**, met je geweldige Queen of Darkness grappen, en **Tammie**, jij lief pittigheidje, kan niet wachten totdat we hier in New York gaan 'gabbing', oja en natuurlijk Melle's hele bucketlist afwerken.

Lieve **Inge**, eerst was je mijn collega, daarna mijn oudcollega en nog later mijn roomie van de laatste maanden voordat ik naar New York ging. Hoe geweldig ben je als je iemand zo spontaan opneemt in je huis als jij deed voor mij. Onder veelvuldig genot van wijntjes, lekkere hapjes, Indisch eten, en (heel erg veel) Bon bon bloc hebben we elkaar tot in de puntjes leren kennen. Hoe fijn was het dat we elkaar lekker direct konden laten reflecteren en inzien wat we deden of waar we mee bezig waren, om elkaar tot inzicht te brengen of juist dat extra duwtje te geven wanneer nodig. Heel erg bedankt voor ALLE duwtjes die jij mij hebt gegeven, je weet precies welke duwtjes in het bijzonder voor mij het verschil hebben gemaakt.

Voor iedereen is het duidelijk dat jij, **Jop**, mijn PhD hubby bent. Vanaf het begin zijn we twee handen op één buik en we begrijpen elkaar met een enkele blik. We hebben elkaar direct door wanneer een van ons een bepaalde benadering hanteert, zowel op werk als daarbuiten, wat hilarische momenten oplevert. Onze etentjes, sleepovers at 'Bed & Breakfast Jop Jans' en stapavonden zijn onbeschrijfelijk. Altijd als ons nummer (Casanova, hoe is dat eigelijk ontstaan?) voorbij komt gaan we vol overgave in elkaar op. Werkelijk, mensen moeten eens weten wat voor hilarische momenten dat heeft opgeleverd! Jopje, jij pittige, slimme, talentvolle, lieve, maar zeker ook professionele man (ik houd van die attitude), bedankt voor werkelijk alles! Alle momenten die je er voor mij was en bent en die we samen beleefd hebben en nog gaan beleven. Onze vriendschap kent geen limiet.

Pap, **Mam**, **Wouter** en **Mieke**, mijn lieve familie met wie ik het zo getroffen heb. Wat geniet ik er altijd van als we samen zijn. Ook al woon ik allang niet meer bij jullie, het voelt nog altijd als thuis en dat zal het ook altijd blijven voelen. **Wouter**, grote broer, en **Miek**, schoonzusje (nog niet officieel en daarom nog koude kant, maar je bent wel ontzettend warm geworden hoor!), het is altijd lachen met jullie en ik weet dat we voor elkaar klaarstaan als we elkaar nodig hebben.

Pap en **Mam**, ik weet dat het is voor jullie de normaalste zaak van de wereld is, maar jullie stonden altijd voor mij klaar en werkelijk niets was jullie te veel. Ik ken weinig mensen die zo'n ontzettend goede band met hun ouders hebben als wij hebben. Jullie liefde en capaciteit voor ons de kinderen kent geen limiet. Ik hoop jullie hierin later te mogen evenaren. De perioden, bij start van mijn PhD als de periode wat meer naar het eind toe waren zwaar voor mij, waarin jullie mij ontzettend veel gesteund hebben en mij belangrijke dingen hebben laten inzien. Lieve **Pap** en **Mam**, jullie hadden geen wetenschappelijke, maar misschien wel de belangrijkste rol tijdens mijn PhD periode en daarom draag ik mijn proefschrift aan jullie op.

Om eerlijk te zijn had ik niet verwacht dat ik deze laatste alinea uberhaupt zou schrijven. Ik had grootste plannen voor New York - daar zou immers mijn hele dating experience starten – maar belangrijker, omdat ik het absoluut niet wilde, was ik ervan overtuigd dat het mij daarom ook niet zou overkomen. Velen waren getuige van deze (nu toch wel naïeve) uitspraak. Maar blijkbaar werkt het zo echt niet, want jij, lieve **Harvey**, bent mij overkomen en linea recta mijn hart binnen gedrongen. Initieel heb ik me hier behoorlijk tegen verzet (wie doet zoiets in de laatste periode van haar PhD, laat staan nog geen 3 maand voor haar emigreren?!). Jij was degene die nergens voor terug deinsde en vooral uitdagingen zag, geen problemen. Het is onbeschrijfelijk hoe jij mij de ruimte gaf tijdens de laatste periode van mijn PhD en mijn laatste periode in Nederland. Deze ruimte geef je me nog steeds, omdat je begrijpt dat ik dit moet doen en ergens naar op zoek ben. Ons gevoel kent letterlijk geen grenzen. Geweldige man, ik ben blij dat je onderdeel uitmaakt van deze belangrijke dag. Daarbij, kan ik niet wachten tot mijn New York avontuur voorbij is en we echt samen kunnen zijn om samen het leven verder te ontdekken. Ik hou van je.

Kirsten

LIST OF PUBLICATIONS

Related to this thesis

Kuipers, K., Diavatopoulos, D. A., van Opzeeland, F., Simonetti, E., van den Kieboom, C. H., Kerstholt, M., Borczyk, M,, van IngenSchenau, D., Brandsma, E. T., Netea, M.G., de Jonge, M. I. Antigen-Independent Restriction of Pneumococcal Density by Mucosal Adjuvant Cholera Toxin Subunit B. *J Infect Dis.* 214(10), 1588-1596 (2016). doi:10.1093/infdis/jiw160

Kuipers, K.[*], Gallay, C.[*], Martínek, V., Rohde, M., Martínková, M., van der Beek, S. L., Jong, W. S., Venselaar, H., Zomer, A., Bootsma, H., Veening, J. W.[#], de Jonge, M. I.[#] Highly conserved nucleotide phosphatase essential for membrane lipid homeostasis in *Streptococcus pneumoniae*. *Mol Microbiol.* 101(1), 12-26 (2015). doi:10.1111/mmi.13312.

Kuipers. K.[*], Daleke-Schermerhorn, M. H.[*], Jong, W. S., ten Hagen-Jongman, C. M., van Opzeeland, F., Simonetti, E., Luirink, J., de Jonge, M. I. Salmonella outer membrane vesicles displaying high densities of pneumococcal antigen at the surface offer protection against colonization. *Vaccine* 33(17), 2022-9 (2015). doi:10.1016/j.vaccine.2015.03.010.

Kuipers, K., van Selm, S., van Opzeeland, F., Langereis, J. D., Verhagen, L. M., Diavatopoulos, D. A., de Jonge, M. I. Genetic background impacts vaccine-induced reduction of pneumococcal colonization. *Submitted.*

Kuipers, K., Jong, W. S. P., van der Gaast-de Jongh, C. E., Houben, D., Opzeeland, F., Simonetti, E., van Selm, S., de Groot, R., Koenders, M. I., Azarian, T., Pupo, E., van der Ley, P., Langereis, J. D., Zomer, A., Luirink, J., de Jonge, M. I. Cross-reactive Th17-mediated protection against pneumococcal carriage with a variable antigen. *Submitted.*

Other publications

Henningham, A.[*], Yamaguchi, M.[*], Aziz, R. K., **Kuipers, K.**, Buffalo, C. Z., Dahesh, S., Choudhury, B., Van Vleet, J., Yamaguchi, Y., Seymour, L. M., Ben Zakour, N. L., He, L., Smith, H. V., Grimwood, K., Beatson, S.A., Ghosh, P., Walker, M. J., Nizet, V., Cole, J. N. Mutual exclusivity of hyaluronan and hyaluronidase in invasive group A Streptococcus. *J Biol Chem.* 289(46), 32303-15 (2014). doi:10.1074/jbc.M114.602847.

van Sorge, N. M.[*], Cole, J. N.[*], **Kuipers, K.**, Henningham, A., Aziz, R. K., Kasirer-Friede, A., Lin, L., Berends, E. T., Davies, M. R., Dougan, G., Zhang, F., Dahesh, S., Shaw, L., Gin, J., Cunningham, M., Merriman, J. A., Hütter, J., Lepenies, B., Rooijakkers, S. H., Malley, R., Walker, M. J., Shattil, S. J., Schlievert, P. M., Choudhury, B., Nizet, V. The classical lancefield antigen of group a Streptococcus is a virulence determinant with implications for vaccine design. *See comment in PubMed Commons belowCell Host Microbe.* 11;15(6), 729-40 (2014). doi:10.1016/j.chom.2014.05.009.

Cole, J. N., Aziz, R. K., **Kuipers, K.**, Timmer, A. M., Nizet, V., van Sorge, N. M. A conserved UDP-glucose dehydrogenase encoded outside the hasABC operon contributes to capsule biogenesis in group A Streptococcus. *J Bacteriol.* 194(22), 6154-61 (2012). doi:10.1128/JB.01317-12.

[*] equal contribution
[#] shared supervision

CURRICULUM VITAE

Kirsten Kuipers was born on November 11th 1988 in Almelo, The Netherlands. She grew up in Rijssen and finished her secondary school (VWO) at de Waerdenborgh in Holten in 2007. She started with her Bachelor Biomedical Sciences at Utrecht University and graduated as Bachelor of Science *cum laude* in 2010. Her interest for infection and immunity was first triggered during a related course as part of the Bachelor program, which led to her enrollment in the Infection and Immunity Master's program at Utrecht University. She performed her Bachelor and first Master internschip in the group of Dr. Kiki Tesselaar and Dr. José Borghans at the Department of Immunology in the Wilhelmina Children's hospital in Utrecht. Under the supervision of Dr. Liset Westera and Dr. Vera van Hoeven, she studied the effect of chronic immune activation on bystander T cells. In addition to the Master curriculum, Kirsten was the chair of the organizing committee of the Master's symposium Infection and Immunity entitled "How to cure the incurable". During her Master courses, host-pathogen interactions inspired her and made her decide to do her second internschip abroad. She travelled to the University of California San Diego in San Diego, the United States and worked at the Department of Pediatrics in the group of Prof. dr. Victor Nizet under the supervision of Dr. Jason Cole and Dr. Nina van Sorge to study Group A streptococcal virulence and immunity. This internship convinced her to further pursue science in the area of host-bacterial interactions, in particular pediatric infectious diseases. After returning to the Netherlands, she obtained her degree Master of Science in 2012 and started her PhD training at the Department of Pediatric Infectious Diseases under the supervision of Dr. Marien de Jonge and Prof. dr. Ronald de Groot at the Radboud University Medical Center in Nijmegen, The Netherlands. Her line of research focused on intranasal vaccination to reduce pneumococcal colonization and to improve the understanding of mucosal immunity in this process. The results of these studies are presented in this thesis and published in peer-reviewed scientific journals. Aside from her PhD studies, Kirsten was a member of the organizing committee of the TULIPS Young Researchers Day in Pediatrics. Kirsten is currently employed as a postdoctoral fellow at the Department of Microbiology in the group of Prof. dr. Jeffrey Weiser at New York University Langone Medical Center in New York, United States. In the coming years, she will continue her research on pneumococcal carriage and aspires to increase the fundamental understanding of pediatric infectious diseases.